THE UNIVERSITY
of EDINBURGH

This thesis has been submitted in fulfilment of the requirements for a postgraduate degree (e.g. PhD, MPhil, DClinPsychol) at the University of Edinburgh. Please note the following terms and conditions of use:

This work is protected by copyright and other intellectual property rights, which are retained by the thesis author, unless otherwise stated.
A copy can be downloaded for personal non-commercial research or study, without prior permission or charge.
This thesis cannot be reproduced or quoted extensively from without first obtaining permission in writing from the author.
The content must not be changed in any way or sold commercially in any format or medium without the formal permission of the author.
When referring to this work, full bibliographic details including the author, title, awarding institution and date of the thesis must be given.

Identification and characterisation of spindle checkpoint silencing factors in *Schizosaccharomyces pombe*

Sadhbh Soper Ní Chafraidh

THE UNIVERSITY *of* EDINBURGH

Thesis presented for the degree of Doctor of Philosophy

Wellcome Trust Centre for Cell Biology

University of Edinburgh

2019

Declaration

I declare that I composed this thesis myself and that the work presented here is my own, except where contributions by others are clearly stated. This work has not been submitted for any other degree or professional qualification.

In Chapter 5, I present work which was previously published in Journal of Cell Science, as Regulated reconstitution of spindle checkpoint arrest and silencing through chemically induced dimerisation *in vivo*. This work was authored by Amin P, Soper Ní Chafraidh S, Leontiou I & Hardwick KG (2019). Priya Amin generated the SynCheckABA system and characterised this arrest. The experiments from this paper which are presented as results in this thesis were carried out by me. I contributed the section of this paper which dealt with checkpoint silencing, specifically, testing the effects of Dis2 binding to $Spc7_{1-666}$-mCherry-PYL. I generated strains, carried out experiments and analysed data for the silencing portion of this work.

Included in the appendices is another paper on which I was a co-author. This work was published in Current Biology, as Generation of a Spindle Checkpoint Arrest from Synthetic Signaling Assemblies, by Yuan I, Leontiou I, Amin P, May KM, Soper Ní Chafraidh S, Zlámalová E & Hardwick KG (2016). This work is referenced throughout the text, and results are presented as background information in Chapter 1 and Chapter 3. I performed experiments to test for dependencies of SynCheck arrest on Bub3 and Sgo2 (presented in Figure 3.1 of this work). I also performed timecourses which demonstrated the effects of Bub3 and Eaf6 on checkpoint arrest kinetics. I collaborated with other authors on timecourse experiments to check TetO dependency, and performed data analysis.

Sadhbh Soper Ní Chafraidh

April 2019

Acknowledgements

As I come to the end of my PhD, I realise how lucky I have been to be surrounded by such supportive people. Firstly, I would like to thank my supervisor, Kevin Hardwick, for all his advice over the years. He was always approachable, and I walked away from each of our meetings feeling more enthused by and knowledgeable about my project than before.

It has been a pleasure to pursue my PhD in such a friendly lab environment. I couldn't have found a warmer or more helpful group of people. Ioanna, Priya, and Karen, it has been a privilege to work alongside all of you over the years. Koly, I have really appreciated your help and enthusiasm since you joined the lab. I also appreciated the advice of Ivan and Onur, who were so helpful when I was just starting out.

I would like to thank the members of my thesis committee, David Finnegan, Patrick Heun and Adele Marston for their valuable insights and guidance. Thanks to Jonathan Millar for providing Spc7 PP1-binding mutant plasmids, as well as interesting discussions.

I thank the Wellcome Trust for funding this PhD. I also thank the Wellcome Trust and ASCB for supporting my attendance at the ASCB 2017 conference, which was one of the best experiences of my academic life and opened my eyes to wonderful cell biology research going on around the world.

I owe a great deal to my family. My parents have always been incredibly supportive of my studies, and especially so during these last few months of writing. I cannot be grateful enough for all their efforts and love, and I thank them for always being there for me.

I am also grateful to my friends, who helped to keep me sane and happy during the PhD process. Special thanks go to Tess and Lisa. I was lucky to have such great company on our Edinburgh adventure and I miss them every day! Thanks to my friends back home, especially the High School girls, who encouraged me to relax when I needed it most.

Thanks to the other students in the Wellcome Trust programme, and to all the friends I have made in Edinburgh. You have made this PhD a wonderful experience. Special thanks to Julian for his work on the high throughput screening software, and for dragging me out of the lab to go to wind band practice!

Last but not least, I want to thank my grandfather, John Caffrey, who nurtured my interest in science and supported me in countless ways over the years (including being my human test subject for science fairs!). His dedication to life-long learning remains an inspiration to me. This thesis may mark the end of my formal education, but there is much left to learn. Granddad, I dedicate this thesis to you.

List of Abbreviations

APC/C: Anaphase promoting complex/cyclosome

Bub: Budding uninhibited by benzimidazoles

CDC: Cell division cycle

CDK: Cyclin-dependent kinase

CENP: Centromere protein

DMSO: Dimethyl sulfoxide

FRAP: Fluorescence recovery after photobleaching

GFP: Green fluorescent protein

KMN: KNL1-Mis12-Ndc80 complex

KT: Kinetochore

Mad: Mitotic arrest deficient

MCC: Mitotic checkpoint complex

nmt/*Pnmt*: No message in thiamine (promoter)

NPC: Nuclear pore complex

ORF: Open Reading Frame

Padh: Alcohol dehydrogenase (promoter)

PCR: Polymerase chain reaction

PMG: *Pombe* minimal medium

PTM: Post-translational modification

RZZ: Rod1-Zwilch-ZW10 complex

SPB: Spindle pole body

TetR/rTetR: (Reverse) tetracycline repressor

tTA/rtTA: (Reverse) transcriptional transactivator

tetO: Tet operator

UTR: Untranslated region

Abstract

In cell division, the spindle-assembly checkpoint (SAC) is an important mechanism which ensures proper segregation of chromosomes into daughter cells by delaying anaphase onset until all chromosomes are correctly attached to the mitotic spindle via their kinetochores. This reduces the risk of aneuploidy, which is associated with severe consequences such as birth defects and cancer. Once all kinetochores have been properly attached the SAC is rapidly silenced, allowing the cell to progress through anaphase.

Several SAC silencing factors have been identified to date but the mechanisms by which silencing occurs remain unclear. This project aims to improve our understanding of SAC silencing mechanisms by identifying factors involved in this process and characterising their functions.

High-throughput genetic screening was carried out in fission yeast (*Schizosaccharomyces pombe*) to identify silencing defective mutants. In designing this genetic screen, we aimed to improve upon previous screens by avoiding false positives due to mutations that lead to prolonged mitotic arrest for reasons unrelated to checkpoint silencing defects, e.g. disruption of kinetochore function. To achieve this, an ectopic synthetic checkpoint mechanism developed as part of previous work in the lab was used to spatially separate checkpoint activation from the kinetochore (Yuan *et al*, 2016).

This screening approach has produced a list of candidates. Assays to confirm and characterise the checkpoint silencing roles of a subset of these factors have been carried out. These factors were selected on the basis of strength of phenotype in the screen and include SWI/SNF component Sol1 and golgi-associated protein Grh1, among others.

Additionally, work was carried out to characterise a previously identified checkpoint silencing factor, Protein Phosphatase 1 (PP1) Dis2 in a synthetic ectopic checkpoint arrest (SynCheckABA). This work illustrated the suitability of this synthetic system as a tool for further study of SAC silencing (Amin *et al,* 2019).

Lay summary

Living cells reproduce by replicating their contents and splitting into two ‘daughter’ cells. During cell replication, the genetic information stored in a cell’s DNA is copied and packaged into chromosomes. Each cell must receive just one full copy of this genetic information, so pairs of chromosomes must be separated and evenly distributed between daughter cells. Improper chromosome segregation is associated with severe consequences, including birth defects and cancer.

To ensure the proper segregation of chromosomes into daughter cells, these events are highly regulated. This is achieved by attaching chromosomes to a spindle apparatus that pulls chromosomes apart in a controlled manner. A surveillance mechanism known as the spindle assembly checkpoint (SAC) detects improperly attached chromosomes and generates a ‘wait’ signal which prevents the cell from proceeding through the later stages of cell division until all chromosomes are properly attached to the spindle. Once chromosomes attach properly, this ‘wait’ signal is rapidly silenced. Regulation of checkpoint silencing is an important but poorly understood process.

This project involved screening approximately 3,000 genes to see if they play a role in SAC silencing. This produced a shortlist of 29 genes which appeared to impact on this process. Additional experiments were performed with several of these genes to confirm whether they were involved in checkpoint silencing. Work to determine what role these factors play in silencing the SAC is underway. This knowledge will provide an increased understanding of SAC silencing mechanisms and may eventually lead to the design of anti-cancer treatments.

List of Figures

Figure 5.7 Schematic model of PP1-dependent SAC silencing pathways.

Chapter 6

Figure 6.1. Phosphoregulation of PP1-binding sites of KNL1^{Spc7}

List of Tables

Contents

CHAPTER 1

Introduction

1.1 The cell cycle

Cells reproduce by a series of events referred to as the cell cycle, during which chromosomes and other components of cells are duplicated and partitioned into two new 'daughter' cells. It is vital that this process is carried out accurately, so that each new cell contains all the components necessary for its survival. Cells ensure orderly progression through the cell cycle by regulating the sequence and timing of these events (for a review, see Nurse, 2000).

The cell cycle is a fundamental process of all living organisms and has been the subject of intensive study. The observation that new cells must be derived from existing cells was first recorded in 1855 by Rudolph Virchow (Nurse, 2000). Since then, the various stages of the cell cycle were identified by microscopy. Molecular mechanisms of cell cycle regulation have been defined in much more detail over the past few decades.

The cell cycle is divided into two main stages, interphase and M-phase (Figure 1.1). During interphase, cells grow and replicate their contents, including organelles, membranes, and other protein and RNA components. The replication of chromosomes occurs once per cell cycle, during a discrete step of interphase (the synthetic, or S phase). M-phase is a highly dynamic stage during which cells divide, which is achieved by undergoing mitosis (nuclear division), followed by cytokinesis (cell division). In many cell types, these phases are separated by gap phases (G1 and G2, before S- and M-phase respectively). These gap phases allow extra time for cell growth and regulatory transitions. Mitosis is a highly dynamic stage of the cell cycle, and is subdivided into several distinct phases, known as prophase, metaphase, anaphase and telophase (Section 1.1.2).

1.1.1 Cell cycle progression

The timing of progression through the cell cycle varies between organisms (for an overview, see Morgan, 2007). Human cells have a relatively long cell cycle, of approximately 18-24 hours. Yeast cells divide every 2-4 hours, depending on growth conditions. The relative

durations of the different phases also vary. For example, in human cells, G1 is the gap between cytokinesis and the beginning of S-phase. Cytokinesis is relatively slow in fission yeast. As a result, the G1 phase may be short or non-existent, as cells enter interphase of the next cell cycle before cytokinesis is completed.

Many complex processes occur during the cell cycle, and regulation is crucial for ensuring these events occur in a timely, ordered fashion. The molecular mechanisms of this regulation have been elucidated in detail. Key model systems which have been used to elucidate the cell cycle include budding yeast (*Saccharomyces cerevisiae*) and fission yeast (*Schizosaccharomyces pombe*). The discovery of *cdc* (cell division cycle) mutants, which experience cell cycle arrests at non-permissive temperatures, was a key step in cell cycle research. The first examples of these genes were identified in *S. cerevisiae* by Lee Hartwell and colleagues. Paul Nurse developed the use of fission yeast as a model organism for cell cycle studies.

An important early focus of cell cycle research was whether the cell cycle was controlled using a timer mechanism, or whether the initiation of later events was dependent on completion of early events. Early evidence suggested that successful completion of certain early events was important for cell cycle progression. For example, initiation of mitosis appeared to depend on completion of DNA synthesis (Hartwell & Weinert, 1989; Rao & Johnson, 1970). However, experiments in frog (*Xenopus laevis*) and fly (*Drosophila melanogaster*) embryos contradicted this view. These cells were found to undergo nuclear division even in the presence of inhibitors of DNA synthesis, which suggested that a simple timer mechanism was responsible for cell cycle progression (Kimelman *et al*, 1987; Raff & Glover, 1988). Eventually, mechanisms were discovered which link initiation of certain events to completion of earlier processes in somatic cells, although these mechanisms are absent in early embryonic cells (Lee & Nurse, 1988; Hartwell & Weinert, 1989; Dasso & Newport, 1990).

The central components of cell cycle regulation were identified to be cyclin-dependent kinases (CDKs) and cyclins. The first cyclin-dependent kinase, Cdc2, was identified in fission yeast as a factor that was required for entry into mitosis (Nurse & Bissett, 1981; Nurse & Thuriaux, 1980; Simanis & Nurse, 1986). It was found that this factor was a highly conserved mitotic regulator, as Cdc2 homologs were identified in many other species, including *S. cerevisiae* Cdc28 and human CDK1 (Lorincz & Reed, 1984; Lee & Nurse, 1987).

Both the human and *S. cerevisiae* homologs functionally complement conditional mutations in fission yeast *cdc2*. Like other regulatory kinases, CDKs can phosphorylate various components of the cell machinery to influence their interactions and/or enzymatic activity. Oscillations in levels of CDK activity occur throughout the cell cycle. This causes cyclical changes in the phosphorylation state of cell cycle machinery, driving initiation of cell cycle events.

Cyclin was first identified in sea urchin studies, carried out by Tim Hunt and colleagues (Evans *et al*, 1983). It was noted that cyclin was important for cell cycle progression, and its levels gradually increase during interphase before rapidly decreasing in mid-mitosis. Cyclin was found to be conserved in vertebrate cells. It was also found that many different cyclins are expressed at distinct stages of the cell cycle (Bhaduri & Pryciak, 2011).

Maturation Promoting Factor (MPF) was purified from frog eggs and found to act as a cell cycle regulator (Masui, 2001). Cdc2 was found to form part of this factor. Work in clams by Joan Ruderman and colleagues illustrated that cdc2 and cyclin A/B interact and led to the discovery that the MPF consisted of both cdc2 and cyclin B (Draetta *et al*, 1989). It was discovered that cyclins regulate CDK activity, to trigger various cell cycle events. Regulation of CDK activity can be controlled in various ways. Different cyclins are expressed at distinct stages of the cell cycle, and confer substrate specificity on CDKs, allowing the same CDK to trigger different events at particular stages (Bhaduri & Pryciak, 2011; Kõivomägi *et al*, 2011).

In higher eukaryotes, multiple cyclins and CDKs play important roles at various stages of the cell cycle (Sherr, 1993) (Figure 1.1). Cyclin D is expressed during G1, when it activates Cdk4/Cdk6. Cdk2-cyclin E is important for S phase initiation. Cyclin A binds to both Cdk1 and Cdk2 at different stages of the cell cycle and is involved in G2/M transition and S-phase maintenance (Pagano *et al*, 1992). Finally, in mitosis, both cyclin B and cyclin A are involved. Cdk1-cyclin B activity is important for entry into mitosis. Each Cdk-cyclin complex is responsible for the activation of the next complex in the sequence, ensuring ordered progression through the cell cycle.

Cdk activity is regulated by multiple mechanisms. Apart from cyclin levels, regulatory phosphorylation/dephosphorylation of cyclins and CDKs themselves also plays a role in CDK activation. In fission yeast, a single CDK, $Cdc2^{Cdk1}$, is responsible for all cell cycle transitions. It associates with different cyclins to achieve this regulation. Cdc13 (cyclin B homolog) is

important for Cdc2^{Cdk1} function in mitosis. Cdc2^{Cdk1} is repressed by phosphorylation, and Wee1 kinase and Cdc25 phosphatase counteract each other to regulate its activation (Parker *et al*, 1992; Parker & Piwnica-worms, 1992; Moreno & Nurse, 1990). Increased expression of Cdc13^{CyclinB} and dephosphorylation of Cdc2^{Cdk1} by Cdc25 act together to activate Cdc2^{Cdk1} towards the end of G2. Initial low levels of Cdc2^{Cdk1}-Cdc13^{CyclinB} activity further drive its own activation in a positive feedback loop (Enoch & Nurse, 1990). Cdc2^{Cdk1}-Cdc13^{CyclinB} can then initiate mitosis. Towards the end of mitosis, Cdc13^{CyclinB} levels rapidly drop as a result of proteasomal degradation (Sullivan & Morgan, 2007).

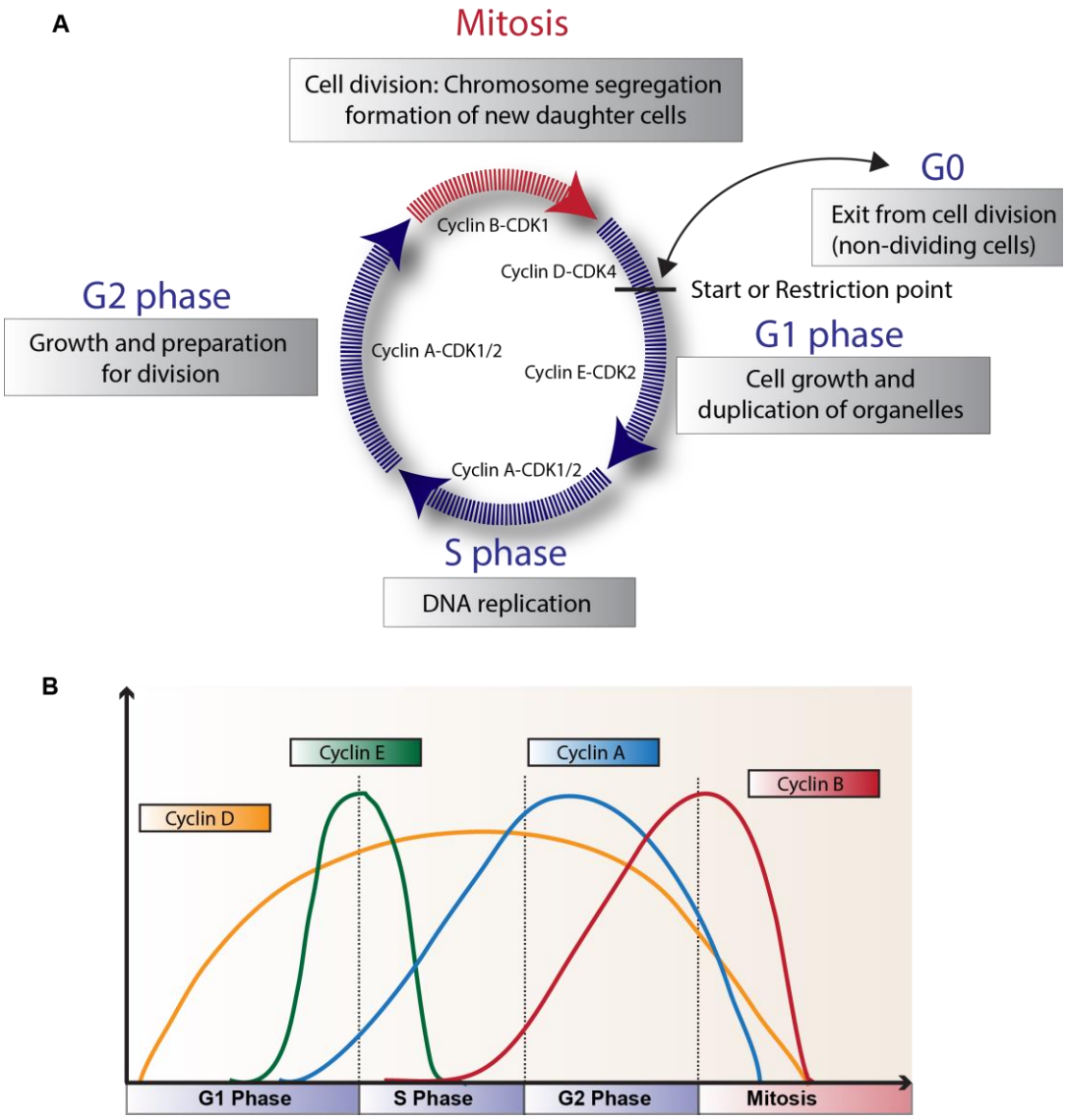

Figure 1.1 Overview of cell cycle and cyclin levels. The cell cycle is composed of two main stages, interphase and mitosis. Interphase includes the G1, S, and G2 phases. During G1, cells grow and replicate organelles. During S phase, DNA is replicated. In G2, cells continue to grow. Mitosis occurs after G2 and involves segregation of replicated chromosomes and division of the cell nucleus. This is followed by cell division. Instead of progressing through the cell cycle, cells may enter a non-proliferative state known as G0. The relevant Cdk-cyclin complexes in higher eukaryotes are indicated for each stage of the cell cycle. (B) Cyclin dependent kinases (Cdks) regulate the cell cycle. Different cyclins are expressed at varying levels throughout the cell cycle, and different Cdk-cyclin complexes have specific roles at different stages in the cycle. In metazoans, Cdk2 interacts with cyclin E and cyclin A during S-phase, and Cdk1 interacts with Cyclin A and Cyclin B during mitosis. Cyclins are rapidly degraded during mitotic exit. Figure adapted from work by Ioanna Leontiou.

1.1.2 Mitosis

During mitosis, the nucleus is divided in preparation for cell division. Mitosis is comprised of several distinct phases. These include prophase, prometaphase, metaphase, anaphase and telophase (for reviews see Mitchison & Salmon, 2001; McIntosh, 2016) (Figure 1.2).

Before mitosis occurs, cells have already replicated their DNA during S-phase. Pairs of replicated chromosomes, also known as sister chromatids, are held together at their centromeres. Cohesion between sister chromatids is maintained by loading cohesin onto chromosome arms during DNA replication. Cohesin is a ring-like complex which consists of four subunits, Mcd1 (also known as Scc1), Smc1, Smc3 and Scc3 (Nasmyth, 2002). Multiple cohesin molecules link sister chromatids together. Premature cohesin removal is inhibited during metaphase by securin. Securin acts by inhibiting separase, an enzyme which cleaves cohesin. During anaphase, upon degradation of securin, cohesin is removed and sister chromatids are separated.

During prophase, chromosomes begin to condense. The mitotic spindle also starts to assemble at this stage. Two microtubule-organising centres (centrosomes in vertebrates, spindle pole bodies in yeast) move apart towards opposite poles of the cell and start to nucleate microtubules. These microtubules are bundled into spindle fibres.

During prometaphase, the nuclear envelope breaks down (in humans and other organisms). This step does not occur in fission yeast, as these cells undergo a closed mitosis in which the nuclear envelope remains intact. Condensation of chromosomes continues. The mitotic spindle is formed and begins to bind to ('capture') sister chromatids at their kinetochores, which are multi-protein structures which assemble on centromeric DNA of each chromosome (Cheeseman & Desai, 2008).

In metaphase, chromosomes are attached to the mitotic spindle. Chromosomes must be bioriented on the spindle for correct segregation to occur, i.e. the kinetochores of a pair of sister chromatids must be attached to opposite spindle poles, so they can be pulled apart (McIntosh, 2012). In vertebrate cells, chromosomes align at a position between the spindle poles (known as the cell mid-zone or 'metaphase plate'). Once all chromosomes are bioriented, anaphase onset can occur. During anaphase, cohesion between sister chromatids is lost, allowing them to be separated and pulled towards opposite spindle poles by spindle fibres (Rieder *et al*, 1995). Correct segregation of chromosomes at this

stage is important for ensuring that all daughter cells receive a full set of genetic material. Failure to segregate chromosomes normally results in cells with an abnormal number of chromosomes, a condition known as aneuploidy. Aneuploidy can have severe consequences for cell viability (Section 1.5.1).

During telophase, the nuclear envelope is reassembled around each new set of chromosomes (except in yeast cells, which remain enclosed in the nucleus throughout the cell cycle). Finally, cells physically cleave into two new daughter cells, each of which contains all necessary components, including a full set of chromosomes.

In organisms capable of sexual reproduction, cells may undergo a different type of cell division called meiosis. Two rounds of chromosome segregation are carried out in these cells, eventually resulting in the production of haploid cells. These can fuse with another haploid cell to form a diploid zygote. There are many similarities between the regulation of mitosis and meiosis, but this thesis focuses on the mitotic cell cycle.

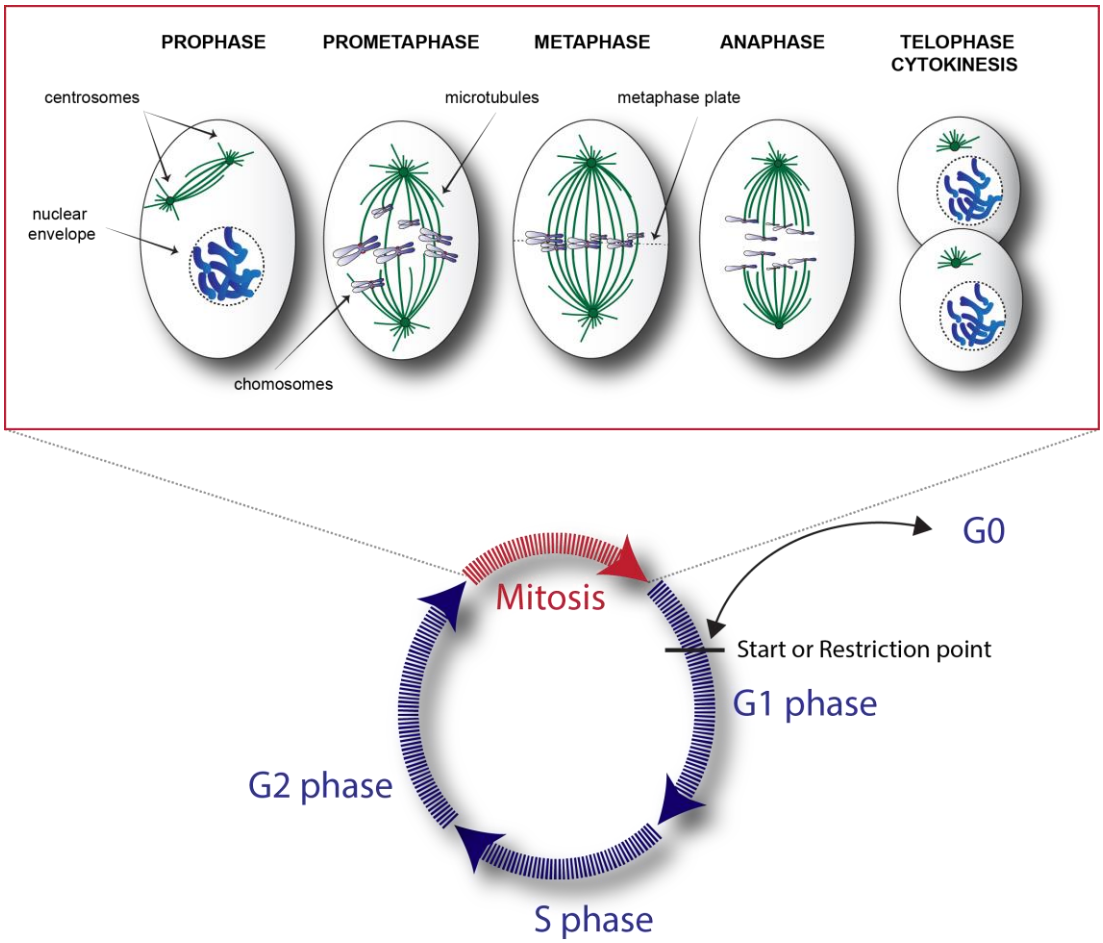

Figure 1.2 Overview of mitosis

Mitosis is divided into several phases; prophase, prometaphase, metaphase, anaphase and telophase. In prophase, chromosomes condense, and spindle poles start to separate (in vertebrates, spindle poles are centrosomes; the yeast equivalents are spindle pole bodies, or SPBs). In prometaphase, the nuclear envelope is disassembled, and the mitotic spindle is formed. During metaphase, chromosomes align at the metaphase plate (indicated by dashed line in the cell midzone). Anaphase onset occurs upon biorientation of all chromosomes on the mitotic spindle. Chromosomes are segregated to opposite poles of the cell. During telophase, nuclear membranes reassemble around the two sets of chromosomes, in preparation for separation into two new daughter cells during cytokinesis. Figure adapted from work by Ioanna Leontiou.

1.1.3 Cell Cycle Checkpoints

To prevent errors in the cell cycle which could have deleterious effects, eukaryotic cells have evolved various regulatory mechanisms. These mechanisms involve several 'checkpoints', which cells must satisfy in order to progress through the cell cycle. The idea of cell cycle checkpoints was first proposed by Weinert and Hartwell (1989). Checkpoints guard against various defects, including errors in DNA synthesis, DNA damage and chromosome segregation (Figure 1.3). Generally, these checkpoints block cells from progressing through the cell cycle, allowing time for errors to be corrected. Together, these checkpoints ensure high fidelity of genomic transmission to daughter cells.

Checkpoint mechanisms are generally composed of components which sense cell cycle defects and amplify the checkpoint signal to ensure a robust cell cycle delay, and components which inhibit cell cycle progression and/or actively repair defects (Lowndes & Marguia, 2000). Mechanisms for deactivating these checkpoints once errors have been corrected are important for allowing cells to proceed through the cell cycle.

One of the first identified checkpoint components was Rad9, which was identified to play a role in responding to DNA damage in *S. cerevisiae* (Weinert & Hartwell, 1988). This DNA damage checkpoint mechanism was found to be highly conserved. This checkpoint can detect various kinds of DNA damage by monitoring for the presence of single-stranded DNA (Lowndes & Marguia, 2000). The effector of this checkpoint is the checkpoint kinase, Chk1 (Walworth *et al*, 1993). Chk1 can block progress from G1/S phase or G2/M, by blocking activation of $Cdk1^{Cdc2/Cdc28}$. It does this by stabilising the inhibitor of $Cdk1^{Cdc2/Cdc28}$, Wee1 kinase. Additionally, it prevents localisation of the $Cdk1^{Cdc2/Cdc28}$ activator, Cdc25 phosphatase, to the nucleus (O'Connell *et al*, 1997; Raleigh & O'Connell, 2000; Lopez-Girona *et al*, 1999). Upon completion of DNA repair, Chk1 is inactivated, allowing cells to progress to mitosis (Latif, 2004).

Another checkpoint, the spindle assembly checkpoint (SAC), regulates the transition from metaphase to anaphase. This checkpoint is also known as the mitotic checkpoint or spindle checkpoint. It promotes accurate chromosome segregation by monitoring for errors in attachment of chromosomes to the mitotic spindle. This checkpoint forms the subject of this thesis and will be explored in detail in the following sections (Section 1.3).

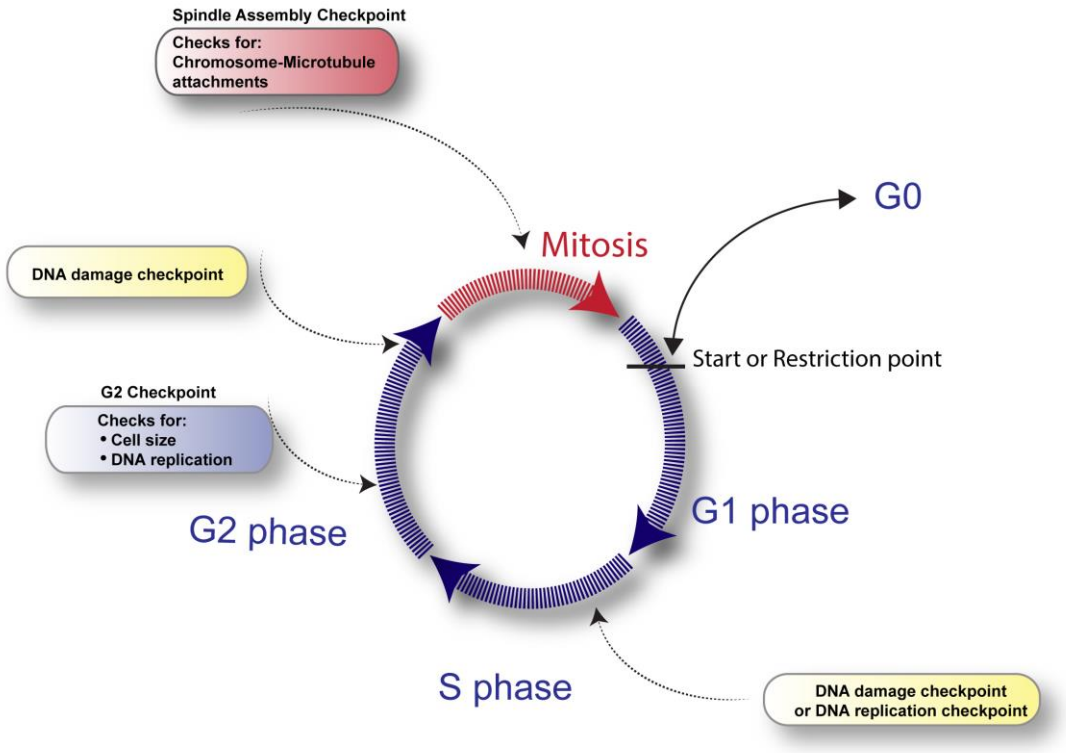

Figure 1.3 Cell cycle checkpoints

Checkpoints regulate the progression of cells through the cell cycle by controlling the activity of Cyclin dependent kinases (Cdks). These checkpoints detect errors in important cell cycle processes and ensure these are corrected before cells progress to the next stage. Checkpoints include the DNA replication checkpoint, the DNA damage checkpoint and the spindle assembly checkpoint. Figure adapted from work by Ioanna Leontiou.

1.2 Metaphase-to-Anaphase transition

1.2.1 Metaphase-to-Anaphase transition

Once all chromosomes have been successfully bioriented, cells can enter anaphase. This transition requires several key steps, as follows:

i) Degradation of cyclin B, which prevents ongoing activation of mitotic effectors (such as Cdk1) by CDK/cyclin B

ii) Removing sister chromatid cohesion

iii) Segregating chromosomes via spindle elongation

Anaphase onset is triggered by the APC/C^{Cdc20}. The APC is an E3 ubiquitin ligase, which brings about anaphase onset by targeting key mitotic proteins for degradation, including cyclins and regulators of sister chromatid cohesion (Barford, 2011). It does this by poly-ubiquitinating proteins to target them for proteasomal degradation. Poly-ubiquitination also requires ubiquitin-activating enzymes (E1s) and ubiquitin-conjugation enzymes (E2s) along with E3 ubiquitin ligases (Hershko & Ciechanover, 1998). The APC needs to interact with the co-activator Cdc20 for its activity in early mitosis. During anaphase, another APC co-activator, Cdh1, takes over this role (for an overview, see Barford, 2011). Cdc20 and Cdh1 are involved in APC substrate recognition.

Degradation of cyclin B (*S. pombe*: Cdc13) inactivates the mitotic kinase Cdk1. This allows Cdk targets to be dephosphorylated, which is important for regulating the final steps in mitosis, including disassembly of the mitotic spindle, cytokinesis.

During metaphase, sister chromatids remain linked to each other by cohesin. During anaphase, upon degradation of securin, cohesin removal can occur, allowing sister chromatids to be separated.

During anaphase, sister chromatids must first be separated and then segregated towards opposite poles of the cell along the mitotic spindle. This segregation is carried out by the mitotic spindle, a bipolar array of microtubules which attach to chromosomes and pull sister chromatids apart towards opposite cell poles. Microtubules bind to chromosomes at their kinetochores, which are large protein structures that assemble on centromeric DNA. Once all chromosomes are bioriented, anaphase onset can occur (reviewed in Tanaka, 2010).

The spindle assembly checkpoint regulates the metaphase-to-anaphase transition. It is important to monitor attachment of chromosomes to the mitotic spindle as incorrect attachments can result in missegregation of chromosomes and aneuploidy. The SAC prevents missegregation by inhibiting activation of the anaphase promoting complex (APC-Cdc20) until all chromosomes are properly attached (Figure 1.4).

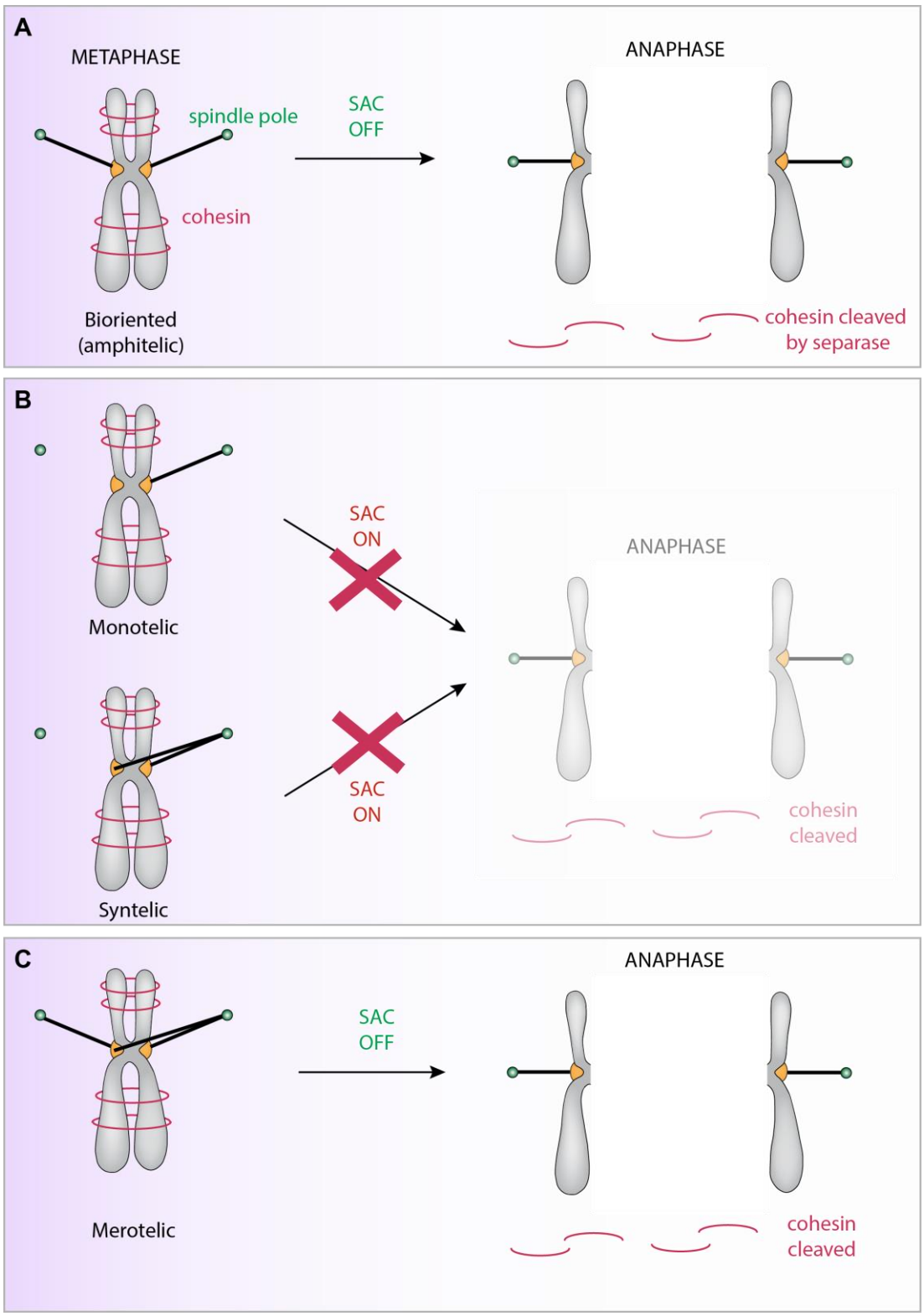

Figure 1.4 Improperly attached chromosomes trigger SAC signalling. See legend over page.

Figure 1.4 Improperly attached chromosomes trigger SAC signalling

Chromosomes need to be bioriented on the mitotic spindle to ensure accurate segregation towards opposite poles. When all chromosomes are correctly attached to the mitotic spindle via their kinetochores, the Spindle Assembly Checkpoint (SAC) is turned off, and cells proceed to anaphase (A). Prior to anaphase, sister chromatids are held together by cohesin, but as cells proceed into anaphase, cohesin is cleaved by the enzyme separase, allowing chromosomes to be separated. In panel B, the SAC remains activated due to errors in kinetochore-microtubule attachment. Unattached kinetochores of monotelic chromosomes activate the checkpoint. The SAC also remains active in the case of syntelic attachments, which lack tension. In panel C, merotelically attached chromosomes are shown; in these, one kinetochore is attached to microtubules from both spindle poles. Since these chromosomes are attached and under tension, they may not be detected by the SAC. However, these merotelic attachments can cause lagging chromosomes and aneuploidy.

1.2.2 Kinetochores

Chromosomes attach to the mitotic spindle microtubules via kinetochores, protein structures which assemble on specialised chromatin domains called centromeres. Kinetochores are highly complex structures, consisting of approximately 100 proteins in vertebrates (Cheeseman & Desai, 2008; Samejima *et al*, 2015).

Kinetochores are broadly organised into 'inner' and 'outer' domains. Inner domain proteins are close to chromatin, and include CCAN network proteins, which constitutively localise to centromeres (Perpelescu & Fukagawa, 2011; Takeuchi & Fukagawa, 2012). Outer kinetochore proteins are recruited to centromeres via CCAN (Figure 1.5).

The outer kinetochore plays an important role in mitosis, as not only is it required for the formation of kinetochore-microtubule (KT-MT) attachments, it also acts as the scaffold for the assembly of the SAC signalling complex.

The outer kinetochore consists of the KMN network (**K**NL1, **M**is12 and **N**dc80 complexes). The KNL1 complex consists of KNL1 (*S. pombe*: Spc7; *S. cerevisiae*: Spc105) and Zwint. KNL1 is particularly important as a scaffold for SAC signalling (Section 1.3). The Mis12 complex consists of Mis12, Pmf1, Dsn1 and Nsl1. This complex is important for tethering the KMN network to the inner kinetochore. The Ndc80 complex consists of Ndc80 (Hec1 in humans), Nuf2, Spc24 and Spc25. Microtubules bind kinetochores by direct interactions with Ndc80 (Biggins *et al*, 2013; Musacchio *et al*, 2017).

The Dam1/DASH complex is an additional component of the outer kinetochore. It has been identified in both *S. cerevisiae* and *S. pombe*, but no orthologs have been identified in

higher eukaryotes. This yeast-specific complex consists of 10 proteins and is involved in microtubule binding. *In vitro* studies suggest that Dam1 complexes oligomerise to form a ring around microtubule plus ends (Miranda *et al*, 2005; Wang *et al*, 2007; Westermann *et al*, 2005), although *in vivo* work in *S. pombe* suggests that formation of this ring structure may not be essential (Buttrick & Millar, 2011).

The Ska (**S**pindle and **k**inetochore **a**ssociated) complex has been identified as an outer kinetochore component in human cells and has been proposed to play a similar role to the Dam1/DASH complex in promoting kinetochore-microtubule attachment (Gaitanos *et al*, 2009; Welburn *et al*, 2009; Hanisch *et al*, 2006).

Kinetochore-microtubule attachment

Bipolar attachment of kinetochores is important for accurate chromosome segregation and satisfaction of the checkpoint. The checkpoint is 'satisfied' when the kinetochore attachment errors that trigger the SAC have been corrected, and the SAC can be switched off. Even a single unattached kinetochore is sufficient to generate a SAC arrest (Rieder *et al*, 1995). A SAC arrest is also generated in response to errors in kinetochore attachment, for example syntelic attachments (where both kinetochores of a pair of chromatids are attached to microtubules from the same spindle pole) (Figure 1.4). Normally, bipolar attachment of sister kinetochores generates tension across the kinetochores, as pulling forces from opposite poles are exerted across the mitotic spindle. This is important for stabilisation of correct microtubule attachments. Work by Bruce Nicklas and Carol Koch (1969) demonstrated that artificially manipulating chromosomes with monopolar attachments to exert tension on them was sufficient to stabilise monopolar attachments. Both syntelic and monotelic attachments (where only one kinetochore in a pair is attached to the spindle) are not under tension.

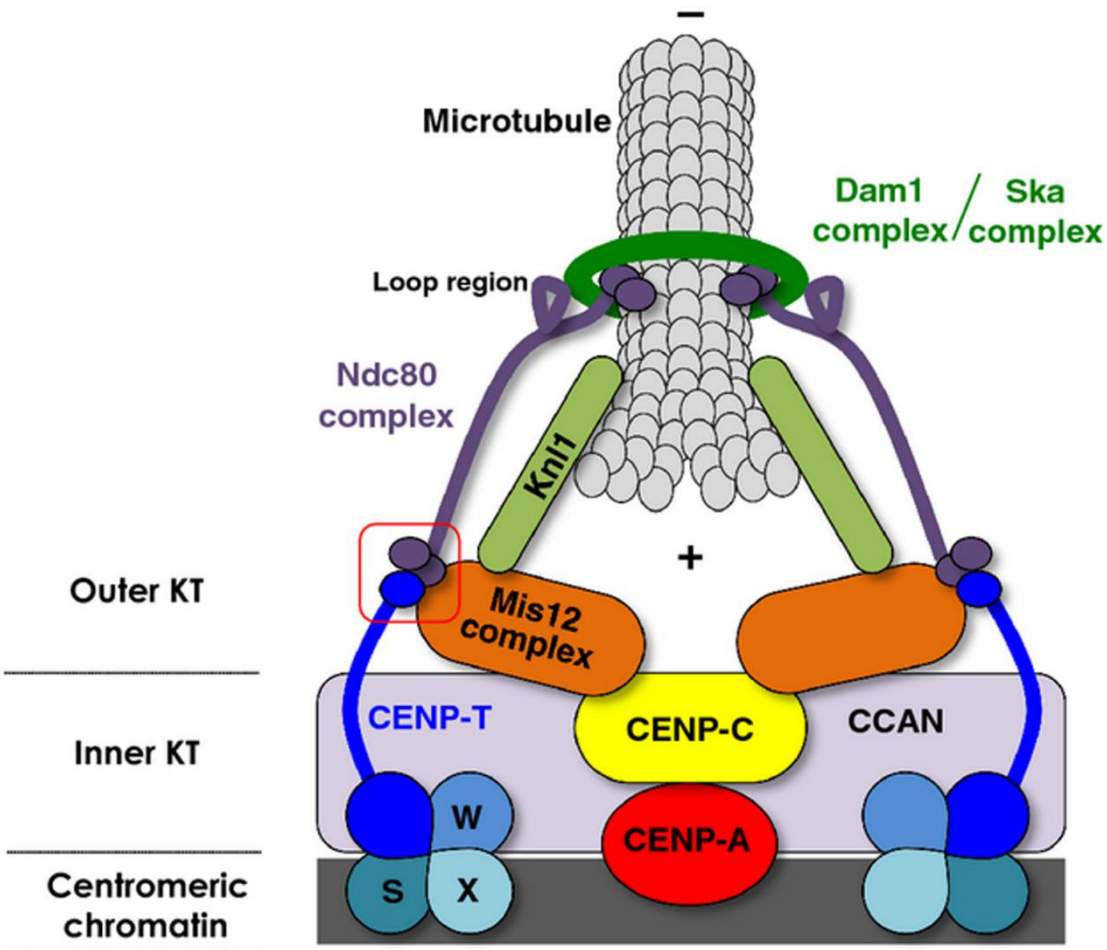

Figure 1.5 Schematic of kinetochore structure. The inner kinetochore consists of CCAN (constitutive centromere-associated network) proteins, such as CENP-A, CENP-C and CENP-T. CCAN proteins mediate the recruitment of outer kinetochore proteins to centromeres. CENP-A nucleosomes interact with CENP-C directly. CENP-C also binds the Nuf2 subunit of the Mis12 complex, part of the KMN network of outer kinetochore proteins (Knl1-Mis12-Ndc80). Additionally, CENP-T interacts with the Ndc80 complex and is important for its localisation to kinetochores. Microtubule binding sites are present in both Ndc80 and Knl1. Microtubule binding to Ndc80 is important for attachment to the mitotic spindle. There are several differences between yeast kinetochores and those of higher eukaryotes. This diagram mainly illustrates the vertebrate kinetochore. The Dam1 complex is thought to promote KT-MT interactions in both budding yeast and fission yeast. The human Ska complex is thought to be analogous to Dam1 complexes in yeast (Welburn *et al*, 2009; Jeyaprakash *et al*, 2012). Image from Yamagishi et al, 2014.

Error correction

Error correction mechanisms exist to remove incorrect microtubule attachments, allowing kinetochores to be reattached correctly. There is evidence to suggest that stabilisation of correct attachments is dependent on tension. In spermatocytes, applying tension to syntelic attachments using a micro-needle apparatus was shown to stabilise these attachments (Nicklas & Koch, 1969).

This tension-sensing error correction mechanism is dependent on the kinase Aurora B, the catalytic component of the Chromosomal Passenger Complex (CPC). The CPC also contains the proteins Survivin, Borealin and INCENP (Adams *et al*, 2001). Aurora B (*S. pombe*: Ark1; *S. cerevisiae*: Ipl1 (Francisco *et al*, 1994)) has been proposed to function as a sensor of intra-kinetochore stretch (Krenn & Musacchio, 2015). Aurora B activity destabilises incorrect attachments by reducing the affinity of KT-MT interactions. Several outer kinetochore targets for Aurora B phosphorylation have been identified (Welburn *et al*, 2010). These targets include Ndc80 and Dam1 (in budding yeast) (Cheeseman *et al*, 2002; Welburn *et al*, 2010). Ndc80 can be phosphorylated by Aurora B on its N-terminal CH (**c**alponin **h**omology) domain, which is involved in microtubule binding (Ciferri *et al*, 2008; Wei *et al*, 2007). This phosphorylation results in loss of microtubule attachment and facilitates recruitment of Mps1. It is thought that tension stabilises KT-MT attachments by stretching kinetochores and spatially separating centrosome-localised Aurora B from these outer kinetochore targets (for a review, see Krenn & Musacchio, 2015). This is supported by observations that outer kinetochore targets of Aurora B (including both artificial targets, such as FRET sensor proteins, and endogenous Aurora B targets) are not phosphorylated while kinetochores are under tension, but continue to be phosphorylated if they are relocated close to Aurora B, e.g. by tethering to CENP-B (Liu *et al*, 2009; Keating *et al*, 2009; Welburn *et al*, 2010).

1.3 The Spindle Assembly Checkpoint

During mitosis the spindle assembly checkpoint (SAC) is responsible for ensuring that chromosomes are properly attached to the mitotic spindle prior to anaphase onset, thus promoting accurate segregation of chromosomes into daughter cells. Errors in

chromosome segregation have severe consequences for human health, including embryonic lethality, birth defects and cancer (reviewed in Kops *et al*, 2005b).

The spindle assembly checkpoint is triggered when kinetochores are improperly attached and prevents progression to anaphase (Figure 1.4). A diffusible signal generated at unattached kinetochores causes the cell to arrest in metaphase, allowing time for proper attachment to be achieved (Rieder *et al*, 1995). This was demonstrated by laser irradiation of centromeres (and their associated kinetochores) on mono-oriented chromosomes in Ptk1 cells. These cells were monitored by light microscopy and it was found that upon destruction of the last mono-oriented centromere, cells rapidly entered anaphase, indicating that the SAC signal was generated by these unattached kinetochores. Upon correct attachment of all kinetochores, the checkpoint signal is turned off (silenced), and cells proceed through anaphase.

Factors involved in SAC-mediated arrest include Mad and Bub proteins (Hoyt *et al*, 1991; Li & Murray, 1991). These Mad (mitotic arrest deficient) and Bub (budding uninhibited by benzimidazole) proteins were identified as being sensitive to the benzimidazole drugs (e.g. benomyl). Benzimidazole inhibits microtubule polymerisation, and low doses of these drugs cause problems in kinetochore-microtubule attachment and activate the SAC. In wild-type cells this causes an increased duration of mitosis ('increased mitotic index') as cells arrest at metaphase to correct errors in kinetochore-microtubule attachment. However, yeast cells which lack a functional checkpoint do not arrest in metaphase, and prematurely exit mitosis. This is likely to result in errors in chromosome segregation and is detrimental to cell viability.

An important research question in spindle checkpoint regulation is how cells sense unattached or incorrectly attached kinetochores and activate the spindle checkpoint in response. Mitotic kinases Mps1 (*S. pombe*: Mph1) and Aurora B (*S. pombe:* Ark1*)* (Funabiki & Wynne, 2013) are recruited to unattached kinetochores (reviewed in London & Biggins, 2014). It has been demonstrated that kinetochores not only mediate microtubule attachment but also act as a scaffold for the assembly of anaphase inhibitory complexes (Rieder *et al*, 1995). This multifunctionality is important for coupling SAC signalling with kinetochore-microtubule (KT-MT) attachment status.

1.3.1 Silencing the SAC signal

The SAC is satisfied by the establishment of stable KT-MT attachments, and the biorientation of all chromosomes on the mitotic spindle. It is important to consider how attachment is detected and related to onset of checkpoint silencing. As discussed in Section 1.2.2, microtubule attachments which are under tension are stabilised. This is believed to be due to tension causing kinetochores to stretch, thus separating Aurora B from its outer kinetochore substrates. However, multiple mechanisms have been proposed to be involved in the onset of checkpoint silencing.

Altering the levels of Mps1 activity or recruitment to the kinetochore can have an important effect on silencing. There is evidence which shows that microtubules compete with Mps1 for access to their binding sites on Ndc80/Nuf2 (Hiruma *et al*, 2015). This means that microtubule binding can physically separate Mps1 from the KNL1 phosphodomain (Aravamudhan *et al*, 2015). However, as Mps1 is highly dynamic in human cells, it is possible that this mechanism may not be sufficient for silencing.

1.3.2 Mechanism of anaphase inhibition by SAC

Anaphase onset is triggered by ubiquitin-mediated degradation of mitotic proteins, including securin and cyclins. This is mediated by the E3 ubiquitin ligase known as the anaphase-promoting complex (APC) (reviewed in Peters, 2006).

The SAC prevents anaphase onset by blocking APC activation. It does so by inhibition of Cdc20, an essential coactivator of the APC. It was observed that Mad2 and Cdc20 are both recruited to and released from kinetochores in a dynamic manner, making them likely candidates for a diffusible signal (Shah *et al*, 2004).

The first inhibitor of the APC/C that was identified was Mad2 (Li *et al*, 1997; DeAntoni *et al*, 2005). An activated form of Mad2 was found to bind and inhibit Cdc20. Mad2 can adopt either an open or closed confirmation (O-Mad2 and C-Mad2, respectively) (DeAntoni *et al*, 2005; Luo *et al*, 2002). C-Mad2 binds to Cdc20 (or Mad1) by adopting a ‘safety belt’ conformation, where the C-terminal tail wraps around the ligand to bind it in place (Luo *et al*, 2002). In O-Mad2, the C-terminal tail is folded back on itself, blocking binding of partners (Figure 1.6).

During SAC signalling, Mad1—C-Mad2 heterotetramers stably associate with kinetochores, where they can dimerise with soluble O-Mad2 and convert it to a C-Mad2 conformation. It was observed from FRAP data (Fluorescence Recovery After Photobleaching) that a highly dynamic pool of Mad2 localised to kinetochores (Shah *et al*, 2004; Vink *et al*, 2006). It was hypothesised that interactions between soluble O-Mad2 and Mad1-C-Mad2 complexes promoted the conversion of the former to C-Mad2, in what has become known as the 'template' model. Confirmation for this hypothesis was provided by crystal structures of Mad1—C-Mad2 and O-Mad2—C-Mad2 dimers (Musacchio & Hardwick, 2002; Mapelli *et al*, 2007).

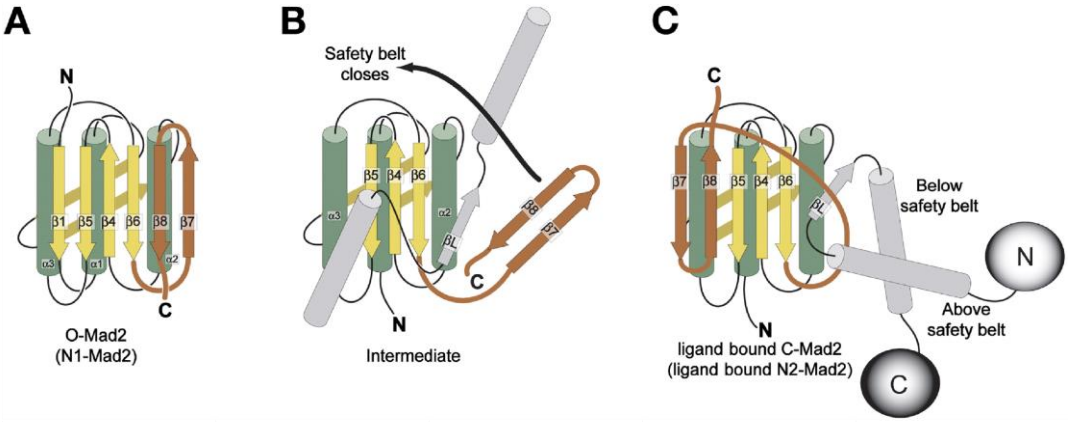

Figure 1.6 Open (O) and Closed (C) conformations of Mad2. O-Mad2 is inactive, with its C-terminal tail folded back upon itself (shown in brown). Upon binding to Mad1 or Cdc20, the C-terminal region of Mad2 closes across the ligand in a 'safety belt' mechanism, locking it in place. Conversion of soluble O-Mad2 to C-Mad2 is promoted by interactions with kinetochore-associated Mad1-C-Mad2 dimers. Figure from Nasmyth, 2005.

BubR1 (Mad3 in yeast) was subsequently also found to inhibit the APC/C (Tang *et al*, 2001). Mad2-Cdc20 and BubR1 act together by forming an inhibitory complex known as the mitotic checkpoint complex, or MCC. The MCC is a more potent inhibitor than either BUBR1 or Mad2 alone (Fang, 2002). The MCC complex consists of Mad2, Mad3/BubR1, Bub3, and Cdc20. This architecture is conserved in model organisms, except for fission yeast, in which the MCC lacks Bub3.

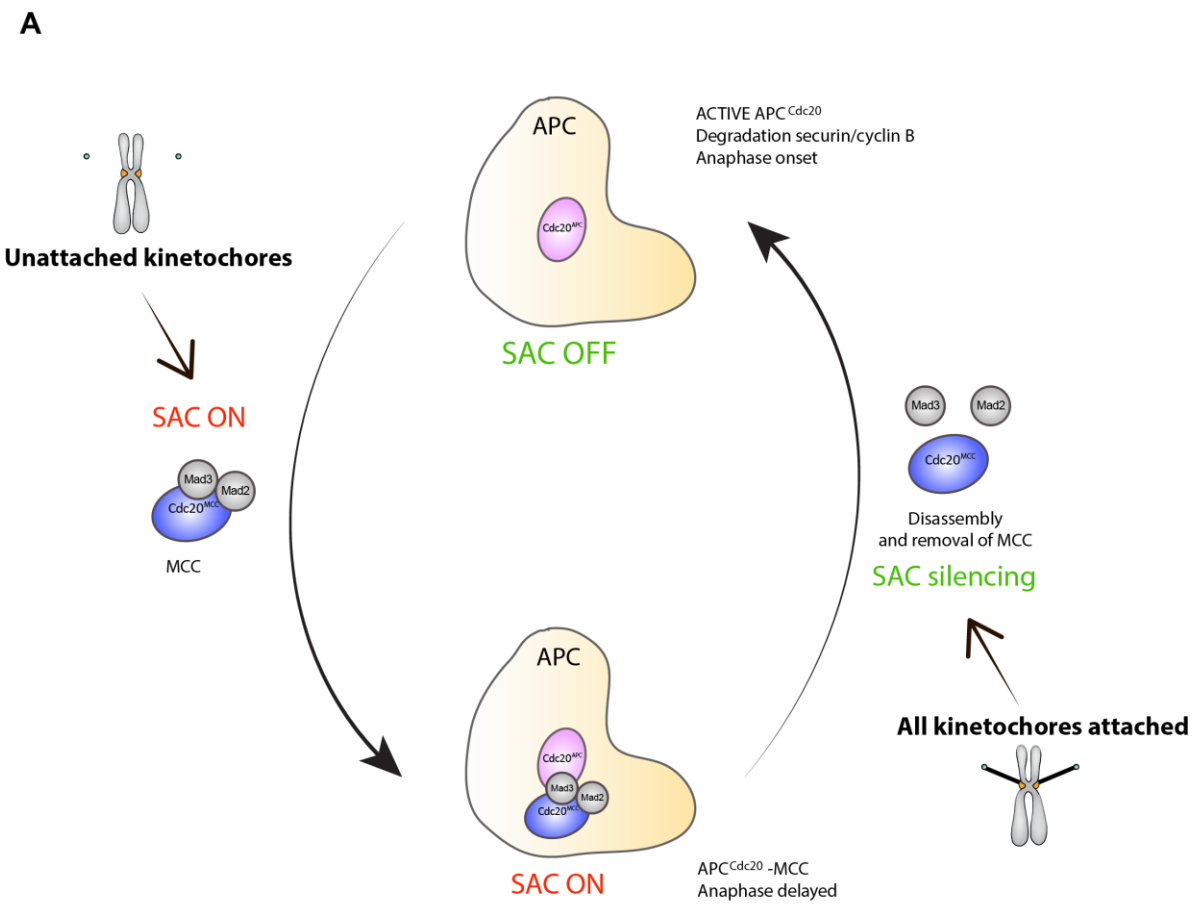

Figure 1.7 The SAC responds to errors in KT-MT attachment by inhibiting APC activation. The APC (Anaphase Promoting Complex) is an E3 ubiquitin ligase which targets key mitotic proteins for degradation, thus promoting anaphase onset. The SAC detects errors in attachment of chromosomes to the mitotic spindle. In response to these errors, the SAC promotes the assembly of APC inhibitors such as the mitotic checkpoint complex (MCC), which consists of $Cdc20^{Slp1}$, Mad2 and Mad3 in *S. pombe*. The MCC can bind to and inhibit APC which already has a second copy of Cdc20 present. Cdc20 is an essential coactivator of the APC, and by inhibiting its activity, APC is maintained in an inactive state. Upon the formation of correct KT-MT attachments, the SAC can be silenced. Disassembly of the MCC is important for checkpoint silencing.

It was found that the MCC binds to and inhibits APC which is already bound to a second copy of Cdc20 (Izawa & Pines, 2015; Alfieri *et al*, 2016) (Figure 1.7). This suggests that the APC/C is poised for activation as soon as the MCC is disassembled. This allows rapid onset of anaphase once the checkpoint is silenced.

Cryo-electron microscopy of MCC-bound human APC has provided insights into the mechanisms by which the MCC inhibits APC activity (Alfieri *et al*, 2016). MCC mainly interacts with the APC via contacts between APC-bound Cdc20 and MCC components (i.e. BubR1 and a second Cdc20 protein). Degron-like motifs of BubR1 interact with the APC-Cdc20 complex and prevent it from recognising substrate degrons. BubR1 also occludes binding sites for the E2-ubiquitin ligase, UbcH10, impeding ubiquitination activity of APC.

1.3.3 Generating the SAC signal

As previously mentioned, the key mechanism by which anaphase inhibitory complexes are formed is by localising spindle checkpoint proteins to kinetochores, including mitotic kinases Aurora B and Mps1 as well as Bub1, BUBR1 (Mad3 in yeast), Mad1 and Mad2.

Mitotic kinases have been found to play a key role in activation of the spindle checkpoint. It was thought that the sole contribution of Aurora B to checkpoint activation was via the error correction mechanism, which destabilises incorrect attachments to generate unattached kinetochores. However, there is growing evidence for the importance of Aurora B for SAC activity (Vanoosthuyse & Hardwick, 2009). Aurora B activity is an important upstream event in SAC signalling, with loss of Aurora B resulting in failure of any other checkpoint components to localise to kinetochores (Heinrich *et al*, 2012; Santaguida *et al*, 2011; Saurin *et al*, 2011). It has been shown in human cells that tethering Mps1 at kinetochores bypasses the requirement for Aurora B. This supports the hypothesis that the primary role of Aurora B in SAC signalling is to localise Mps1 at kinetochores.

Mps1 as a master regulator of SAC signalling

Mps1 has pleiotropic functions in mitosis. Mps1 is involved in chromosome biorientation in both yeast and vertebrate cells (Maure *et al*, 2007; Maciejowski *et al*, 2017). In budding yeast, Mps1 was identified to be important for spindle pole body (SPB) duplication, however this function is not conserved in the fission yeast homolog (Mph1) (Winey *et al*, 1991; He *et al*, 1998). Mps1 plays a highly conserved role in checkpoint signalling, although *C. elegans* lacks an Mps1 homolog (Essex *et al*, 2009). There is evidence to suggest that *C. elegans* Polo-like kinase (PLK-1) functionally substitutes for Mps1 in the spindle checkpoint by phosphorylating KNL-1 (Knl1 homolog) (Espeut *et al*, 2015).

Mps1 regulates the recruitment of MCC components in a stepwise manner. There are two main modules involved in SAC signalling, the KNL1-Bub3-Bub1 interaction and the Mad1-Mad2 interaction.

Mps1 phosphorylates the outer kinetochore protein KNL1 (Spc7) at its MELT motifs ([**M**/I][**E**/D/N][I/**L**/M][S/**T**]) (London *et al*, 2012; Yamagishi *et al*, 2012). Once phosphorylated, these motifs recruit Bub3-Bub1 complexes (Shepperd *et al*, 2012) (Figure 1.8). This binding is mediated through Bub3, although Bub1 interactions with KNL1 may stabilise the interaction (Krenn *et al*, 2012; Primorac *et al*, 2013).

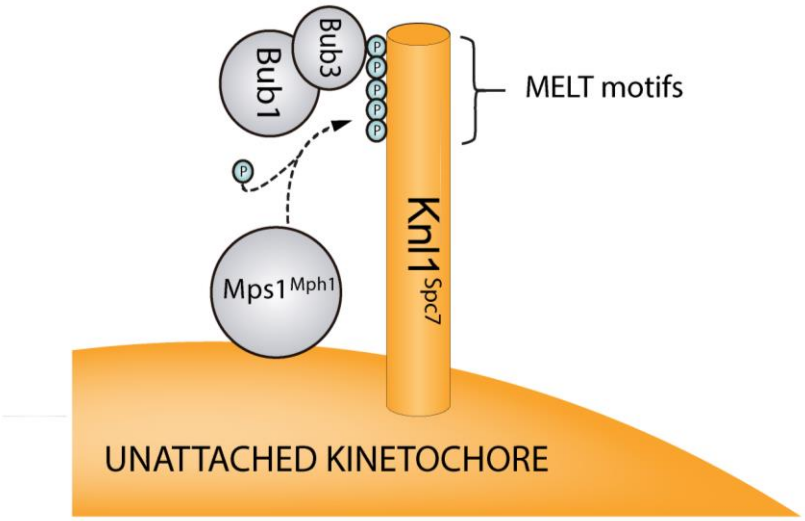

Figure 1.8 Phosphorylation of MELT motifs in Knl1/Spc7 is a key upstream event in SAC activation. $Mps1^{Mph1}$ phosphorylates MELT motifs in N-terminus of $KNL1^{Spc7}$. This phosphorylation is required for recruitment of Bub3-Bub1 to unattached kinetochores.

BUBR1 (Mad3) is recruited to kinetochores via the KNL1-Bub3-Bub1 scaffold (Overlack *et al*, 2015). Initially it was thought that this interaction was mediated by direct interactions between Bub3 and BUBR1, however it is now believed that Bub1 is important for BUBR1 recruitment.

It is hypothesised that the KNL1-Bub3-Bub1 scaffold generates an arrest, and that phosphorylation of Bub1 by Mps1 allows it to recruit Mad1-Mad2, which results in robust inhibition of the APC by promoting the formation of the MCC complex (Figure 1.9). Work in budding yeast has demonstrated that the generation of the Mad1-Bub1 complex is a hallmark of checkpoint signalling (London & Biggins, 2014; Brady & Hardwick, 2000). Recent

data from our lab has detected the Mad1-Bub1 complex in fission yeast and demonstrated that disrupting this interaction abolishes the checkpoint (Yuan *et al*, 2016).

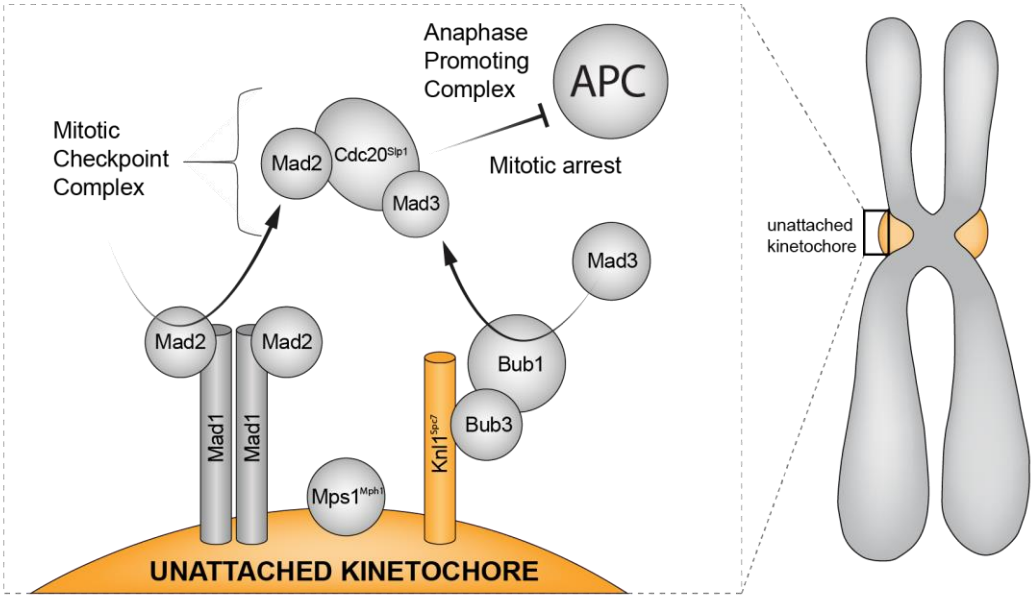

Figure 1.9 Schematic of endogenous spindle assembly checkpoint. Unattached kinetochores generate a checkpoint signal which triggers mitotic arrest, allowing attachment defects to be corrected before cells pass through anaphase. This is achieved by the repression of the anaphase promoting complex (APC) by the mitotic checkpoint complex (MCC). Checkpoint proteins including Mps1 kinase, Knl1 and Mad1 localise to kinetochores, where they are believed to act as a scaffold to guide the assembly of complexes involved in delaying anaphase onset, i.e. the MCC. Some checkpoint proteins stably associate with kinetochore-bound proteins, e.g. Bub1, Bub3 and Mad2, whereas others interact in a dynamic fashion (indicated by curved arrows), e.g. Mad2 and Mad3. Adapted from Yuan *et al*, 2016.

1.3.4 Non-kinetochore sites of checkpoint activation

Although kinetochores are the principal site of MCC formation, there is evidence to suggest that anaphase-inhibitory complexes also function away from the kinetochore. It has been demonstrated that anaphase inhibitory complexes are present during interphase in HeLa cells (Sudakin *et al*, 2001), and can also be formed in *S. cerevisiae* cells which lack functional kinetochores (Fraschini *et al*, 2001). It has also been observed that Mps1 which lacks a kinetochore-binding domain is capable of delaying mitotic exit in MEF cells (Foijer *et al*, 2014) and RPE1 cells (Rodriguez-Bravo *et al*, 2014). The essential functions of BubR1 in mitosis can also be carried out by an N-terminal fragment which cannot localise to kinetochores (Malureanu *et al*, 2009).

This pre-mitotic, kinetochore-independent pool of anaphase inhibitors defines a minimum duration of interphase in unperturbed cells by preventing premature mitotic exit before new kinetochores assemble and can generate a SAC response (Meraldi *et al*, 2004).

It has been shown in humans and *S. cerevisiae* that Mad1-Mad2 complexes associate with the nucleoplasmic side of nuclear pore complexes during interphase (Campbell *et al*, 2001; Scott *et al*, 2005), where they can interact with soluble Mad2 and catalyse its structural conversion to allow it to bind Cdc20 (Rodriguez-Bravo *et al*, 2014).

1.3.5 Non-checkpoint functions of checkpoint/MCC components

Several of the proteins involved in the SAC have additional, non-checkpoint associated functions. These pleiotropic functions are important to bear in mind when interpreting studies of SAC function. For example, Bub1 has non-checkpoint functions including roles in chromosome congression and stabilisation of kinetochore-microtubule attachments (Klebig *et al*, 2009; Warren *et al*, 2002; Williams *et al*, 2007). Bub1 also affects error correction of KT-MT attachment, as localisation of shugoshin (and the CPC) to centromeres depends on Bub1-dependent phosphorylation of histone H2A (Boyarchuk *et al*, 2007; Kitajima *et al*, 2004, 2005; Fernius & Hardwick, 2007; Kawashima *et al*, 2010).

A Golgi-localised pool of Mad1 has been discovered in mammalian cell lines (Wan *et al*, 2014). Mad1 associates with the Golgi independently of Mad2. Mad1-depletion experiments suggest that this pool of Mad1 promotes α-integrin secretion and affects cell migration, although the mechanism for these functions is unclear.

Mps1 is also involved in spindle pole duplication and error correction (for a review see Pachis & Kops, 2018).

1.4 Silencing the SAC

Despite its importance in cell cycle regulation, relatively little is known about the mechanisms for silencing SAC signalling. Although certain aspects of silencing are becoming clearer, such as the mechanism by which kinetochore-microtubule attachment triggers silencing, our understanding of how the generation of SAC complexes at the kinetochore is

shut off or how the activity of existing complexes throughout the nucleus/cell is quenched is incomplete.

In the absence of continued MCC generation at unattached kinetochores, spontaneous dissociation of MCC components may occur. However, the rate at which SAC silencing is achieved suggests that active processes are involved. Degradation of cyclin B has been observed to occur soon after the completion of correct kinetochore attachment (Clute & Pines, 1999). However, the rate of spontaneous dissociation of anaphase inhibitory complexes is relatively slow. It has been shown that after release of HeLa cells from a nocodazole-induced SAC arrest, the association of Cdc20 with Mad2 is quickly lost in wild-type cells. However, in cells with both the known SAC silencing protein p31 and ubiquitin-conjugating enzyme UbcH10 depleted, Mad2 and Cdc20 can still be co-immunoprecipitated 90 minutes post-release (Reddy *et al*, 2007). Thus the existence of SAC silencing mechanisms explains the disparity between the slow rate of spontaneous MCC:APC complex dissociation *in vivo* and rapid anaphase onset (for a review, see Ciliberto & Shah, 2009).

Balancing the activities of mitotic kinases and phosphatases plays an important role in controlling SAC signalling. Phosphorylation of APC subunits, Cdc20, and other checkpoint proteins regulates their mutual affinities and activity (Kramer *et al*, 2000). It has been demonstrated that tension across kinetochores can trigger checkpoint silencing by spatially separating Aurora B from its substrates. Additionally, microtubule attachment can block Mps1 from binding to Ndc80 (Aravamudhan *et al*, 2015). Spatially separating these mitotic kinases from their substrates allows dephosphorylation to occur.

Protein phosphatases have been identified to play an important role in SAC silencing. PP1 (Vanoosthuyse & Hardwick, 2009; Meadows *et al*, 2011; Pinsky *et al*, 2009; Rosenberg *et al*, 2011) and PP2A-B56 (Nijenhuis *et al*, 2014) have been found to play important roles.

There appear to be multiple redundant mechanisms involved in checkpoint silencing, at least in vertebrate cells. In addition to regulation of silencing by phosphatases, other known silencing mechanisms including dynein-mediated stripping of checkpoint proteins from the kinetochore upon microtubule attachment (Howell *et al*, 2001). Various mechanisms to disrupt MCC complexes have been identified, including a $p31^{comet}$ dependent pathway (Xia *et al*, 2004; Yang *et al*, 2007) and Cdc20 ubiquitination (Reddy *et al*, 2007).

Mechanisms of these silencing pathways are described in more detail in the following section.

1.4.1 PP1^{Dis2} is a conserved checkpoint silencing factor

Protein phosphatase PP1^{Dis2} has been identified to play a conserved role in silencing the spindle checkpoint (Meadows *et al*, 2011; Pinsky *et al*, 2009; Vanoosthuyse & Hardwick, 2009; Nijenhuis *et al*, 2014). PP1 (*S. cerevisiae*: Glc7) is a widely expressed Ser/Thr phosphatase. It acts upon thousands of substrates across all stages of the cell cycle (Winkler *et al*, 2015), including Retinoblastoma protein in G1 (Hendrickx *et al*, 2009), MCM4 in S-phase (Hiraga *et al*, 2014), Cdc25 in G2, and Aurora A/B in M-phase. Like other phosphatases, PP1 is regulated by interactions with different subunits. PP1 has approximately 200 such confirmed interactors, which confer specificity upon its interactions by influencing its localisation and substrate specificity (Hendrickx *et al*, 2009).

PP1 plays multiple roles during mitosis, and deletion of PP1 has been demonstrated to cause a mid-mitotic arrest, with abnormal mitotic spindle organisation and over-condensed chromosomes (Axton *et al*, 1990; Chen *et al*, 2007; Hisamoto *et al*, 1994). In *S. cerevisiae*, loss of Glc7 function results in a lethal metaphase arrest, which indicates that it has important functions in mitosis (Hisamoto *et al*, 1994; Bloecher & Tatchell, 1999).

Studying the functions of PP1 presents several challenges. Knockdown experiments are problematic. In many organisms, PP1 has several isoforms which exhibit functional redundancy. This makes knockdown experiments with individual isoforms uninformative (Cheng *et al*, 2000; Kirchner *et al*, 2007). Additionally, the broad functionality of PP1 complicates analysis of knockdown experiments due to pleiotropic effects.

Discovery of PP1^{Dis2} SAC silencing functions

Ohkura *et al* identified **d**efective **i**n **s**ister chromatid disjoining genes (*dis1, 2* and *3*) in *S. pombe* (Ohkura *et al*, 1988). *Dis* mutants enter mitosis normally but experience defects during mitosis. Despite failure to disjoin sister chromatids, chromosome condensation and spindle elongation still occur in *dis* mutants, resulting in unequal segregation of chromosomes (Ohkura *et al*, 1988).

Dis2 was found to be a catalytic subunit of protein phosphatase PP1. Two such PP1 catalytic subunits are found in *S. pombe*, Dis2 and Sds21 (Ohkura *et al*, 1989). These have partially overlapping functions. Dis2 is highly conserved, with 82% sequence homology to rabbit PP1 (Ohkura *et al*, 1989).

Dis2 is enriched in the nucleus, but has a broad cellular distribution (Ohkura *et al*, 1989; Alvarez-Tabarés *et al*, 2007; Matsuyama *et al*, 2006). Dis2 mutants have multiple defects, including disrupted mitotic spindle structure, spindle degradation, chromosome condensation, regulation of RNA Pol II transcription termination and cell polarity (Ohkura *et al*, 1989; Vanoosthuyse & Hardwick, 2009; Kokkoris *et al*, 2014; Parua *et al*, 2018).

$PP1^{Dis2}$ was first identified to play a role in spindle checkpoint silencing in fission yeast (Vanoosthuyse & Hardwick, 2009; Meadows *et al*, 2011). Previous research in this lab demonstrated that although *dis2Δ* cells enter a SAC arrest normally, they experience prolonged mitotic arrest, which suggests that they are unable to effectively silence the checkpoint.

One of the challenges of studying checkpoint silencing is that it is difficult to distinguish whether a prolonged mitotic arrest is due to failure of chromosomes to biorient or defects in silencing itself. To overcome this limitation, this lab devised a system for separating these functions (Vanoosthuyse & Hardwick, 2009) (Figure 1.10). For these experiments, strains were used which contained the cold-sensitive tubulin mutant *nda3-KM311*. Depolymerisation of microtubules at the restrictive temperature prevented these cells from satisfying the SAC and caused prolonged metaphase arrest. These strains also contained an analogue-sensitive allele of Aurora kinase (Ark1-as), allowing Ark1 to be inhibited upon the addition of 1NMPP1 (ATP analogue). By inhibiting Ark1 during the metaphase arrest, cells were unable to maintain activation of the SAC, and wild-type cells exited from metaphase even in the absence of microtubules, i.e. independently of chromosome biorientation.

In this *nda3-KM311 ark1-as* assay, *dis2Δ* cells were unable to efficiently exit metaphase arrest, even after Ark1 inhibition. This defect was found to be specific to Dis2, as deletion of other phosphatases, including Sds21, Clp1 (Cdc14 homolog) and Par1 (PP2A) did not have an effect (Vanoosthuyse & Hardwick, 2009). The *dis2Δ* phenotype was found to occur under more physiological conditions, i.e. when checkpoint signalling was deactivated by microtubule attachment, using *nda3-KM311* strains without Ark1 inhibition. This result has been confirmed in several other studies, where the absence of kinetochore-localised PP1

has been shown to cause failure to silence the checkpoint signal even when the checkpoint is satisfied by microtubule reattachment (Meadows *et al*, 2011; Pinsky *et al*, 2009; Rosenberg *et al*, 2011).

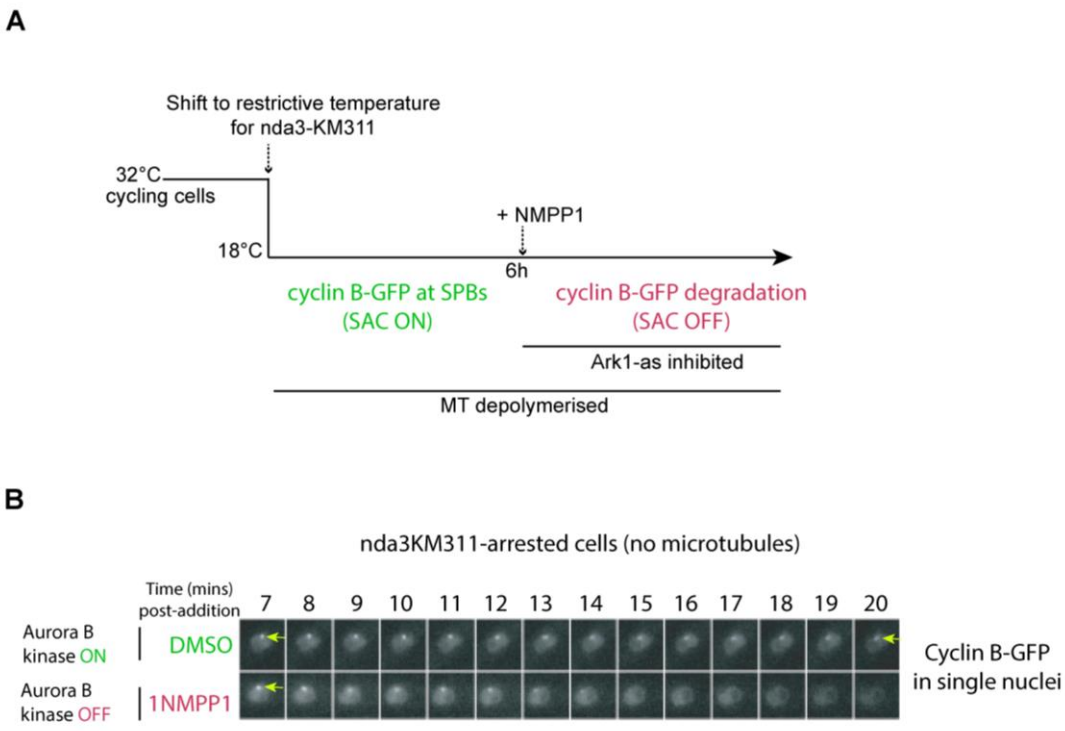

Figure 1.10 *nda3-KM311 ark1-as* assay for checkpoint silencing. (A) Schematic diagram of silencing assay. The SAC was activated by shifting cells with the cold-sensitive tubulin mutant *nda3-KM311* to the restrictive temperature. At 6 hours, the majority of cells were arrested in metaphase, as determined by high levels of cyclin B localised to spindle pole bodies (SPBs). The analogue-sensitive mutant kinase Ark1 was inhibited by adding 1NMPP1 (DMSO for controls). As a readout of checkpoint activity, cyclin B levels were monitored by live cell microscopy. (B) Microscopy timecourse of cells illustrating the progressive loss of cyclin B-GFP at SPBs as wild-type cells silence the SAC, in the absence of microtubules (Vanoosthuyse & Hardwick, 2009).

Although the precise mechanisms of PP1-mediated silencing are not understood, these experiments demonstrated that $PP1^{Dis2}$ is required to dephosphorylate Ark1 (Aurora B) targets (Vanoosthuyse & Hardwick, 2009). There is evidence to suggest that Aurora B is counteracted by PP1 in several systems, including human and yeast cells (Pinsky *et al*, 2009; Emanuele *et al*, 2008; Wang *et al*, 2008).

It is unclear what the important downstream targets of $PP1^{Dis2}$ are for silencing. Dephosphorylation of KNL1 MELTs appears to be important, although there are likely to be additional downstream targets (London *et al*, 2012; Nijenhuis *et al*, 2014).

It is notable that although knocking out $PP1^{Dis2}$ function has a severe impact on checkpoint silencing in fission yeast, it does not completely abolish checkpoint silencing in either yeast or human cells (Vanoosthuyse & Hardwick, 2009; Nijenhuis *et al*, 2014), which suggests that other redundant pathways are involved.

Regulation of $PP1^{Dis2}$ silencing functions

Recruitment of $PP1^{Dis2}$ to kinetochores has been demonstrated to be important for its checkpoint silencing functions. PP1 is targeted to kinetochores via $KNL1^{Spc7}$ (Liu *et al*, 2010; Rosenberg *et al*, 2011; Meadows *et al*, 2011). In human cells, kinetochore-localised Aurora B has been demonstrated to phosphorylate PP1-docking sites at the amino terminus of $KNL1^{Spc7}$, blocking $PP1^{Dis2}$ recruitment (Liu *et al*, 2010). $PP1^{Dis2}$ can be recruited following removal of Aurora B from the kinetochore upon the establishment of stable kinetochore-microtubule attachments. A separate pool of $PP1^{Dis2}$ is recruited to the mitotic spindle via kinesins Klp5 and Klp6 (Meadows *et al*, 2011).

$KNL1^{Spc7}$ has been found to contain conserved PP1-binding motifs, SILK and RVxF (Egloff *et al*, 1997). In *S. pombe* these conserved sequence motifs are KGILK and RRVSF respectively. Mutation of the RVSF motif (either by deletion or substitution with alanines) was shown to abolish PP1 binding in yeast and human cells (Meadows *et al*, 2011; Liu *et al*, 2010; Rosenberg *et al*, 2011). The role of the SILK motif has been more controversial. Some studies did not observe an effect of ablating this motif (Liu *et al*, 2010), whereas others have found that it reduces PP1 affinity, albeit in a less dramatic manner than deleting RVSF (Meadows *et al*, 2011; Espeut *et al*, 2012; Bajaj *et al*, 2018). Recently, crystallographic and NMR studies demonstrated that SILK (along with RVxF and another binding motif, ΦΦ) directly contacts PP1 (Bajaj *et al*, 2018) (Figure 1.11). It was demonstrated in the same study that the N-terminal portion of KNL1 containing these motifs is sufficient for recruiting PP1 in human cells (aa residues 23-80; SILK is 25-28, RVSF is 58-61).

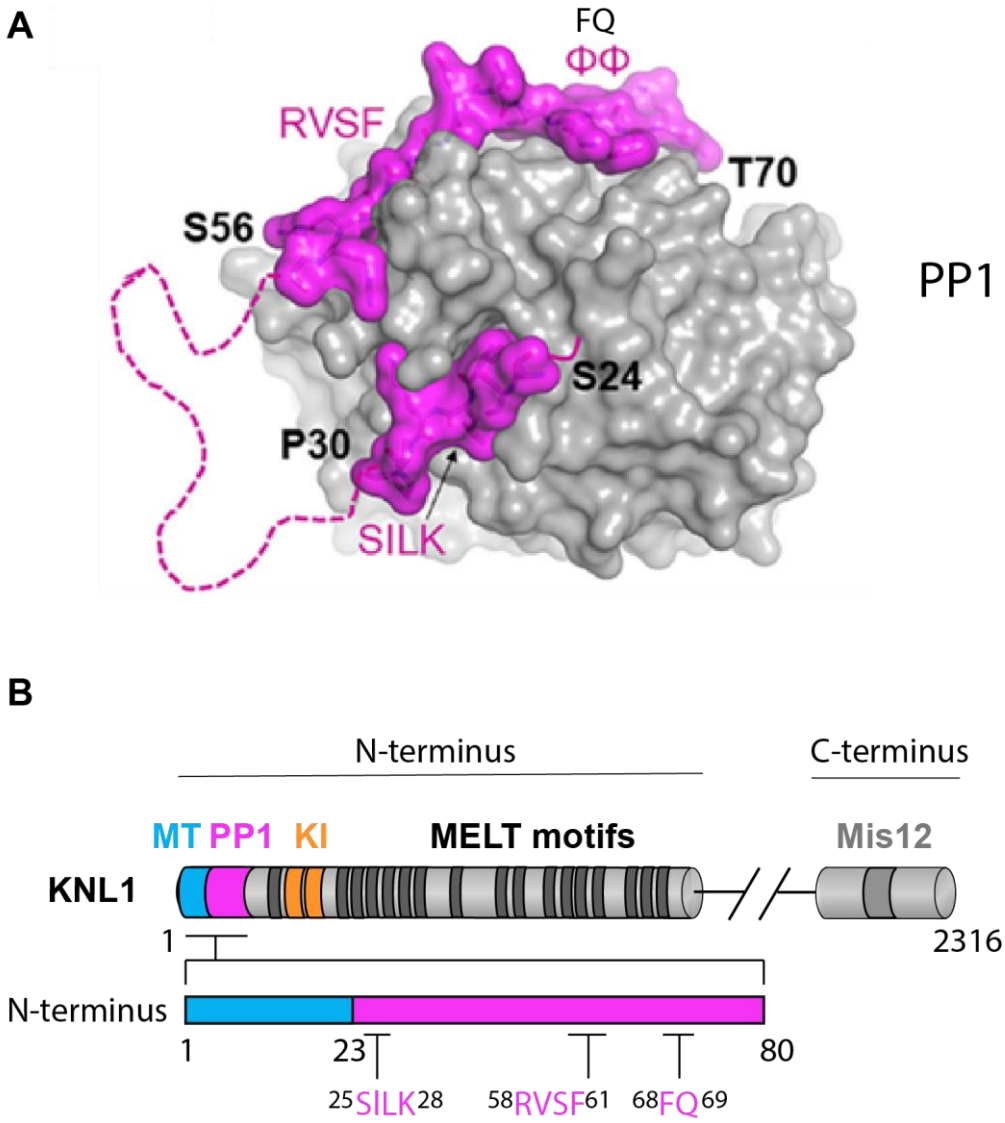

Figure 1.11 Human KNL1 binds to PP1 via direct interactions with SILK, RVSF and ΦΦ domains. (A) Crystal structure of $KNL1_{23-80}$ bound to PP1 holoenzyme. KNL1 fragment shown in magenta, PP1 in grey. A flexible linker separates the SILK and RVSF motifs. (B) Schematic of KNL1 binding domains. PP1-binding domains (SILK, RVSF and ΦΦ) are shown in magenta, microtubule binding region in blue, KI motifs in orange, and MELT motifs in dark grey. The C-terminal Mis12-binding domain is also shown (light grey). Figure adapted from Bajaj *et al*, 2018.

PP1 recruitment to kinetochores via Knl1

PP1 is recruited to kinetochores specifically during metaphase. Regulation of PP1 binding appears to be dependent on Aurora B activity. Both the **SS**ILK and RV**S**F motifs of KNL1 contain conserved Aurora B consensus sites, which have been demonstrated to be phosphorylated by Aurora B both *in vivo* and *in vitro* (Ser24, Ser25 and Ser60) (Welburn *et*

al, 2010; Kettenbach *et al*, 2011). Phosphomimic mutants (S-D substitution) of these residues have been demonstrated to block PP1 binding (Liu *et al*, 2010; Bajaj *et al*, 2018). In contrast, mutating these residues to non-phosphorylatable alanine residues caused only a mild reduction in PP1 binding (Liu *et al*, 2010). Increasing Aurora B activity at the outer kinetochore by tethering Aurora B to Mis12 (of the KMN network) results in reduced levels of PP1 recruitment to kinetochores (Liu *et al*, 2010). These Aurora B consensus sequences are conserved in fission yeast KNL1^{Spc7}, although it has not been confirmed that Aurora B^{Ark1} is responsible for their phosphorylation in this organism.

A model of regulation of PP1 silencing activity has emerged. Aurora B activity excludes PP1 from kinetochores by phosphorylating binding motifs on KNL1. Phosphatase PP2A-B56 acts to counteract this inhibition and promote PP1 binding. PP2A-B56 is recruited to phosphorylated BUBR1 (Mad3 homolog) during prometaphase (Wang *et al*, 2016). During metaphase, there is a balance between phosphorylation and dephosphorylation of Aurora B targets (Nijenhuis *et al*, 2014). When the SAC is satisfied, Aurora B is spatially separated from its outer kinetochore targets, which allows dephosphorylation to occur. Dephosphorylation of KNL1 binding sites allows PP1 to be recruited to kinetochores, where it can silence the SAC by dephosphorylating mitotic proteins. Important targets of PP1 remain to be discovered, however PP1 activity has been shown to counteract phosphorylation of KNL1 MELT motifs and the recruitment of checkpoint proteins, e.g. Bub3-Bub1 (London *et al*, 2012; Nijenhuis *et al*, 2014).

The N-terminal region of KNL1^{Spc7} is also involved in microtubule binding. This binding is not required for forming tension-bearing KT-MT attachments or for SAC activation, as these functions are mediated through Ndc80, but is involved in checkpoint silencing (Espeut *et al*, 2012). There is a basic patch immediately upstream of the SILK motif that is important for microtubule binding (Espeut *et al*, 2012; Bajaj *et al*, 2018), however the region containing the SILK and RVSF motifs has recently been shown to also be involved in microtubule binding (residues 1-80; contains two binding domains, at residues 17-34 and 53-80) (Bajaj *et al*, 2018). Phosphorylation of SILK by Aurora B also negatively regulates microtubule binding. Microtubules and PP1 cannot bind KNL1 simultaneously, and it has been shown that PP1 has a much higher affinity than microtubules for KNL1 (Bajaj *et al*, 2018). It is possible that microtubule binding aids in recognition of attachment status and may facilitate active transport of PP1 to KNL1 (Kim *et al*, 2010b), where it displaces KNL1-microtubule interactions and silences the checkpoint (Espeut *et al*, 2012; Bajaj *et al*, 2018).

PP1 recruitment to kinetochores via Klp5/Klp6

Fission yeast Klp5 and Klp6 are members of the kinesin-8 motor protein family (West *et al*, 2001; Garcia *et al*, 2002a). Kinesin-8 family members include processive, plus-end directed molecular motors that concentrate at kinetochores early in mitosis (for a review, see Messin & Millar, 2014). Kinesin-8 proteins are involved in microtubule depolymerisation, kinetochore dynamics and anaphase onset (Mayr *et al*, 2007; Stumpff *et al*, 2008). Other kinesin-8 family members include Kip3 (budding yeast) (DeZwaan *et al*, 1997) and KLP67A (Drosophila) (Pereira *et al*, 1997), as well as Kif18A, Kif18B and Kif19 in humans (Zhu & Jiang, 2005; Stout *et al*, 2011; Tanenbaum *et al*, 2009).

Mutation of either Klp5 or Klp6 results in aberrant chromosome movements and stabilisation of microtubules, which results in abnormally long metaphase spindles (Garcia *et al*, 2002b; Gergely *et al*, 2016; Meadows *et al*, 2011; West *et al*, 2001, 2002; Klemm *et al*, 2018). Although microtubule depolymerase activity has been reported for some kinesin-8 members, e.g. budding yeast KIP3 (Gupta *et al*, 2006; Varga *et al*, 2006), fission yeast kinesins Klp5 or Klp6 were found not to have measurable depolymerisation activity *in vitro* for stabilised microtubules (Grissom *et al*, 2009).

A separate pool of PP1 Dis2 is recruited to the mitotic spindle via Klp5 and Klp6 binding sites (Meadows *et al*, 2011). Both Spc7- and Klp5/Klp6-bound pools of Dis2 have been shown to play a role in checkpoint silencing, although recruitment to Klp5/Klp6 appears to play a more minor role, and cells are generally able to silence the arrest, albeit less efficiently, in *klp5Δ*/*klp6Δ*/double mutant strains (Meadows *et al*, 2011).

The motor activity of Klp5/Klp6 is important for many of their functions, as motor-defective mutants display most of the defective phenotypes associated with their deletion mutants, including chromosome biorientation defects. However, motor activity appears to be unnecessary for the spindle checkpoint silencing function of these proteins in the absence of microtubules (Meadows *et al*, 2011). In contrast, disrupting the PP1-binding sites of these proteins results in phenotypes indicative of defects in checkpoint silencing, including sensitivity to microtubule depolymerising drugs and delays in anaphase onset, despite having normal metaphase spindle length (Meadows *et al*, 2011).

1.4.2 Dynein-mediated stripping of checkpoint proteins to spindle poles

It has been observed that a range of SAC proteins localise to spindle poles upon formation of kinetochore-microtubule attachments, including Mad2, Mad1, BubR1 and Mps1. It has been proposed that 'stripping' of checkpoint components from kinetochores to spindle poles plays a role in checkpoint silencing. Dynein/dynactin, a minus-end-directed microtubule motor complex, was noted to be involved in movement of Mad2 to spindle poles (Howell *et al*, 2001). Dynein remains localised at unattached kinetochores until stable microtubule attachments are formed, which allow it to 'walk' along microtubules and relocalise its cargo to spindle poles. This is thought to prevent formation of new MCC, as proteins are no longer under the influence of regulatory phosphorylation by centromere-localised Aurora B (Famulski *et al*, 2011; Howell *et al*, 2001).

Kinetochore proteins RZZ *(***R**od: **Z**w10: **Z**wilch*)* and Spindly are involved in this process (Gama *et al*, 2017; Ying *et al*, 2009; Griffis *et al*, 2007; Kops *et al*, 2005a). Spindly is required for recruiting dynein to kinetochores (Griffis *et al*, 2007).

Several observations suggest that 'stripping' is unlikely to be crucial for SAC silencing. Firstly, it has been shown that checkpoint proteins Mad1 and Mad2 localise to spindle poles even in the absence of Spindly, albeit at lower levels (Gassmann *et al*, 2010). Secondly, this model assumes that spindle pole localised MCC components cannot inhibit APC/C. This assumption is called into question by the fact that kinetochores are not the only site at which APC/C inhibitory complexes can form (Essex *et al*, 2009; Kulukian *et al*, 2009; Malureanu *et al*, 2009; Vanoosthuyse *et al*, 2009b). Finally, it has been demonstrated that removal of Mad2 from kinetochores is not a requirement for anaphase onset (Canman *et al*, 2002).

It appears this mechanism is not conserved in yeast, which lack RZZ and Spindly homologs. Additionally, dynein is not essential for SAC silencing in yeast (Courtheoux *et al*, 2007).

1.4.3 Inactivation of Mad2 by p31^{comet}/TRIP13

Another vertebrate-specific mechanism of checkpoint silencing involves Mad2 inactivation by TRIP13 and p31^{comet}. As discussed in Section 1.3.2, a key event in MCC assembly is the conversion of O-Mad2 (open) to its active form, C-Mad2 (closed), which is capable of binding Cdc20.

Evidence for the role of p31^{comet} in SAC silencing has been confirmed in several studies, with p31^{comet} knockdown resulting in delayed mitotic exit (Habu *et al*, 2002; Xia *et al*, 2004). p31^{comet} overexpression can disrupt SAC signalling.

p31^{comet} and Mad2 are both HORMA domain proteins. Generally, HORMA domains appear to be important for various protein-protein interactions, and a common feature of HORMA domain-containing proteins is their ability to interact with chromatin (Aravind & Koonin, 1998). Crystal structures of p31^{comet} reveal a very similar structure to C-Mad2 (Yang *et al*, 2007). This structural mimicry is important for its silencing function. It was found that p31^{comet} forms a heterodimer with C-Mad2, which resembles the Mad2 dimers formed at unattached kinetochores (Xia *et al*, 2004; Mapelli *et al*, 2007; Yang *et al*, 2007). It was proposed that p31^{comet} could bind to kinetochore-localised Mad1—C-Mad2 dimers and block them from catalysing the conversion of O-Mad2 to C-Mad2. However, it appears that kinetochore localisation of p31^{comet} may not be necessary for its silencing functions. O-Mad2 levels are not affected by p31^{comet} kinetochore localisation (Westhorpe *et al*, 2011) and p31^{comet} has been demonstrated to bind C-Mad2 in both soluble and APC/C-bound MCC (Teichner *et al*, 2011; Westhorpe *et al*, 2011), suggesting that it functions downstream of kinetochores.

In cooperation with TRIP13, p31^{comet} promotes MCC disassembly (Westhorpe 2011) (Eytan *et al*, 2014; Wang *et al*, 2014b; Westhorpe *et al*, 2011). p31^{comet} and BubR1 share similar Mad2-binding interfaces, so p31^{comet} may compete with BubR1 for Mad2 binding, blocking the formation of the MCC complex (Chao *et al*, 2012; Yang *et al*, 2007).

TRIP13 is an ATPase which localises to kinetochores during mitosis, and physically interacts with p31^{comet}. It is a member of the 'ATPases associated with diverse cellular activities' (AAA+) family. AAA+ ATPases use energy extracted from ATP hydrolysis to remodel or translocate target substrates. Previous studies have shown that ATP hydrolysis is required for MCC disassembly, although it was unclear what process this was required for (Miniowitz-Shemtov *et al*, 2010). It has been demonstrated that TRIP13 ATPase activity is required for p31^{comet}-mediated silencing (Wang *et al*, 2014b; Eytan *et al*, 2014; Tipton *et al*, 2012). TRIP13 depletion delays metaphase-to-anaphase transition due to prolonged MCC activity (Wang *et al*, 2014b).

TRIP13 has been shown to be capable of binding to and unfolding the MAD2 N-terminal domain (Wang *et al*, 2014b). Unfolding of just a few N-terminal residues of Mad2 has been

shown to destabilise the C-terminal 'safety belt' region of Mad2 from its closed conformation and promote Cdc20 release (Wang *et al*, 2014b; Eytan *et al*, 2014). p31^{comet} increases the efficiency of this process, but there are conflicting reports as to whether it is required or not. Other results suggest that while TRIP13 is essential for converting C-Mad2 to O-Mad2, ablation of p31^{comet} only partially compromises this inactivation (Ma & Poon, 2016). Structural and *in vitro* studies suggest that p31^{comet} is involved in both recruiting TRIP13 to Mad2, and activating TRIP13 (Tipton *et al*, 2012; Wang *et al*, 2014b; Ye *et al*, 2015). Recently, structural and molecular modelling approaches have improved our understanding of the mechanics of the conformational conversion of Mad2 by TRIP13 (Alfieri *et al*, 2018).

This mechanism has a major effect on silencing in vertebrates, with some studies showing it is essential for mitotic exit. However, it has also been shown that p31^{comet} and TRIP13 are not essential for an unperturbed mitosis (Ma & Poon, 2016). It has also been observed that TRIP13-deficient mice (with a strongly hypomorphic allele) are viable and phenotypically normal, despite being born at sub-mendelian ratios (Li & Schimenti, 2007).

TRIP13 is also involved in checkpoint activation

TRIP13 also appears to be required for SAC activation (Nelson *et al*, 2015; Ma & Poon, 2016). It was found that TRIP13 deficient cells contain exclusively C-Mad2 (Ma & Poon, 2016). Activation of the SAC may require dynamic conversion of C-Mad2 to O-Mad2, rather than just the presence of C-Mad2 (see Musacchio, 2015).

Despite being conserved between humans and *C. elegans*, this mechanism is unlikely to be found in yeast. Both fission and budding yeast lack a p31^{comet} homolog (Vleugel *et al*, 2012). While *S. pombe* also lacks a TRIP13 ortholog (Wu & Burgess, 2006), the *S. cerevisiae* TRIP13 homolog, Pch2, is only expressed during meiosis (San-Segundo & Roeder, 1999).

1.4.4 Additional mechanisms for MCC disassembly

There is evidence to suggest additional pathways for MCC disassembly. Recently, it was proposed that CCT chaperonin plays a role in release of Cdc20 in an ATP-dependent process (Kaisari *et al*, 2017). CCT chaperonin is an essential complex required for the folding of many proteins (Yam *et al*, 2008). Hershko and colleagues purified a factor which was

associated with MCC disassembly, and demonstrated by immunoblotting and mass spectrometry that this factor consisted of CCT chaperonin subunits (Kaisari *et al*, 2017). Finally, they demonstrated *in vitro* that recombinant CCT5 contributes to MCC dissociation.

Several studies have indicated the importance of APC/C-mediated ubiquitination for the release of MCC bound to APC/C (Reddy *et al*, 2007). These experiments were performed *in vitro*, in the absence of proteasomes, which demonstrates that this effect is independent of protein degradation. However, until recently it was unclear what the important targets of this ubiquitination were. By incubating MCC-bound APC/C with components of the ubiquitination machinery, it was demonstrated that Cdc20, and to a lesser extent BubR1, are poly-ubiquitinated and that this contributes to removal of MCC components from APC/C (Eytan *et al*, 2013; Sitry-Shevah *et al*, 2018).

1.4.5 Mitotic slippage

Cells usually successfully biorient chromosomes and silence the checkpoint before exiting mitosis. In some cases, cells may fail to satisfy the checkpoint. There are several possible outcomes for these cells: they may die, exit mitosis without dividing, or else override the SAC signal. In yeast, cells may exit a prolonged SAC arrest by inhibition of Cdk1/cyclin B activity, e.g. by inhibitory phosphorylation, allowing cells to progress through the cell cycle even in the absence of correct KT-MT attachments (Wolfe & Gould, 2004; Rudner *et al*, 2000; Minshull *et al*, 1996). This process is known as adaptation. Vertebrate cells can undergo 'mitotic slippage', where gradual degradation of cyclin B results in cells bypassing the active SAC (Brito & Rieder, 2006). It has been suggested that adaptation and SAC silencing may be related processes.

An important factor involved in mitotic exit which has been implicated in adaptation is Cdc14 (Toda *et al*, 2012). Cdc14 is an essential gene required for progression through anaphase in *S. cerevisiae*. Cdc14 is a phosphatase that acts directly upon effectors of mitotic exit. Cdc14 is sequestered in the nucleolar chromatin for most of the cell cycle and is released in two waves which are regulated by the FEAR (Cdc **F**ourteen **E**arly **A**naphase **R**elease) and MEN (**M**itotic **E**xit **N**etwork) pathways (Geymonat *et al*, 2002; Stegmeier *et al*, 2002; D'Amours & Amon, 2004). Cdc14 activity is important for several different processes which occur during anaphase. Cdc14/FEAR activity has been shown to be involved in stabilising anaphase spindles, regulating nuclear positioning and segregation of repetitive

DNA and activation of motors required for spindle elongation. Cdc14/FEAR activates mitotic exit by promoting MEN activation, in a positive feedback loop. The FEAR pathway only mediates Cdc14 release into the nucleus and does not affect CDK inactivation. Later, the MEN pathway releases Cdc14 into the cytoplasm, where it can dephosphorylate Clb-CDK and its downstream targets.

Components of the FEAR network include kinetochore protein Slk19, nucleolar protein Spo12 and its homolog Bns1, Esp1 (Separase homolog) and polo kinase Cdc5 (Stegmeier et al, 2002; Visintin et al, 2003). FEAR is negatively regulated by Pds1 (Securin homolog), which inhibits Esp1, and Fob1 (Cohen-Fix & Koshland, 1999; Tinker-Kulberg & Morgan, 1999; Sullivan & Uhlmann, 2003; Stegmeier *et al*, 2004).

Cdc14 is sequestered in the nucleolus by the anchor protein Cfi1/Net1, where it remains in an inactive state. Association with this inhibitor is reported to be regulated by phosphorylation (Azzam *et al*, 2004). Phosphomutant versions of Cfi1/Net1 exhibit similar phenotypes to FEAR pathway mutants. It is likely that the FEAR pathway promotes Cdc14 release by promoting Cfi1/Net1 phosphorylation. Cdc5 has been demonstrated to disassemble Cdc14-Cfi1/Net1 *in vitro* (Shou *et al*, 2002), and several studies suggest that it is involved in Cfi1/Net1 phosphorylation (Visintin *et al*, 2003). However, other studies suggest that mitotic CDKs are involved in this regulation (Azzam *et al*, 2004).

The organisation of the FEAR pathway remains unclear. Models based on genetic interaction data have suggested that Esp1, Slk19 and Cdc5 function in one branch and Spo12, Bns1 and Fob1 function in another (Visintin *et al*, 2003), or that Cdc5 acts in a third branch (Roccuzzo *et al*, 2015). Alternative models have all components interacting in a single branch (Liang *et al*, 2013).

Histone PTMs have been postulated to play a role in Cdc14 release (Hwang & Madhani, 2009), which indicates that chromatin modifiers may be involved in Cdc14 regulation. One chromatin modifier, RSC, has been identified to play a role in mitotic exit via the FEAR pathway. Deletion of the Rsc2 subunit of RSC results in a mitotic exit defect in conditions where the MEN is partially compromised, like FEAR pathway mutants (Rossio *et al*, 2010). Deletion mutant phenotypes suggest that RSC is involved in phosphorylation of Net1 and activation/nucleolar release of Cdc14. This paper also shows a direct interaction of RSC with Cdc5. Several possible explanations for this defect were investigated. Altered recruitment of Cdc5 to chromatin regions was ruled out as a possible explanation, as were defects in

Cdc5 binding to rDNA. It was suggested that RSC mediates changes in chromatin structure which influence interactions between Cdc14 and Net1, which are bound to different rDNA sequences via Cdc5 (Rossio *et al*, 2010). It is also possible that RSC plays a role in mitotic exit independently of its chromatin-binding activity.

Most FEAR proteins have homologs in yeasts and in more complex, multicellular eukaryotes (higher eukaryotes), however the existence of a FEAR-related network has not been demonstrated in higher eukaryotes to date (D'Amours & Amon, 2004). In higher eukaryotes many of these components play a role in cytokinesis rather than in inactivation of mitotic CDKs. MEN proteins play a conserved role in cytokinesis, with Cdc14 involved in *S. pombe* (SIN, Septation Initiation Network) and *C. elegans* (Trautmann *et al*, 2001; Chen *et al*, 2006; Gruneberg *et al*, 2002).

1.5 Importance of studying SAC silencing

1.5.1 Therapeutic potential of SAC silencing factors

Studies of spindle checkpoint signalling are of biomedical importance. Aneuploidy is a common feature of cancers and may contribute to oncogenesis. Perturbations to spindle checkpoint signalling are found in many tumour types.

Impaired SAC signalling may contribute to genome instability by allowing premature mitotic exit. Defects in SAC silencing may also have a detrimental effect by delaying mitotic exit. SAC silencing factors which have been associated with cancers include TRIP13, which is overexpressed in several tumour types and has been associated with chromosomal instability (Banerjee *et al*, 2014; Larkin *et al*, 2012). p31 has also been found to be overexpressed in cancers, with levels of p31 affecting the sensitivity of cells to antimitotic drugs (Ma *et al*, 2012).

SAC signalling is a potential target for cancer therapies, which could avoid problems associated with traditional chemotherapeutics (for a review, see Ruan *et al*, 2018). These problems include toxicity and resistance of some tumour types to treatment with these drugs.

Traditional chemotherapeutics include taxanes and vinca alkaloids, which act by disrupting microtubule function. These anti-mitotic drugs prevent proliferation of cancerous cells by disrupting mitotic spindle assembly and promoting apoptosis. Cells are arrested in mitosis

for prolonged periods. However, there is variation between tumour types in the their tendency to undergo apoptosis in response to anti-mitotic drug treatments (Gascoigne & Taylor, 2008; Shi *et al*, 2008; Milross *et al*, 1996). There is a risk that some cells may undergo mitotic slippage and escape apoptosis, resulting in aneuploid cells which may resume the cell cycle.

Second generation anti-mitotics have been developed to address these issues. These drugs target mitotic regulators, including Mps1, Plk1, Aurora kinase and APC/C (Chan *et al*, 2012; Mason *et al*, 2017; Jackson *et al*, 2007). However, these have reduced efficacy compared to drugs which disrupt spindle assembly (Bavetsias & Linardopoulos, 2015; Gutteridge *et al*, 2016).

Inhibition of mitotic exit may be a useful alternative strategy. This approach could be particularly effective for killing cancer cells which are prone to mitotic slippage, have increased resistance to apoptosis, or have reduced SAC activity. The potential efficacy of this approach has been illustrated by a study involving Cdc20 inhibition. Inhibition of Cdc20 by RNAi was shown to kill cells efficiently and prevent mitotic slippage in several solid-tumour derived human cancer cell lines (Huang *et al*, 2009). As Cdc20 acts as a co-activator of APC and is required for anaphase onset, inhibition of Cdc20 prevents cells from exiting a mitotic arrest. This study found that cyclin B1 degraded more slowly upon directly inhibiting Cdc20 by RNAi than when a SAC arrest was triggered by kinesin-5 inhibition. Cdc20 inhibition led to a longer mitotic arrest. It is likely that the increased efficacy of this treatment in killing cells was due to this longer time spent in mitosis, which increased the likelihood that cells would die by apoptosis before exiting mitosis.

Mitotic exit could also be blocked by inhibition of checkpoint silencing factors, including $PP1^{Dis2}$. Selective inhibition of PP1 by overexpression of NIPP1 (nuclear inhibitor of PP1) has been shown to impair tumour growth in mouse xenografts (Winkler *et al*, 2015). Identification of novel spindle checkpoint silencing factors could identify additional cancer drug targets.

1.5.2 Prospects for further studies of SAC

Despite SAC activation being well-characterised, our view of checkpoint silencing remains unclear. It will be important to identify additional factors involved in SAC silencing. Key regulators and downstream effectors of identified pathways (e.g. $PP1^{Dis2}$) remain to be

determined, and it is possible that additional redundant mechanisms exist. Improved understanding of checkpoint silencing will have important therapeutic implications.

1.5.3 *S. pombe* as a model for studying SAC silencing

The relative simplicity of yeasts makes them attractive systems for studying chromosome segregation. For example, budding yeast kinetochores have approximately 50 protein components (Biggins *et al*, 2013), compared to ~100 proteins in vertebrates (Cheeseman & Desai, 2008; Samejima *et al*, 2015). Despite this, kinetochore architecture is highly conserved between eukaryotes.

There are some notable differences in the fission yeast SAC that should be borne in mind when considering our results. For example, Bub3 is required for SAC activity in humans and *S. cerevisiae* but is dispensable in *S. pombe*. Bub3 plays a role in silencing the checkpoint in *S. pombe* (Vanoosthuyse *et al*, 2009b). Silencing mechanisms found in vertebrate cells, including dynein-mediated stripping of Mad2 and $p31^{comet}$/TRIP13-mediated Mad2 inactivation, are not conserved in *S. pombe*. However, $PP1^{Dis2}$ plays an important, conserved role in *S. pombe* SAC silencing.

1.6 High-throughput genetic screens

Genetic screens are a powerful approach for identifying genes involved in a biological process. In designing a genetic screen, one needs to consider the following:

1) Identifying the process of interest
2) Predicting the phenotypes of mutants defective in that process
3) Designing a method for identifying mutants with that phenotype

The information obtained from such screens can be used to suggest specific follow-up studies to confirm gene function. For example, physical interactions can be confirmed by cross-linking mass spectrometry, and biochemical assays or *in vivo* experiments can be designed to probe gene function.

In this study, we aim to identify genes involved in silencing the spindle checkpoint, by screening for genetic mutants which are defective in this process. Defects in checkpoint silencing are likely to cause prolonged mitotic arrest, which can be determined by measuring the mitotic index of cells. This can be directly established by imaging cells during the transition from metaphase to anaphase, for example with fluorescently labelled tubulin. It can also be estimated by measuring colony growth on solid media. In cases of severe delays in metaphase, increased levels of cell death might be observed. This could be measured by microscopy, or by adding a vital dye to media to stain dead cells.

The design of the genetic screen carried out as part of this project is described in more detail in Chapter 3. In the following sections, background information is presented on the resources used, specifically the Bioneer haploid deletion library, and synthetic checkpoint system (SynCheck).

1.6.1 Screening the Bioneer deletion library

The development of large-scale single gene deletion libraries for yeast has proved to be a valuable aid for dissecting gene function and interactions. Initial studies in *S. cerevisiae* showed the utility of such studies (Winzeler *et al*, 1999; Birrell *et al*, 2001; Ooi *et al*, 2001). The development of similar *S. pombe* deletion libraries provides a powerful tool for such studies in this organism (Kim *et al*, 2010a; Deshpande *et al*, 2009; Pan *et al*, 2012; Lie *et al*, 2018).

Many genes in *S. pombe* have yet to be characterised, especially non-essential genes. It is likely that some of these genes have important functions, especially those that are highly conserved (Wood *et al*, 2019). By performing a high-throughput screen, we expected that some of the identified genes may play a role in silencing the SAC.

Unfortunately, the use of a deletion library means that we are unable to analyse essential genes. There are several alternative screening methods that could be used to avoid this problem (see Chapter 6 for a discussion of alternative screening strategies). However, since high levels of redundancy have been observed in vertebrate checkpoint silencing, we hypothesise that many checkpoint silencing genes may be non-essential.

In this study we screened the Bioneer haploid deletion library, version 2.1 (Bioneer v2.1). We aimed to perform an extensive screen for checkpoint silencing factors. This collection

contains single-gene deletion strains for 3004 non-essential *S. pombe* genes. This covers a substantial portion of the *S. pombe* genome, which consists of slightly over 5000 genes in total (see https://www.pombase.org/status/statistics, release version: 30th Jan 2017). The number of genes annotated as non-essential in the PomBase database is currently 3574 (10th December 2019).

It should be noted that there have been some problems associated with strains from the Bioneer library (v2.1). Thirty-one strains from this collection have been reported to lack the specified gene deletion (work from Henry Levin lab; see https://dornsife.usc.edu/pombenet/bioneer-reports/).

1.7 SynCheck, a synthetic checkpoint system

We needed to develop a query strain that would sensitise strains to the effects of defects in checkpoint silencing. This sensitivity will be particularly important if multiple redundant pathways, each with minor effects on silencing efficiency, are involved. To achieve such a query strain, we aimed to generate a mutant with a stronger spindle checkpoint and ideally one which was inducible, so that we could easily compare the effects of the mutation with and without the checkpoint activated and thus rule out secondary effects.

For our query strain we opted to use an inducible, synthetic version of the spindle checkpoint that has recently been developed in our lab (Yuan *et al*, 2016). This 'SynCheck' system was developed to allow dissection of key checkpoint components and mechanisms away from the highly complex kinetochore architecture.

This query strain has several advantages which make it suitable for our purposes. By generating the spindle checkpoint at an ectopic location, false positives due to mutants which disrupt KT-MT attachment may be ruled out. Additionally, unlike previous screens performed in our lab, it does not rely on overexpression of Mph1 to induce the checkpoint. This is important because Mph1 overexpression could have pleiotropic effects.

The SynCheck screen was designed on the principle that promoting interactions between upstream effectors of the spindle checkpoint (Mph1 kinase and the kinetochore protein Spc7) is sufficient to generate a checkpoint-mediated metaphase arrest. Initially this was done by co-tethering these two proteins to a location on chromosome arms (Figure 1.12). The tetracycline transcriptional activation system was used to achieve this co-localisation.

The tetracycline transcriptional activation system is based on a tetracycline repressor (TetR) protein identified in *E.coli* (Gossen & Bujardt, 1992). TetR is capable of binding to both tetracycline antibiotic and to a 19bp operator sequence, *tetO*. The binding of TetR protein to *tetO* can be modulated by the addition of tetracycline to growth media. In the original 'tetOFF' system, TetR only binds to *tetO* in the absence of tetracycline. A second system, 'tetON', was developed by introducing point mutations to TetR to reverse the effect of tetracycline on binding. In this system the mutant protein, reverse transcriptional transactivator (rTetR) can only bind to *tetO* upon the addition of anhydrotetracycline (a tetracycline derivative).

The SynCheck system we employ in this study is based on the TetON system. Fusion proteins of key upstream spindle checkpoint effectors with an N-terminal rTetR domain were used to co-target these proteins to a 112-copy *tetO* array on a chromosome arm (*arg3* locus, chromosome I) (Yuan *et al*, 2016). It was found that co-targeting Mph1 and Spc7 proteins was sufficient to generate an ectopic spindle checkpoint-mediated arrest. These fusion proteins had their kinetochore localisation domains removed (i.e. the C-terminus of Spc7, and first 302 N-terminal residues of Mph1 (Petrovic *et al*, 2014, 2016; Heinrich *et al*, 2012).

The induction of the SynCheck arrest is controlled by regulating the expression of the rTetR-Mph1 construct. While rTetR-Spc7 is constitutively expressed under an *adh21* promoter, an inducible *nmt* promoter (*nmt81*, no message in thiamine) is used for rTetR-Mph1. This allows it to be conditionally expressed, when thiamine is removed from media.

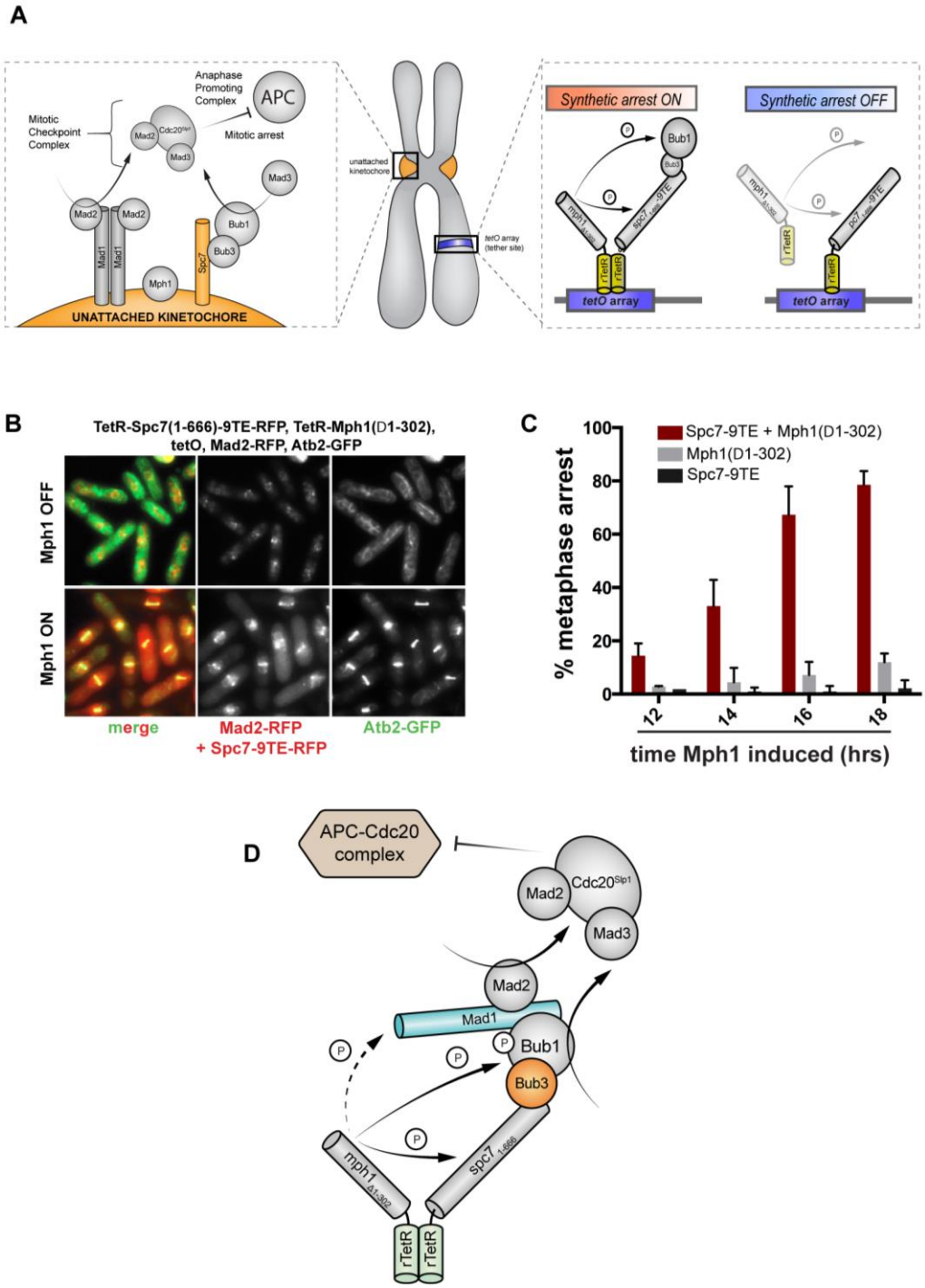

Figure 1.12 – Synthetic Checkpoint (SynCheck) system. See legend over page.

Figure 1.12 – Synthetic Checkpoint (SynCheck) system. (A) Schematic diagram illustrating SynCheck design. Instead of checkpoint proteins being recruited to endogenous kinetochores, the signal can be induced independently of kinetochore attachment status by promoting ectopic interactions between key checkpoint proteins, i.e. Spc7 and Mph1. This system was designed to recruit rTetR-Spc7 and rTetR-Mph1 constructs to a *tetO* array on a chromosome arm, upon the addition of anhydrotetracycline. It was later found that this tethering to the chromosome arm was unnecessary and that the rTetR fusion proteins simply needed to be co-expressed to dimerise and induce checkpoint signalling. The checkpoint can be induced by controlling rTetR-Mph1 expression. rTetR-Mph1 is expressed when thiamine is removed from the media, whereupon it can interact with rTetR-Spc7 to generate a checkpoint-dependent metaphase arrest. (B) Images illustrating cycling cells and cells in SynCheck-induced metaphase arrest. In the presence of thiamine, cells do not express rTetR-Mph1 (Mph1 OFF) and the SynCheck signal is not induced. When thiamine is removed from the media, rTetR-Mph1 is expressed (Mph1 ON). Anhydrotetracycline addition to media facilitates binding of rTetR-Mph1 and rTetR-Spc7 fusion proteins to a *tetO* array on a chromosome arm, promoting interactions between these proteins and generating a metaphase arrest. This arrest can be visualised by looking for short thick metaphase spindles, as are seen here for Mph1 ON, in comparison to long interphase spindles (shown in green, atb2-GFP). (C) Timecourse experiment illustrating kinetics and dependencies of SynCheck arrest. Levels of cells in a SynCheck-induced metaphase arrest peak approx. 16-18h after thiamine wash-out from media. Control strains containing either rTetR-Mph1 or rTetR-Spc7 constructs alone do not arrest. D) Model of SynCheck mechanism of action. Upon dimerisation of rTetR-Mph1 and rTetR-Spc7, Mph1 phosphorylates Spc7 MELT motifs, allowing Bub3-Bub1 to be recruited. Mad1-Mad2 is subsequently recruited. Phosphorylation of checkpoint proteins Mad1 and Bub1 by rTetR-Mph1 may be important in this process. Local concentration of checkpoint proteins promotes the assembly of the mitotic checkpoint complex (MCC). Figure adapted from (Yuan *et al*, 2016).

1.8 Alternative Silencing Assay – SynCheckABA

In this study, checkpoint silencing candidates are tested in various SAC systems, including an alternative synthetic checkpoint, SynCheckABA. This system involves chemically induced dimerisation by abscisic acid.

Chemically induced dimerisation (CID) is a method of controlling specific protein-protein interactions with small molecules. Examples of CID include rapamycin, gibberellin, auxin and abscisic acid systems. The most well-known of these is rapamycin, which induces strong binding between two proteins which are fused to rapamycin-binding domains. However, there are several disadvantages to this system, as the tight binding is difficult to reverse. Other systems offer several advantages, such as reduced toxicity, and the ability to rapidly wash out small molecule inducers and abolish dimerisation. Plant-based systems

have the advantage of limiting interaction with other yeast proteins, resulting in fewer off-target effects.

Abscisic acid (ABA) is a plant phytohormone. *In vivo*, ABA induces binding between the PYL domain of the ABA receptor PYL1 and the ABI domain of PP2C phosphatase ABI1 (Miyazono *et al*, 2009). By fusing the ABI domain and the PYL domain to two proteins of interest, this system can be applied to study interactions involved in a range of different processes (Liang *et al*, 2011). These fusion proteins do not interact until the addition of ABA to media, after which dimerization typically occurs within just a few minutes.

SynCheckABA was recently developed in our lab as a way of studying the spindle checkpoint ectopically (Amin *et al*, 2019), thus bypassing kinetochore complexity. It operates along similar principles to the original SynCheck rTetR system, in that it forces heterodimerisation between the upstream checkpoint proteins Mph1 and Spc7.

As in the original SynCheck, the fusion proteins of Mph1 and Spc7 had their kinetochore localisation domains removed. $Spc7_{1\text{-}666}$ was fused to a C-terminal PYL domain (residues 33-209) and an *adh21* promoter (Tanaka et al, 2009). $Mph1_{\Delta 1\text{-}302}$ was fused to a C-terminal ABI domain (residues 126-423) and expressed under an *adh41* promoter (Figure 1.13A).

SynCheckABA strains also contained the *cdc25-22* mutation, which was used to synchronise cultures by blocking cells in G2 upon shifting temperature to 36°C. Dimerisation of the Mph1-ABI and Spc7-PYL fusion proteins and metaphase arrest occurred within 30 minutes of ABA addition to synchronous cultures (Figure 1.13B). This arrest was demonstrated to be dependent on downstream spindle checkpoint factors (e.g. Mad1) (Amin *et al*, 2019). SynCheckABA can induce an arrest independently of endogenous checkpoint activation at kinetochores (i.e. when endogenous Mph1 is deleted). Examination of arrest kinetics revealed that the number of arrested cells usually peaks one hour after ABA addition.

SynCheckABA has several advantages over rTetR-based SynCheck which make it more suitable for studying checkpoint silencing. In contrast to the rTetR-based system, fine-tuned control of checkpoint signalling is possible with SynCheckABA. In the rTetR system, dimerisation is constitutive, and the arrest is controlled on a transcriptional level. Expression of the rTetR-Mph1, driven by a *nmt* promoter, requires several hours of growth in media lacking thiamine. The resulting arrest peaks at around 14h post-induction and is not completely synchronous. Termination of this arrest is not easily controlled. However, in SynCheck ABA, checkpoint arrest is initiated by the addition of ABA, which induces an arrest

within 30 minutes. ABA can be washed out rapidly, allowing cells to silence the checkpoint signal and escape from the metaphase arrest. This latter feature is particularly important for our purposes, as it allows us to directly monitor the rate of checkpoint silencing.

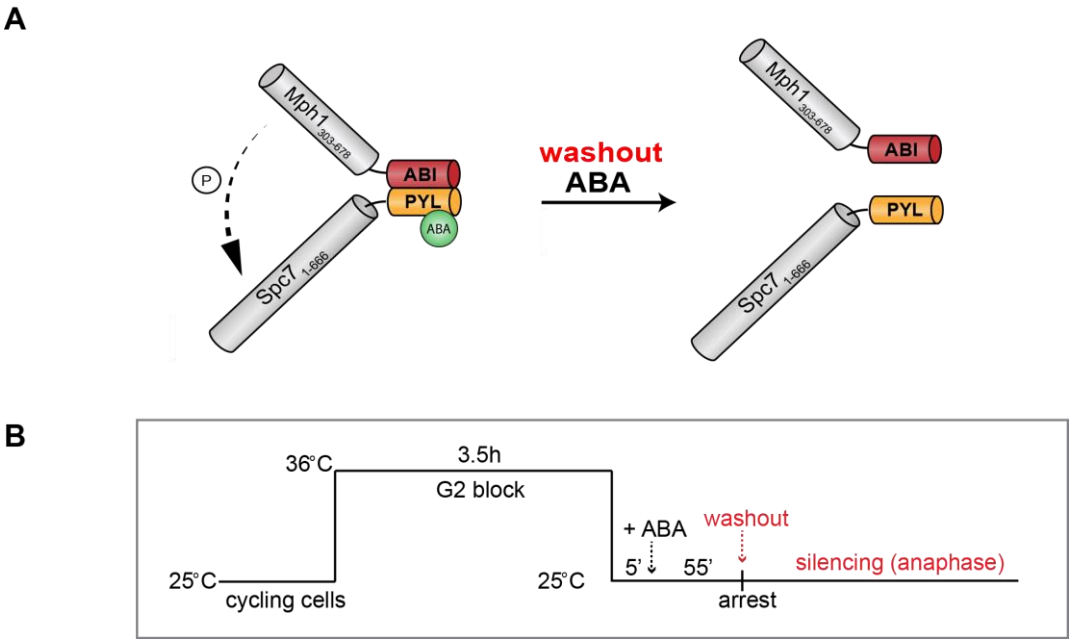

Figure 1.13 Silencing of spindle checkpoint signalling after ABA wash-out. (A) Representation of the dissociation of Mph1-Spc7 heterodimers after ABA wash-out. (B) Schematic of silencing workflow. Cells are pre-synchronised in G2 (via *cdc25-22* mutation, at 36°C), followed by shifting cultures to 25°C to allow release into mitosis. Checkpoint arrest is induced through the addition of ABA, and ABA is subsequently washed out after 60 min incubation, allowing silencing of checkpoint to occur.

1.9 Project overview

This project was designed to provide further insight into the mechanism of SAC signalling. Specifically, I set out to study checkpoint silencing.

Using fission yeast *S. pombe* as a model organism, the objective was to identify factors involved in SAC silencing by performing a high-throughput screen. Our approach differs from earlier attempts by employing a synthetic checkpoint to spatially separate SAC signalling from the kinetochore, thus eliminating false positives obtained as a result of mutations which disrupt kinetochore attachment and persistently activate the checkpoint. This synthetic approach identified several potential silencing factors, enabling resources to be focused on the most promising candidates.

In addition to studying candidates from the screen, I analysed a known silencing factor, $PP1^{Dis2}$, in more detail. This work attempts to establish the use of the synthetic checkpoint system to further study of $PP1^{Dis2}$ silencing mechanisms.

1.10 Aims

The goal of this project was to improve our understanding of SAC silencing mechanisms. More specifically, the aims were to:

i) Perform a high-throughput genetic screen for SAC silencing factors (Chapter 3)

ii) Analyse SAC silencing factors in more detail, including:

- Candidates from the screen (Chapter 4)
- Known checkpoint silencing factor Dis2 (Chapter 5)

CHAPTER 2

Materials and Methods

2.1 Yeast methods (*S. pombe*)

2.1.1. *S. pombe* growth media

Yeast cells were grown in either YES or PMG media. Recipes for liquid media are shown in Table 2.1. For solid media, 2% w/v agar was added. Media was sterilised by autoclaving before use. Additives such as supplements and drugs were filter-sterilised and added after autoclaving.

Liquid cultures were usually grown in dry shaking incubators at 30°C, except in the case of temperature-sensitive mutants.

Yeast Extract Supplemented (YES) media contains thiamine, which results in the repression of *nmt* promoters. Additional thiamine (at a final concentration of 15µM) was added as a precaution when culturing SynCheck strains, where repression of rTetR-Mph1 expression from the *nmt81* promoter was desired. YES is a rich growth medium but amino acid supplements were added to ensure all nutrients were present in sufficient amounts.

Pombe Minimal Glutamate (PMG) media requires the addition of amino acid supplements (which allows for the omission of one or more amino acids when amino acids are supplemented, facilitating selection for auxotrophic markers). It also lacks thiamine, allowing genes under the control of *nmt* promoters to be expressed. Thiamine can be added to PMG (at a final concentration of 15µM) to repress *nmt*-driven expression. If adding thiamine to PMG solid media, it was added at double the concentration (30µM).

Clear PMG was used for microscopy as it reduces background fluorescence seen when imaging GFP-tagged constructs. This is because filter-sterilised D-glucose is added after

autoclaving (final concentration 2% w/v), avoiding the yellow colour caused by caramelisation of glucose.

Anhydrotetracycline (aTC) was added to yeast cultures at a final concentration of 10µM to induce binding of rTetR to *tetO* sequences. A 1000X stock was prepared in DMSO, filter-sterilised and stored at -20°C.

Phloxin B plates were made by adding 10 mg/L of phloxin B to PMG agar with supplements. Plates were made with or without thiamine (at a final concentration of 15µM).

Media/Solution	Ingredient
YES	yeast extract (0.5%), D-glucose (3%), 1X supplements*, 1X minerals*, 1X vitamins*
PMG	Potassium hydrogen phthalate (14.7 mM), Na_2HPO_4 (15.5 mM), L-glutamic acid, monosodium salt (25.4 mM), D-glucose (2%), 1X supplements*, 1X minerals*, 1X vitamins*
SPA (synthetic sporulation agar)	D-glucose (1%), KH_2PO_4 (0.1%), agar (3%), 0.2X supplements*, 1X minerals*, 1X vitamins*
*Supplements mix (20X)	Adenine (3.2 g/L), arginine (1.6 g/L), histidine (1.6 g/L), leucine (3.2 g/L), uracil (1.6 g/L), lysine (1.6 g/L)
*Vitamins mix (1000X)	Biotin (10 mg/L), pantothenic acid (1 g/L), nicotinic acid (10 g/L), inositol (10 g/L)
*Minerals mix (1000X)	Boric acid (80.9 mM), MnSO4 (23.7 mM), $ZnSO_4.7H_2O$ (13.9 mM), $FeCl_3.6H_2O$ (7 mM), molybdic acid (2.47 mM), KI (6.02 mM), $CuSO_4$.$5H_2O$ (1.6 mM), citric acid (47.6 mM)
G418	150 µg/ml G418 sulphate
CloNAT	100 µg/ml CloNAT
Hygromycin	100 µg/ml hygromycin

Table 2.1. Recipes for *S. pombe* growth media and additives

2.1.2. *S. pombe* strain construction

Cells were revived from freezer stocks and plated on YES overnight. To perform mating crosses, strains of opposite mating types were mixed on a SPA plate and incubated at 30°C. Formation of tetrads was checked for under a light microscope.

Random spore analysis (RSA) was performed by taking a small loopful of tetrads from mating plates and adding them to 200µl dH_2O and 1µl glusulase extract (MP Biomedicals) and incubating for 1-2 days at 37°C to remove parent strains and digest the asci containing spores. Spores were then washed with sterile water and plated on YES plates. Once colonies appeared (up to 3 days after plating at 32°C) they were streaked out and replica plated to selective media. Other desired components of strains were screened for by PCR or Western blotting, or by microscopy to detect fluorescently tagged constructs. Stocks of desired strains were stored at -80°C in YES with 50% glycerol.

In some instances, tetrad dissection was performed instead of RSA. Tetrad dissection was performed using a Singer MSM 400 microscope/micromanipulator system. After performing crosses on SPA plates, tetrads were plated to YES plates and placed about 3mm apart in a line, using the micromanipulator. Tetrads were incubated at 37°C for 3-5 hours, until ascus walls broke down. The micromanipulator was used to separate each tetrad into a horizontal line of four individual spores, approximately 5mm apart. Spores were incubated at the appropriate temperature (usually 30°C) until colonies formed. Phenotypes of these colonies was then assessed by replica plating and/or microscopy.

2.1.3. *S. pombe* transformation

Transformation by electroporation

Cells were grown to mid-exponential phase (OD_{600}=0.5) in YES medium. Cells were harvested by centrifugation (1701 x g for 2.5min at 20°C) and washed once in 1ml ice-cold water and again in 1ml 1M sorbitol. The final resuspension was in ice-cold 1M sorbitol at a density of 1-5 X 10^9 ml. 10µl DNA (1500ng) + 40µl of cell suspension were added to chilled Eppendorfs and incubated on ice for 5 mins. Samples were transferred to chilled electroporation cuvettes (0.2cm gap).

Electroporation was carried out using a BioRad electroporator at 1.5kV, 200 Ω, 25µF. Upon electroporation, 0.5ml of ice-cold 1M sorbitol was added to the cuvette immediately and

the cell suspension was returned to a chilled 1.5ml tube. Cells were plated directly onto minimal selective medium (washing in 1ml dH2O prior to plating optional). Alternatively, cells were allowed to recover on YES plates prior to replating to drug-containing selective media.

Lithium acetate transformation

Alternatively, cells were transformed using a lithium acetate transformation protocol (Ito *et al*, 1983). Exponentially growing cells were harvested and washed with 25ml dH_2O before being resuspended in 1ml dH_2O. 1 x 10^8 cells were aliquoted for each transformation. Water was removed by centrifuging cells (1701 x g, 2.5 mins). Cells were then resuspended in 100mM lithium acetate buffer (pH 4.9) and incubated at 30°C for 30 minutes. Cells were then pelleted and resuspended in 290µL of PEG buffer (50% w/v polyethylene glycol 3350, 0.1M lithium acetate (pH4.9)) with 2-4µg (5-10µL) of the DNA construct to be transformed. This transformation mixture was incubated at 30°C for 60 minutes, before undergoing heat shock at 42°C for 15 minutes. Cells were harvested by centrifugation and either plated immediately to selection media or allowed to recover by growing in YES liquid media overnight at 30°C before plating (particularly in the case of drug-resistant selection).

Transformed colonies were confirmed by PCR and/or Western blotting to check expression.

2.1.4. *S. pombe* strains used in this study

ID	Genotype
SS5	*cen2-GFP, lys1::Padh15-rTetR-mCherry-spc7(1-666)-9TE:ura5, Pnmt81-rTetR-mph1(Δ1-302):leu1*
SS6	*eaf6Δ::kanR, lys1::Padh15-rTetR-mCherry-spc7(1-666)-9TE:ura4, tetO:kanR, Pnmt81-rTetR-mph1(Δ1-302):leu1*
SS7	*pof9Δ::kanR, lys1::Padh15-rTetR-mCherry-spc7(1-666)-9TE:ura4, tetO:kanR, Pnmt81-rTetR-mph1(Δ1-302):leu1*
SS8	*spc19Δ::kanR, lys1::Padh15-rTetR-mCherry-spc7(1-666)-9TE:ura4, tetO:kanR, Pnmt81-rTetR-mph1(Δ1-302):leu1*
SS9	*gcn5Δ::kanR, lys1::Padh15-rTetR-mCherry-spc7(1-666)-9TE:ura4, tetO:kanR, Pnmt81-rTetR-mph1(Δ1-302):leu1*
SS10	*mop1Δ::kanR, lys1::Padh15-rTetR-mCherry-spc7(1-666)-9TE:ura4, tetO:kanR, Pnmt81-rTetR-mph1(Δ1-302):leu1*
SS11	*apc14Δ::kanR, lys1::Padh15-rTetR-mCherry-spc7(1-666)-9TE:ura4, tetO:kanR, Pnmt81-rTetR-mph1(Δ1-302):leu1*
SS12	*duo1Δ::kanR, lys1::Padh15-rTetR-mCherry-spc7(1-666)-9TE:ura4, tetO:kanR, Pnmt81-rTetR-mph1(Δ1-302):leu1*
SS13	*apc15Δ::natR, lys1::Padh15-rTetR-mCherry-spc7(1-666)-9TE:ura4, tetO:kanR, Pnmt81-rTetR-mph1(Δ1-302):leu1*
SS14	*apc15Δ::hygR, lys1::Padh15-rTetR-mCherry-spc7(1-666)-9TE:ura4, tetO:kanR, Pnmt81-rTetR-mph1(Δ1-302):leu1*
SS20	*PEM-2, Pnmt81-rTetR-mph1(Δ1-302):leu1*
SS22	*dis2Δ::hygR, lys1::Padh15-rTetR-mCherry-spc7(1-666)-9TE:ura4, tetO:kanR*
SS29	*PEM-2, Pnmt81-rTetR-mph1(Δ1-302):leu1, lys1::Padh15-rTetR-mCherry-spc7(1-666)-9TE:ura4*
SS38	*dis2Δ::hygR, Pnmt81-rTetR-mph1(Δ1-302):leu1*
SS42	*bub3Δ::kanR, Pnmt81-rTetR-mph1(Δ1-302):leu1, lys1::Padh15-rTetR-mCherry-spc7(1-666)-9TE:ura4*
SS43	*eaf6Δ::kanR, Pnmt81-rTetR-mph1(Δ1-302):leu1, lys1::Padh15-rTetR-mCherry-spc7(1-666)-9TE:ura4*
SS45	*mad2Δ::kanR, Pnmt81-rTetR-mph1(Δ1-302):leu1, lys1::Padh15-rTetR-mCherry-spc7(1-666)-9TE:ura4*
SS46	*mad2Δ::kanR, Pnmt81-rTetR-mph1(Δ1-302):leu1, lys1::Padh15-rTetR-mCherry-spc7(1-666)-9TE:ura4*
SS47	*ell1Δ::kanR, Pnmt81-rTetR-mph1(Δ1-302):leu1, lys1::Padh15-rTetR-mCherry-spc7(1-666)-9TE:ura4*
SS48	*ell1Δ::kanR, Pnmt81-rTetR-mph1(Δ1-302):leu1, lys1::Padh15-rTetR-mCherry-spc7(1-666)-9TE:ura4*
SS49	*apc15Δ::kanR, Pnmt81-rTetR-mph1(Δ1-302):leu1, lys1::Padh15-rTetR-mCherry-spc7(1-666)-9TE:ura4*
SS50	*apc15Δ::kanR, Pnmt81-rTetR-mph1(Δ1-302):leu1, lys1::Padh15-rTetR-mCherry-spc7(1-666)-9TE:ura4*
SS64	*SPBC29A3.05Δ::kanR, Pnmt81-rTetR-mph1(Δ1-302):leu1, lys1::Padh15-rTetR-mCherry-spc7(1-666)-9TE:ura4*
SS65	*eaf1Δ::kanR, Pnmt81-rTetR-mph1(Δ1-302):leu1,*

	lys1::Padh15-rTetR-mCherry-spc7(1-666)-9TE:ura4
SS66	*SPBC20f10.10Δ::kanR, Pnmt81-rTetR-mph1(Δ1-302):leu1, lys1::Padh15-rTetR-mCherry-spc7(1-666)-9TE:ura4*
SS67	*SPBC18H5.08CΔ::kanR, Pnmt81-rTetR-mph1(Δ1-302):leu1, lys1::Padh15-rTetR-mCherry-spc7(1-666)-9TE:ura4*
SS68	*SPBC21C3.08cΔ::kanR, Pnmt81-rTetR-mph1(Δ1-302):leu1, lys1::Padh15-rTetR-mCherry-spc7(1-666)-9TE:ura4*
SS69	*ogm4Δ::kanR, Pnmt81-rTetR-mph1(Δ1-302):leu1, lys1::Padh15-rTetR-mCherry-spc7(1-666)-9TE:ura4*
SS70	*mug112Δ::kanR, Pnmt81-rTetR-mph1(Δ1-302):leu1, lys1::Padh15-rTetR-mCherry-spc7(1-666)-9TE:ura4*
SS77	*reg1Δ::kanR, Pnmt81-rTetR-mph1(Δ1-302):leu1, lys1::Padh15-rTetR-mCherry-spc7(1-666)-9TE:ura4, PEM-2*
SS91	*sol1Δ::kanR, adh41-mph1(Δ1-302)-3xHA-ABI:leu2, cdc25-22, adh15-mCherry-atb2:natR*
SS92	*reg1Δ::hygR, adh41-mph1(Δ1-302)-3xHA-ABI:leu2, cdc25-22, adh15-mCherry-atb2:natR*
SS93	*SPCC18B5.5CΔ::hygR, adh41-mph1(Δ1-302)-3xHA-ABI:leu2, cdc25-22, adh15-mCherry-atb2:natR*
SS95	*psy2Δ::hygR, adh41-mph1(Δ1-302)-3xHA-ABI:leu2, cdc25-22, adh15-mCherry-atb2:natR*
SS96	*tls1Δ::kanR, adh41-mph1(Δ1-302)-3xHA-ABI:leu2, cdc25-22, adh15-mCherry-atb2:natR*
SS98	*grh1Δ::kanR, adh41-mph1(Δ1-302)-3xHA-ABI:leu2, cdc25-22, adh15-mCherry-atb2:natR*
SS99	*nup37Δ::kanR, adh41-mph1(Δ1-302)-3xHA-ABI:leu2, cdc25-22, adh15-mCherry-atb2:natR*
SS100	*SPAC227.17cΔ::kanR, adh41-mph1(Δ1-302)-3xHA-ABI:leu2, cdc25-22, adh15-mCherry-atb2:natR*
SS101	*sol1Δ::kanR, adh41-mph1(Δ1-302)-3xHA-ABI:leu2, lys1::Padh21-spc7(1-666)-mCherry-2xFLAG-PYL:ura4, cdc25-22, adh15-mCherry-atb2:natR*
SS102	*reg1Δ::hygR, adh41-mph1(Δ1-302)-3xHA-ABI:leu2, lys1::Padh21-spc7(1-666)-mCherry-2xFLAG-PYL:ura4, cdc25-22, adh15-mCherry-atb2:natR*
SS103	*SPCC18B5.5CΔ::hygR, adh41-mph1(Δ1-302)-3xHA-ABI:leu2, lys1::Padh21-spc7(1-666)-mCherry-2xFLAG-PYL:ura4, cdc25-22, adh15-mCherry-atb2:natR*
SS105	*psy2Δ::hygR, adh41-mph1(Δ1-302)-3xHA-ABI:leu2, lys1::Padh21-spc7(1-666)-mCherry-2xFLAG-PYL:ura4, cdc25-22, adh15-mCherry-atb2:natR*
SS106	*tls1Δ::kanR; adh41-mph1(Δ1-302)-3xHA-ABI:LEU2, lys1::Padh21-spc7(1-666)-mCherry-2xFLAG-PYL:ura4; cdc25-22, adh15-mCherry-atb2:natR*
SS108	*grh1Δ::kanR, adh41-mph1(Δ1-302)-3xHA-ABI:leu2, lys1::Padh21-spc7(1-666)-mCherry-2xFLAG-PYL:ura4, cdc25-22, adh15-mCherry-atb2:natR*
SS109	*nup37Δ::kanR; adh41-mph1(Δ1-302)-3xHA-ABI:leu2, lys1::Padh21-spc7(1-666)-mCherry-2xFLAG-PYL:ura4, cdc25-22,*

	adh15-mCherry-atb2:natR
SS110	*SPAC227.17cΔ::kanR, adh41-mph1(Δ1-302)-3xHA-ABI:leu2, lys1::Padh21-spc7(1-666)-mCherry-2xFLAG-PYL:ura4, cdc25-22, adh15-mCherry-atb2:natR*
SS111	*sol1Δ::kanR*
SS112	*reg1Δ::hygR*
SS113	*SPCC18B5.5CΔ::hygR*
SS115	*psy2Δ::hygR*
SS116	*tls1::kanR*
SS118	*grh1Δ::kanR*
SS119	*nup37Δ::kanR*
SS120	*SPAC227.17cΔ::kanR*
SS121	*lys1::Padh21-spc7(1-666, Δ136-150)-mCherry-PYL-2xFLAG:ura4, Padh41-mph1(303-678)-3xHA-ABI:leu2, cdc25-22, Padh15-atb2-RFP:natR*
SS122	*lys1::Padh21-spc7(1-666, Δ331-345)-mCherry-PYL-2xFLAG:ura4, Padh41-mph1(303-678)-3xHA-ABI:leu2, cdc25-22, Padh15-atb2-RFP:natR*
SS123	*Padh41-mph1(303-678)-3xHA-ABI:leu2, lys1::Padh21-spc7(1-666, Δ136-150)-mCherry-PYL-2xFLAG:ura4, cdc25-22, Padh15-atb2-RFP:natR*
SS128	*dis2Δ::hygR, Padh41-mph1(303-678)-3xHA-ABI:leu2, lys1::Padh21-spc7(1-666)-mCherry-2xFLAG-PYL:ura4, cdc25-22, Padh15-mCherry-atb2:natR, cdc13-GFP:leu*
SS130	*klp6Δ::ura4 Padh41-mph1(303-678)-3xHA-ABI:leu2, lys1::Padh21-spc7(1-666)-mCherry-2xFLAG-PYL:ura4, cdc25-22, Z:Padh15-mCherry-atb2:natR, cdc13-GFP:leu, ark1-as:hygR*
SS158	*klp6Δ::ura4, Padh41-mph1(303-678)-3xHA-ABI:leu2, lys1::Padh21-spc7(1-666, Δ136-150, Δ331-345)-mCherry-2xFLAG-PYL:ura4, cdc25-22, Z:Padh15-mCherry-atb2:natR, cdc13-GFP:leu, mph1Δ::natR*
SS144	*sol1Δ::kanR, ark1-as3::hygR, cdc13-gfp::leu, nda3-KM311*
SS145	*sol1Δ::kanR, ark1-as3::hygR, cdc13-gfp::leu, nda3-KM311*
VV1472	*PEM-2, dis2Δ::hygR, ade6-210, leu1-32, ura4-D18, h-MTL:cycS*
VV1525	*PEM-2, bub3Δ::hygR, ade6-210, leu1-32, ura4-D18, h-MTL:cycS*
KMP501	*PEM-2, mad2Δ::hygR, ade6-210, leu1-32, ura4-D18, h-MTL:cycS*
PA175	*lys::adh21-spc7(1-666)wt-flag-mCherry-PYL:ura, adh41-mph1(303-678)-GFP-ABI:leu2, mph1Δ:natR, cdc25-22*
JM5349	*klp6::ura4, cdc13-gfp, ark1-as, nda3-KM311*
KMP010	*ade6-210, leu1-32, ura4-D18*
KMP011	*ade6-210, leu1-32, ura4-D18*
KMP477	*PEM-2, ade6-210, leu1-32, ura4-D18, h-MTL:cycS*
VV1381	*ark1-as3::hygR, cdc13-gfp, nda3-KM311*
VV1388	*ark1-as3::hygR, cdc13-gfp, nda3-KM311, dis2Δ::ura4*

IY230	*lys1::adh15-rTetR-mCherry-spc7(1-666)-9TE:ura4, tetO:kanR, Pnmt81-rTetR-mph1(Δ1-302):leu1, mad2-GFP*
IY222	*lys1::adh15-rTetR-mCherry-spc7(1-666)-9TE:ura4, Pnmt81-rTetR-mph1(Δ1-302):leu1, mad2-GFP*
IY240	*lys1::adh15-rTetR-mCherry-spc7(1-666)-9TE:ura4, tetO:kanR, Pnmt81-rTetR-mph1(Δ1-302):leu1, mad2-GFP, bub3Δ::hygR*
IL322	*lys1::adh15-rtTA-mCherry-spc7(1-666)-9TE:ura4, tetO:kanR, Pnmt81-rtTA-mph1(Δ1-302):leu1, atb2-GFP:leu1, mad2-RFP:natR*
IL375	*lys1::adh15-rtTA-mCherry-spc7(1-666)-9TE:ura4, Pnmt81-rtTA-mph1(Δ1-302):leu1*
PA284	*adh41-mph1(Δ1-302)-3xHA-ABI:leu2, cdc25-22, adh15-mCherry-atb2:natR, ura-*
PA252	*adh41-mph1(Δ1-302)-3xHA-ABI:leu2, mph1Δ::natR, lys::adh21-spc7(1-666)-PYL:ura; cdc25-22, adh15-mCherry-atb2:natR, bub1-GFP:his*
PA338	*adh41-mph1(Δ1-302)-3xHA-ABI:leu2, lys::adh21-spc7(1-666)-PYL:ura, cdc25-22, adh15-mCherry-atb2:natR, cdc13-GFP:leu*

Table 2.2 *S. pombe* strains used in this work. I constructed strains (SS) for this work. Other strains used include those made in this lab by Vincent Vanoosthuyse (VV), Karen May (KMP), Priya Amin (PA), Ioanna Leontiou (IL) and Ivan Yuan (IY). Strain JM5349 was a gift from Jonathan Millar.

2.2 DNA methods

2.2.1 Genomic DNA extraction

Yeast genomic DNA extracts were prepared using a protocol adapted from the single tube LiOAc-SDS lysis method (Lööke *et al*, 2011).

2.2.2 DNA Purification/EtOH precipitation

DNA was precipitated from aqueous solutions by adding the 3 volumes ice-cold 96% ethanol, 1/10 volume 3M sodium acetate solution and 1/10 volume 3M sodium chloride solution. After mixing well and incubating at -20°C for 20 min, tubes were centrifuged at maximum speed for 10 min at 4°C. Supernatant was removed, and the pellet washed with 500µl 70% ethanol before centrifuging tubes for another 5 min. After removing the supernatant, pellets were allowed to dry before being resuspended in dH_2O or TE buffer.

2.2.3 PCR Amplification of DNA fragments

For polymerase chain reactions (PCR) homemade Taq polymerase was used (see Table 2.3 for default conditions). For samples requiring higher proof-reading activity, Q5 High-Fidelity Master Mix 2X (New England Biolabs) was used in accordance with manufacturer's instructions.

Steps	Temperature (°C)	Time
Denature DNA	94	2 min
i) Denature DNA	94	30 sec
ii) Anneal primers	55	30 sec
iii) Extension	68	1 min/kb
Repeat i)-iii) 35X		
Final extension step	68	10 min
End of PCR	10	∞

Table 2.3 PCR default settings for lab Taq polymerase

2.2.4 Primers used in this study

ID	Name	Sequence (5'-3')
SS05	Ptef F	CGGATCCCCGGGTTAATTAA
SS21	Mph1 5UTR F 700	CCTGTTTTGCTTGATGGC
SS23	Mph1 3UTR R 600	ATGTCTGAGTTAATTCGTCCT
SS26	Mph1 5UTR F	AATCTATACGTCCTTGGTGT
SS27	Mph1 3UTR R	TCATGACTTCGATTCACACT
SS30	pAdh21 F	GTGCCTTCGCTTTTCTTTA
SS31	mCherry 53 R	CGCATGAACTCCTTGATGATG
SS32	Lys F	GCTCGTATGTTGTGTGGA
SS33	Lys R	GAAAGCAACCTGACCTACAG
SS34	Spc7 5UTR F	GCATCATCGTAGTCTACCGT

SS35	pAdh21 F2	TTGCCGATGTTACTTGGGGAG
SS43	sol1 5'UTR F	ACGTTTGCGA GATTTAAAGG AA
SS44	sol1 3'UTR R	AATTGTTGCAATGCGTAGAATG
SS45	reg1 Bahler F	ACTTGAAACATCTACGTCCTGGATACAATTGTTGCATTTAGGG AGTTAGCCATCACGAATTGTGTTGGTAATTTGTTTGC – CGGATCCCCGGGTTAATTAA
SS46	reg1 Bahler R	CCATAAATCAGATGTCACATCACTTCAATAAAATAAAAAGCTC CAGATTTGAATAATTATTTTTTGAAGGCATTTCAAAA – GAATTCGAGCTCGTTTAAAC
SS47	reg1 5UTR F	GTACATATCCATTTCCCCCAGA
SS48	reg1 3UTR R	CACTTTTGTAAATAAAGGCCCG
SS51	SPCC18B5.05c 5UTR F	CCCTTCATTAGGGAATGTTGAA
SS52	SPCC18B5.05c 3UTR R	GACACAAAATCATAAACCGCTG
SS55	ppk15 5'UTR F	AAGTGTTTCCCTTTGTTCCAGA
SS56	ppk15 3'UTR R	TTGGCGATTTGTGAATGTCTAC
SS57	psy2 Bahler F	GTCTTCACTTTTGAAAATTTGGTGACGAACGCCAACGTCGTAA ATTCGAAGCTGACGTCTACCCTTAATCCGCCGTAGAA – CGGATCCCCGGGTTAATTAA
SS58	psy2 Bahler R	AAAATACGATGTCCATATGATGATTCACTTGCATTACAATCTTC TAGAGTTTTTGGAGCTTCCCTTTTTATGTTCATCTTGAATTCGA GCTCGTTTAAAC
SS59	psy2 5UTR F	TGCAATCTACGGTATTGCATTC
SS60	psy2 3UTR R	GTCCCTTAATGAACAACCCAAA
SS63	tls1 5UTR F	ACGAAACAATCCTACTCCCTGA
SS64	tls1 3UTR R	TAACGATTCCCAAACAACTCCT
SS67	gyp2 5UTR F	AGTACTCGAACCTCACACCCAT
SS68	gyp2 3UTR R	CATAAGAAAATGGCCCATCAAT

SS71	grh1 5UTR F	AAGAGCGGTGATTGCTTCCA
SS72	grh1 3UTR R	GCAACAGTTTGGCAAGGTTCA
SS75	nup37 5UTR F	GTTACCTGCAACACCATATCAC
SS76	nup37 3UTR R	TCAATTCAAATCGCATATCGG
SS79	SPAC227.17c 5UTR F	CAGCAATGATATGAGCAGAAGG
SS80	SPAC227.17c 3UTR R	CCCCGCCAACTATAAACAATTA
SS83	reg1 Bahler F2	TGCTGTATAGCTATTTATCAAAGCTATAATTATATTGGAAACTTGAAACATCTACGTCCTGGATACAATTGTTGCATTTA – CGGATCCCCGGGTTAATTAA
SS84	reg1 Bahler R2	CCGGCGGAAGTAATACAACATTCAATGCGCTATTTAGAAAACCAAGATAAACTCAACTGCATACAAGTATTAATTTACAT – GAATTCGAGCTCGTTTAAAC
SS89	ppn1 5'UTR	GATGGTGTAGCGAAGGGTTTAG
SS90	ppn1 3'UTR	TTTTTGGCCATCATGTTTGTT
SS93	sds22 5UTR F	ATTAAGCTGCAATTGGGATTGT
SS94	sds22 3UTR R	TATACGCAATTCTTTTCCAGCA
SS97	sds23 5UTR F	AGTTTTACCTTGCTGGGATGAA
SS98	sds23 3UTR R	TCAAGAGGCAAAGTTTCAATCA
SS101	ppe2 5UTR F	ACTAATAATGGTGGAGCAACCG
SS102	ppe2 3UTR R	ATGTTTGAAAACCGAGCATTTT
SS105	glc9 5UTR F	AAGTAGATGTTTGGCCATTGCT
SS106	glc9 3UTR R	GTACAACCAAAGTGAAAAGGGC
SS109	reg1 CDS F	TCAGAACAGGACACCCAACAT
SS110	reg1 CDS R	TCATTATCGTCGGCTCCAGTA
KM65	Reg1 5'UTR F	ATCCCCTTGAAACAACAGTAG
KM66	Reg1 3'UTR R	GTGTACACCAATATGAACGC
KM79	Reg1 5'UTR F1	TGAATTTCAGACTTATCAGTT

KM80	Reg1 3’UTR R1	ACATTAGAAGACGAGTCATTGAG
KM67	Duo1 5’UTR F	TCATGTTATGACTTATTTTAC
KM68	Duo1 3’UTR R	ACTTTCTCATAAGTTTAGGAG
KM69	gcn5 5’utr F	TGCCGAGTTTCCTTAAGTTTT
KM70	gcn5 3’utr R	CATGACTTGTTCTGATAACAT
KM71	eaf6 5’utr F	GATCTCGGAATTCGTTGGTT
KM72	eaf6 3’utr R	CACACGTTACATAAGAGATGC
KM87	Pof9 5’UTR	TTGATTCGTGCAATGACTACACC
KM88	Pof9 3’UTR	TTTTCTCACTTATTTAATCACCG
KM89	Pof9 F1	TTGTGAAAATCCATGCTGGTCG
KM90	Pof9 R1	AGTGAATTTGATGTGGAATGGAAAC
KM91	SPBC17G9.12C 5’UTR	TAACCATACTACTTCTTCTAGCC
KM92	SPBC17G9.12C 3’UTR 1602	TTTACATAGAAGCCAAGAGAGATG
KM77	pFA6 EcoR1 F (Ptef)	CCAGCTGAGAATTCGTACGCTGCA
CPN10	KanR CPN10	GATGTGAGAACTGTATCCTAGCAAG
KM235	BUB3 5’UTR F	TGTCAGAATCAGCTCCTTTGC
KM236	BUB3 3’UTR R	TTATATAAATATGGTCTTGCG
KM237	DIS2 5’UTR F	TTTGTAGAGCAGCAAGATTTAG
KM238	DIS2 3’UTR R	TCCACCGATAGCAAACAGAA
PA30	spc7(1-666) + pac1 site R	ACCATGTTAATTAACCCGGGGATCCGATTCAAAGTTGAAATTGATTTT
PA33	spc7 + nhe1-NLS F	agaattGCTAGCATGCCTAAGAAGAAGCGTAAAGTTATGCCAACATCGCCTCGTCG
PA92	PYL R	GTGAACTCGTCCTGGGTGGCCAT
PA93	adh 724 F	GGGTGGTGGACAGGTGCCTTCG
AS61	ADHterm-FW	CTCTTATTGACCACACCTCTACC

AS62	lys1-Rev	GTGATGTGTCTGGGAAAGGCAGAG
IL017	3' URA4	TCAGCAAAGACTTTCTCA
IL018	5'Ura4	TGAAATACTCTAGCATCC

Table 2.4 List of primers used in this work. Primers with IDs starting SS were constructed for this study. Other primers used were constructed by Karen May (KM), Priya Amin (PA), Ioanna Leontiou (IL), and Alicjia Sochaj (AS).

2.2.5 Plasmids used in this study

Plasmid	Vector backbone	ID/Source
P_{adh21}-spc7$_{1-666}$-mCherry-2×FLAG-PYL (PP1-binding site mutants) (pIY03 vector backbone)	pIY03 vector	This work
Padh41-Mph1$_{303-678}$-3xHA-ABI	pRad41 vector	Amin *et al*, 2019
pLYS1K-Spc7(Δ136-150) 'ΔA'	pLYS1K	Gift from Jonathan Millar
pLYS1K -Ura4-Spc7(Δ331-345) *'ΔB'*	pLYS1K	Gift from Jonathan Millar
pLYS1U-Padh15-NLS-2xFLAG-rtTA-mCherry-Spc71-666-9TE	pLYS1U.	pIY10/ Yuan *et al,* 2016
PLYS1U-Padh15-NLS-2xFlag-rTetR-Spc7$_{(1-666)}$	pLYS1U.	Yuan *et al,* 2016
Pnmt81-2xFlag-rTetR-Mph1$_{303-678}$	pHFF81C vector	Yuan *et al*, 2016

Table 2.5 List of plasmids used in this work.

2.2.6 Restriction endonuclease digestion

Restriction enzymes obtained from New England Biolabs or Roche were used in accordance with the manufacturer's instructions.

2.2.7 Ligation

Ligation reactions were carried out using T4 Quick Ligase (New England Biolabs) in accordance with the manufacturer's instructions.

2.2.8 Bacterial transformations

For transformations, DNA was added to thawed competent *E. coli* cells (DH5α, made in our lab) and gently mixed. The mix was incubated on ice for 30 min, followed by heat-shocking for 45 seconds at 42°C. 400µl of SOC media was added and cells were incubated at 37°C for 1 hour with shaking. Cells were then spun down for 2 min (4000rpm) and 250ml media was removed. The pellet was then resuspended in the remaining volume. 1:10 and 1:4 dilutions were prepared in SOC media for plating onto selective media (kanamycin or ampicillin) at 37°C overnight for selection of transformants.

2.2.9 Sequencing

All sequencing was carried out by Genepool (University of Edinburgh). Samples were prepared using BigDye v3.1 Cycle Sequencing Kit (Applied Biosystems) in accordance with the manufacturer's instructions.

2.3 Protein methods

2.3.1 *S. pombe* protein extracts

10-25ml of cells were grown overnight (30°C, 250 RPM) in the appropriate medium to mid-exponential phase (OD_{600}=0.6) and harvested by spinning down (1701 x *g*, 2 min 30 s) and transferring to a screw-cap tube. Cells were washed with 1ml of ice-cold water before pellets were measured and normalised. 100µl lysis buffer (as in Table 2.6) was added for a cell pellet of 0.03g, along with silica beads. Cells were broken by bead-beating (2x 30 s, with 1 min on ice in between beating cycles) before an equal volume of 2X sample buffer (with 0.2M dithiothreitol) was added. Cells were briefly vortexed and incubated at 95°C for 5 min to denature protein. Cell debris was pelleted by centrifugation (10,621 x *g*, 5 min, 4°C).

Component	Concentration
HEPES pH7.6	50mM
KCl	70mM
$MgCl_2$	1mM
EGTA	1mM
Triton-X-100	0.1%
$NaVO_4$	1mM
Pefabloc	20mM
CLAAPE*	1:2000

Table 2.6 Lysis buffer composition. * CLAAPE is a protease inhibitor mix composed of chymostatin, leupeptin, aprotinin, antipain, pepstatin and E-64, all dissolved in DMSO at a final concentration of 10 mg/ml each.

For analysis of unstable proteins, e.g. Spc7-mCherry-PYL, cells were broken directly into 2X sample buffer, with CLAAPE mix, Pefabloc, DTT and microcystein (1µl) added immediately before use.

2.3.2 Resolving proteins on SDS-PAGE gels

12.5% resolving gels were prepared as outlined in Table 2.7. A layer of butanol-1-ol was added to ensure gel surface was level. Once the gel was set, the alcohol layer was removed and stacking gel (prepared as in Table 2.7) was added. A 1X stock solution of stacking gel without gelling components added was prepared and stored at -4°C. 5ml of this solution was used per (10cm X 20cm) gel and gelling components were added immediately prior to pouring.

Steps	Volume added
HEPES pH7.6	4.7ml
KCl	0.75ml
$MgCl_2$	3.75ml
EGTA	***to 15ml***
Gelling agents: **(added last)**	
APS (ammonium persulfate)	150µl (10%)
TEMED	15µl

Table 2.7 Components of 12.5% acrylamide gel

Proteins were resolved by running on SDS-PAGE gels for 90 min at 120-160V in SDS-PAGE buffer (50 mM Tris, 384 mM glycine, 2% SDS).

2.3.3 Western blotting

Once proteins had been resolved by electrophoresis on SDS-PAGE gels, transfer of protein to nitrocellulose membranes was carried out using a semi-dry transfer unit (Hoefer, TE77) at 150 mA for 1.5-2.5 hours in semi-dry transfer buffer (25mM Tris, 130mM glycine, 20% methanol).

Membranes were blocked in blocking solution (1x PBS, 0.08% Tween 20, 5% w/v dried skimmed milk (Marvel)) for up to 30 min at room temperature before incubation overnight in primary antibody at 4°C. Membranes were then washed 3 times with PBS + 0.08% Tween for 10 min each. Secondary antibody was applied for 1 hour at room temperature. A further 3 washes of PBS + 0.08% Tween were performed to remove unbound antibody.

Proteins were visualised by chemiluminescence using an ECL detection kit (SuperSignal West Pico or SuperSignal West Femto, Pierce) according to the manufacturer's instructions. Membranes were covered with clear acetate and exposed to X-ray film (Agfa Healthcare). Films were developed using a SRX-101A Film Processor (Konica-Minolta).

2.3.4 Antibodies used in this work

Antibody	Species	Concentration	Source
Primary antibodies			
Anti-tubulin (TAT1)	Mouse	1:1000	Gift from Keith Gull
Anti-Mph1	Sheep T	1:1000	Hardwick lab
Anti-FLAG M2	Mouse	1:1000	Sigma-Aldrich
Anti-HA 12CA5	Mouse	1:1000	Kumiko/Earnshaw lab
Anti-Spc7	Sheep	1:1000	Hardwick lab
Anti-GFP	Sheep	1:1000	Hardwick lab
Secondary antibodies (all HRP-conjugated)			
Anti-sheep	Donkey	1:5000	Jackson Immuno-Research
Anti-mouse	Donkey	1:5000	GE Healthcare
Anti-rabbit	Sheep	1:5000	GE Healthcare

Table 2.8 List of antibodies used in this work

2.4 Microscopy

Fluorescence microscopy was performed using a Zeiss Axiovert 200M inverted epi-fluorescent microscope (Carl Zeiss Ltd.) equipped with a 100x 1.49 N.A. objective lens and a CoolSnap CCD camera (Photometrics). Slidebook v5.5 software (Intelligent Imaging Innovations Inc.) was used to acquire and analyse images. Acquisition settings were as follows: 300ms exposure (FITC & TRITC), 2x binning, Z-series over 3µm range in 0.5µm steps (7 planes).

Fixed samples for microscopy were prepared by centrifuging 1.5ml of culture for 1 min at 6000 rpm. Cell pellets were fixed in 200–500µl of 100% ice-cold methanol. To image cells, 8µl of the cell suspension was added to a glass slide. Once the methanol had evaporated, 2 µl DAPI (0.4µg/ml) was added to the sample and a glass cover slip was placed on top. Cells were imaged immediately as described above. Typical exposure setting for imaging DAPI was 100ms.

2.5 Checkpoint assays and checkpoint silencing assays

2.5.1. Synthetic checkpoint arrest assay (SynCheck, rTetR system)

To induce a synthetic arrest in strains containing Mph1 kinase fragments driven by the *nmt81* promoter, exponentially growing cells were obtained by growth in liquid PMG medium (with thiamine) at 30°C with shaking for 6-8 hours to load cells with thiamine. Cells were harvested (1701 x *g*, 2 min 30 s) and washed twice with 50ml PMG and split into two PMG cultures, one with thiamine added and one without. aTC was added to both cultures and cells were grown at 30°C with shaking for 6-20 hours, with samples taken for microscopy at regular intervals. Cells were imaged immediately.

2.5.2. Serial dilution growth assays

Strains were pre-grown on PMG plates (with and without thiamine) for 24 hours. Serial tenfold dilutions of cells were prepared in PMG media without thiamine (1, 1/10 and 1/1000 dilutions) in a 96-well plate. A pinning device was used to transfer cells to phloxin-containing plates (with and without thiamine added). Plates were usually incubated at 30°C

(except when using temperature sensitive strains). Plates were photographed and scanned 24 and 48 hours after plating.

For phloxin B serial dilution growth assays, plates were made by adding phloxin B to PMG agar at a concentration of 10mg/L. Amino acid supplements were also added. Plates were made with and without thiamine.

Strains were examined for defects in spindle checkpoint by plating to benomyl-containing media. Benomyl was added to boiling YES agar at concentrations ranging from 0-10 μg/ml. Plates were used within 2 days of pouring, to avoid degradation of the drug over time.

2.5.3. *nda3-KM311* block-and-release checkpoint silencing assays

Cells were spindle checkpoint arrested by depolymerising microtubules using cold-sensitive *nda3-KM311* mutants (Hiraoka *et al*, 1984). Log-phase cultures were shifted to 18°C for 6 hours, until 80-90% of cells were checkpoint arrested. Cultures were shifted back to 25°C and samples were taken every ten minutes to monitor rates of mitotic exit. Samples were fixed in ice-cold methanol. Microscopy was performed to visualise levels of cyclin B (Cdc13-GFP).

2.5.4. Assays with an abscisic acid based synthetic checkpoint, SynCheckABA

cdc25-22 synchronisation

Cells were grown on YES plates at 25°C for 1-2 days. These were pre-cultured in liquid YES (10ml) with added amino acid supplements for 6-8 hours, before inoculating over-night cultures. The next day, log-phase cultures were shifted to the non-permissive temperature of 36°C and incubated for 3.5 hours to block cells in G2. Cultures were shifted back to 25°C after this, to release them from G2.

Induction of synthetic arrest by ABA addition

After synchronising cells in G2, cultures were released and after 5 minutes ABA was added (Sigma Aldrich A1049, final concentration 250μM). DMSO was added to control cultures at the same volume.

ABA wash-out and SynCheckABA silencing assays

Cells were incubated with ABA for 60 mins to induce a synthetic checkpoint arrest. Following induction of SynCheckABA arrest, cells were washed three times with 50ml YES to remove ABA. 1.5ml samples of cultures were taken immediately after wash-out and at various timepoints after release (e.g. 30 minute intervals, for up to 2 hours). Samples were immediately preserved in ice-cold methanol and stored at -20°C.

2.6 SynCheck Genetic Screen of Bioneer deletion collection

Construction of PEM-2 SynCheck strain

PCR was used to amplify rTetR-Mph1 (*leu1:Pnmt81-rTetR-mph1*$_{(303-678)}$) and rTetR-Spc7 (*lys1::Padh15-rTetR-mCherry- spc7*$_{1-666}$*-9TE:ura4*) cassettes from plasmids. These constructs were transformed by electroporation into a PEM-2 genetic background (Roguev *et al*, 2007). Transformants were identified based on ura and leu auxotrophic markers and were confirmed by PCR/immunoblotting.

Genetic crosses (for screen)

3004 G418-resistant single-deletion haploid strains were obtained from the Bioneer v2.1 library (Kim *et al*, 2010a). Genetic crosses were performed according to the usual PEM-2 protocol (Roguev *et al*, 2007, 2018). The PEM-2 SynCheck strain (SS29: *leu1:Pnmt81-rTetR-mph1*$_{(303-678)}$, *lys1::Padh15-rTetR-mCherry-spc7*$_{1-666}$*-9TE:ura4, PEM-2*) was used as a query strain which was crossed with the Bioneer v2.1 library (using a Singer ROTOR robot).

Library strains were thawed, replica plated to YES media and incubated at 30°C for 2-3 days. Strains were then condensed from a 96-strain to a 384-strain array format using a Singer RoTor robot.

In the meantime, the PEM-2 SynCheck query strain was grown in a lawn on YES plates (with additional thiamine). Once strains were sufficiently grown, the isolates from the library were mated with the SynCheck query strain by pinning strains on to SPA agar plates together. Each cross was performed in quadruplicate, so the array was pinned in 1536-strain format.

After sporulation, the PEM-2 background allowed for selection against parental strains, diploids and h+ haploid cells on the basis of cycloheximide sensitivity. Desired progeny were selected for based on G418 resistance and auxotrophic markers. Cycloheximide concentration in screen selection plates was 250µg/ml, and G418 was used at a final concentration of 200µg/mL G418.

Plates with and without thiamine (+Th/-Th) added were used as control and test plates respectively, to determine the effects of inducing rTetR-Mph1 expression/SynCheck

activation in these strains. These plates contained phloxin B, a dye which stains dead cells pink.

Images of plates were acquired on a flatbed scanner at 24-hours, 48-hours, and 1-week post-plating. Plates were scored for strain growth and colour by eye.

Quantification of high-throughput screen results

To more rigorously quantify strain phenotypes, software was used to measure colony size and normalise values. By automating analysis, we hoped to achieve rapid, quantitative and unbiased scoring of screen phenotypes. SGAtools/gitter was selected for this purpose (Wagih & Parts, 2014; Wagih *et al*, 2013). SGAtools successfully recognised the array layout in all plates, unlike some other software tested, e.g. Spotsizer (Bischof *et al*, 2017). This software corrects for some factors which may affect growth, e.g. differences in growth conditions between plates and between strains plated in different positions on the same plate.

To quantify the screen, scanned images were uploaded to SGAtools website. These plates were cropped to size and rotated, but not subjected to any other processing. To obtain scores for the -Th condition, the experimental strains were compared with parental control strains (Bioneer library strains). Colony areas were normalised by SGAtools for each plate (Baryshnikova *et al*, 2010; Wagih *et al*, 2013). The software then computed scores and p-values for each strain based on the four replicates tested. The same process was repeated for +Th plates. Finally, the +Th score was subtracted from the score for the -Th condition to give an adjusted score which represents the effect of inducing SynCheck signalling on phenotypes.

Strains were ranked based on this adjusted score. Large negative values indicate a strong synthetic sickness phenotype. A threshold value of -0.2 (or +0.2 for strains with a synthetic positive interaction) was applied to data.

Results from the analysis with SGAtools can be found in Appendix 1.6.

2.7 SynCheckABA yeast strain construction

2.7.1 PP1-binding mutant strain construction

Padh21-Spc7$_{1-666}$-mCherry-2×FLAG-PYL (PP1-binding site mutants)

Plasmids containing full-length Spc7 PP1-binding mutants (ΔA, deletion of residues 136–150; ΔAB, deletion of residues 136-150 and residues 331– 345) (provided by the Millar laboratory, University of Warwick) were used as PCR templates to amplify mutant versions of Spc7$_{1-666}$. NheI-NLS and PacI restriction sites were introduced during amplification, allowing Spc7 constructs to be digested and ligated into digested pIY03-derived vector backbone, which also contained a C-terminal mCherry-2×FLAG-PYL tag (pLYS1U-Padh21-NLS-Spc7$_{1-666}$-mCherry-2XFLAG-PYL, see Amin *et al*, 2019). These constructs were amplified by PCR and transformed into fission yeast strains which contained *adh41-mph1-3xHA-ABI*, *atb2-RFP* and *cdc25-22*. Efforts were also made to generate a strain with just the B motif deleted, but no transformants were obtained.

CHAPTER 3

A High-throughput Genetic Screen to Identify Novel Spindle Assembly Checkpoint Silencing Factors

3.1 Introduction

The overall aim of this project is to better understand the spindle assembly checkpoint (SAC), with a specific focus on how the SAC is silenced. The SAC plays an important, highly conserved role in genomic stability. Mechanisms of SAC activation and silencing are worthy of detailed investigation. Studies of the SAC have identified therapeutic targets for cancer treatment (Section 1.5.1). Insights gained from SAC silencing studies in *S. pombe* may make valuable contributions to the understanding of this fundamental cell cycle process and of cell signalling mechanisms in general.

This chapter recounts our efforts to identify novel SAC silencing factors. Our rationale in taking this approach is that the discovery and characterisation of novel SAC silencing factors will suggest possible mechanisms of action which can be investigated further. As we have seen in the Introduction (Section 1.4), several independent SAC silencing mechanisms have been identified in vertebrates to date, including dynein-mediated stripping of checkpoint proteins from microtubule-attached kinetochores, and $p31^{comet}$-mediated inhibition of Mad2. The existence of multiple redundant mechanisms indicates that there may be additional undiscovered pathways at work in silencing the spindle checkpoint. The possibility of identifying SAC silencing components which operate independently of known pathways is an argument in favour of using a high-throughput screening strategy.

Additionally, a wide-scale screen may provide useful information on known SAC silencing mechanisms. Many of the pathways that have been identified to date are not well-characterised, so a genetic screen may identify important components of these pathways. For example, protein phosphatase PP1 Dis2 has been found to play a highly conserved role in SAC silencing, and has a particularly strong effect in *S. pombe* (Pinsky *et al*, 2009; Vanoosthuyse *et al*, 2009a). Despite its established importance for SAC silencing, key targets and regulators of this pathway have yet to be determined.

3.1.1. Overview of screening strategy

We conducted a high-throughput genetic screen to identify novel SAC silencing factors. Specifically, we set out to screen the Bioneer single-gene deletion haploid library (v2.1) of *S. pombe*. To sensitise strains to the effect of mutations which disrupt SAC silencing we used a synthetic checkpoint system, SynCheck (Yuan *et al*, 2016). This system allows us to induce a checkpoint-mediated arrest by promoting interactions between SAC proteins independently of their localisation to unattached kinetochores. This system is both inducible and ectopic, which offers several advantages for our purposes (Section 1.7).

A Singer RoTor robot was used to mate the synthetic checkpoint (SynCheck) query strain with strains from the Bioneer haploid library of 3004 single-gene null mutants (Kim *et al*, 2010a). The synthetic checkpoint was induced, and strains were spotted out in quadruplicate on agar plates containing phloxin B dye. Data analysis was carried out to determine which gene deletions cause reduced fitness upon checkpoint induction.

Genetic screens

High-throughput genetic screens are a powerful tool for identifying genes involved in a biological process (Section 1.6). In designing a screen, it may be useful to sensitise strains to the effects of defects in a process, so that the observed phenotype is more obvious. This can be achieved by using a background strain with a mild defect in the process under investigation and crossing it with mutant strains. If a second mutation exacerbates the phenotype of the original 'query' strain, this indicates that it is involved in the same process. Phenotypes due to such genetic interactions are known as 'synthetic' interactions.

For this screen, increasing the sensitivity of strains to checkpoint silencing defects is likely to be particularly important. This is because multiple redundant pathways may be involved, each with minor effects on silencing efficiency. For the query strain used, we aimed to generate a mutant with a stronger spindle checkpoint, and ideally one which was inducible. Query strains which are inducible/conditional mutants are often particularly useful in genetic screens. Having a query strain which grows normally under uninduced conditions makes it easier to work with and allows for direct comparison of the mutant phenotype alone and in combination with the defect induced by the query mutation, helping to rule out secondary effects of the genetic background of the query strain.

A previous high-throughput screen involving inducible Mph1 overexpression

Previous efforts by our lab to identify spindle checkpoint silencing mutants included a high-throughput screen which employed a query strain with inducible Mph1 overexpression. An Mph1 cassette was inserted which was under the control of an inducible *nmt81* promoter (no message in thiamine) (Basi *et al*, 1993; Maundrell, 1993). Thiamine represses expression from this promoter, and so removal of thiamine from media resulted in overexpression of Mph1 (approx. 6-fold), followed by a metaphase delay mediated by spindle checkpoint proteins. This slight delay did not have a significant impact on cell fitness in isolation, but when combined with mutants which were impaired in checkpoint silencing cells experienced more profound metaphase delays (visible as reduced colony sizes) and increased levels of cell death. However, there were concerns that this approach generated a high level of false positives. This was because Mph1 has pleiotropic functions, including chromosome biorientation, which increases the likelihood that its overexpression would have off-target effects.

Another complication of this screening strategy was that the overexpressed Mph1 could localise to kinetochores, and potentially exacerbate the effect of mutations which caused defects in microtubule-kinetochore attachment. Increased activation of the SAC by these mutants could result in a synthetically sick phenotype when Mph1 was overexpressed, resulting in false positive results from the screen. This concern was particularly relevant in relation to the several kinetochore proteins which were identified in the Mph1 overexpression screen (e.g. Dam1/DASH complex subunits Duo1, Spc19).

To address these issues, we opted to use a synthetic version of the spindle checkpoint that has recently been developed in our lab as our query strain (Yuan *et al*, 2016) (Section 1.7).

SynCheck

The SynCheck system was designed on the principle that promoting interactions between upstream effectors of the spindle checkpoint (Mph1 kinase and outer kinetochore protein Spc7) is sufficient to generate a checkpoint-mediated metaphase arrest. Constructs of Mph1 and Spc7 with their kinetochore localisation domains removed were generated. The tetracycline transcriptional activation system was used to achieve co-localisation of these protein fragments. rTetR-Spc7 was constitutively expressed, whereas rTetR-Mph1$_{\Delta 1\text{-}302}$ was

expressed from a *nmt81* promoter, so expression could be induced by removal of thiamine from media. Addition of anhydrotetracycline to media allowed rTetR-Mph1 and rTetR-mCherry-Spc7 constructs to co-localise to *tetO* sequences which had been introduced to a chromosome arm. Heterodimerisation of these proteins generated a checkpoint-mediated metaphase arrest (see Appendix 2; Yuan *et al*, 2016).

3.1.2. Characterisation of SynCheck

In preparation for carrying out the high-throughput screen, additional characterisation of the SynCheck system was needed. Firstly, the effect of the *tetO* array on the strength of the arrest was examined. It was found that varying the size of the array (from 0-112 *tetO* repeats) has only a minor effect on the efficiency of the arrest (work by P. Amin). In collaboration with I. Leontiou, I confirmed that the kinetics of the arrest are similar with and without the tetO.

Secondly, work was carried out in our lab which confirmed that the rTetR domains of the Spc7-9TE and Mph1 fusion proteins are still required for the arrest, although addition of anhydrotetracycline is not necessary. Surprisingly, simply expressing fusion proteins of Spc7 and Mph1 with rTetR domains allowed them to form heterodimers. This activated checkpoint signalling away from the kinetochore (Figure 3.1A). It was also demonstrated that this arrest did not require endogenous Mph1 and could operate independently of endogenous checkpoint activation. Dependency of the arrest on various downstream checkpoint components was tested (Figure 3.1B). Synthetic checkpoint signalling was demonstrated to generate a Mad1-Bub1 complex (Yuan *et al*, 2016). Details of the work described above have been published (Yuan *et al*, 2016, see Appendix 2).

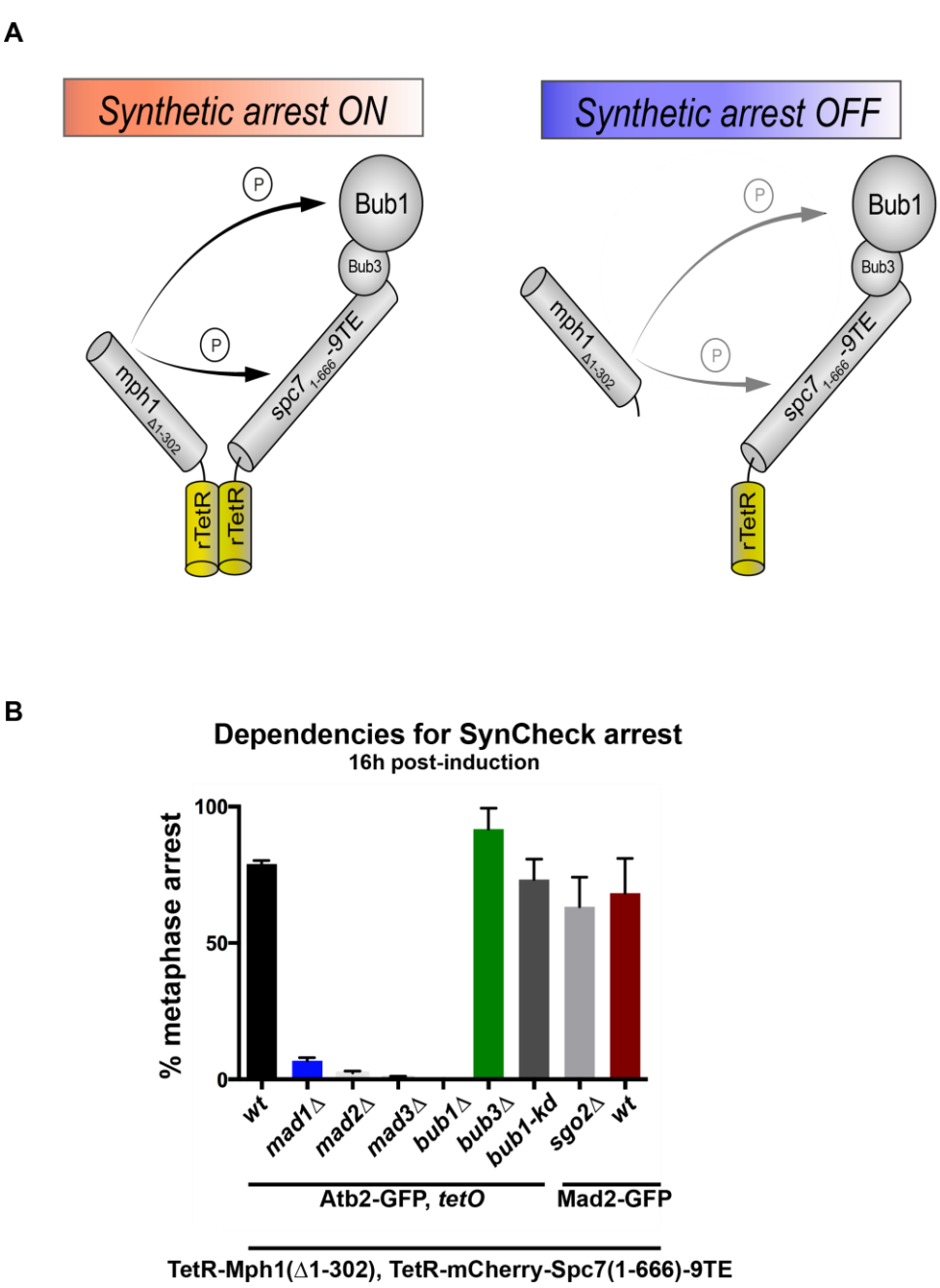

Figure 3.1 Characterisation of SynCheck. (A) Revised model of SynCheck action. It was found that tethering checkpoint proteins to the chromosome arm was unnecessary, and that the rTetR fusion proteins simply need to be co-expressed to dimerise and induce checkpoint signalling. Signalling was confirmed to occur only when both Spc7 and Mph1 protein constructs contained an rTetR domain, and heterodimerisation was shown to be required for checkpoint activity. (B) SynCheck arrest is dependent on Mad1, Mad2, Mad3 and Bub1, but independent of Bub3, Bub1 kinase activity (kd = kinase dead mutant) and Sgo2. SynCheck-mediated metaphase arrest was induced in these cells by washing out thiamine, allowing expression of rTetR-Mph1 from its *nmt81* promoter. Percentages of cells arrested in metaphase at 16h post-induction (approximate time for peak numbers of cells in metaphase in wild-type control) are shown here for each strain. Experiments were repeated (at least) three times. More than 100 cells were analysed per strain. Data is

plotted as mean ± s.d. All strains contain a fluorescent marker to allow metaphase arrested cells to be identified by microscopy (Atb2-GFP in the majority of strains shown, which allows short metaphase spindles to be visualised; the exception is the *sgo2Δ* strain which was had been constructed in a different genetic background (Mad2-GFP, which localises to spindle pole bodies during metaphase), which was compared with a wild-type SynCheck control which also contained Mad2-GFP.

3.1.3. Chapter Aims

The aims of this chapter are as follows:

i) Establish whether SynCheck could be successfully used to test for checkpoint silencing defects (Section 3.2)

ii) Describe the design and execution of a high-throughput screen for SAC silencing mutants (Sections 3.3 and 3.4)

iii) Analyse the results obtained from this screen, and present a list of candidate genes involved in SAC silencing (Section 3.4)

3.2 SynCheck as a system for testing SAC silencing function

For the purposes of this genetic screen, it was necessary to confirm that the SynCheck strain did indeed exhibit synthetic sickness phenotypes when combined with mutations which cause defects in spindle checkpoint silencing.

It had previously been noted that SynCheck strain survival was severely reduced after induction of a synthetic arrest in liquid cultures (Ivan Yuan and Ioanna Leontiou, data not shown). When cells were grown in liquid cultures without thiamine to induce a SynCheck arrest (checkpoint arrest peaks at 16h after thiamine wash-out; cells were grown for 14-20h in these experiments) and subsequently plated to thiamine-containing media in attempt to 'rescue' arrested cells, many cells were unable to recover and went through few or no cell divisions before dying. Such a severe phenotype would prohibit us from conducting a screen with SynCheck, because if the query strain itself was severely sick or lethal upon checkpoint induction, it could not be used for identifying synthetic phenotypes when combined with a checkpoint silencing mutant. We hoped that inducing the checkpoint on solid media would have a less severe impact on cell fitness, possibly due to solid media providing more spatial cues to guide cell division, e.g. gradients of nutrients in media.

To confirm that the SynCheck system was suitable for identifying candidate checkpoint silencing mutations a small-scale pilot screen was performed. We aimed to compare strain fitness between conditions where the spindle checkpoint is induced and not induced, thus specifically looking at the effect of the gene deletion on checkpoint silencing. We planned to do this by plating strains on to solid media with thiamine (+Th) and without thiamine (-Th) and comparing the effects on cell growth for four independent replicates. This experiment was also designed to check that the proposed methods for assessing strain fitness in the high-throughput screen were suitable for detecting such phenotypes.

To increase the sensitivity of the screen, strains were grown on plates containing phloxin B. Phloxin B is a vital dye which specifically stains dead cells red. This is because the dye is excluded by intact membranes of healthy cells. Cells might go through a few rounds of cell division before thiamine is depleted from cells and the synthetic spindle checkpoint is induced, or until the effects of subtle defects in spindle checkpoint silencing become apparent. As such, measuring colony size alone might not reveal silencing defects. Phloxin B has been used in yeast studies as a vital dye for some time (Kucsera *et al*, 2000; Tange &

Niwa, 1995), and has been recently demonstrated to be useful for increasing the sensitivity of high-throughput yeast screens for synthetically sick phenotypes (Lie *et al*, 2018).

Apc15 encodes a small subunit of the APC and *apc15Δ* cells exhibit defects in checkpoint activation, so both SynCheck *apc15Δ* and the wild-type strains were used as negative controls for defects due to checkpoint silencing. Known checkpoint silencing defective mutant, *bub3Δ,* was used as a positive control, and was expected to have a synthetically sick phenotype. It would be informative to see how other confirmed checkpoint silencing mutations behave in combination with the synthetic checkpoint strain, to assess whether a synthetically sick phenotype is observed for all SAC silencing mutants, or just a subset. $PP1^{Dis2}$ plays a conserved role in chromosome segregation (Pinsky *et al*, 2009; Espeut *et al*, 2012; Liu *et al*, 2010; Nijenhuis *et al*, 2014) and has been shown to have a relatively strong effect on checkpoint silencing in *S. pombe* (Vanoosthuyse & Hardwick, 2009; Meadows *et al*, 2011), so it is reasonable to expect that *dis2Δ* cells would be noticeably synthetically sick in the presence of an induced synthetic checkpoint arrest. However, attempts to obtain a SynCheck *dis2Δ* strain by both mating crosses and transformation ran into difficulties due to a strong synthetically sick phenotype (Chapter 5).

We also aimed to test a subset of candidates from the previous Mph1 overexpression screen. These included DASH complex subunits Spc19 and Duo1, Gcn5 (the SAGA complex histone acetyltransferase catalytic subunit), Eaf6 (NuA4 histone acetyltransferase complex subunit), Pof9 (an F-box protein), and Mop1 (a conserved fungal protein). Most of these candidates had been verified using independent silencing assays, e.g. recovery from checkpoint arrest after *nda3-KM311* block and release (K. May, unpublished data; see Section 4.5.2 for a description of *nda3-KM311* assay). Some of these candidates did not have a phenotype in *nda3-KM311* assays but had a particularly strong phenotype in the screen, e.g. *gcn5Δ.* It is possible that these deletions affect checkpoint silencing in a microtubule-dependent manner. Candidate strains were constructed by transforming the synthetic checkpoint strain with deletion constructs. These strains were confirmed to have similar protein expression levels of rTetR-Mph1 by western analysis (Appendix 1.3).

Serial dilution growth assays were performed with these strains (Section 2.5.2). As can be seen in Figure 3.2, SynCheck strains grew on both +Th and -Th plates, although there were more dead cells on -Th plates. However, there were clear phenotypic differences between SynCheck alone and in combination with the *bub3Δ* mutation. Deletion of *bub3* resulted in

a much more severe growth defect on -Th plates, along with a dark red colour, indicating many dead cells.

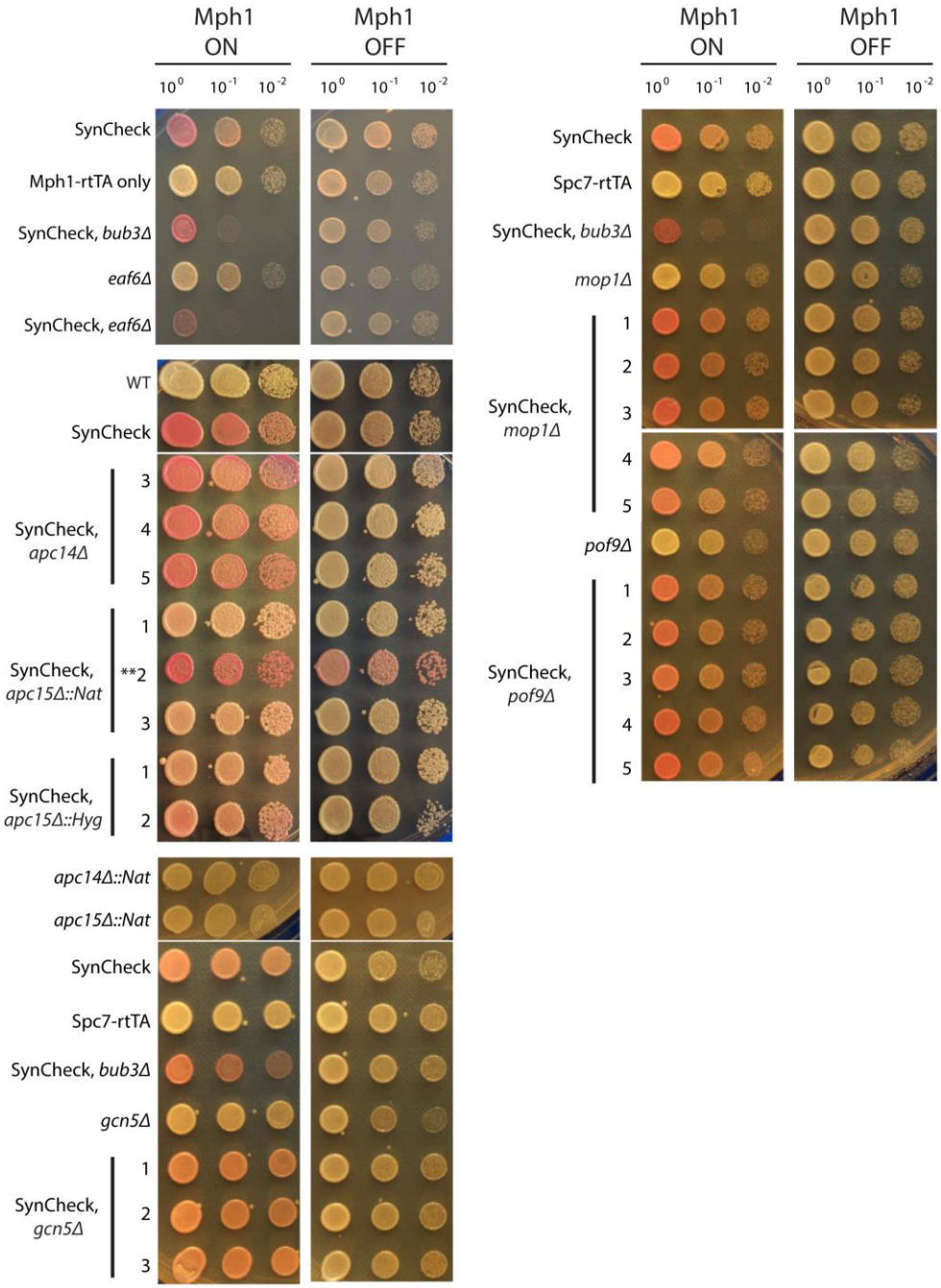

Figure 3.2. Serial dilution growth assays to assess checkpoint silencing defects. Growth assays were performed to assess suitability of plating cells to +/-Th media containing phloxin B dye as a method for detecting phenotypes of SAC silencing mutants in a SynCheck arrest. Phloxin B dye is taken up by dead cells and causes sick colonies to be pink. Growth assays show 10-fold serial dilutions of strains indicated. All strains grow well on +Thiamine plates, where rTetR-Mph1 is not expressed. Upon induction of the synthetic checkpoint by plating on -Thiamine media, SynCheck alone is slightly sick, as can be seen by pale pink colour indicating sick/dead cells. More severe phenotypes are seen when

SynCheck is combined with deletion of known checkpoint silencing factor Bub3. Eaf6 is a candidate checkpoint silencing mutant identified in a previous screen in our lab, and *eaf6Δ* is also synthetically sick in combination with SynCheck arrest. Other candidates from the Mph1 overexpression screen were also tested but did not have a phenotype in this assay.

Deletion of checkpoint silencing factor Bub3 caused a synthetically sick phenotype in this assay. Differences in cell viability between *bub3Δ* and wild-type strains were noticeable for strains pre-grown on –Th plates and transferred to +/–Th phloxin plates. Strains grown on +Th plates but transferred to –Th were less sick, but differences in viability were still noticeable between strains. For cells that were maintained on +Th plates, all strains were viable and no phenotypic differences could be observed between strains.

Of the six candidate SAC silencing-defective mutations tested in this assay, only *eaf6Δ* appeared to be synthetically sick. As expected, *apc15Δ* was found to rescue the SynCheck strain from the mild reduction in viability it exhibits on -Th plates. Its phenotype resembled strains which lack synthetic checkpoint activity (e.g. strains which lack rTetR-Mph1, and express rTetR-Spc7 alone). This is further evidence that the viability defects seen for the synthetic checkpoint strain are checkpoint-dependent, and not due to other effects of removing thiamine from growth media.

These results indicate that the synthetic checkpoint strain is sufficiently viable to be used for a genetic screen. Phloxin B growth assays were demonstrated to be sensitive enough to detect differences in viability between the checkpoint strain alone and in combination with mutants which disrupt checkpoint silencing. It may be possible to adjust the strength of the effect of synthetic checkpoint induction on cell viability by pre-plating on either +/-Th before transferring to -Th plates.

3.3 Designing a high-throughput genetic screen

The results above indicate that the SynCheck strain is suitable for sensitising cells to the effect of checkpoint silencing mutations in our screen. The synthetically sick phenotypes generated could be observed in phloxin B growth assays. This confirmed the suitability of our proposed experimental design for a large-scale screen.

For this screen, we used the Bioneer haploid single-gene deletion library (v2.1). This collection contains 3004 deletion strains, approximately 84% of *S. pombe* non-essential

genes (Kim *et al*, 2010a; Pan *et al*, 2012). These genes are replaced by a G418-resistance cassette (*kanMX4/kanR*), which facilitates selection for the deletion genotype in crosses.

Several checkpoint silencing factors identified to date, including Bub3 and Dis2, are non-essential in *S. pombe*. Despite this limitation, the Bioneer library is a convenient resource which allows us to examine a large portion of the *S. pombe* genome.

3.3.1 Generating Query strain in a PEM-2 genetic background

In the process of our screen, haploid strains containing a single gene deletion (i.e. Bioneer library strains) were crossed with strains containing the SynCheck components (rTetR-Spc7, rTetR-Mph1). After mating and sporulation have occurred, each of the desired components can then be selected for by using unique selectable markers (leu and ura auxotrophy for rTetR-Mph1 and rTetR-Spc7 constructs respectively; G418 resistance for deletions from the Bioneer library).

Apart from selecting for these desired components, it was necessary to efficiently select against any other cells which were present, including heterozygous diploid cells. It was also important to prevent re-mating by selecting for a single mating type. To achieve these ends a PEM-2 genetic background was utilised in our query strain.

The PEM-2 system allows for the rapid generation of double mutants. It utilises a recessive allele which confers resistance to cycloheximide, to allow selection against parental cells and diploids (Figure 3.3; also see Roguev *et al*, 2007). This system also ensures mating type selection (to prevent re-mating) by inserting an additional copy of the dominant wild-type cycloheximide-sensitive (*cycS*) allele in close proximity to one of the mating type alleles (*h-*). This ensures that only h+ progeny may exhibit cycloheximide resistance, if they contain the cycloheximide resistance (*cycR*) allele at the endogenous location.

To obtain this query strain the components of the synthetic checkpoint arrest were transformed into a PEM-2 background by electroporation. rTetR-Mph1 expression levels were analysed by western blotting to confirm that these were similar to the original SynCheck strain (Appendix 1.2). Serial dilution growth assays were performed to confirm the optimum concentration of cycloheximide prior to carrying out the screen (Appendix 1.3).

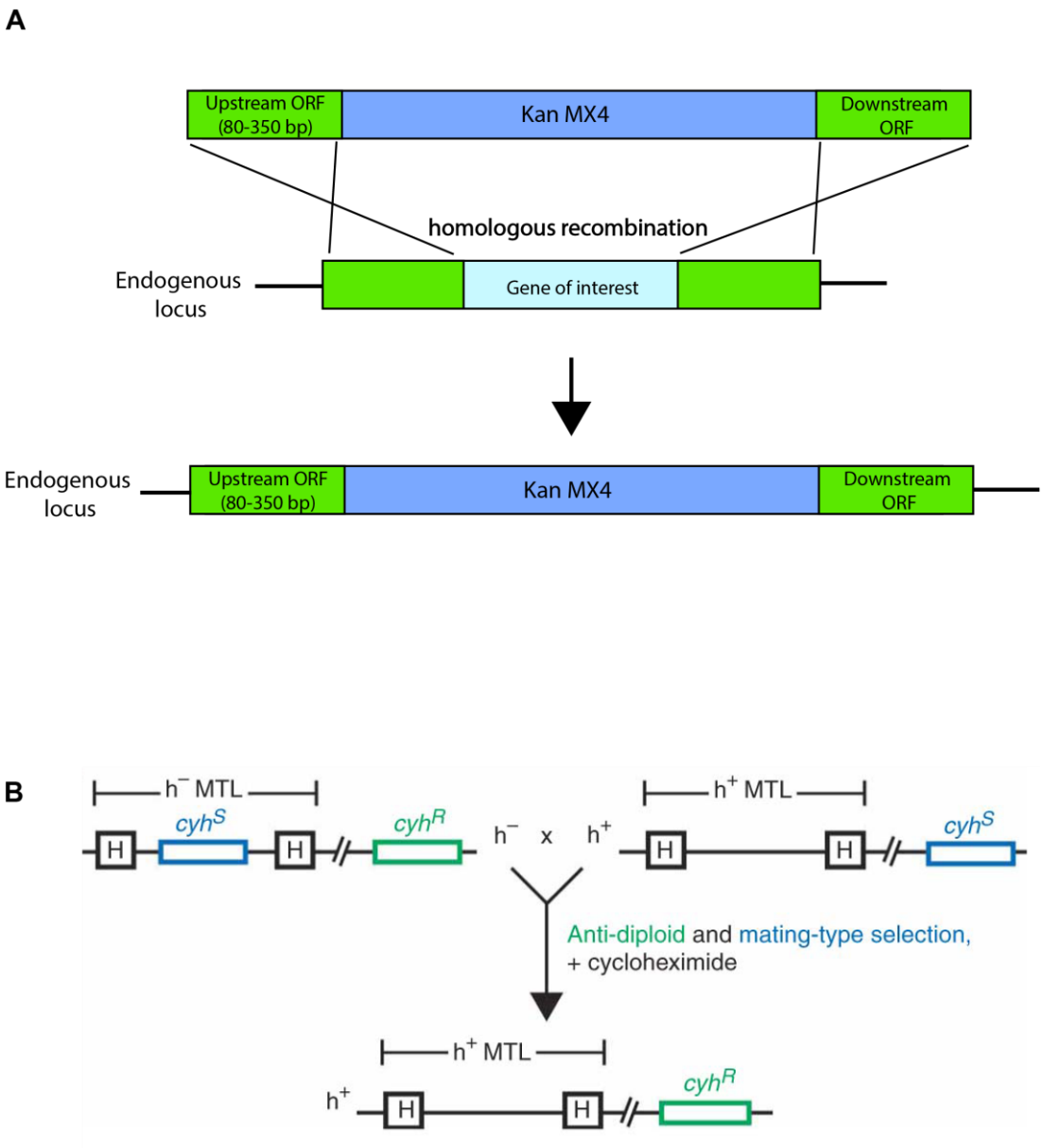

Figure 3.3 Features of high-throughput screen design. (A) Gene deletion cassette containing the *kanMX4* gene flanked by regions of homology to the gene of interest. The cassette replaced the open reading frame (ORF) of the gene of interest by homologous recombination. (B) PEM-2 is a strategy for high-throughput double mutant strain construction. A dominant cycloheximide sensitive (*cyhS*) allele is expressed from within the mating type locus (MTL; i.e. *mat,* indicated by boxes labelled 'H' in figure) of *h-* cells while a recessive resistance allele (*cyhR*) is expressed from the endogenous locus, resulting in a cycloheximide sensitive phenotype. After meiosis, the only cells able to survive on media containing cycloheximide are haploids of the opposite mating type (*h+*) which retain the *cycR* allele at the endogenous locus. PEM-2 diagram from Roguev *et al*, 2007.

3.3.2 Pilot screen

Before proceeding to the full high-throughput screen, a pilot experiment was conducted on a single test plate from the library (365 strains) to confirm that everything was working optimally. The workflow of the screen is described in detail in Chapter 2 (Section 2.6).

This test plate consisted of four 96-strain plates from the Bioneer library which were condensed into a 365-strain array (strain list in Appendix 1.4.1). These plates were chosen based on inclusion of various strains of interest. These included positive controls, e.g. known checkpoint silencing mutant *bub3Δ*, and a candidate from the Mph1 overexpression screen performed in our lab, *eaf6Δ.* This plate also included negative controls in the form of strains deficient in spindle checkpoint activation, i.e. *mph1Δ*, *mad1Δ* and *apc15Δ* strains. Control strains *bub3Δ* and *eaf6Δ* both displayed a synthetically sick phenotype, as they had in the smaller scale experiment. Other candidates identified from this pilot screen are summarised in Figure 3.4B. Some strains produced larger, paler colonies on -Th plates, appearing to be healthier in combination with rTetR-Mph1 expression.

A

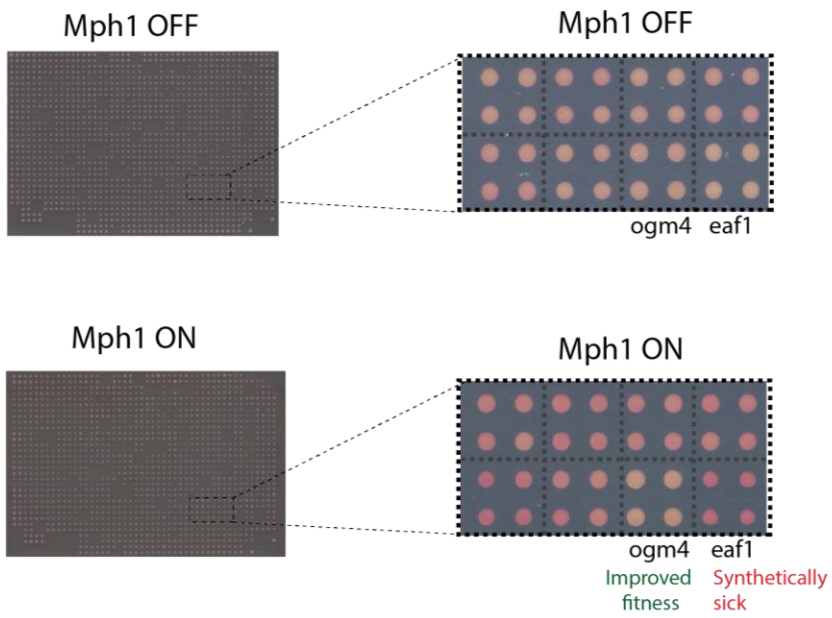

B

Synthetically sick upon checkpoint induction	
bub3	mitotic spindle checkpoint protein
SPBC16H5.08c	ribosome biogenesis ATPase, Arb family
vps71	chromatin remodeling complex subunit (Swr1 complex)
ell1	RNA polymerase II transcription elongation factor SpELL
eaf1	RNA polymerase II transcription elongation factor SpEAF (ELL associated factor)
psl1	cyclin pho85 family
SPBC21C3.08c	ornithine aminotransferase

Figure 3.4 Pilot screen for SAC silencing factors (A) Sample of phenotypic readouts from screen. 1536-array plates are shown on the left. On the right, a close-up of 8 adjacent strains illustrates the different phenotypes which can be observed. Phloxin B is taken up by dead cells and causes sick colonies to be pink. Most strains are a pale pink colour when SynCheck has not been induced (i.e. on thiamine-containing plates). On plates without thiamine, synthetically sick genetic interactions can be observed, e.g. *eaf1Δ* shows reduced growth and darker pink colour. Some deletions appear to improve cell fitness, e.g. *ogm4Δ*. Strains are plated in quadruplicate. (B) Table of hits from pilot screen (scored by eye for colony size and colour).

3.4 High-throughput genetic screen

The high-throughput screen was carried out in a similar manner to the pilot screen described above. After crossing the library with the SynCheck query strain and selecting for desired progeny, strains were pre-plated to +/-Th plates for 2 days before re-plating to +/-Th plates containing phloxin B dye. Images were acquired on a flatbed scanner at 24, 36 and 48 hours post-plating.

Synthetically sick strains were identified by manual analysis of screen phenotypes. Each replicate was scored for colony size and intensity of red colour. Efforts were made to avoid bias due to plate position (for example, strains in outer rows may grow better due to decreased competition for nutrients) by carefully comparing strains with near neighbours. Results were compared between -Th plates and +Th control plates, as well between parental Bioneer deletion strains and double mutants. This helped to rule out secondary effects not specifically due to synthetic checkpoint induction, as well as controlling for single mutant phenotypes.

For all observed hits, semi-quantitative scores were given for each attribute (0 = no phenotype, 1 = mild, 2 = strong), and strains were ranked based on severity of phenotypes. Preference was given to strains where both low growth and phloxin red phenotypes were observed.

3.4.1 Results of high-throughput screen

Thirty gene deletions were identified as having reduced fitness in the SynCheck background when the checkpoint was induced (Table 3.1 and Appendix 1.5). Eight of these were selected for further verification on the basis of strength of phenotype, as will be discussed in more detail in Chapter 4.

The screen successfully detected a synthetically sick phenotype for positive control, *bub3Δ*. No spindle checkpoint gene deletions (e.g. *mad2*) were synthetically sick, as expected. Some gene deletions rescued the mild reduced viability phenotype of SynCheck on -Th plates.

Many SAC components were first discovered by the sensitivity of gene deletions to benomyl, a microtubule-depolymerising drug. It is possible that checkpoint silencing factors may also be detected by altered sensitivity to benomyl. There are nine strains annotated in

Pombase as benomyl resistant. It is possible that if SAC silencing is mildly impaired or delayed, cells will have more time to correct KT-MT attachment errors caused by spindle poisons, potentially resulting in increased viability. The results of the high-throughput screen were examined to see if any of these gene deletions were also synthetically sick in a SynCheck arrest, as taken together both phenotypes could support further study of these factors. Unfortunately, none of these gene deletions were present in the Bioneer library. This illustrates one of the limitations of this screen; there are several non-essential genes which are either not included in the Bioneer v2.1 collection, or which were not able to be successfully revived from freezer stocks. Only 2918 of the 3004 Bioneer strains were successfully revived and analysed in this screen. The PombeNet website has records of several problem or missing strains in the Bioneer collection (http://www-bcf.usc.edu/~forsburg/Bioneer.html). One notable omission is *dis2*Δ, which would have been a valuable positive control strain, as a known SAC silencing factor with a strong effect.

It was investigated whether any of the previously reported problems with the Bioneer library affected strains identified as candidates in this screen. No problems were found to have been recorded for any of these strains.

3.4.2 Verification of candidates

Further verification of candidates identified from the high-throughput screen was carried out. Serial dilution growth assays were performed on strains isolated from mating crosses performed as part of the high-throughput screen. The purpose of this analysis was to confirm the observed phenotype by repeating the same experiment (comparing growth and viability of cells between +/-Th media, in the presence of phloxin B dye). This experiment was designed to give a general indication of the reproducibility of phenotypes observed in the large-scale screen and to verify individual factors tested. Repeating the experiment in the serial dilution growth assay format removed the variable of position effects which may have influenced growth on the high-throughput screening plates. This approach yielded more easily observable phenotypes due to the larger format and was also cheaper and quicker to carry out than repeats of the high-throughput screen.

Strains were grown on PMG +Th plates at 30°C for two days before resuspending cells in liquid PMG media, serially diluting tenfold and re-plating to +/-Th plates containing phloxin

B dye. For all strains tested, parental deletion strains were used as a negative control. Between two and four isolates were tested for each strain.

Gene ID	Gene name	Gene function	Verified by growth assay	Parental strain phenotype
SPAC14C4.11	vtc2	polyphosphate synthetase	Yes	
SPCC1223.02	nmt1/thi3	no message in thiamine Nmt1	Yes	Strongly reduced viability on -Th
SPCC18B5.05c		phosphomethylpyrimidine kinase	Yes (strong)	Slightly reduced viability on -Th
SPAC227.15	reg1	protein phosphatase regulatory subunit Reg1	Yes	
SPBC30B4.04c	sol1	SWI/SNF complex subunit Sol1	Yes (strong)	
SPAC4F10.18	nup37	WD repeat protein, human NUP37 family	Yes (strong)	
SPAC926.03	rlc1	myosin II regulatory light chain	Yes	
SPAC589.02c	med13	mediator complex subunit Srb9	Yes	
SPBC3B8.02	php5	CCAAT-binding factor complex subunit Php5	Inconclusive	
SPAPJ696.01c	vps17	retromer complex subunit Vps17	Inconclusive	
SPCC1672.04c	cox 19	mitochondrial copper ion transport protein	Yes	
SPBC691.04	mss116	mitochondrial ATP-dependent RNA helicase	Yes (strong)	
SPBC216.01c	psy2	DNA damage response protein	Yes	
SPCC1259.11c	gyp2	GTPase activating protein Gyp2	Inconclusive	Strongly reduced viability -Th
SPAC1D4.01	tls1	sequence orphan	Yes (strong)	
SPAC1B3.16c	vht1	vitamin H transporter Vth1	No	
SPBC29A10.06c		conserved fungal protein	Inconclusive	
SPAC23H3.08c	bub3	mitotic spindle checkpoint protein Bub3	Yes	
SPAC823.03	ppk15	serine/threonine protein kinase Ppk15	Yes	
SPAC1D4.02c	grh1	human GRASP protein homolog	No	
SPAC227.17c		conserved protein (fungal and plant)	Yes (strong)	
SPBC3E7.16c	leu3	2-isopropylmalate synthase	Inconclusive	
SPCC777.08c	bit61	HbrB family protein	Yes	
SPBC11B10.05c	rsp1	random septum position protein Rsp1	Inconclusive	
SPBP8B7.18c		phosphomethylpyrimidine kinase	Yes	Slightly reduced growth on –Th

Figure 3.5 Summary of candidates from high-throughput screen. Selected hits from high-throughput screen of Bioneer library v2.1 are shown, along with results from when these strains were retested in growth assays (serial dilution assay; Figure 3.6). Any unusual phenotypes of parental strains in the high-throughput screen control plates are noted.

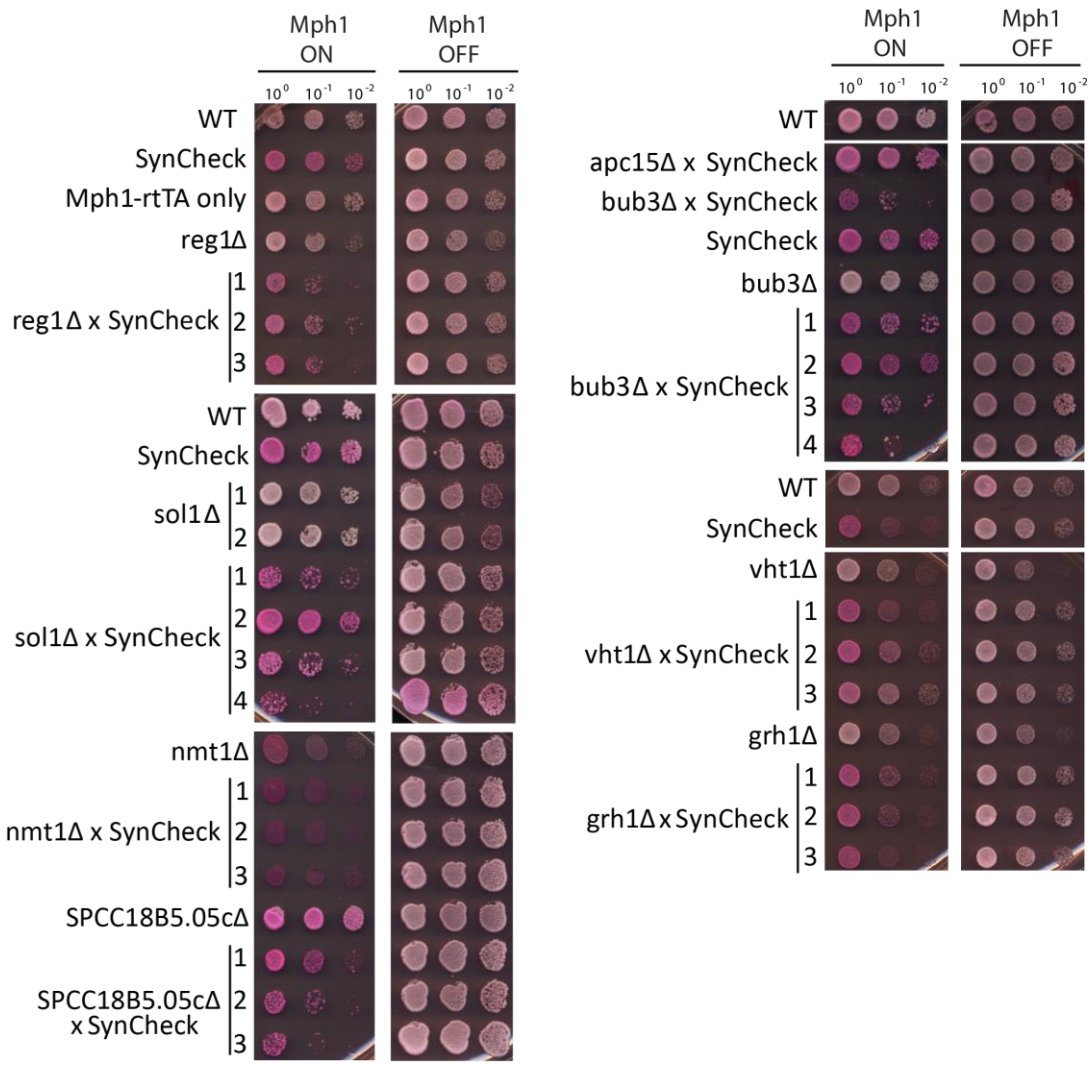

Figure 3.6 Verification of selected candidates from high-throughput screen. Candidates from the high-throughput screen were re-tested to confirm phenotype. Multiple isolates of each deletion strain were generated during the high-throughput screening process. These isolates were stored and retested in serial dilution growth assays to confirm their phenotype. Strains were grown on PMG +Thiamine plates for two days before resuspending cells in liquid PMG media, serially diluting tenfold, and re-plating to + and -Thiamine plates containing phloxin B dye.

Overall, most of the strains tested had a reproducible synthetically sick phenotype in the high-throughput screen and serial dilution growth assay experiments. Positive control *bub3Δ* exhibited a synthetically sick phenotype when grown on -Th. Figure 3.5 reports whether a synthetically sick phenotype was observed in serial dilution growth assays for each candidate strain tested. Particularly strong phenotypes were noted, to help identify which candidates are the most promising for further characterisation, i.e. *bub3Δ, sol1Δ,*

SPCC18B5.05cΔ, mss116Δ, nup37Δ, SPBP8B7.18cΔ and *bit61Δ*. These strains also had a strong phenotype in the high-throughput screen, with the exception of *bit61Δ,* which had a mild phenotype in the screen but a more pronounced phenotype in this assay.

Several of the factors retested did not have a detectable phenotype. These were mostly strains which were only noted as having a weak phenotype in the screen. It is possible that these irreproducible phenotypes were false positives in the screen. It is also possible that some of strains did have checkpoint silencing defects, but the effects were very minor.

For some strains, it was noted that upon checkpoint induction a few pale, large colonies grew against a background of very sick cells. This effect could be caused by contamination with wild-type cells, however another possible explanation is that these cells were accumulating checkpoint suppressor mutations. These cells were not directly tested to confirm this, but it is possible that they could be losing expression of the synthetic checkpoint components or accumulating mutations in downstream components of the spindle checkpoint machinery. Alternative silencing pathways could also be upregulated.

Some of the parental control strains were noted to also have a phenotype when grown on -Th plates. These were *nmt1Δ*, *SPCC18B5.05cΔ* and *SPBP8B7.18cΔ*. These are all known to be involved in thiamine biosynthesis.

Serial dilution growth assays were also performed to compare candidates identified and isolated from the pilot screen to the same strain in the high-throughput screen. Although many of the hits identified in the pilot screen were not identified by manual analysis of the full screen, retesting isolates side-by-side showed that at least in some instances, these phenotypes were reproduced by strains from the high-throughput screen. This perhaps illustrates the limitations of the sensitivity of this method of screening. This could potentially be overcome by carrying out more repeats of the full-scale experiment. Some of the pilot screen isolates also no longer displayed a phenotype in these growth assays. This lack of reproducibility may indicate that these were false positive results. However, some of these strains did show a phenotype in growth assays performed immediately after the pilot assay, so it may be possible that checkpoint suppressor mutations were accumulated before making freezer stocks.

Ideally, we would also repeat the full-scale screen several times to further verify candidates and to identify additional hits.

3.4.3 GO term analysis

Gene ontology (GO) term analysis was carried out on this list of candidates, using the Bioneer library as a reference (edited for missing strains). We used the Generic Gene Ontology Term Mapper to bin the genes into GO terms and GO Term Finder (https://go.princeton.edu/cgi-bin/GOTermFinder) to check for enrichment. Unfortunately, no processes were found to be significantly enriched in our data, except for those involving thiamine biosynthesis. This enrichment (10% vs 0.2%, P-values <0.006) is most likely due to the experimental design of growing cells on plates lacking thiamine to induce rTetR-Mph1 expression, rather than a functional link between this pathway and spindle checkpoint silencing.

Several of the candidates identified are involved in gene expression. Med13, Php5, Rps2302 and Sol1 are involved in gene transcription, Tls1 is a splicing factor and Mss116 is a predicted ATP-dependent RNA helicase thought to be involved in mitochondrial gene transcription. Although these candidates may have an indirect effect on checkpoint silencing via their effects on gene expression, it is also possible that they play a more direct role in silencing.

Several candidates have genetic interactions which are consistent with a role in SAC silencing. *grh1* and *SPCC18B5.05c* have reported genetic interactions with *mph1*, while *sol1* and *tls1* have interactions with *apc10*, which encodes a component of the APC. *tls1* is reported to have a negative genetic interaction with *klp6*, a known checkpoint silencing factor in *S. pombe* (Ryan *et al*, 2012; Meadows *et al*, 2011).

Several mitochondrial factors were identified as SAC silencing candidates, including Cox19 (predicted), SPBC28E12.04, Yta4/Msp1 (predicted), Leu3 and Mss116. These were not selected for further analysis in this work but may be worthy of investigation in future studies. In particular, *mss116* deletion had a strong phenotype, and has also been reported to display a synthetic growth defect in combination with *dis2Δ* (Buttrick *et al*, 2011). There is evidence to support a link between mitochondria and cell cycle progression (Esposito *et al*, 2011).

To illustrate general properties of the shortlisted candidates, analysis was performed using PomBase's QuiLT (Quick Little Tool) (Figure 3.7). QuiLT provides a graph where one horizontal line corresponds to one gene, across all categories. For ease of interpretation, I sorted genes by each category and combined the results into one figure, so horizontal lines

in this analysis do not represent a single gene. This analysis showed that just under half of these genes are relatively uncharacterised and have either inferred or unknown functions.

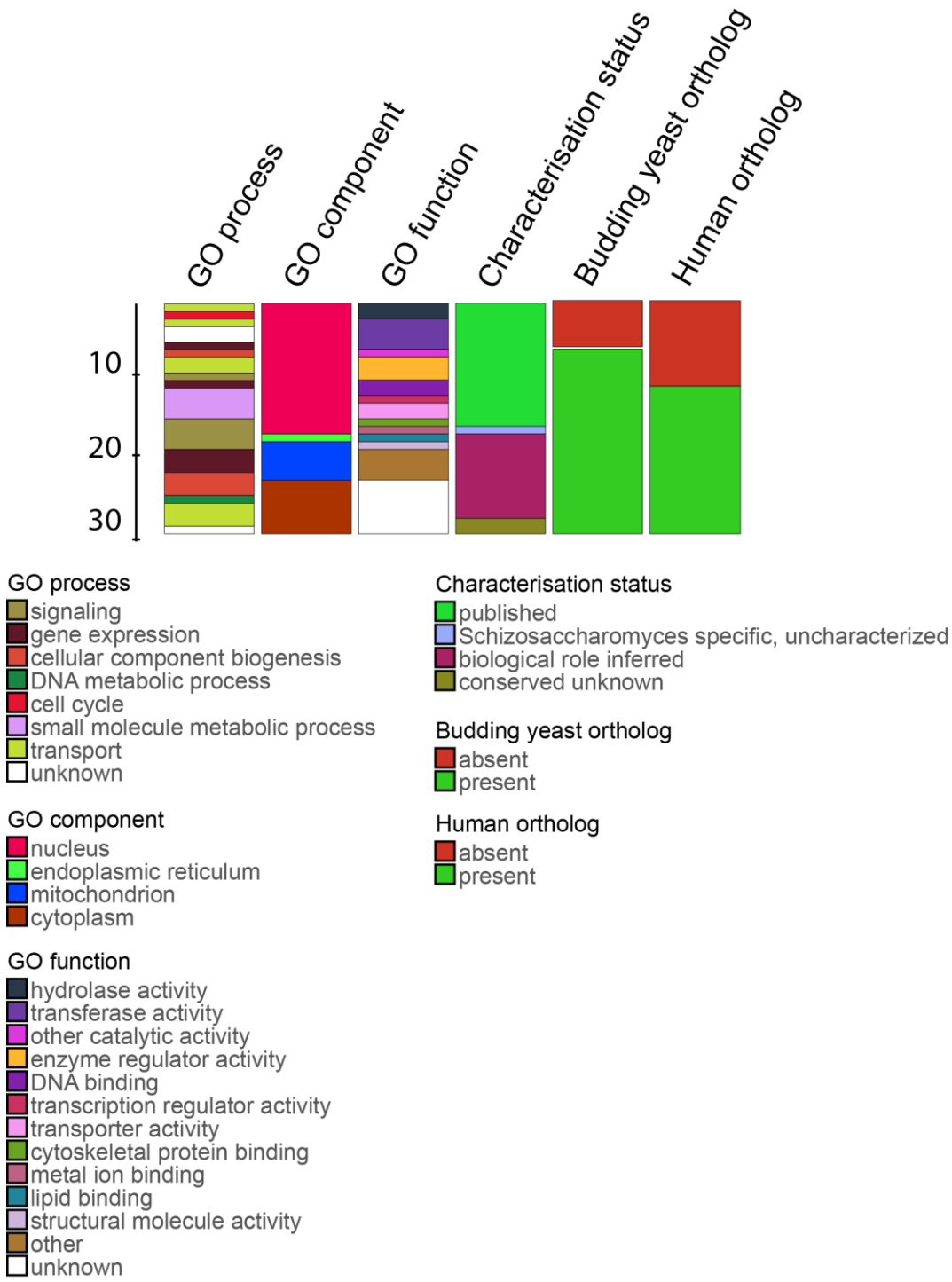

Figure 3.7 Analysis of GO term annotations and orthologs of SAC silencing candidates identified in the high-throughput screen. Analyses were performed using the Quick Little Tool (QuiLT) resource by PomBase. Figure adapted from graphics generated by QuiLT.

The next chapter of this thesis focuses on the verification of a subset of the factors identified by manual analysis of the high-throughput screen. There are additional control experiments which could be informative to carry out in the high-throughput SynCheck system, which are discussed in Section 3.4.6. However, due to time constraints and limitations of the SynCheck genetic background (e.g. leaky expression of rTetR-Mph1 from the *nmt81* promoter), we decided to shift our attention to verifying a subset of these factors. This verification involved assays in independent checkpoint silencing assays.

3.4.4 Quantification

To more rigorously quantify strain phenotypes, software (SGAtools/gitter; Wagih & Parts, 2014; Wagih *et al*, 2013) was used to measure colony size and normalise values (Section 2.6).

Analysis was initially performed for one plate from the screen and it was noted that several of the manually identified strains were identified as having a relatively strong effect (Figure 3.8). Of the eight strains identified by manual analysis of these plates, two were not scored by the software (*rsp1Δ, SPAC1D4.01Δ*), four were confirmed by the software to be amongst the top ten strains with the biggest reduction in growth on -Th *(vht1Δ, grh1Δ, SPCC18B5.05cΔ* and *mss116Δ*; range between -0.42 and -0.18). The two remaining strains, *SPBC29A10.06cΔ* and *vps17Δ*, both have reduced growth on -Th, however this is a weaker effect (scores are -0.068 and -0.058 respectively; this puts them at position #59 and #66 in list of strains with most reduced growth from this plate). It should be noted that when scored manually, these two strains were both identified as candidates based on red colour, and only *SPBC29A10.06cΔ* was noted to have a mild reduction in growth on -Th.

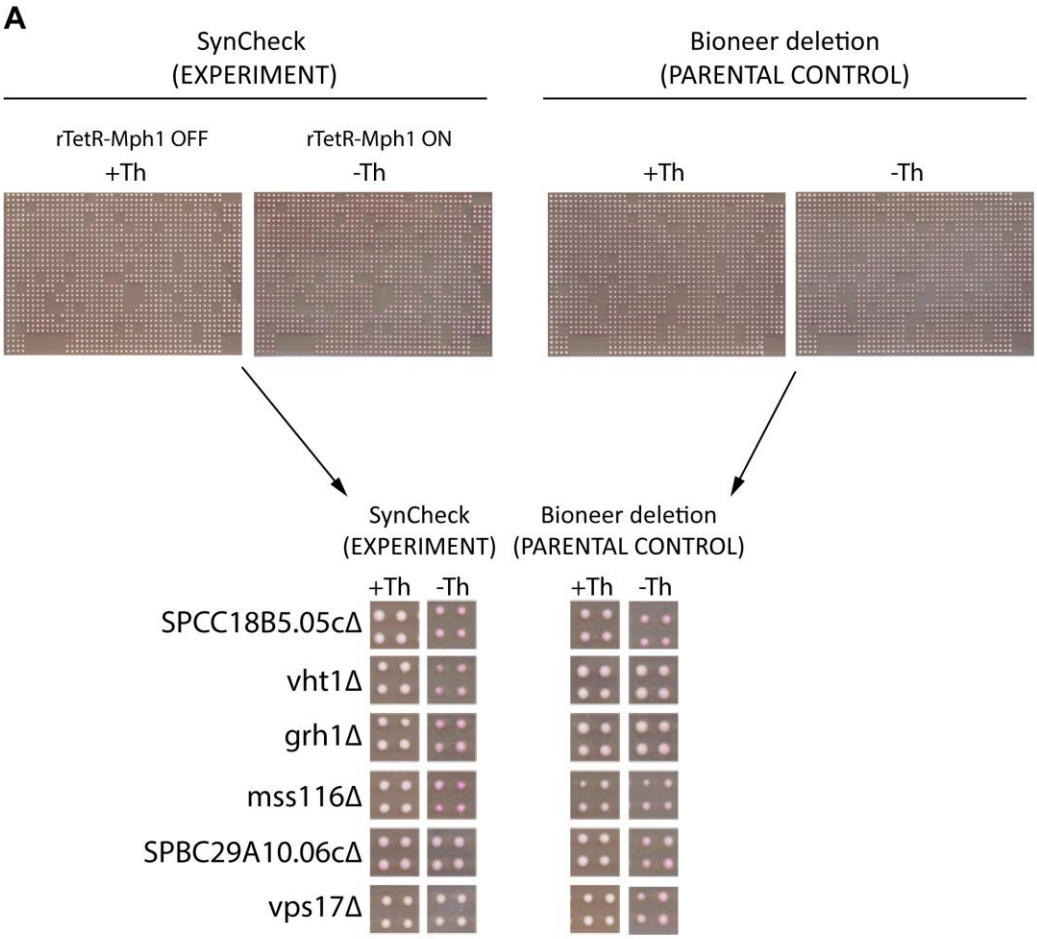

B

Gene ID	Gene name	Normalised colony size				SCORE
		+Th, EXPERIMENT	-Th, EXPERIMENT	+Th, CONTROL	-Th, CONTROL	
SPCC18B5.05c	-	1.08785	0.79996	1.0219	0.93675	**-0.20587**
SPAC1B3.16c	vht1	0.96053	0.62507	0.88287	0.94847	**-0.42149**
SPAC1D4.02c	grh1	0.92194	0.82984	1.10048	1.25502	**-0.24048**
SPBC691.04	mss116	0.97833	0.75155	0.79521	0.74419	**-0.18876**
SPBC29A10.06c	-	0.88406	0.82567	1.23431	1.24197	**-0.06826**
SPAPJ696.01c	vps17	0.68905	0.56942	0.83962	0.77323	**-0.0576**

Figure 3.8 Quantitative analysis of high-throughput screen plates with SGAtools. (A) Plates from high-throughput screen, with enlarged images of strains identified as candidates by eye. (B) Quantitative results for the indicated strains using SGAtools. Score is the difference in the normalised colony size values for the experimental strain between -thiamine and +thiamine conditions, minus the difference in these values for the parental strains.

This approach was extended to the rest of the high-throughput screen plates (data in Appendix 1.6). A rigorous cut-off of -0.2 was applied, strains with p-values <0.05 are shown.

This resulted in a list of 134 hits out of the 2518 library strains analysed. Note that some strains were not analysed due to gaps in the library. Other strains are missing from final screening plates due to failure to transfer all strains correctly using the Singer RoTor robot. Not all strains were successfully scored by the software, which was usually due to missing isolates.

GO term analysis was performed on the strongest candidates (as described in Section 3.4.3). For this analysis we used a gene list consisting of the thresholded table of hits produced by SGAtools and the strongest hits manually identified by colour (11 additional strains). Unfortunately, no terms were found to be significantly enriched in this data.

Efforts were made to quantify colour of strains in a similar manner, however difficulties with software have prevented this for the time being. Some of these software platforms, e.g. Colonyzer (Lawless et al, 2010), are difficult to run for those without programming experience. Even after enlisting help from experienced programmers, there were technical difficulties with Colonyzer. Consultations with Dr. Julian Mak led to the development of a MATLAB programme with some of the desired capabilities, particularly the ability to measure the intensity of red colour. However, this programme still requires further testing and optimisation.

3.4.5 Synthetic rescue phenotypes identified in screen

In this screen, we also identified strains which had phenotypes indicative of increased viability (i.e. paler colony colour due to reduced uptake of phloxin dye, indicating fewer dead cells, and/or increased colony area) when thiamine was removed from media to induce a SynCheck arrest. Gene deletions which improve viability could have this effect by increasing efficiency of checkpoint silencing (e.g. by deletion of a negative regulator of SAC) or by impairing checkpoint activation.

Although these strains are not the focus of the present study, they may be interesting candidates for future work on the spindle checkpoint, and as such we have listed the strongest 'rescue' phenotypes (Table 3.1). Quantitative analysis with SGAtools was performed using a threshold of +0.2 or above, i.e. at least at 20% increase in normalised colony size between +Th and -Th conditions, resulting in a list of 181 strains (Appendix 1.6.2).

GO term analysis was performed for strains with improved viability upon SynCheck induction. The candidate list for this analysis consisted of 37 strains identified manually (Table 3.1), along with the list produced by quantitative analysis. This strain list was not significantly enriched for any process or function GO terms.

Some candidates were identified by both manual analysis and quantitative analysis, including *swd3*, *SPAC4A8.06c* (which encodes a predicted esterase/lipase), *tal1* (which encodes a predicted transaldolase) and *set3* (histone lysine methyltransferase). Candidates with strong colour phenotypes include *dep1* and *snt1*, both of which encode components associated with the Rpd3L histone deacetylase complex (Shevchenko et al, 2008), and *clr5*, which is also involved in chromatin organisation (Hansen et al, 2011).

Gene ID (Δ)	Gene name	Gene function	Paler	Larger	Verified by quantification
SPBC354.03	*swd3*	WD repeat protein Swd3	2	2	Yes
SPBC29A3.21		sequence orphan	2	2	Not scored
SPAC19D5.03	*cid1*	poly(A) polymerase Cid1	2	2	Yes
SPAC4A8.06c		esterase/lipase	2	1	Yes
SPBC21C3.02c	*dep1*	Sds3-like family	2	1	Not scored
SPAC22E12.19	*snt1*	histone deacetylase complex subunit	2	1	Not scored
SPCC550.07	*fah1*	acetamidase	2	1	Not scored
SPAC1565.01		conserved fungal protein	2	1	Not scored
SPAC15A10.10	*mde6*	Muskelin homolog	2	1	Yes
SPCC1020.06c	*tal1*	transaldolase	2	0	Yes
SPAC1250.03	*ubc14*	ubiquitin conjugating enzyme Ubc14	1	2	Not scored
SPAC29B12.08	*clr5*	Clr5	1	1	No
SPAC22E12.04	*ccs1*	metallochaperone Ccs1	1	1	No
SPAC343.20		sequence orphan	1	1	No
SPAC22E12.11c	*set3*	histone lysine methyltransferase Set3	1	0	Yes
SPBC32H8.07	*git5, gpb1*	heterotrimeric G protein beta subunit Git5	1	0	No
SPAC23H3.13c	*gpa2, git8*	heterotrimeric G protein alpha-2 subunit Gpa2	1	0	No
SPAC3A11.02	*cps3, mug188, scp3*	zinc finger protein Cps3	1	0	No
SPAC4H3.02c	*swc3*	Swr1 complex subunit Swc3	1	0	Yes
SPAC18G6.13		sequence orphan	1	0	No
SPBC1703.03c	*syo2*	armadillo repeat protein, nucleocytoplasmic transport	1	0	No
SPCC1753.02c	*git3*	G-protein coupled receptor Git3	1	0	No
SPAC13A11.03	*mcp7, mnd1, mug32*	meiosis specific coiled-coil protein Mcp7	0	2	Yes
SPAC23D3.11	*ayr1*	1-acyldihydroxyacetone phosphate reductase	0	2	Not scored
SPBC16G5.13	*ptf2*	Mst2 histone acetytransferase acytyltransferase complex subunit	0	2	Not scored
SPBC725.15	*ura5*	orotate phosphoribosyltransferase Ura5	0	2	No

SPCC24B10.18		human Leydig cell tumor 10 kDa protein homolog	0	2	Yes
SPAC823.10c		mitochondrial carrier with solute carrier repeats	0	2	Yes
SPBC13E7.04	*atp16*	F1-ATPase delta subunit	0	2	Yes
SPBC1773.17c		hydroxyacid dehydrogenase	0	1	No
SPBC21C3.20c	*git1*	C2 domain protein Git1	0	1	No
SPBC887.11	*pus2*	tRNA pseudouridylate synthase Pus2	0	1	No
SPAC10F6.11c	*atg17*	kinase activator	0	1	No
SPCC736.09c	*tfx1*	TRAX	0	1	No
SPAC2C4.05		cornichon family protein	0	1	No
SPCC24B10.09	*rps1702*	40S ribosomal protein S17	0	1	Yes
SPBC21C3.11	*ubx4*	UBX domain protein Ubx4	0	1	Yes

Table 3.1 Gene deletions which displayed synthetic rescue phenotypes in a SynCheck background. Upon removal of thiamine from media, these strains exhibited phenotypes which indicated improved growth (i.e. increased colony area) and reduced cell death (reduced uptake of phloxin dye, resulting in paler colour) relative to other strains. The strength of each phenotype was ranked on a scale from 0-2 (0 = no observable phenotype, 1 = observable phenotype, 2 = strong phenotype, i.e. very pale or very large colonies). Results for each of these strains from quantitative analysis of colony areas using SGAtools software is indicated.

It was noted that some of the gene deletions which 'rescued' cell growth in the quantified list were in fact synthetically sick when scored by eye, including *sol1Δ* and *gyp2Δ*. This is because phloxin B uptake by dying cells was not considered in the automated analysis. This illustrates the benefits of using phloxin B to increase the sensitivity of the screen.

When GO term analysis was performed on candidates identified by manual analysis only, two clusters of genes had enriched processes; one cluster of 5 proteins was involved in cellular response to oxygen-containing compounds, and another cluster of 4 proteins was involved in response to carbohydrates (including carbohydrate homeostasis, sugar-mediated signalling pathways) and G-protein coupled receptor signalling. The only enriched component was Rpd3L-expanded complex, which is part of the chromatin remodelling machinery (p-values >0.01).

As with the synthetically sick strains, the first step in studying these candidates should be to confirm whether these phenotypes are reproducible and if they are due to effects on SynCheck activity or silencing. The same assays described in this chapter and the independent checkpoint silencing assays described in Chapter 4 are likely to be similarly useful for characterising these strains. It will be necessary to shortlist candidates of interest to focus on for these assays.

For example, *swd3* could be an interesting candidate for further study. *swd3Δ* was associated with one of the strongest improved viability phenotypes upon SynCheck activation. Swd3 is part of the Set1-COMPASS complex, a histone methyltransferase which targets histone H3 lysine 4 (H3K4) residues (Roguev *et al*, 2003). This complex plays an important role in transcription regulation and *swd3Δ* might indirectly affect SAC activity by altering the expression of checkpoint proteins (Beilharz *et al*, 2017). However, the Set1-COMPASS might play a more direct role in regulating SAC activity by methylating proteins involved in the checkpoint. Set1 complexes have previously been shown to methylate non-histone targets in other organisms, such as *S. cerevisiae*, where Set1 is required for methylation of DAM/DASH component Dam1 (Zhang *et al*, 2005). It would be interesting to test if Dam1 and/or other mitotic proteins are targeted by Set1 in *S. pombe*.

Six other genes which encode components of the Set1-COMPASS complex (*ash2*, *set1*, *shg1*, *spf1*, *swd1*, *swd2*) were also screened (Roguev *et al*, 2003). None of these were observed to have phenotypic effects when analysed by eye, but upon quantification with SGAtools, *swd2Δ* and *shg1Δ* were associated with increases in relative colony areas following SynCheck activation (increased growth of +0.19 and +0.15 respectively, slightly

under the threshold of +0.2). However, deletion of *set1*, which encodes the catalytic component of this complex, did not have much effect on cell viability.

3.4.6 Controls for high-throughput screen

Chapter 4 discusses experiments which were carried out to verify a subset of hits identified in the full-scale screen. Although the results of this give an indication of the reliability of this screen and verify the individual factors in question, it would be useful to carry out controls on the high-throughput platform.

A single plate (384 strains) from the Bioneer library was crossed with a query strain which contained rTetR-Mph1 alone, without the rTetR-Spc7 construct. The effects of inducing rTetR-Mph1 expression were tested by following the same protocol used for the high-throughput screen with the original query strain. This experiment aimed to test whether phenotypes observed in the screen were due to off-target effects of rTetR-Mph1 expression. Although the rTetR-Mph1 construct lacks a kinetochore localisation domain and is thus unlikely to contribute to the generation of endogenous SAC signal, it may affect non-checkpoint functions of Mph1.

Unfortunately, the screen plate which was selected for this smaller scale experiment did not contain many of the deletion mutations which exhibited strong synthetically sick phenotypes in the full SynCheck screen, limiting the conclusions we can draw from comparison of the two data sets. Four deletion mutants tested in this experiment were identified as synthetically sick by quantitative analysis of colony area in the SynCheck screen (*bit61Δ, ubi5Δ, SPAC806.04cΔ* and *mug165Δ*). Of these, only *bit61Δ* was still synthetically sick when rTetR-Mph1 was expressed in the absence of rTetR-Spc7. This indicates that although some candidates may be false positives due to pleiotropic effects of Mph1, the SynCheck screen identified strains which are sick due to SynCheck activity. Future work on candidate mutants identified from the screen should include control experiments using this rTetR-Mph1 strain to test whether rTetR-Mph1 expression alone is sufficient to produce synthetically sick (and synthetic rescue) phenotypes.

3.5 Conclusions

1) SynCheck-based genetic screen

In this chapter, it was demonstrated that the SynCheck system is suitable for detecting checkpoint silencing mutants. Previously identified checkpoint silencing mutant *bub3Δ* exhibited synthetic sickness phenotypes in both serial dilution growth assays and in the high-throughput screen plating format. Phloxin B was particularly useful in identifying these synthetically sick phenotypes.

As discussed (Section 3.1.1), an alternative high-throughput screen for SAC silencing factors was previously conducted in this lab. This earlier screen aimed to sensitise strains to the effects of SAC silencing defects by inducing overexpression of endogenous Mph1. The results obtained from these two screens are compared in Table 3.2.

	Mph1 OE	SynCheck
Analysis method	Manual scoring of strains (by colour and colony size)	Manual scoring of strains (by colour and colony size)
Longlisted candidates	60	30
General properties of candidates	Many candidates involved in: - Gene expression - Signalling - Small molecule metabolic processes Significantly enriched for: - DAM/DASH components (outer kinetochore)	Many candidates involved in: - Transcription - Signalling Significantly enriched for: - Thiamine biosynthesis
Candidates in common	***SynCheck manual scoring (colour/size):*** *bub3*, *reg1*, *SPBC28E12.04* ***SynCheck quantification data (size):*** *eaf6*, *vip1*, and *clr1*	

Table 3.2 Comparison of results from a previous high-throughput screen which utilised inducible overexpression of Mph1 (Mph1 OE) with results from the SynCheck screen. Note that quantification of colony area with SGAtools was only performed for the SynCheck screen, so results are not presented here, apart from in 'candidates in common', which compares SynCheck candidates (identified from indicated method of analysis) with candidates identified by manual scoring of Mph1 OE data.

As expected, SynCheck was apparently successful in removing potential sources of false positive results. SynCheck allowed us to induce metaphase arrest without relying on Mph1 overexpression. This is expected to have reduced false positives due to off-target effects of Mph1 overexpression. In comparison with a previous screen which relied on Mph1 overexpression, our screen yielded noticeably fewer hits (30 hits, vs. 60). There was little overlap between the two candidate lists, although positive control *bub3Δ* was synthetically sick in both screens. Ectopically inducing the checkpoint may have eliminated false positives due to mutants which perturb kinetochore attachment. Kinetochore components were not found in the manually curated candidate list from this screen, nor were they enriched in the list generated by the SGAtools software. Several of the hits from the

previous Mph1 overexpression screen were proteins involved in kinetochore structure and kinetochore-microtubule attachment (e.g. Dam1/DASH complex subunits Duo1 and Spc19).

To aid in the quantification and analysis of the large dataset generated by this screen we planned to use software designed for analysing high-throughput SGA plates, to quantify cell growth and colour. This approach was intended to be complementary to manual analysis of plates, as combining these two sets of results will provide an extra level of verification. Quantification of colony size allowed normalisation of data to account for differences between plates, and the SGAtools software is designed to account for other biases, such as plating position. We hoped that software would be useful in increasing the sensitivity of the screen to small differences in colour and/or size. This appears to be the case, as many additional candidates were identified by quantification using SGAtools. These remain to be verified in independent silencing assays but could form the basis of future studies.

An important control experiment will be to perform this screen with each of the SynCheck components (rTetR-Mph1 and rTetR-Spc7) in isolation, to check that expression of these constructs is not affecting strain viability or silencing efficiency. Both constructs have their kinetochore localisation domains deleted, and it has been demonstrated in a wild-type background that neither of these constructs alone can induce an arrest (Yuan *et al*, 2016). However, it is possible that they may be affecting other cellular process which could be exacerbated by certain deletion mutants.

2) Candidates identified in screens

This screen has provided us with a list of candidate checkpoint silencing factors which may form the basis of further studies. Several of these candidates form the subject of the next chapter, where further efforts to characterise these mutants and to confirm their role in SAC silencing are discussed. Now that these candidates have been identified, several more questions must be considered.

i) Are these candidates truly involved in spindle checkpoint silencing or are they false positives?

It will be important to demonstrate that the apparent SAC silencing defects observed here can be reproduced in independent silencing assays. It should be noted that in this

screen, we are not directly observing silencing defects, but using reduced strain fitness in the presence of synthetic checkpoint activation as a proxy. It is possible that for some strains the effect on growth is not mediated via the SAC. This question may be addressed by using microscopy to directly follow the progression of cells through the cell cycle after inducing a SAC arrest, e.g. by monitoring degradation of Cdc13-GFP, or the persistence of metaphase spindles labelled with Atb2-RFP. The rTetR-based SynCheck system is not suitable for these timecourse experiments, as induction of SAC signaling by this method cannot be rapidly shut off. The following chapter describes independent checkpoint silencing assays conducted on these candidates. These experiments feature SynCheckABA, an alternative synthetic checkpoint system which has the advantage of being rapidly reversible (Chapter 4).

ii) Do these factors play a direct or indirect role in checkpoint silencing?

iii) Are these factors involved in known checkpoint silencing pathways or are they part of undiscovered pathways?

This can be investigated by testing for genetic interactions with known checkpoint silencing factors or by identifying physical interactors, e.g. by Co-IP/mass spectrometry.

Many candidates identified in this screen have not been previously associated with the SAC or SAC silencing. It is possible that components of novel mechanisms have been identified from this screen. GO term analysis was carried out to check if any processes or functions were significantly enriched in our candidate lists. Unfortunately, this analysis did not suggest any informative associations. Several of the factors identified are uncharacterised or have only been assigned putative functions. These factors may be particularly promising for future analysis.

Once these questions have been answered for these candidates, additional work will need to be carried out to determine their mechanisms of action in spindle checkpoint silencing.

Several of the candidates identified in this screen are involved in gene expression. Although these mutations may have an indirect effect on checkpoint silencing via gene expression, it is also possible that they play a more direct role in silencing. This has been shown to be the case in separate studies for some chromatin remodellers. For example, in *S. cerevisiae*, the RSC chromatin remodeling complex has been shown to be directly involved in mitotic exit.

The Rsc2 subunit of this complex has been shown to physically interact with polo kinase Cdc5, and is involved in the Cdc14 early anaphase release pathway (FEAR pathway) (Rossio *et al*, 2010).

Some of the candidates identified in this screen appear to be particularly promising, as they have been linked to known checkpoint silencing factors in previous studies. For example, Reg1, which is studied in more depth in the following chapter, is a known interactor of PP1 Dis2 in *S. pombe* (Vanoosthuyse & Hardwick, 2009) and has been shown in *S. cerevisiae* to regulate PP1 activity (Tabba *et al*, 2010; Tu & Carlson, 1995). It is plausible that Reg1 could be involved in regulating checkpoint silencing functions of Dis2. In addition to Reg1, deletion of Mss116, a predicted mitochondrial ATP-dependent RNA helicase, had a strong phenotype in our screen, and has been documented to have a synthetic growth defect with *dis2Δ* (Buttrick *et al*, 2011).

Taken together, these results indicate that this screening method is likely to have provided several promising candidates for further studies of SAC silencing.

Future directions

In the future, it would be beneficial to conduct additional replicates of the high-throughput screen to help account for biases due to batch effects. It is likely that repeat experiments may provide a slightly different set of hits, including some which may not have been detected thus far. A screen can be described as 'saturated' when the same genes are repeatedly identified in multiple experiments (Forsburg, 2001). There are several different iterations of this screening strategy that could provide additional hits. For example, the sensitivity of the screen could potentially be increased by introducing mutations in a known checkpoint silencing factor. This would only isolate a subset of silencing mutants that are involved in parallel pathways but sensitised screen such as this could be a useful addition to the data obtained from the original screen design.

This screening approach could also be expanded to test additional control strains. For example, screening in a genetic background in which endogenous *mph1* is deleted would prevent checkpoint proteins from localising to kinetochores and ensure that the endogenous SAC is not active. This would eliminate any effect that the endogenous SAC might have on SynCheck phenotypes, and ensure that phenotypes observed are fully independent of KT-MT attachment. Another potentially interesting control experiment

would be to test the effects of using different rTetR-Spc7 constructs. The rTetR-Spc7 construct used in this screen had some, but not all, of its MELT motifs replaced with phosphomimic mutations (T9E). During the initial design of the SynCheck strain it was thought that phosphorylation of rTetR-Spc7 MELT motifs by rTetR-Mph1 might be less efficient than phosphorylation interactions involving the endogenous proteins, and so the phosphomimetic version of rTetR-Spc7 was used to ensure that downstream spindle checkpoint components could still be recruited. However it has since been shown that in the presence of rTetR-Mph1, the rTetR-Spc7-WT construct induces a synthetic checkpoint arrest much more efficiently than rTetR-Spc7-9TE (Yuan *et al*, 2016). Using this query strain might increase the sensitivity of the screen, allowing detection of additional candidates.

The implementation of software to quantify colour phenotypes would improve the quality of data generated by this screening strategy.

CHAPTER 4

Characterisation of checkpoint silencing candidates

4.1 Introduction

The genetic screen discussed in Chapter 3 identified a list of single gene deletions which are likely to cause defects in spindle checkpoint silencing (Figure 3.5). This chapter describes the selection and further characterisation of a subset of these candidates. Verification of these candidates will not only shed light on their individual contributions to SAC silencing but will also validate the approach taken in the high-throughput screen.

To select candidates, multiple sources of information were considered. Apart from our high-throughput screen data, we also looked at data from the Mph1 overexpression screen previously conducted in our lab, as well as performing a literature search on promising candidates. The *S. pombe* database, PomBase (www.pombase.org), was a useful resource for searching for previously annotated features and functions of these proteins (Lock *et al*, 2018; Wood *et al*, 2012).

The first step in characterising these candidates involved investigating their deletion phenotypes in a wild-type background. After this, independent checkpoint silencing assays were performed to test whether phenotypes observed for these strains in the rTetR-based SynCheck system were in fact due to SAC silencing defects. These additional silencing assays involved experiments with a reversible synthetic checkpoint system (SynCheckABA). Another assay with an endogenous SAC arrest induced by *nda3-KM311* cold-mediated microtubule depolymerisation was also employed.

4.2 Aims of chapter

The aims of this chapter were to:

i) Select a subset of candidates for further analysis (Section 4.3)

ii) Characterise selected candidates in more detail, including examination of deletion mutant phenotypes in a wild-type background (Section 4.4)

iii) Verify selected candidates in independent SAC silencing assays (Section 4.5)

4.3 Selection of candidates for further verification

To focus our efforts on the most promising candidates from the screen, we aimed to narrow our focus to a subset of the original list of candidates identified by eye (Figure 3.5). Quantitative analysis of the screen results using SGAtools had not been completed at this stage, so this data was not taken into consideration. It was our aim to select 10 or fewer hits for additional verification and characterisation. Candidates were primarily selected based on severity of the synthetically sick phenotype seen in the high-throughput screen, with the aim of selecting genes that have a relatively strong effect on checkpoint silencing. Only candidates with a phenotype that was successfully reproduced in serial dilution growth assay experiments were selected (Figure 3.2).

An exception to these criteria was made for *grh1Δ*, as we wanted to include one strain that had a mild phenotype in the screen. This was to take into consideration that some SAC silencing factors may have mild phenotypes, especially if there are multiple redundant silencing pathways in operation. A synthetically sick phenotype was not evident for *grh1Δ* in the spot assays, however the relatively mild phenotype may have been difficult to detect in this assay.

Finally, we wanted to ensure as far as possible that the shortlisted genes were likely to be involved in checkpoint silencing, based on available information about their biological functions, localisation and interactions. These selection criteria are discussed in more detail below.

Several candidates with likely alternative explanations for phenotypes seen in the screen were removed from consideration. These included genes involved in thiamine biosynthesis (e.g. *nmt1Δ, SPBP8B7.18cΔ*), as removal of thiamine from screen plates resulted in reduced growth of the parental strains, which could complicate the interpretation of synthetically sick phenotypes in combination with SynCheck. However, one gene involved in thiamine biosynthesis, *SPCC18B5.05c*, was retained in the shortlist for further analysis. In this case, the *SPCC18B5.05cΔ* parental strain was only moderately sick in the absence of thiamine, and it was still possible to observe a particularly strong synthetically sick phenotype in combination with SynCheck. Its gene product is a kinase which localises to the nucleus, so it could plausibly play a direct role in checkpoint signalling. However, it remains likely that its

phenotype is simply due to defects in thiamine production. If this is the case, this strain may be a good control in other assays which do not involve thiamine.

Preference was given to strains which were annotated as having a function which could be related to a direct role in spindle checkpoint silencing (e.g. signalling proteins, such as kinases and phosphatases and their regulatory subunits, including *reg1* and *psy2*).

We also considered whether candidates had genetic or physical interactions with SAC components. Reg1 has been demonstrated to physically interact with known checkpoint silencing factor PP1 Dis2 in fission yeast and is predicted to be involved in its regulation (Vanoosthuyse *et al*, 2014). In *S. cerevisiae,* the Reg1 homolog has been demonstrated to regulate PP1 (Glc7) (Tabba *et al*, 2010). *mph1Δ* has been reported to have a negative genetic interaction with *grh1Δ*, but have a positive interaction with *SPCC18B5.05cΔ* (i.e. the double mutant phenotypes are, respectively, more severe and less severe than would be expected from the individual effects of single mutants) (Ryan *et al*, 2012). Cells lacking the APC component Apc10 have synthetic genetic interactions with *sol1Δ* and *tls1Δ*. *tls1Δ* is reported to have a negative genetic interaction with *klp6Δ*, which is known to be involved in regulation of PP1 Dis2-mediated silencing (Ryan *et al*, 2012; Meadows *et al*, 2011). However, as Tls1 is a splicing factor, *tls1Δ* has many genetic interactions which are likely to be indirect, and due to gene expression effects.

Conserved uncharacterised genes are also among the shortlisted candidates, e.g. *SPAC227.17c*. These are promising candidates, as they have functions which are important enough to be highly conserved. The fact they have not previously been subjected to detailed study makes it more likely that our efforts will reveal interesting new features of these genes. *S. pombe* has 410 identified conserved genes of unknown function, and these are likely to have many important functions worthy of in-depth study (Wood *et al*, 2019).

Based on these considerations, eight candidates were selected for further verification (Figure 4.1).

Gene ID	Gene name	Product	Darker	Smaller	Verified by growth assay	Verified by software	GO biological process	GO cellular component
SPCC18B5.05c	-	phosphomethylpyrimidine kinase (predicted)	2	2	Yes	Yes	thiamine biosynthetic process	cytosol, nucleus
SPAC227.15	reg1	protein phosphatase regulatory subunit Reg1	2	2	Yes	Yes (strong)	signalling, carbohydrate metabolic process	cytosol, PP1 complex, fungal-type vacuole membrane
SPBC30B4.04c	sol1	SWI/SNF complex subunit Sol1	2	2	Yes	No	chromatin remodelling, regulation of transcription by RNA Pol II	SWI/SNF complex
SPAC4F10.18	nup37	nucleoporin, WD repeat Nup37	2	2	Yes (strong)	Yes	nucleocytoplasmic transport	cytosol, nuclar pore (outer ring)
SPBC216.01c	psy2	protein phosphatase PP4 complex regulatory subunit 3 Psy2 (predicted)	1	1	Yes	Not scored	DNA repair, negative regulation of sister chromatid cohesion	nuclear chromatin, protein phosphatase 4 complex
SPAC1D4.01	tls1	splicing factor Tls1	1	1	Yes (strong)	Not scored	regulation of mRNA splicing	cytosol, spliceosomal complex
SPAC1D4.02c	grh1	human GRASP protein family Golgi protein (predicted)	1	0	No	Yes	ER to Golgi vesicle-mediated transport, Golgi organisation	cell division site, cell tip, cytosol, Golgi apparatus, nucleus
SPAC227.17c	-	conserved eukaryotic protein;	1	0	Yes (strong)	No*	-	-

Figure 4.1 Summary of selected candidate mutants from high-throughput screen. (A) Table listing candidate checkpoint silencing mutants selected for further investigation. The strength of the phenotypes from manual scoring of the high-throughput screen are ranked on a scale from 0-2 (0 = no observable phenotype, 1 = observable phenotype, 2 = strong phenotype, i.e. very pale or very large colonies). Table summarises results of subsequent serial dilution growth assay experiments, as well as information on gene ontology (GO) terms as annotated in PomBase. It is noted whether candidates were verified by quantitative analysis of colony area by the SGAtools software (Appendix 1.6).

Genotypes of the selected strains were confirmed by PCR amplification of the target gene region with primers which anneal in 5' and 3' UTRs (untranslated regions) of each gene (Figure 4.2). In wild-type strains, the entire gene coding sequence (CDS) would be amplified, along with approximately 200bp each of the 5' and 3' UTRs. For genes which had successfully been deleted, the entire CDS should be replaced by the 1.5kb Bioneer deletion construct, which contains the G418 resistance cassette and flanking sequences designed to act as a 'barcode' for identifying which constructs had integrated.

The PCR fragments obtained for each candidate deletion were analysed by gel electrophoresis to confirm that they did not correspond with products obtained for the wild-type genes and instead were the expected size for the introduction of the deletion cassette in the designated region. All candidate deletions gave the expected results, except for *reg1Δ*.

There is a risk that when the Bioneer deletion cassettes were transformed into these strains they could have integrated in locations other than the endogenous locus. The Bioneer

deletion cassettes also contain portions of gene UTRs to facilitate homologous recombination with the target gene, so it is possible that primers targeted against UTR regions would amplify cassettes that had integrated in the incorrect location. If this was the case, we could expect to see two bands for the PCRs performed with these UTR primers, one corresponding to the Bioneer construct and one amplified from the endogenous locus where the wild-type gene was still present. As this was not seen for any of the candidates tested, it appears that the wild-type genes were successfully replaced by the deletion cassette. However, to address this concern, PCR primers targeting regions further upstream of the endogenous gene could be used to confirm that the deletion cassettes inserted in the correct location. It could also be demonstrated that the wild-type gene was deleted by using primers targeting regions within the CDS. No product should be obtained for strains with the CDS successfully deleted.

For the PCR with primers in the UTRs of *reg1*, the same size bands were observed for both wild-type control strain and the Bioneer deletion strain which corresponded to the expected size for the wild-type band (data not shown). A similar result was seen using different primer sets which annealed at various locations in *reg1* UTRs and the CDS (coding sequence). As a known interactor of silencing factor Dis2, Reg1 is an interesting candidate, so I continued to investigate this strain despite these issues. A different *reg1Δ* deletion mutant had previously been generated in the lab by replacing the *reg1* open reading frame (ORF) with the hygromycin resistance cassette (constructed by K.May). This *hygR* deletion construct resulted in a band of the expected size when amplified with primers targeting the upstream and downstream UTRs (Figure 4.2B) and was used for all subsequent work involving *reg1Δ*.

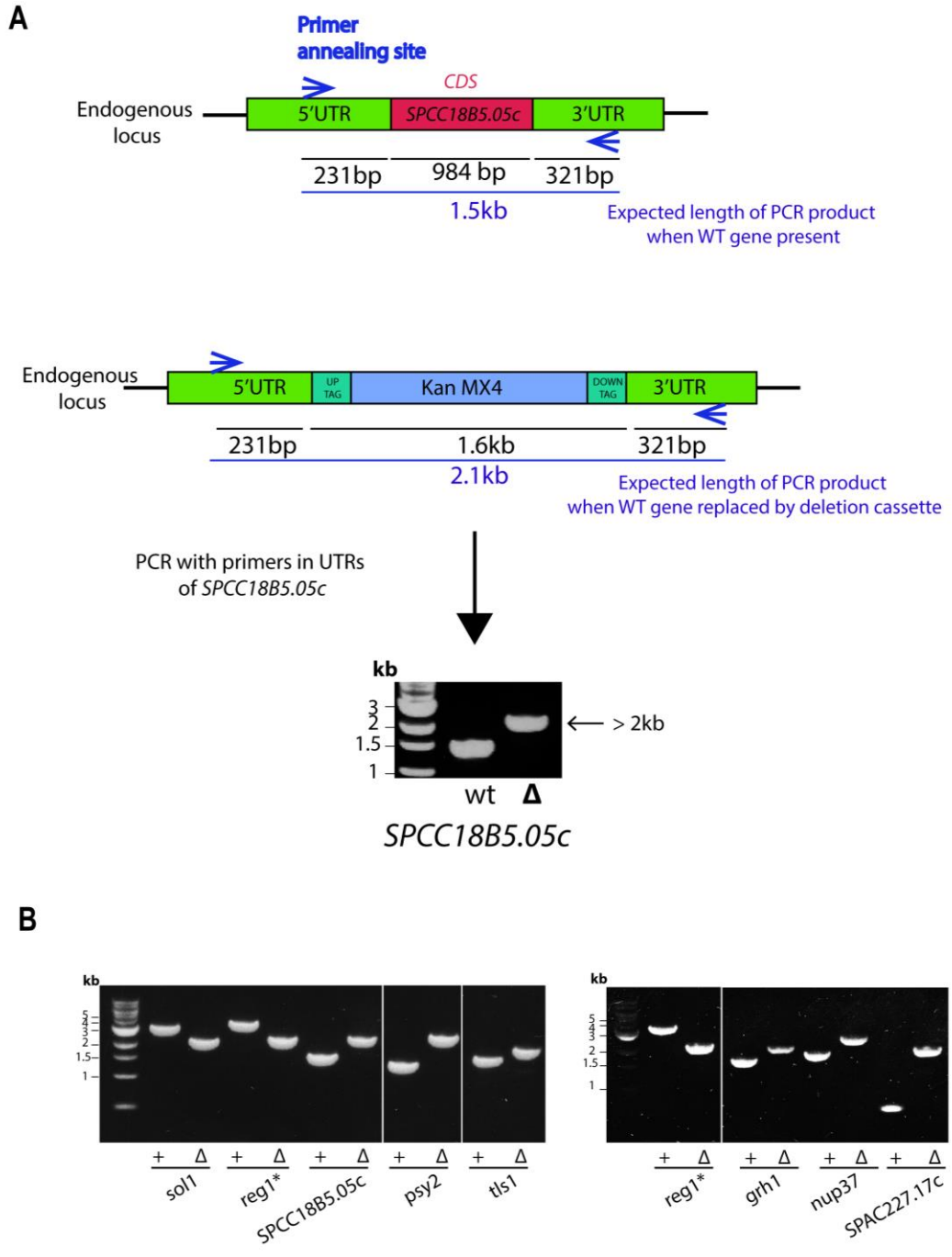

Figure 4.2 Verification of strain genotypes for selected candidates from high-throughput screen. (A) Schematic illustrating PCR strategy used to verify Bioneer deletion strain genotypes, using the *SPCC18B5.05c* gene as an example. PCRs were performed using primers in gene UTRs. There is a difference in the expected PCR product size for strains which have the wild-type genes and those which have the wild-type gene replaced with the deletion cassette. For *SPCC18B5.05c*, the expected size for the PCR product is 1.5kb where the wild-type gene is present (wt), and 2.1kb where it has been replaced with the Bioneer G418 resistance cassette (Δ). (B) Gel electrophoresis of PCR products from amplifying the regions between 5' and 3' UTRs of the indicated genes in wild-type (+) and the

corresponding Bioneer deletion strains (Δ). In each case, product sizes for Bioneer candidate deletion strains differ from those obtained for the wild-type gene template, and these bands correspond to the expected size for the insertion of the G418-resistant gene deletion cassette (*kanMX4*). *Unlike other strains shown here, *reg1Δ* is not from the Bioneer library and is marked with *hygR* instead of *kanMX4*.

The *tls1* mutation in the Bioneer deletion library has previously been reported to only remove a small portion of the gene (the majority of the HEP59 domain is deleted, amino acids 130-244, out of a total of 254 residues). This mutation has been reported to cause loss-of-function of *tls1* in the context of telomere silencing (Wang *et al*, 2014a). It should be noted that two of the genes identified in this screen as likely SAC silencing factors, *tls1* and *grh1,* are located in close proximity to each other (on opposite strands of chromosome I) (Figure 4.3). The coding sequences (CDS) of each of these genes overlap with the UTRs of the other gene. Thus, deletions of the CDS of each gene could potentially affect the expression of the other, e.g. by altering mRNA stability. It is likely that just one of these genes is involved in checkpoint silencing, and its silencing functions are disrupted by both the *tls1Δ* and *grh1Δ* mutations. Further investigation will be required to determine which of these genes is involved in silencing (as discussed in Section 6.1).

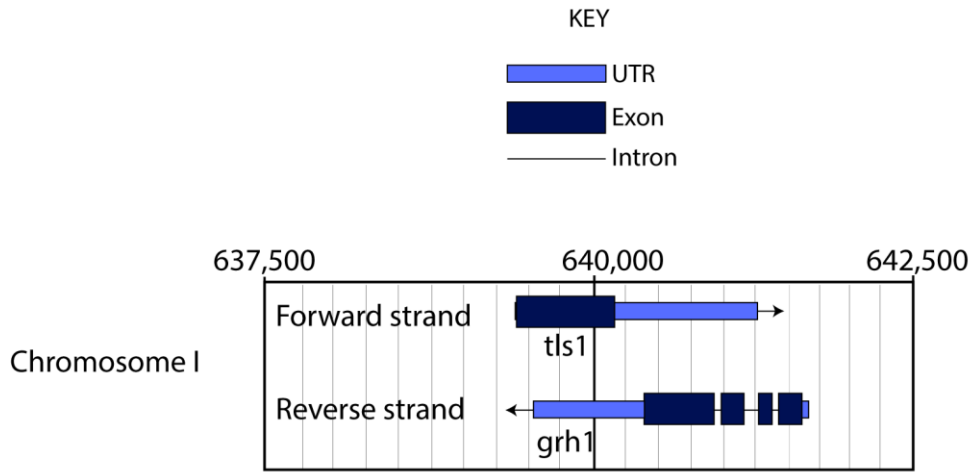

Figure 4.3 *grh1* and *tls1* have overlapping genes. Forward and reverse strands of chromosome I, nucleotides 637,500-642,500. The *grh1* CDS is 1,229 nucleotides long, from 641,627-640,399. Including UTRs, it extends from 641,680-639,545. Tls1 is encoded on the reverse strand. The *tls1* CDS is 639,411-640,175, and with UTRs it extends from 639,405-641,280. The coding sequences of each gene overlap with UTR regions of the other gene.

4.4 Characterising null mutants of candidate SAC silencing factors

The first step we took in characterising these candidates was to determine the effects of the gene deletions in a wild-type background. The phenotypes of these strains were tested in various environmental conditions. Additional phenotypes of these deletions could indicate that these genes have pleiotropic functions. They may indicate something about their role in checkpoint silencing or could be important to consider when designing checkpoint silencing experiments. For example, if any of the mutants were cold-sensitive, an assay involving cold-induced microtubule depolymerisation (i.e. using *nda3-KM311* mutant) to induce a checkpoint arrest might not be suitable.

To construct these deletions in a wild-type background, G418-resistant gene deletion cassettes were amplified from Bioneer library strains, using primers which anneal in gene UTRs (the same primers as were used for confirming deletions in Bioneer library strains, Figure 4.2). For *reg1Δ*, the Bioneer strain was not used and genomic DNA from a strain which has the CDS replaced by a hygromycin resistance cassette was used as a template instead. The constructs and primers used are illustrated in Figure 4.4.

These deletion cassettes were transformed into a wild-type background by electroporation and transformants were selected based on G418 resistance (or HygR for *reg1Δ*). Transformants were confirmed by PCR, using the same primers which anneal in gene UTRs.

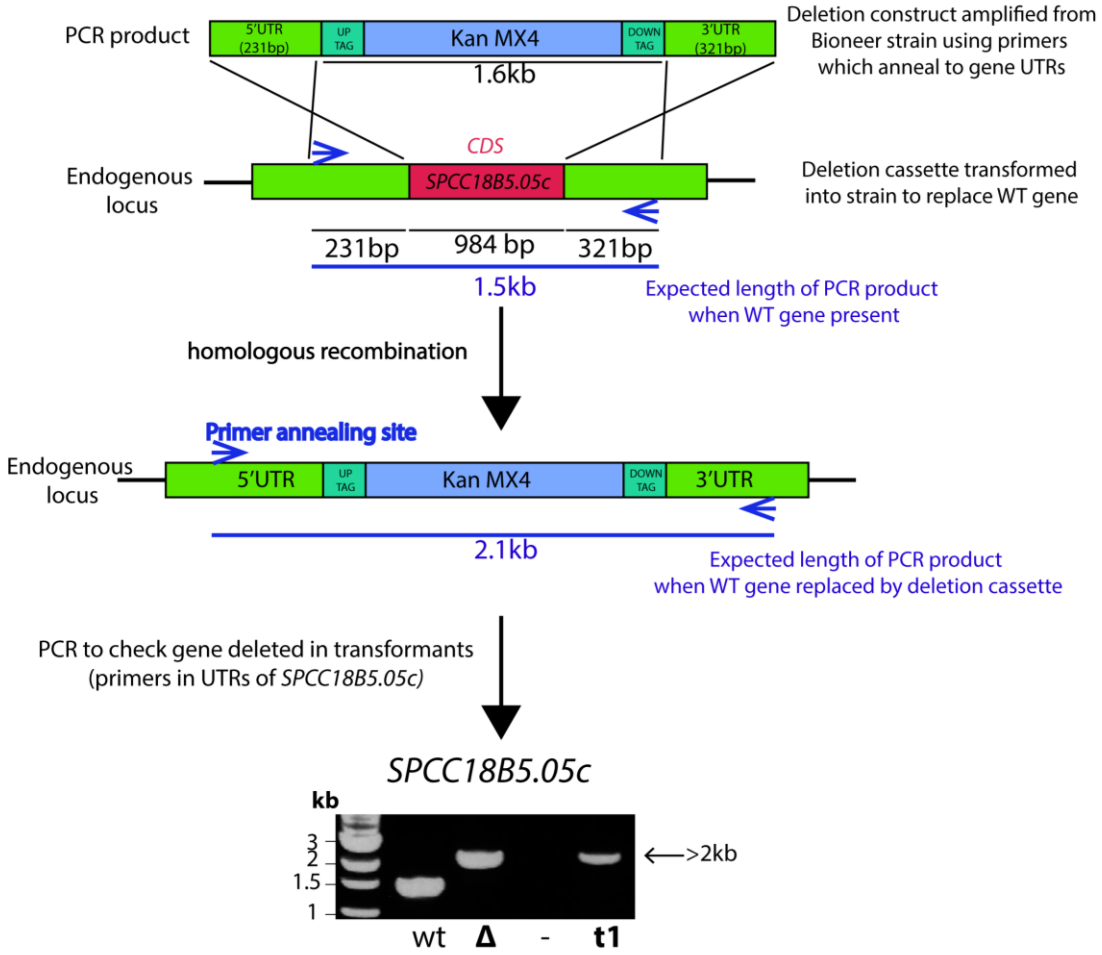

Figure 4.4 Gene deletion cassettes from Bioneer library strains were used to construct candidate checkpoint silencing mutants in various genetic backgrounds. General features of strain construction are illustrated using the *SPCC18B5.05c* gene as an example. Deletion cassettes were amplified from Bioneer deletion strains using primers which anneal in the UTRs, approximately 200bp up- and down-stream from coding sequence (CDS). Other strains, e.g. wild-type or SynCheckABA strains, were transformed with these PCR products. To test whether genes were successfully deleted in transformants, PCRs were performed with the same primers that were used to amplify the cassettes from the Bioneer strains. There is a difference in the expected PCR product size for strains which have the wild-type gene and those which have the wild-type gene replaced with the deletion cassette. For *SPCC18B5.05c*, the PCR product expected for the wild-type gene is 1.6kb (wild-type control, 'wt') and the deletion product is approx. 2.1kb (band for the corresponding deletion strain from the Bioneer library, 'Δ'). The image from gel electrophoresis shows that a transformant (t1, transformed into SynCheckABA strain background) has a product which corresponds to the size of the deletion cassette.

Strains were examined for temperature sensitivity by performing serial dilution growth assays on YES plates and incubating at 18°C, 25°C and 32°C (Figure 4.5A). At least two isolates of each of the candidate strains were tested in each experiment (except for *nup37Δ* and *SPAC227.17cΔ*, for each of which only one transformant was obtained). These experiments were repeated on at least two separate occasions. Temperature-sensitive strains were used as controls, including *cdc25-22* (sensitive at 32°C) and *nda3-KM311* (cold-sensitive at 18°C). Benomyl-sensitive controls included strains with single gene deletions of SAC components i.e. *mad1Δ* and *bub3Δ.*

All strains grew similarly to the wild-type strain at 25°C. Apart from the temperature-sensitive control strains, which displayed the expected phenotypes, none of the strains tested were temperature-sensitive at 18°C. At 32°C, *tls1Δ* and *SPAC227.17cΔ* strains had reduced growth.

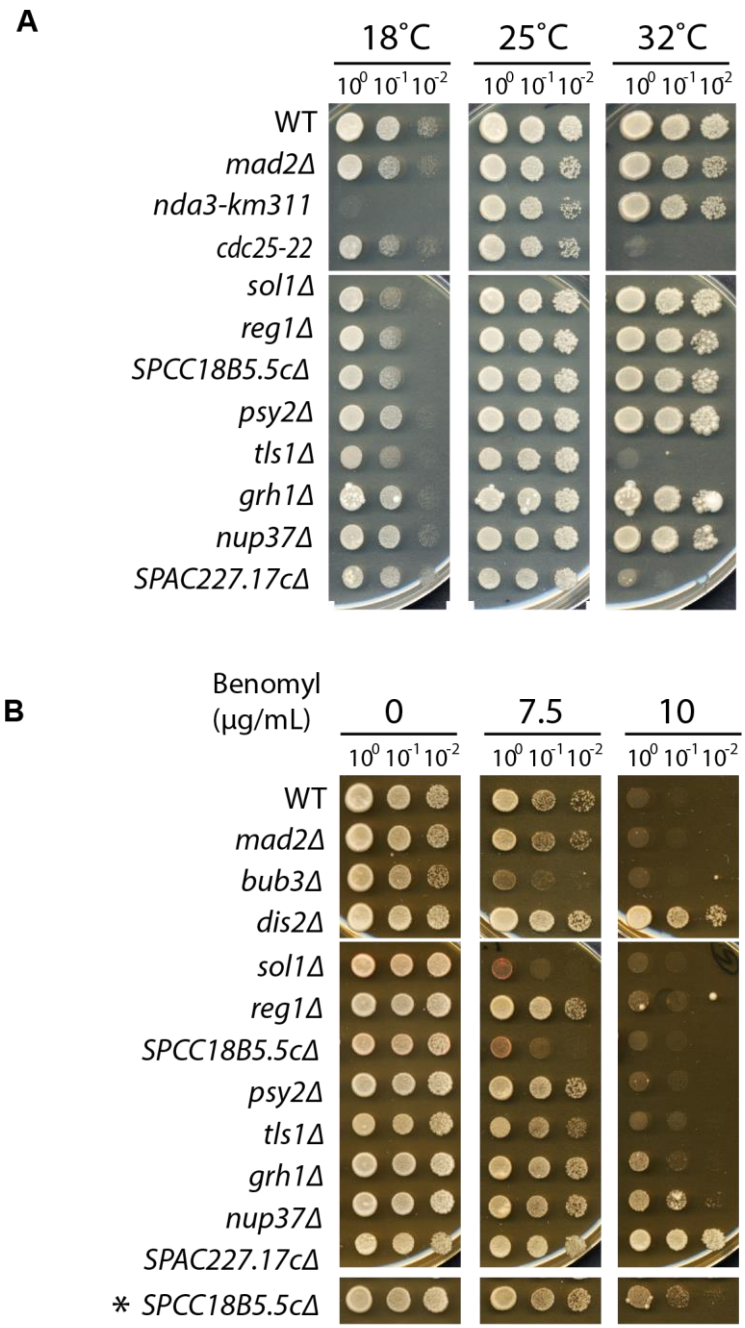

Figure 4.5 Phenotypes of deletion mutants in a wild-type background. (A) Temperature-sensitivity test. Serial dilution growth assays were performed on strains with the indicated gene deletions in a wild-type (WT) background. Strains were grown on YES plates at 25°C for 48h, resuspended in YES and serially diluted (tenfold) before being spotted on to YES plates (with amino acid supplements) which were incubated for 1 week at the indicated temperatures. Strains were tested for growth at 18°C, 25°C and 32°C. Multiple isolates of each strain were tested (for all strains except *nup37Δ* and *SPAC227.17cΔ*). This experiment was carried out in duplicate. *cdc25-22* was used as a temperature-sensitive control (at restrictive temperature of 32°C), *nda3-km311* used as cold-sensitive control. *tls1Δ* and *SPAC227.17cΔ* strains are temperature sensitive at 32°C. (B) Benomyl-sensitivity test.

Growth assays shown were carried out as in (A), on plates with 0, 7.5 and 10µg/ml benomyl. Strains were incubated at 25°C for 1 week. Strains with deletions of spindle checkpoint genes, i.e. *mad2Δ* and *bub3Δ,* were used as benomyl sensitive controls*. dis2Δ*, *SPAC227.17cΔ* and *nup37Δ* appear to be benomyl resistant in this assay.

Serial dilution growth assays on benomyl plates were performed in parallel with the temperature-sensitivity experiments (Figure 4.5B). Benomyl is a microtubule-depolymerising drug. Sensitivity to benomyl may be caused by various defects, including impaired spindle checkpoint activity, microtubule stability, and efficiency of membrane pumps at removing drugs.

Many conserved SAC proteins were first identified in benomyl-plating experiments in budding yeast, including Mad1, Mad2, Mad3 and Bub1 (Li & Murray, 1991; Hoyt *et al*, 1991). Low levels of benomyl partially depolymerise microtubules, causing unattached kinetochores. Cells with a functional spindle checkpoint arrest in metaphase under these microtubule-destabilising conditions. Although this increases the mitotic index of these cells, it allows them to maintain their viability, as the checkpoint protects against errors in chromosome segregation. Although yeast cells are viable without a functional checkpoint under normal conditions, in a perturbed mitosis the risk of chromosome missegregation is increased. Lack of a functional checkpoint can therefore result in aneuploidy and cell death in this assay.

Plates with concentrations of benomyl ranging from 0µg/mL to 10µg/mL (0, 2.5, 7.5 and 10µg/mL) were used to judge relative sensitivity of strains. By confirming that the candidate deletions from the screen do not cause benomyl sensitivity, we can infer that the candidate deletions are not important for activation of the spindle checkpoint.

Wild-type cells were resistant to up to 7.5µg/mL of benomyl. Consistent with previous studies, we observed *mad2Δ* to have a weak phenotype on benomyl plates, and *bub3Δ* was more sensitive, with moderately reduced growth at 7.5µg/ml.

Deletion of *sol1* has previously been reported to cause benomyl sensitivity, as have deletions of other components the SWI/SNF complex, including the catalytic component, Snf22 (Monahan *et al*, 2008). *sol1Δ* strains were confirmed to be sensitive to benomyl at concentrations of 7.5µg/ml. Sol1 is involved in transcription, therefore the fact that *sol1Δ* has multiple defective phenotypes is unsurprising, since it is likely to have pleiotropic, indirect effects on many cellular processes.

dis2Δ was resistant to benomyl in these experiments (up to 10µg/ml). *SPAC227.17cΔ* showed a similar resistance phenotype. *nup37Δ* also had slightly increased benomyl resistance. Dis2 has been recorded to have pleiotropic functions and cells lacking Dis2 may have increased resistance for several reasons. It would be interesting to test whether any of these deletions stabilise microtubules, which could cause this phenotype.

4.5 Verification of candidates in independent silencing assays

Additional checkpoint silencing assays were carried out to determine whether the shortlisted genes are involved in SAC silencing or whether they are false positives. The SynCheck system could yield false positives due to possible pleiotropic effects of slight Mph1 overexpression, defects in thiamine biosynthesis, or other screen-specific factors, so it is important to rule these possibilities out.

Additionally, rebuilding and confirming the phenotypes of the deletion mutants in different genetic backgrounds eliminates the possibility that additional mutations which may have been present in the Bioneer library strains were responsible for the observed phenotypes.

SynCheck has several limitations for studying checkpoint silencing, most notably that once rTetR-Mph1 expression is induced it is not easily reversible, which makes it difficult to induce and monitor checkpoint silencing directly. It will also be important to determine that these genes are involved in silencing the endogenous checkpoint, even though this may not be as easy to study.

It is sometimes the case that checkpoint silencing phenotypes may be apparent in one assay but not detectable in another assay. For example, the strength of the checkpoint signal generated can affect how much of an impact impaired silencing has, and this varies across different assays (e.g. completely depolymerising microtubules using cold-sensitive tubulin mutant *nda3-KM311*, vs. partial depolymerisation induced by low levels of spindle poisons). In addition, some methods of checkpoint induction may preclude the study of certain silencing pathways. For example, an ectopically induced SAC arrest such as SynCheck (in an *mph1Δ* background) will not identify kinetochore-dependent events in checkpoint silencing. For this reason, it will be useful to conduct multiple independent silencing assays.

4.5.1 Alternative synthetic checkpoint: ABA system

Shortlisted candidates were tested in an alternative SynCheck system which has recently been developed (Amin *et al*, 2019). SynCheckABA is a synthetic ectopic checkpoint system which operates along similar principles to the original SynCheck rTetR system, in that it forces heterodimerisation between the upstream checkpoint proteins Mph1 and Spc7. Instead of relying on rTetR-induced dimerisation, it utilises an abscisic acid (ABA) based system (Section 1.8).

Strain construction of SynCheckABA with candidate gene deletions

SynCheckABA strains were transformed with the same gene deletion cassettes that were used for wild-type strain transformations (Figure 4.6). The SynCheckABA strains used contained Atb2-mCherry, which allows microtubules to be visualised, and the *cdc25-22* mutation to allow synchronisation of cells in G2.

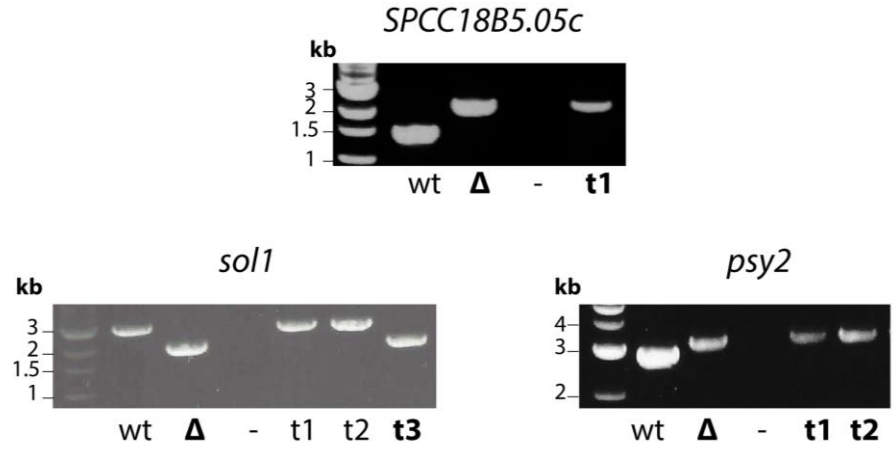

Figure 4.6 SynCheckABA strains were transformed with Bioneer deletion constructs. Images of gel electrophoresis of PCR products from primers in UTRs of other candidate genes to check whether transformations into SynCheckABA strain background resulted in successful gene deletion. Template DNA sources indicated as follows: 'wt' = wild-type, 'Δ' = corresponding deletion strain from the Bioneer library, '-' = no DNA, 't' = transformant (in SynCheckABA genetic background). All of the SynCheckABA strains with deletions of SAC silencing candidate genes that were used in this study were confirmed by PCR.

SynCheckABA silencing timecourse experiments

Silencing timecourses were carried out with these strains. Cells were synchronised in G2 by shifting cells to 36°C for 3.5h. Cells were released from this block by shifting to 25°C. ABA was added five minutes after release, to activate the spindle checkpoint by inducing formation of Spc7-PYL—Mph1-ABI heterodimers (Figure 1.13). Cultures were incubated for 60 mins to allow cells to arrest in the checkpoint. Cells were then washed to remove ABA and abolish checkpoint activation, allowing us to analyse the ability of cells to silence the checkpoint and exit from mitosis.

Samples were taken at 30-min intervals after ABA wash-out and preserved in methanol, before immediately checking by microscopy for the presence of metaphase spindles (Figures 4.7 and 4.8). Wild-type cells silence SynCheckABA signalling rapidly. Approximately 40% of WT cells have silenced the arrest within 30 minutes of wash-out and almost all cells have silenced within 60 minutes. A particularly dramatic failure to silence the arrest was seen for *sol1Δ* cells. Indeed, even more cells seemed to accumulate in the arrest over the course of the experiment. Other strains exhibited more subtle delays in silencing, such as *grh1Δ* and *psy2Δ*.

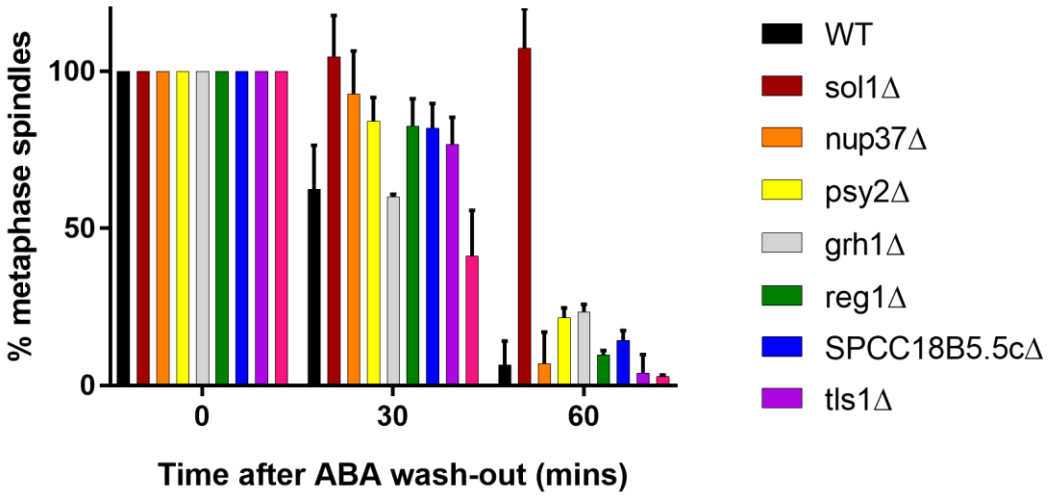

Figure 4.7 Checkpoint silencing in SynCheckABA is severely compromised by *sol1* deletion and is also reduced by other candidate checkpoint silencing mutants identified in the high-throughput screen. Quantification of release from SynCheckABA arrest. Timecourse experiments were performed to monitor strains with one of several candidate checkpoint silencing factors deleted for their ability to silence a SynCheckABA-induced arrest. Cells were scored as metaphase arrested if they had short metaphase spindles and a single mass of condensed chromatin. More than 100 cells were analysed per strain at each timepoint. Data are plotted as mean ± s.d. Time points were analysed at the time of ABA wash-out (time zero) and 30- and 60-minutes post-wash.

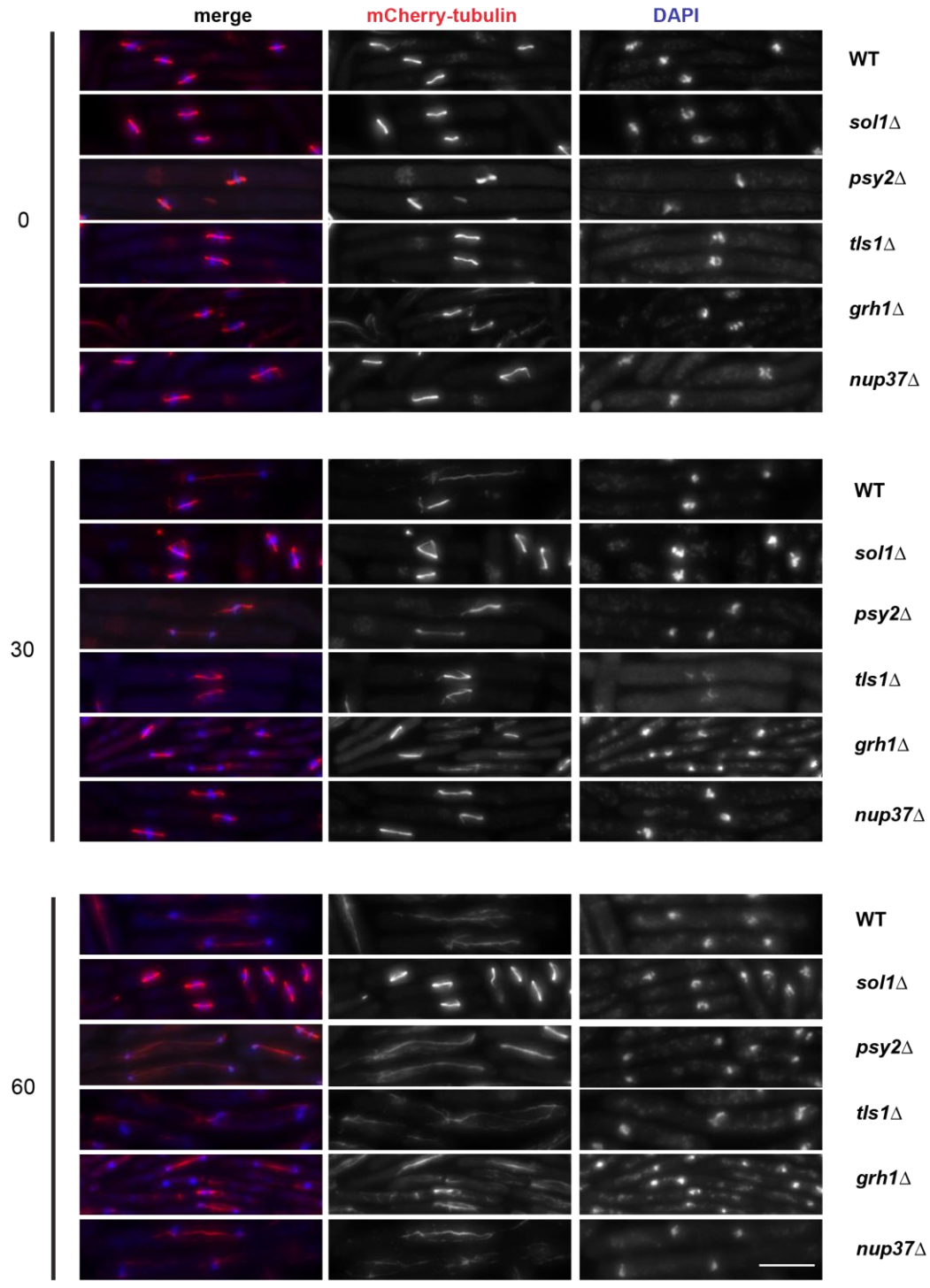

Figure 4.8 Microscopy timecourse experiment reveals profound delay in SynCheckABA silencing for *sol1Δ*. These microscopy images correspond to the quantification data shown in Figure 4.7. Timecourse experiments were performed to monitor strains with one of several candidate checkpoint silencing factors deleted for their ability to silence a SynCheckABA-induced arrest. Images of cells with indicated genes deleted. Microtubules are seen in red (mCherry-tubulin), and chromatin in blue (DAPI). Time points were analysed at the time of ABA wash-out (time zero) and 30- and 60-min post-wash. Scale bar: 10 µm.

No silencing defect was observed for *SPAC227.17cΔ* in this assay. It is possible that temperature-sensitivity of this strain at 32°C may have affected this result. Some other strains may have minor reductions in silencing efficiency that are within the error bars, e.g. *reg1Δ, SPCC18B5.05cΔ*. Increasing the sensitivity of our methods to small delays in SAC silencing might resolve the issue of whether these deletions cause real but minor delays in silencing. It may be useful to perform additional repeats of SynCheckABA timecourses with smaller timepoint intervals (e.g. every 10 minutes).

Comparison of Mph1$_{(303-678)}$-3HA-ABI levels in strains assayed

Immunoblotting was performed to test the expression levels of the Mph1-ABI construct (Figure 4.9). This assay was performed to determine whether any of the synthetically sick phenotypes observed in this assay could be due to changes in levels of Mph1-ABI and thus in the strength of the arrest, rather than effects on checkpoint silencing. In Figure 4.9, it is shown that Mph1-ABI levels do not differ much between most of the deletion mutant strains. Transfer of the Mph1-ABI bands for *nup37*Δ and SPAC227.17cΔ was partially blocked by a bubble, however from what can be seen of the bands it seems expression levels are similar to other strains. However, two *sol1Δ* isolates both had noticeably increased levels of the Mph1-ABI construct. This may be due to overexpression of the construct, either at the transcriptional or translational level, or due to altered protein stability. Sol1 may affect Mph1 levels directly or indirectly, i.e. by altering expression levels of other proteins. It is likely that the increased levels of Mph1-ABI contribute to the strong synthetically sick phenotype of *sol1Δ* in the SynCheckABA silencing assay.

We also attempted to assess the levels of Spc7-PYL construct. Unfortunately, constructs containing Spc7$_{1-666}$ are in general large and unstable proteins, and our lab has experienced difficulty in assessing the levels of such proteins by immunoblotting. Degradation of Spc7-PYL proteins in these samples prevented interpretation of the blots performed to date.

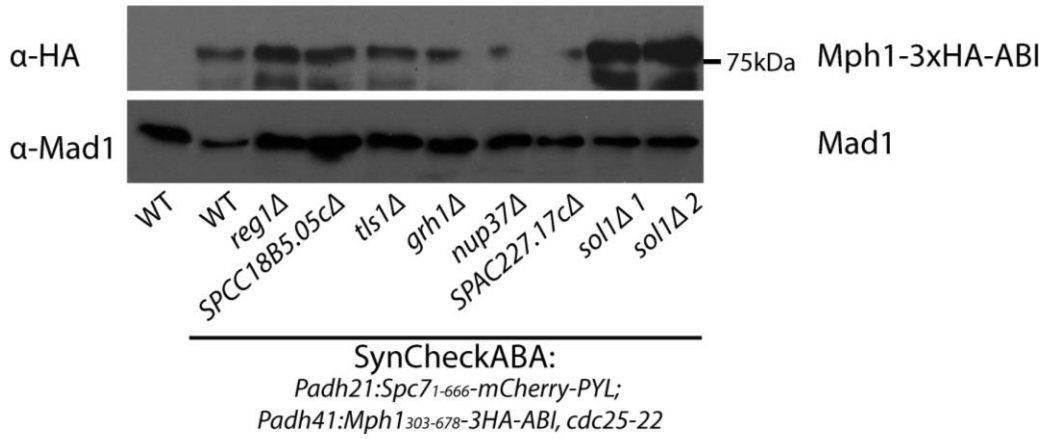

Figure 4.9 Expression levels of Mph1-ABI are similar in most of the deletion mutant strains tested in the SynCheckABA silencing assay. Protein extracts from the strains indicated were run on a 10% SDS-PAGE gel. The immunoblot from this gel was probed with α-HA antibody to detect the Mph1-3xHA-ABI construct. The immunoblot was re-probed with α-Mad1 as a loading control. Transfer of the Mph1-ABI bands for *nup37Δ* and *SPAC227.17cΔ* was partially blocked by a bubble.

4.5.2 Recovery from nda3-KM311 mitotic arrest assay

The effects of *sol1* deletion on checkpoint silencing were also tested in a *nda3-KM311* arrest. Unlike the previous assays which have employed synthetic ectopic checkpoints, this assay tests silencing of the endogenous spindle checkpoint.

Depolymerisation of microtubules triggers the endogenous spindle checkpoint by causing microtubule-kinetochore attachment errors. Depolymerisation can be induced in multiple ways, including the addition of spindle poisons to media (e.g. carbendazim, thiabendazole). Another method utilises the cold-sensitive tubulin mutant *nda3-KM311* (Hiraoka *et al*, 1984). By shifting cells to the restrictive temperature (below 20°C) microtubules can be completely depolymerised. In wild-type cells, this induces a robust, spindle assembly checkpoint mediated metaphase arrest.

Depolymerisation of microtubules via *nda3-KM311* can be rapidly reversed by shifting cultures back to room temperature, allowing the checkpoint to be satisfied as kinetochore-microtubule attachments form. By conducting experiments in strains with Cdc13-GFP (cyclin B), progression through mitosis can be visualised. Cdc13-GFP is highly expressed and

localises to spindle pole bodies during metaphase. Levels of Cdc13-GFP rapidly decline as cells are released from the checkpoint arrest and enter anaphase.

nda3-KM311 cell cultures were shifted to 18°C for 6 hours, until 80-90% of cells were arrested (Figure 4.10). Cultures were shifted back to 25°C and samples were taken every ten minutes to monitor rates of mitotic exit. Microscopy was performed to assess levels of cyclin B.

The control strain used was *dis2Δ*, which has previously been demonstrated to have checkpoint silencing defects in similar *nda3-KM311* arrests (Vanoosthuyse & Hardwick, 2009). In our experiments *dis2Δ nda3-KM311* strains were very sick, which is likely to be due to pleiotropic functions of Dis2. *dis2Δ* cells arrested in metaphase, and this arrest persisted throughout the 30-minute experiment, whereas wild-type cells had fully escaped from the arrest within 20 minutes.

sol1Δ did not appear to have a strong effect on checkpoint silencing in this system. It is possible that there is a minor delay which is difficult to detect as microtubule repolymerisation and escape from mitosis occurs relatively quickly in this assay. Repeating these experiments with smaller timepoint intervals (e.g. 5 mins) may enable the detection of subtle silencing defects. Ability to silence the SAC after exposure to different microtubule depolymerising conditions, e.g. carbendazim (CBZ), should also be tested.

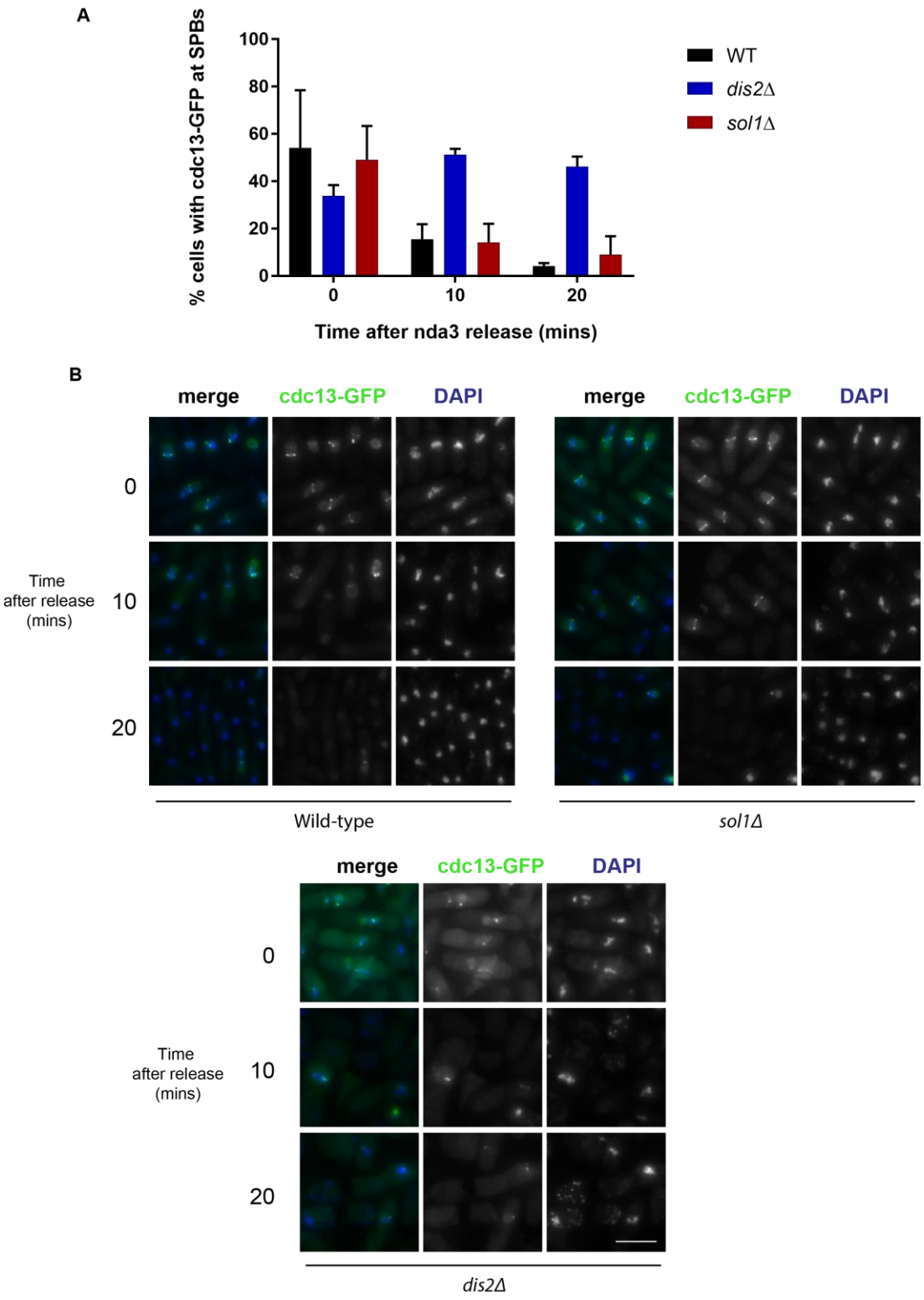

Figure 4.10 *sol1Δ* does not result in a strong checkpoint silencing phenotype in an endogenous checkpoint arrest triggered by cold-induced microtubule depolymerisation. See legend on next page.

Figure 4.10 *sol1Δ* does not result in a strong checkpoint silencing phenotype in an endogenous checkpoint arrest triggered by cold-induced microtubule depolymerisation. Timecourse experiments were performed in a *nda3-KM311* genetic background. At the restrictive temperature of 18°C, *nda3-KM311* cells depolymerise microtubules, resulting in activation of the endogenous spindle checkpoint due to unattached kinetochores. To monitor efficiency of spindle checkpoint silencing, cells were shifted back to the permissive temperature (25°C) and monitored for their ability to escape from metaphase arrest. (A) Quantification of number of arrested cells at various timepoints after returning cultures to the permissive temperature. Cells were scored as arrested if Cdc13-GFP was enriched at spindle poles. This experiment was repeated two times. More than 200 cells were analysed per strain at each time point. (B) Images of cells with indicated genes deleted. Cdc13-GFP is seen in green and chromatin in blue (DAPI). Time points were analysed from the time of shifting cultures to 25°C (time zero) and 10- and 20-min post-shift. Scale bar: 10µm.

4.6 Conclusions

This chapter has discussed our efforts to verify a subset of the candidates identified in Chapter 3. Eight candidates were selected for further analysis. Candidates *sol1Δ* and *grh1Δ* have been confirmed to have silencing phenotypes that are reproduced in another spindle checkpoint arrest system, SynCheckABA. Interesting features of these candidates are discussed in more detail below. In general, this work has provided a good starting point for further characterisation of these factors. The fact that silencing phenotypes observed in the high-throughput screen have been verified in direct, independent assays of checkpoint silencing function confirms the validity of the screening strategy described in Chapter 3. This suggests that additional candidates identified in this SynCheck screen may also merit further study.

General phenotypes of candidate deletions

Deletion strains were constructed in a wild-type background to test if they caused other phenotypic effects. Benomyl resistance was observed for *SPAC227.17cΔ* and *nup37Δ*, as well as *dis2Δ*. A temperature sensitive phenotype at 32°C was discovered for *tls1Δ* and *SPAC227.17cΔ*.

It would be interesting to test the effect of these candidate mutations on spindle morphology and cell cycle progression. Strains could be constructed with fluorescently tagged tubulin and progression of cells through the cell cycle could be monitored by

microscopy. As part of this analysis, we could also test what effect growth at 32°C has on the temperature sensitive mutants. By identifying which stages of the cell cycle are disrupted at the non-permissive temperature, we may gain additional insights into gene function.

Evaluation of sol1Δ phenotypes in different checkpoint silencing assays

Loss of the SWI/SNF component Sol1 appeared to have a particularly catastrophic effect on checkpoint silencing in SynCheckABA assays, as well as having a strong synthetically sick phenotype in the rTetR SynCheck screen. However, this effect was not reproduced in a *nda3-KM311* arrest. It is encouraging that *sol1Δ* had a phenotype in multiple assays, as this reduces the likelihood that it was a false positive in the screen. However, it will be important to address why this mutation did not have an effect in the *nda3-KM311* assay, and in particular whether *sol1Δ* has an effect in assays which involve the endogenous checkpoint rather than a synthetic ectopic checkpoint.

It is likely that the strong synthetically sick phenotype for *sol1Δ* seen in the SynCheckABA assay is due to raised levels of the Mph1-ABI construct in these strains. One possible explanation for this is that Sol1 does not contribute to checkpoint silencing, but rather *sol1* deletion results in increased levels of Mph1-ABI, generating a stronger SAC signal which is more difficult to silence. Alternatively, regulation of Mph1 levels may be important for checkpoint silencing.

It remains to be tested whether expression of the rTetR-Mph1 constructs or endogenous Mph1 are affected in SynCheck rTetR and *nda3-KM311* assays, but this will be an important question to follow up on in future studies. It is possible that *sol1Δ* impacts expression from the *adh41* promoter but not from the endogenous *mph1* promoter. If the phenotypes of *sol1Δ* in SynCheck/SynCheckABA systems are due (at least in part) to overexpression of the Mph1 construct, it may be that the *nda3-KM311* assay does not show a phenotype because endogenous Mph1 is not overexpressed in response to *sol1* deletion. If this were the case, *sol1* might not be relevant in the context of the endogenous checkpoint or else might be one of multiple redundant mechanisms that exist in the endogenous context.

Follow-up work to investigate this could initially focus on increasing the sensitivity of the *nda3-KM311* assay, as even strains with deletions of known checkpoint silencing factors such as *bub3Δ* have relatively mild phenotypes in this assay. One way this could be

achieved is by sampling at shorter time intervals. Additionally, alternative silencing assays involving the endogenous checkpoint could be performed. For example, metaphase arrest could be induced by adding microtubule depolymerising drugs such as CBZ to liquid cultures, and then the drug could be washed out and progress through anaphase monitored by microscopy timecourses.

Sol1 is a regulatory component of the SWI-SNF chromatin remodelling complex. Another component of the SWI/SNF complex, Snf59, had a synthetically sick phenotype in the previous Mph1 overexpression screen (work by Karen May). To confirm that defects in SWI/SNF activity are responsible for the checkpoint silencing phenotype of *sol1Δ*, a strain lacking the catalytic component of SWI-SNF, Snf22, could be tested in these silencing assays to see if it has a similar phenotype. This gene is inessential but was not present in the Bioneer v2.1 library.

It is possible that *sol1Δ* phenotypes are due to an indirect effect mediated via changes in the transcription of other intermediate factors. Altered levels of proteins involved in the SAC could disrupt the balance between checkpoint activation and checkpoint silencing. *sol1Δ* could cause increased levels of Mph1 by affecting its transcription or the transcription of other factors which regulate Mph1 levels (i.e. proteins with roles in translation, splicing, post-translational modification and protein turnover). However, these phenotypes could also be due to a non-transcriptional effect of remodelling chromatin structure or to possible chromatin-independent functions of Sol1.

Many genetic interactions are reported for SWI/SNF, which is unsurprising due to its role in transcription. As such, it is likely that this deletion will have pleiotropic effects which may complicate analysis of its contributions to checkpoint silencing.

sol1Δ has been reported to be cold-sensitive, although our temperature-sensitivity assays did not reproduce this phenotype (Monahan *et al*, 2008). Those assays were carried out at 16°C, whereas our experiment was carried out at 18°C, so it is possible that at lower temperatures we would have seen this defect. It is possible that this cold-sensitivity may have affected the results of the *nda3-KM311* assay, which is another reason why it will be important to conduct additional checkpoint silencing assays with the endogenous SAC which do not involve shifting cells to low temperatures.

This work also investigated other features of *sol1Δ* which may be helpful in designing and interpreting the results of future SAC silencing experiments. The results obtained in our

assays reproduced the benomyl sensitive phenotype reported previously (Monahan *et al*, 2008). Other studies have reported abnormal interphase microtubule morphology in *sol1Δ* cells. Altered microtubule stability may explain the benomyl sensitivity of this strain. *sol1Δ* also results in small vegetative cells (Navarro & Nurse, 2012; Hayles *et al*, 2013).

Future directions: alternative checkpoint silencing assays

So far only *sol1Δ* has been tested for the ability to silence a *nda3-KM311* checkpoint arrest. It would be interesting to test other candidates in this assay, although it may be difficult to detect milder silencing phenotypes, as strains silence this arrest relatively quickly (within about 20 minutes). In particular, candidates which have a detectable phenotype in our SynCheckABA experiments should be retested in this assay, i.e. *grh1*.

Alternative silencing assays include various microtubule poisons (e.g. CBZ, TBZ). It may also be useful to test recovery from an arrest in the absence of microtubules. Silencing factors have been identified which carry out their checkpoint silencing activity independently of kinetochore-microtubule attachment, e.g. Bub3 and Dis2 (Vanoosthuyse & Hardwick, 2009; Vanoosthuyse *et al*, 2009b). In these experiments, a checkpoint arrest was induced by *nda3-KM311* microtubule depolymerisation. These strains contained an analogue-sensitive allele of Ark1, which could be inhibited to abolish checkpoint activation, permitting checkpoint silencing in the absence of microtubules.

CHAPTER 5

Protein phosphatase $PP1^{Dis2}$ in SAC silencing:

SynCheckABA as a system for dissection of silencing mechanisms

5.1 Introduction

The aim of this project is to improve our understanding of spindle checkpoint silencing by identifying and characterising factors involved in this process. Chapters 3 and 4 have dealt with the identification of novel SAC silencing candidates. This chapter aims to take a more in-depth approach, by studying a previously identified checkpoint silencing factor, PP1 Dis2.

$PP1^{Dis2}$ is a phosphatase, which silences the checkpoint by dephosphorylating targets of mitotic kinases, e.g. Aurora B (Ark1) (Vanoosthuyse & Hardwick, 2009). $PP1^{Dis2}$ is a promising candidate for further analysis, as it plays a conserved role in SAC silencing, and *dis2Δ* causes a severe SAC silencing defect in yeast (Meadows *et al*, 2011; Pinsky *et al*, 2009; Vanoosthuyse & Hardwick, 2009; Nijenhuis *et al*, 2014; Liu *et al*, 2010). Despite being a confirmed silencing factor, little is known about how Dis2 is regulated or its relevant substrates for SAC silencing (see Section 1.4.1 for detailed introduction).

$PP1^{Dis2}$ is recruited to $KNL1^{Spc7}$ via two conserved motifs (SILK and RVSF), also referred to as the 'A' and 'B' motifs respectively) in its N-terminal domain (Rosenberg *et al*, 2011; Meadows *et al*, 2011; Espeut *et al*, 2012; Liu *et al*, 2010). Mutation of both the A and B motif have been shown to result in defects in SAC silencing in *S. cerevisiae* and *S. pombe* (Rosenberg *et al*, 2011; Meadows *et al*, 2011). Indeed, this pathway is of particular importance in yeast, as mutation of *S. cerevisiae* RVSF to a PP1-binding defective version (RASA) leads to a lethal metaphase block (Rosenberg *et al*, 2011). This mechanism appears to be highly conserved, as KNL1 PP1-binding sites have also been demonstrated to affect PP1 recruitment and checkpoint silencing (Liu *et al*, 2010; Nijenhuis *et al*, 2014). In human cells, PP1 binding to KNL1 is regulated by Aurora B activity. Aurora B directly phosphorylates the SILK and RVSF binding motifs in KNL1 (Welburn *et al*, 2010; Bajaj *et al*, 2018). Phosphorylation of the RVSF has been demonstrated to disrupt KNL1:PP1 association (Liu *et al*, 2010).

In *S. pombe* it has been shown that a second pool of $PP1^{Dis2}$ is recruited to the mitotic spindle via kinesin-8 family motor proteins Klp5 and Klp6 (Section 1.4.1). This pool of PP1 has also been demonstrated to be important for checkpoint silencing (Meadows *et al*, 2011).

In this work, both the rTetR SynCheck and SynCheckABA systems were employed to study Dis2. These systems, particularly SynCheckABA, offer several advantages for studying checkpoint silencing (Section 1.8). In the current work, we aimed to demonstrate the utility of this system for studying checkpoint silencing factors in general.

Interactors of Dis2 have been identified previously (Vanoosthuyse *et al*, 2014), although it remains unclear which of these factors are relevant for regulating its spindle checkpoint silencing functions, as Dis2 has many functions and acts in multiple parts of the cell. This is an important question, which we hope these synthetic checkpoint systems can address. Our simplified, ectopic systems will aid in the identification of relevant interactors of checkpoint silencing proteins.

5.2 Aims of chapter

The aims of this chapter are to further characterise the role of $PP1^{Dis2}$ in checkpoint silencing and to establish whether SynCheckABA is a suitable system for studying its mechanisms. Specifically, our aims were to:

i) Examine the effects of deleting Dis2 and its interactors in the rTetR SynCheck system (Section 5.3)
ii) Establish whether PP1 Dis2 is involved in silencing SynCheckABA arrest (Section 5.4)
iii) Confirm whether regulation of Dis2-mediated silencing in SynCheckABA involves the same pathways as in the endogenous checkpoint, specifically:

- whether Spc7 recruits Dis2 to the SynCheckABA signalling platform (Section 5.4.1)
- if kinesin-8 (Klp5/Klp6) is involved in Dis2-mediated silencing of SynCheckABA (Section 5.4.2)

5.3 *dis2Δ* in rTetR-based SynCheck system

5.3.1 Impact of *dis2Δ* on viability of rTetR SynCheck strains

In preparation for the high-throughput screen described in Chapter 3, we used known checkpoint silencing defective mutants as controls for testing the sensitivity of the SynCheck screening method. For this purpose, we intended to use *bub3Δ* and *dis2Δ.* However, it was challenging to generate a strain with *dis2Δ* in the SynCheck system. Efforts were made to transform *dis2Δ* strains with SynCheck constructs. This yielded strains with *dis2Δ* and either rTetR-Spc7 or rTetR-Mph1, but strains with both constructs could not be obtained. Several different mating strategies did not yield the desired genotype. A few candidates were obtained which contained all auxotrophic and drug resistant markers, however when tested by western blotting none were found to express both rTetR-Mph1 and rTetR-Spc7. This may be due to strong selective pressure on synthetically sick strains to acquire suppressor mutations.

We hypothesised that these difficulties in constructing the *dis2Δ* SynCheck strain could be due to this strain being inviable. In the SynCheck system, rTetR-Mph1 expression is controlled by a *nmt81* promoter. This promoter is known to have low level, 'leaky' expression even when cells are grown in the presence of thiamine. This could result in mild induction of the SynCheck signal. Although wild-type cells can usually overcome this low-level signal, viability could be impacted for strains with particularly severe SAC silencing defects.

To test this hypothesis more directly, tetrad dissection was performed on crosses designed to obtain *dis2Δ* in combination with rTetR-Spc7 and rTetR-Mph1 (Figure 5.1). A *dis2Δ* rTetR-Mph1 strain was crossed with a SynCheck strain (rTetR-Spc7, rTetR-Mph1). In this cross all progeny would have rTetR-Mph1. Assuming normal segregation of alleles, 25% of progeny would have each parental phenotype, 25% would have both *dis2Δ* and rTetR-Spc7 and 25% would have neither (Figure 5.1A). If *dis2Δ* was synthetically lethal in combination with SynCheck we would expect 75% of spores to be viable. From this tetrad dissection experiment only 55% of spores were viable (Figure 5.1B).

The viable spores from these tetrad dissections were tested for markers for *dis2Δ* (hygromycin resistance), rTetR-Spc7 (auxotrophic for uracil but not lysine) and rTetR-Mph1 (leucine auxotrophy). The genotypes of viable spores were inferred from these phenotypic markers (Figure 5.1C).

14% of progeny had only the rTetR-Mph1 construct and were viable. This is lower than the expected result of 25%, which could indicate that viability is generally reduced for all progeny in this cross due to the presence of rTetR-Mph1.

dis2Δ rTetR-Mph1 had a similar effect to the rTetR-Mph1 only strain. The strain containing both constructs (rTetR-Mph1 and rTetR-Spc7) and the *dis2* deletion had further reduced viability, with only 7% of surviving progeny having the phenotypic markers for this genotype. This is consistent with our hypothesis that low-level activation of SynCheck could be causing synthetic sickness in combination with *dis2Δ.*

In the absence of *dis2Δ*, progeny with rTetR-Spc7 and rTetR-Mph1 are viable. It is notable that there were more surviving progeny with both rTetR-Spc7 and rTetR-Mph1 than rTetR-Mph1 alone; at 22%, this is close to the expected value of 25%. rTetR-Spc7 (and SynCheck activity) could have a beneficial effect on spore viability (on media containing thiamine) compared to rTetR-Mph1 alone. It will be important to confirm this result by repeating these crosses with higher numbers of spores. Possible explanations could include that rTetR-Spc7 is a good substrate for rTetR-Mph1, and that by forming heterodimers with rTetR-Mph1 it could reduce the number of rTetR-Mph1 homodimers formed, both of which could impact on the activity of the rTetR-Mph1 kinase.

A

Mating cross for tetrad dissection:

IL375: Pnmt81-rTetR-mph1(Δ1-302):leu1, lys1::adh15-rTetR-mCherry-spc7(1-666)-9TE:ura4 dis2+

X

SS38: Pnmt81-rTetR-mph1(Δ1-302):leu1, dis2Δ::hygR

↓

Progeny genotype	Phenotype	Expected % spores
Pnmt81-rTetR-mph1(Δ1-302):leu1, lys1::adh15-rTetR-mCherry-spc7(1-666)-9TE:ura4, dis2+	leu + lys -, ura + HygS	25%
Pnmt81-rTetR-mph1(Δ1-302):leu1, dis2Δ::hygR	leu + HygR	25%
Pnmt81-rTetR-mph1(Δ1-302):leu1, lys1::adh15-rTetR-mCherry-spc7(1-666)-9TE:ura4, dis2Δ::hygR	leu + lys -, ura + HygR	25%
Pnmt81-rTetR-mph1(Δ1-302):leu1, dis2+	leu + HygS	25%

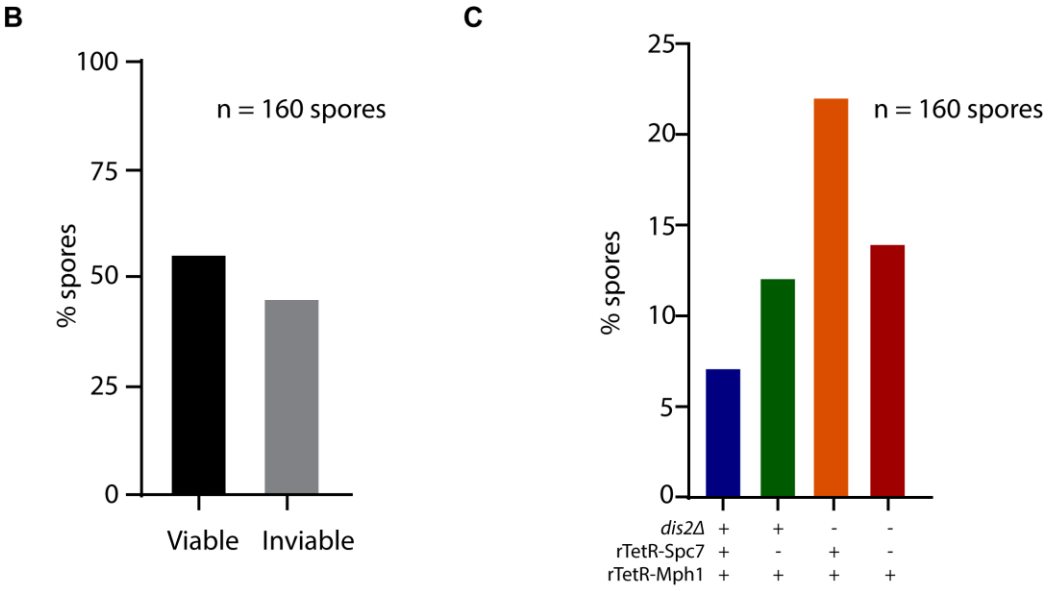

Figure 5.1 Effects of deleting PP1 Dis2 in the SynCheck system. (A) Schematic illustrating the expected genotypes of progeny from a cross between parental strains **SS38: *Pnmt81-rTetR-mph1(Δ1-302):leu1, lys1::adh15-rTetR-mCherry-spc7(1-666)-9TE:ura4*** and **IL375: *Pnmt8-rTetR-mph1(Δ1-302):leu1, dis2Δ::hygR*.** Phenotypic markers are indicated, with '+' denoting auxotrophy for a given amino acid. Hygromycin sensitivity is indicated as either resistant (R) or sensitive (S). (B) Quantification of viable and inviable spores obtained from tetrad dissection of this cross, with (C) genotypes of these spores, as determined from auxotrophic and drug resistant markers. Tetrad dissection was performed in collaboration with Koly Aktar. n = 160 spores.

To test whether rTetR-Mph1 contributes to the reduced viability of *dis2Δ* rTetR-Mph1 strains, tetrad dissection of crosses between one parental strain with *dis2Δ* and another with just rTetR-Mph1 could be performed. In this cross we would expect 25% of strains to have both *dis2Δ* and rTetR-Mph1 and another 25% to have *dis2Δ* alone. If fewer spores are obtained with *dis2Δ* rTetR-Mph1 than with *dis2Δ* alone, this would support the hypothesis that leaky rTetR-Mph1 expression plays a role in the reduced viability of these strains.

To test whether the detrimental effect of rTetR-Spc7 on viability in progeny with *dis2Δ* observed in this cross is dependent on the presence of rTetR-Mph1 (and thus may be due to leaky SynCheck activation) it would be useful to carry out additional crosses. A parental strain with *dis2Δ* could be crossed with an rTetR-Spc7 strain to examine the effects of these genotypes on spore viability individually and in combination with each other.

Due to time constraints, additional tetrad dissection experiments were not carried out. It also remains to be confirmed by western blotting whether the viable *dis2Δ* isolates from this cross express rTetR-Spc7 and rTetR-Mph1. Even if we have eventually obtained *dis2Δ* SynCheck strains from this cross, the ability to tightly control SynCheckABA induction will make it a more useful assay for studying Dis2 function than the rTetR-based system. For this reason, we shifted our attention to constructing *dis2Δ* SynCheckABA strains (Section 5.4).

5.3.2 Regulators of PP1 Dis2

Like other phosphatases, PP1 acts on a wide range of substrates, spanning a range of cellular processes and locations. Interactions with regulatory proteins are required to confer specificity on PP1. These interactors function to target PP1 to substrates or to modulate PP1 activity. It would be informative to identify which interactors of Dis2 are important for regulating its activity in silencing the checkpoint.

Co-immunoprecipitation of fission yeast Dis2 and mass spectrometry of these samples has yielded a list of specific Dis2 interactors (Vanoosthuyse *et al*, 2014). It is possible that several of these interactors represent regulators of Dis2 activity in the context of checkpoint silencing. Deletion mutants of several of these factors are contained within the Bioneer library. Of these, *reg1Δ* had a strong synthetically sick phenotype in the SynCheck screen. Other deletions of PP1 interactors tested in the SynCheck screen included *lys9Δ*,

glc9Δ, *tea4Δ*, *uri1Δ*, *ppn1Δ*, *ppe2Δ*, *rad24Δ* and *rad25Δ*. None of these strains were noted to have a phenotype when plates from the high-throughput screen was analysed.

We retested these strains in phloxin B serial dilution growth assays to see if any subtle defects could be detected (Figure 5.2). None of the strains exhibited a clear phenotype in this assay, except for *lys9Δ* which had a synthetic defect in two of the three isolates tested. It might be informative to retest some of these deletions in a more sensitive, direct assay of silencing, e.g. timecourse experiments using SynCheckABA or CBZ arrests. Some other interactors of PP1 Dis2 which were not tested in the Bioneer screen but might also be relevant for SAC silencing include Sds22, Bud27, Ucp3, Rpb1 and Ypi1.

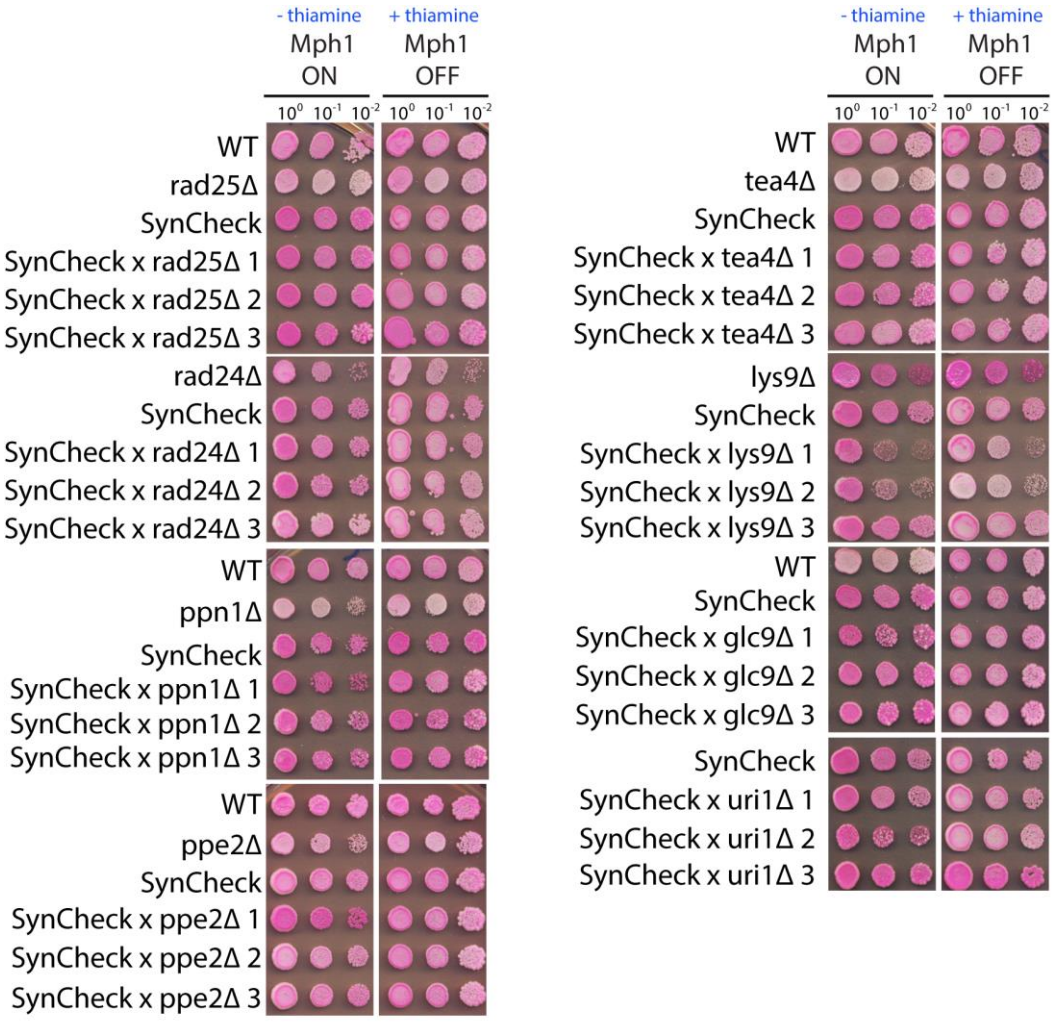

SynCheck: *rTetR-mph1(Δ1-302), rTetR-mCherry-spc7(1-666)-9TE, PEM-2*

Figure 5.2 Serial dilution growth assays of strains with deletions of Dis2 interactors in a SynCheck background. Phloxin B dye is taken up by dead cells, causing sick colonies to be

darker pink. Growth assays show 10-fold serial dilutions of the indicated strains. Multiple isolates were obtained with each genotype (individual isolates indicated by a number in figure). Growth is shown for conditions where SynCheck arrest was induced (- thiamine) and uninduced (+ thiamine).

5.4 *dis2Δ* in SynCheckABA system

SynCheckABA has several advantages over the original SynCheck system (Section 1.8). This synthetic checkpoint is under tight temporal control, with checkpoint activation only occurring upon addition of ABA to media. It was therefore possible that this tightly controlled system would facilitate the study of *dis2Δ* mutants. Importantly, induction of this synthetic arrest is rapidly reversible, by washing ABA from cells. This allows silencing of the checkpoint to be monitored in timecourse experiments.

5.4.1 Recruitment of Dis2 via Spc7 PP1-binding motifs

To test whether $PP1^{Dis2}$ is recruited to the SynCheckABA signalling platform by PP1-binding motifs in Spc7-PYL (Section 2.7.1) we constructed strains with versions of Spc7-PYL which lacked the KGILK (A) and RRVSF (B) binding motifs (Figure 5.3).

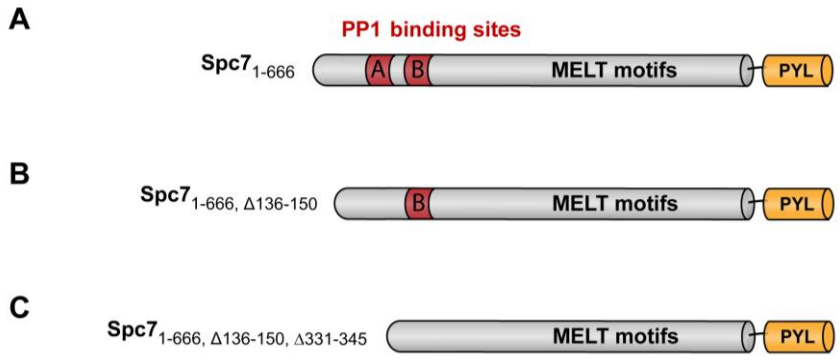

Figure 5.3 Schematic of $Spc7_{1-666}$-PYL constructs with binding sites for $PP1^{Dis2}$ deleted.

Timecourse experiments were performed to determine whether checkpoint silencing was affected by these mutants. As described in Chapter 4, SynCheckABA timecourses were conducted by synchronising cells in G2 using *cdc25-22*, before releasing at 25°C, and adding ABA to arrest at metaphase. After 60 mins, cells were washed to remove ABA and

terminate checkpoint signalling. Cyclin B degradation (Cdc13-GFP) was monitored to assess progression through anaphase over a period of 90 min.

Deletion of the A motif caused a 30-minute delay in spindle elongation, and the double mutant ΔAB caused an even more profound delay (Figure 5.4). These results indicate that both sites play a role in checkpoint silencing. There were delays in constructing a strain with only the B motif deleted, but it would be useful to test the effect of this mutation in the future to get a clearer idea of the individual contributions of each mutation to the double mutant phenotype.

We suspect that the delay in spindle elongation is due to failure to recruit PP1 Dis2 to the Mph1-ABI–Spc7-PYL platform (model in Figure 5.4C). To confirm this, co-immunoprecipitation experiments comparing levels of Dis2 bound to wild-type and mutant Spc7-PYL constructs could be performed.

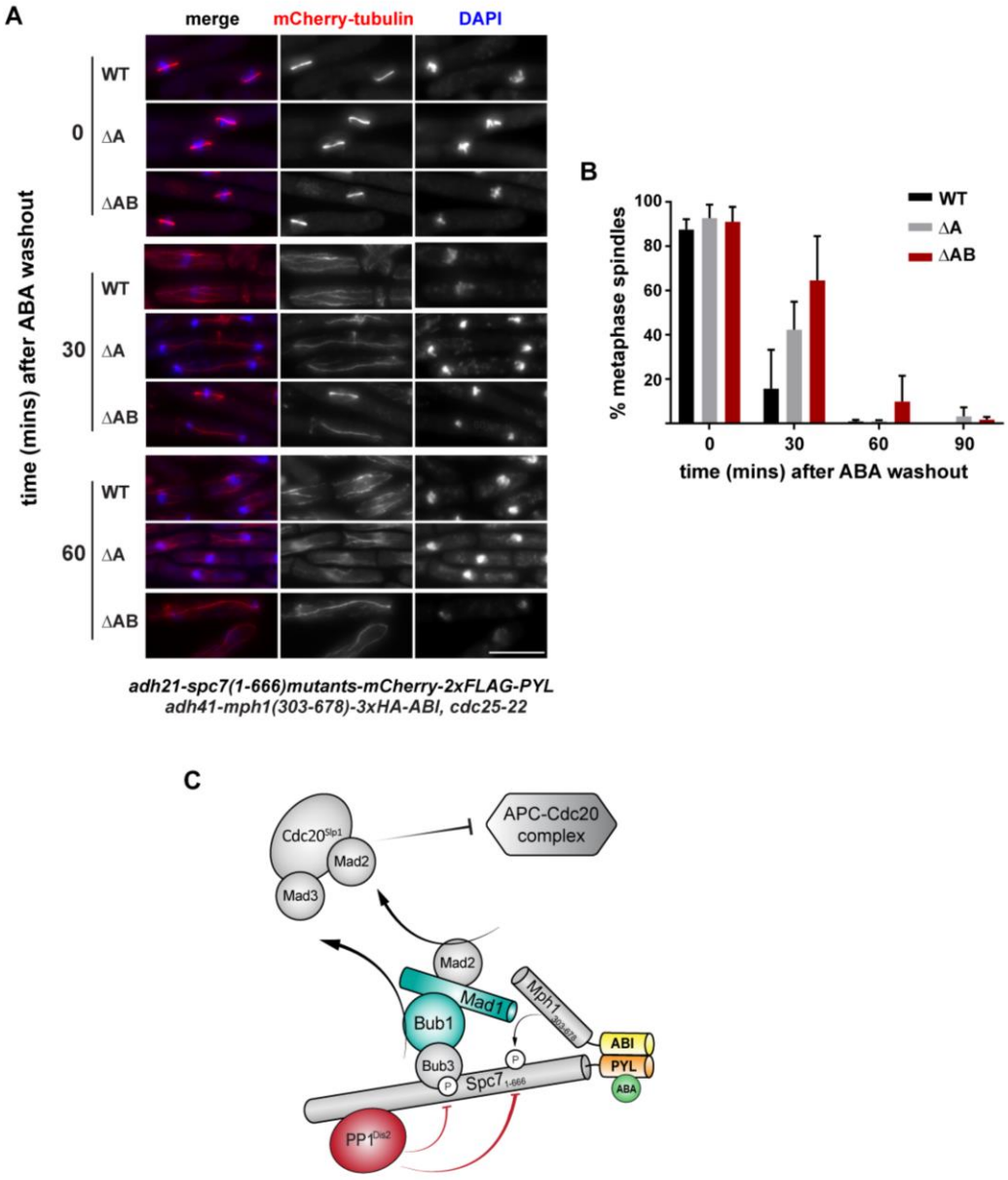

Figure 5.4 Checkpoint silencing in SynCheckABA is delayed by deletion of Spc7^{KNL1} binding sites for PP1^{Dis2}. (A) Images of cells expressing wild-type Spc7$_{1-666}$ (WT) or Spc7$_{1-666}$ mutants with deletion of the A motif alone (ΔA) or of both the A and B motifs (ΔAB). ABA wash-out was performed (at time zero) and time points were analysed 0, 30- and 60-minutes post-wash. Scale bar: 10µm. (B) Quantification of release from checkpoint arrest in WT, ΔA and ΔAB strains. The experiment was repeated three times. More than 100 cells were analysed per strain at each time point. Data are plotted as mean ± s.d. (C) Schematic illustration of checkpoint silencing in SynCheckABA system. Checkpoint activators (Mph1-ABI) and silencing factors (PP1) bind in close proximity on the Spc7-PYL scaffold. The balance of their respective activities determines levels of MCC produced, and whether anaphase onset is inhibited. Figure adapted from Amin *et al*, 2019.

5.4.2 Recruitment of Dis2 via Klp5/Klp6 heterodimers

A second pool of PP1 Dis2 localises to endogenous kinetochores via motor proteins Klp5 and Klp6 (kinesin-8 homologs). To test whether this pathway is also involved in silencing the ectopic SynCheckABA arrest, Klp6 was deleted. Klp5 and Klp6 function as a heterodimer, so deleting Klp6 should be sufficient to abolish this localisation.

Mutation of either Klp5 or Klp6 results in aberrant chromosome movements and stabilisation of microtubules (Garcia *et al*, 2002b; Gergely *et al*, 2016; Meadows *et al*, 2011; West *et al*, 2001, 2002; Klemm *et al*, 2018). Metaphase spindles are unusually long, and so measuring spindle elongation is not a suitable method for scoring progression through the arrest. In these experiments, Cdc13-GFP depletion was used to monitor checkpoint silencing.

Timecourse experiments of SynCheckABA silencing were performed as for the Spc7 PP1-binding site mutants (Section 5.4.1). Deletion of Klp6 was found to significantly reduce silencing efficiency and rate of cyclin B degradation (Figure 5.5). This phenotype is likely to be due to loss of Dis2 recruitment to the mitotic spindle.

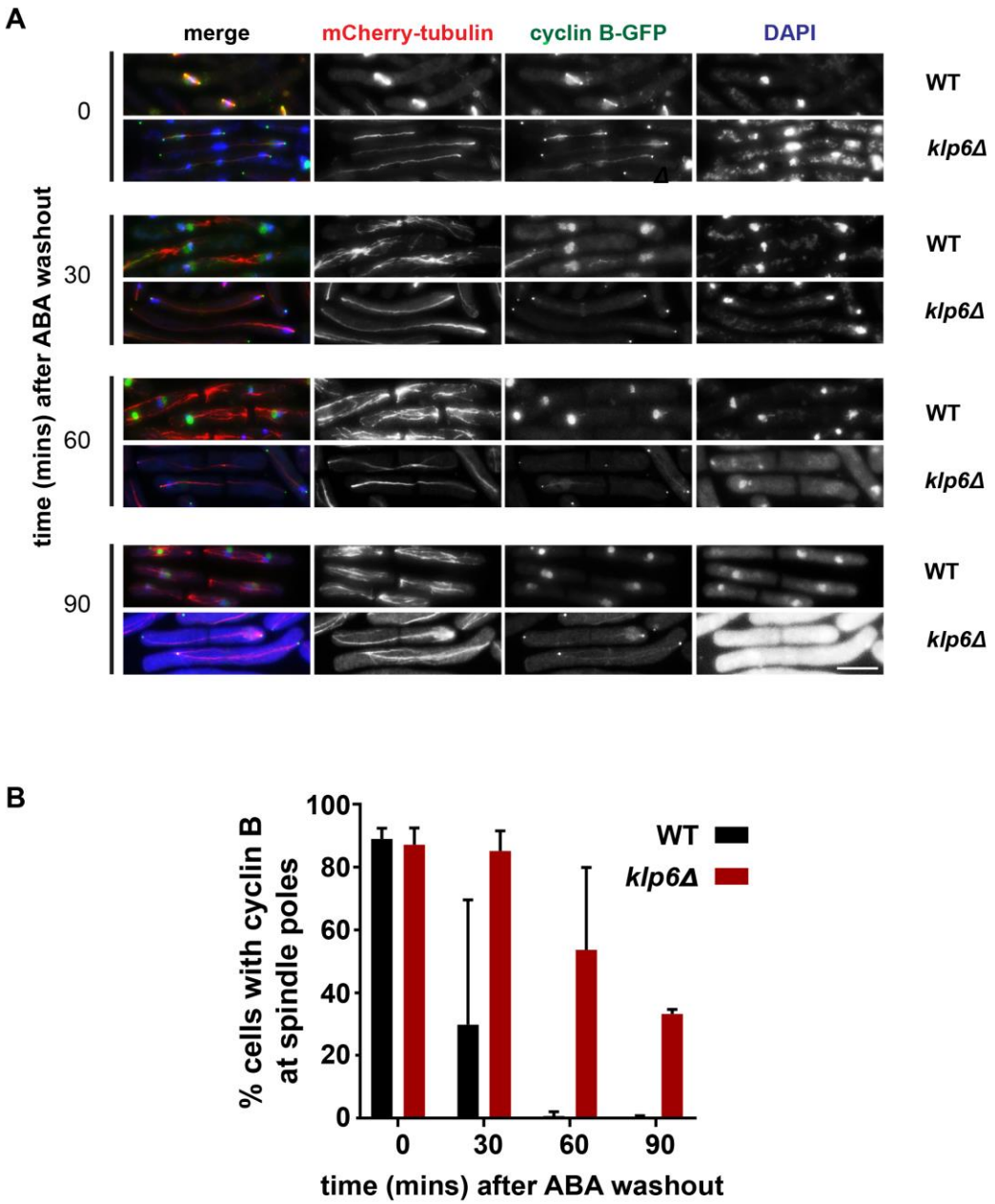

Figure 5.5 Checkpoint silencing in SynCheckABA is also delayed when other recruitment sites for PP1 are removed from spindles. (A) Deletion of Klp6 (kinesin-8) impairs silencing efficiency. Images of cells with and without Klp6 deleted are shown after ABA wash-out (time zero) and 30, 60- and 90-min post-wash. Microtubules are seen in red (mCherry-Atb2), cyclin B in green (Cdc13-GFP) and chromatin in blue (DAPI). Scale bar: 10µm. (B) Quantification of this release from checkpoint arrest in strains with (WT) and without Klp6 (*klp6Δ*). Cells were scored as arrested if Cdc13-GFP was enriched at spindle poles. This experiment was repeated three times. More than 100 cells were analysed per strain at each time point. All data are plotted as mean ± s.d. Figure adapted from Amin *et al*, 2019.

5.4.3 Effects of deleting Dis2 in SynCheckABA

To directly test whether Dis2 plays a role in silencing SynCheckABA, *dis2* was deleted in this system. *dis2Δ* cells were sick even in the absence of synthetic checkpoint induction, as microscopy images reveal many dead cells and cells with defects in cell morphology (Figure 5.6). They also exhibit significant mitotic delays. These defects are likely due to pleiotropic functions of Dis2 in mitosis.

Upon induction of the SynCheckABA arrest and subsequent wash-out, the *dis2Δ* strain experienced extreme defects in checkpoint silencing, as levels of metaphase arrested cells did not decrease over the 90 minute timecourse.

This result confirms that Dis2 is important for silencing of the SynCheckABA arrest and supports our hypotheses that the phenotypes caused by deletion of Spc7 PP1-binding motifs or Klp6 are a result of their roles in Dis2 recruitment.

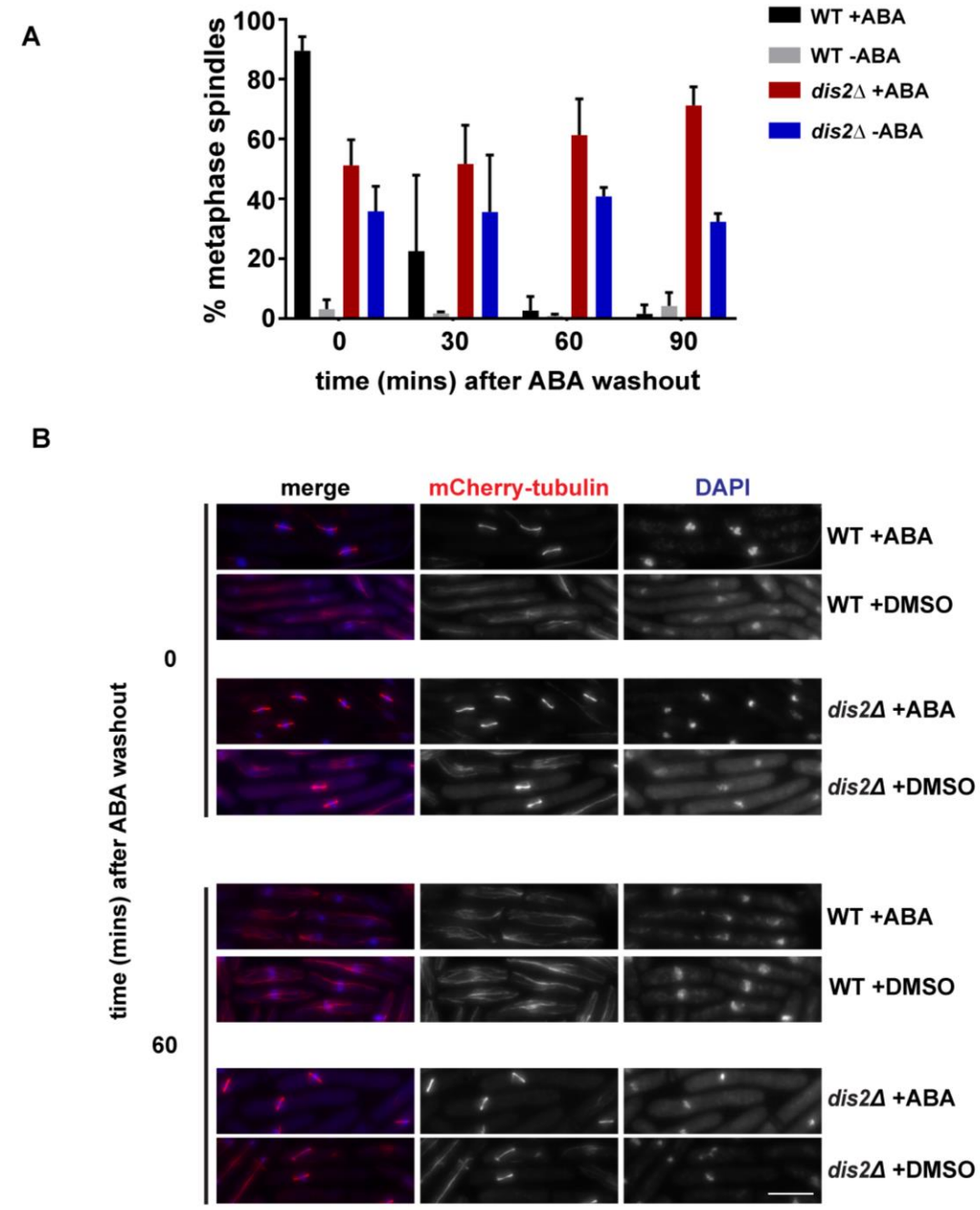

Figure 5.6 Checkpoint silencing in SynCheckABA is severely delayed when PP1^{Dis2} is deleted. (A) Quantification of the release from the checkpoint arrest is shown for wild-type and *dis2Δ* cells (plus ABA or DMSO). Cells were scored as metaphase arrested if they had short metaphase spindles and a single mass of condensed chromatin. Results for DMSO controls show that *dis2Δ* cells are generally sick, but that ABA addition induces the SynCheckABA, resulting in elevated levels of metaphase-arrested cells. This arrest persists for >60 m after ABA wash-out as *dis2Δ* cells struggle to silence the checkpoint. This experiment was repeated three times. More than 200 cells were analysed per strain at each time point. (B) Images of cells with and without Dis2 deleted are shown after ABA wash-out (time zero) and 60 min post-wash. Microtubules are seen in red (mCherry-Atb2), and chromatin in blue (DAPI). Scale bar: 10 µm. Figure adapted from Amin *et al*, 2019.

5.5 Conclusions

5.5.1 Model of Dis2 involvement in SynCheckABA

Dis2 is an important, conserved silencing factor. PP1 binds to Spc7 at its N-terminus, at sites which are near the conserved MELT motifs. When phosphorylated by Mph1, the MELT motifs can be bound by Bub3-Bub1 complexes and initiate MCC formation (Shepperd *et al*, 2012). Thus, Spc7 acts as a scaffold for both activation of the spindle checkpoint by Mph1 kinase and silencing by PP1 Dis2 phosphatase (Meadows *et al*, 2011) (Figure 5.7). It is likely that the proximity of these sites is important for integrating these two opposing functions.

The results presented here (and in Amin *et al*, 2019) provide support for the hypothesis that Dis2 is important in silencing the arrest induced by SynCheckABA. As deletions of Spc7 PP1-binding sites or Klp6 also delay silencing, and both of these are involved in recruiting PP1 Dis2 during silencing of the endogenous SAC, this indicates that the same pathways could also be responsible for recruiting Dis2 in SynCheckABA (model in Figure 5.7).

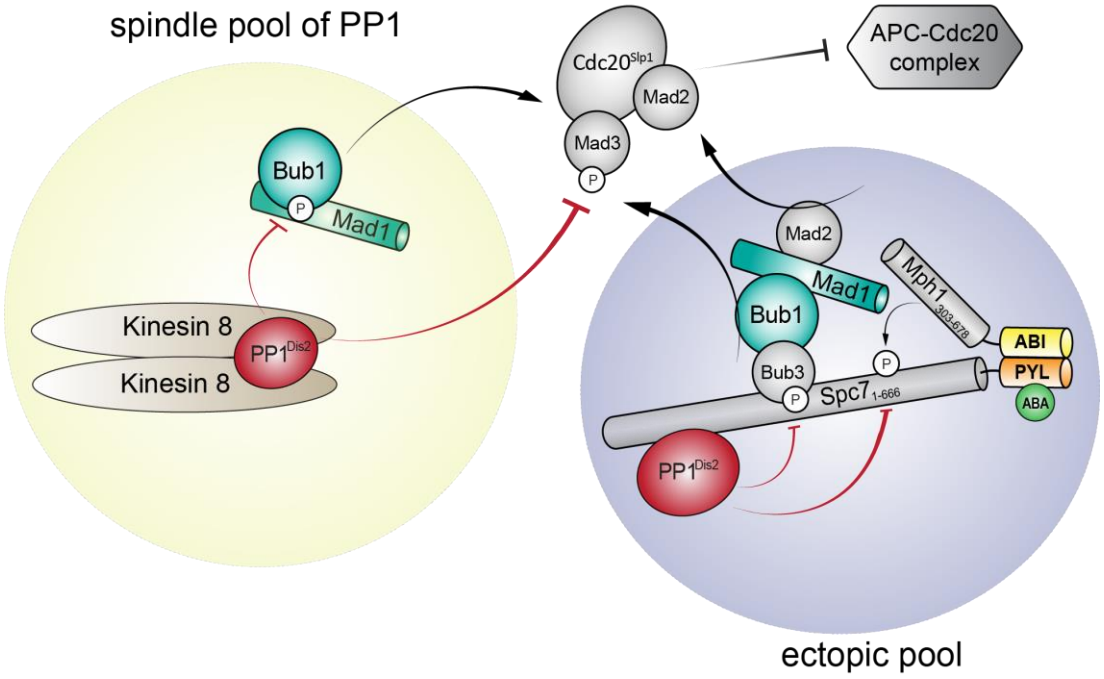

Figure 5.7 Schematic model of PP1-dependent SAC silencing pathways. This model shows two pools of PP1, one recruited via Spc7 A and B motifs to the ectopic SynCheckABA Spc7-Mph1 scaffold, and a second pool recruited via interaction with kinesin-8 (Klp6) to the mitotic spindle. These two pools co-operate to enable checkpoint silencing by inhibiting MCC formation and activity. Model from Amin *et al*, 2019.

These results are important, as not all aspects of silencing will necessarily be preserved in the SynCheckABA system. Any kinetochore-specific factors or processes will not be reproduced at the ectopic signalling platform. This shows that at least some endogenous checkpoint silencing factors are important for exit from a SynCheckABA arrest, which supports our view of this system as an important tool for studying SAC silencing. SynCheckABA will be useful in studying Dis2 in more depth, and in the study of novel checkpoint silencing factor mechanisms.

As we have seen from poor viability of *dis2Δ* in both the SynCheck and SynCheckABA backgrounds even in the absence of checkpoint induction, pleiotropic effects of deleting Dis2 make these strains difficult to work with and complicate analysis of its silencing functions. The Spc7 and Klp6 mutant strains constructed in this work could selectively

disrupt regulation of Dis2 silencing pathways and allow dissection of these mechanisms without disrupting other Dis2 functions.

5.5.2 Future directions

Future work will involve testing double mutants with *spc7ΔAB* and *klp6Δ*, to see if simultaneously disrupting both pathways of Dis2 recruitment abolishes silencing of SynCheckABA, like *dis2Δ*.

Another aim would be to construct Spc7 with the B motif deleted individually. Although it is possible to infer that the B motif has an important contribution to Dis2 recruitment from the more severe checkpoint silencing defect of ΔAB compared to ΔA, it would be informative to see this effect in isolation. In other studies, the B motif has been shown to be more important for Dis2 recruitment (Meadows *et al*, 2011; Liu *et al*, 2010). However, there is evidence to suggest that the A motif also plays an important role in this process, but some studies support its involvement (Meadows *et al*, 2011; Espeut *et al*, 2012; Bajaj *et al*, 2018). Our results support a role for the A motif, as ΔA has clear silencing defects even when the B motif is intact. It is possible that this role is more significant in the ectopic context, in the absence of other interactions, than at kinetochores.

The experiments described in this chapter were performed in strains with endogenous Mph1, so there is a possibility that checkpoint activation and/or silencing may involve kinetochores. It has been demonstrated that endogenous Mph1 is not required for either SynCheckABA arrest or for the subsequent silencing of this arrest (Amin *et al*, 2019). However, it has not been ruled out that kinetochores might make a non-essential contribution to SynCheckABA silencing. A focus of future work will be to repeat silencing assays with *klp6Δ* strains in a *mph1Δ* background.

Despite being a key checkpoint silencing factor, important downstream targets of Dis2 remain to be determined. One of the advantages of the synthetic checkpoint systems are that they avoid the complexity of kinetochores, which may prove useful in identifying key regulatory interactions of Dis2. Future studies will focus on testing known interactors of Dis2 to see whether they are involved in regulating its silencing functions in SynCheckABA. Candidates identified in Vanoosthuyse *et al*, 2014 will be of particular interest. As discussed in Chapter 4, Reg1 is one such PP1 Dis2 interactor which also came out as a candidate from our SynCheck screen (rTetR system). However, in the SynCheckABA system deletion of Reg1

did not have a strong effect on silencing. It may be possible to sensitise strains to the effects of deleting interactors such as Reg1 by disrupting one of the paths of Dis2 recruitment, i.e. constructing double mutants with either *spc7ΔAB* or *klp6Δ*. This approach could also demonstrate which pathway of Dis2 regulation such factors are involved in.

CHAPTER 6

Discussion

This project aimed to improve our understanding of spindle checkpoint silencing. The motivation behind this goal is that the spindle checkpoint is a fundamental cellular process and studying it in more detail could enhance our understanding of cell cycle checkpoints and signalling in general. Increased knowledge of checkpoint silencing may have therapeutic applications, for example in cancer treatment. Specifically, we aimed to identify novel factors involved in SAC silencing and characterise these in more detail. Our approach was divided into two main sub-aims:

1) Identify novel checkpoint silencing factors in a high-throughput screen
2) Characterise known checkpoint silencing factor $PP1^{Dis2}$

This chapter will discuss each of these aims in turn and evaluate how the results presented in this work have contributed to their fulfilment. It will also tackle the issue of how these findings fit into the broader context of research on spindle checkpoint silencing.

6.1 Identifying new components of SAC silencing pathways

This project set out to perform a high-throughput screen to identify candidate checkpoint silencing factors in *S. pombe*. This was done by testing the ability of strains from a single-gene deletion library to overcome a metaphase arrest induced by a synthetic, ectopic version of the spindle checkpoint (SynCheck). The rationale behind performing a high-throughput screen was that since spindle checkpoint silencing has not been extensively studied to date, there may be undiscovered pathways which could be identified by taking a broad approach.

To date, checkpoint silencing factors have been identified in a number of ways:

- $PP1^{Dis2}$ was discovered to play a role in checkpoint silencing in fission yeast after being selected as a likely candidate, based on observations that it counteracted phosphorylation by Aurora B in other systems (Vanoosthuyse & Hardwick, 2009; Pinsky *et al*, 2006; Emanuele *et al*, 2008; Wang *et al*, 2008).

- In humans, PP1 and PP2A-B56 were identified as hits in an RNAi screen for phosphatases involved in silencing (Nijenhuis *et al*, 2014).
- p31^{comet} was identified in HeLa cells in a screen for Mad2 interactors (Habu *et al*, 2002). This screen was not specifically aiming to identify checkpoint silencing factors but trying to characterise Mad2 more generally. TRIP13 and p31 co-operate to deactivate Mad2 and disassemble the MCC. TRIP13 was identified as a candidate checkpoint silencing factor in a data-mining study which searched for proteins which were reported to co-localise or physically interact with a query set of known mitotic and kinetochore proteins (Tipton *et al*, 2012). TRIP13 was shortlisted for further study on the basis that it localises to kinetochores and interacts with p31^{comet} (Tipton *et al*, 2012; Rual *et al*, 2005; Stelzl *et al*, 2005).
- The silencing mechanism of dynein-mediated stripping of SAC proteins from kinetochores was predicted based on a few observations. It was observed that several kinetochore components, including SAC components such as Mad2, were relocalised to spindle poles. This relocalisation was found to be dependent on microtubules, which led investigators to suspect a microtubule motor such as dynein was involved (Howell *et al*, 2001). The importance of stripping of SAC components from kinetochores for silencing was supported by the demonstration that cells fail to silence the checkpoint when Mad1 is constitutively tethered to kinetochores (Maldonado & Kapoor, 2011).

A unifying feature of the discoveries of the SAC silencing mechanisms described above is that the search parameters were restricted, either by looking for interactors of a specific protein, or by investigating a particular cellular phenomenon, e.g. localisation of Mad2 to SPBs. Where screens were performed, these were limited to a specific class of proteins (e.g. phosphatases). Although these approaches have been successful in identifying several silencing mechanisms, the lack of a comprehensive screening strategy to date raises the possibility that additional mechanisms remain to be discovered. This observation supports our view that a high-throughput screen for silencing factors, like the one performed as part of this project, is likely to provide valuable new insights. Our approach to this study was novel in that this was the first time that the SynCheck system had been used in a genetic screen.

Candidate checkpoint silencing factors were identified from this high-throughput screen (Section 3.4). Preliminary characterisation was carried out on several of the most promising

candidates, including temperature and benomyl-sensitivity assays. Independent checkpoint silencing assays were also performed on these candidates, to confirm their role in silencing. Two candidates, *sol1Δ* and *grh1Δ* had a synthetically sick phenotype that was reproducible in another synthetic checkpoint system, SynCheckABA (Section 4.5). These shortlisted candidates are ready to be studied in more detail, and longlisted candidates may form the basis of future studies. As such, the results from this screen are likely to be a useful resource for investigating checkpoint silencing.

It remains a possibility that kinetochore enrichment of SAC components is important for silencing the SynCheck arrest. However, no kinetochore proteins were identified as candidates in this screen, in contrast to the results of the previous Mph1 overexpression screen (unpublished work by Karen May), in which 7/64 candidates localise to kinetochores/centromeres. This indicates that any involvement of kinetochores in silencing the SynCheck arrest is likely to be minimal. It may be that localisation of silencing factors to the Mph1-Spc7 signalling platform is sufficient for silencing to occur, or that silencing processes occur away from kinetochores/in cytoplasm/nucleoplasm.

The screening approach that was developed in this work could be extended and improved by repeating the screen with additional query strains. These include using a query strain which has the same SynCheck components, but with endogenous Mph1 deleted. As localisation of $Mps1^{Mph1}$ to kinetochores is a key upstream event in SAC signalling, this will have the advantage of eliminating any contribution of the endogenous checkpoint to amplification or silencing of the SynCheck signal (Ciliberto & Hauf, 2017). This will aid in interpretation of our results by removing any false positives due to disruption of KT-MT attachment, although many of these are likely to have been removed already due to ectopic induction of the arrest. Deletion of endogenous, kinetochore-localised Mph1 has been shown to have a negligible effect on the efficiency of SynCheck arrest (Yuan *et al*, 2016).

Sensitivity is an important consideration in screen design. Various assays for checkpoint silencing vary in the levels of SAC signal which are generated. The stronger the SAC signal, the more likely it is that silencing defects will be apparent, even for factors which only have a mild effect on silencing. However, if the checkpoint signal is too strong, even wild-type cells may struggle to escape the arrest, which will prevent evaluation of synthetically sick phenotypes. The sensitivity of the SynCheck strain used in this screen appears to be

appropriate for identifying candidate silencing factors, since positive control *bub3Δ* was identified. However, additional candidates with weaker silencing phenotypes may be identified by increasing sensitivity. This could be achieved by introducing a mild silencing defective mutation to the SynCheck query strain, e.g. *bub3Δ*.

This screen was performed with an rTetR-Spc7-9TE construct in which some, but not all, of the Spc7 MELT motifs were replaced with phosphomimic mutations. A wild-type version of the rTetR-Spc7 construct could be used in subsequent iterations of this screening strategy. In the presence of rTetR-Mph1, the rTetR-Spc7-WT construct has been shown to induce a checkpoint arrest much more efficiently than rTetR-Spc7-9TE. This suggests that these nine substitutions are not fully mimicking phosphorylation. By modulating the efficiency of the SAC arrest the sensitivity of the screen could be altered, which could result in different candidates being identified in screens using each of these constructs.

A limitation of this screening strategy is that only non-essential genes can be tested. Alternative approaches could be used to screen for essential factors in the future. An approach that could be combined with our existing screen set-up is to use an alternative library which contains conditional mutants, e.g. temperature-sensitive alleles. Some work has been done on developing these resources for fission yeast (Armstrong *et al*, 2007), but these are not yet widely available. Alternatively, a library of auxin-induced degron alleles could be constructed for the essential genes in *S. pombe*. Some progress has been made in developing such alleles, but further technical improvements are probably necessary before a full library of 'inducible-knockout' alleles can be constructed (Kanke *et al*, 2011). Alternatively, a mutagenesis screen could be performed. Mutagenic screens have the advantage of generating not only complete loss-of-function mutants, but also conditional mutants in essential genes, such as temperature-sensitive alleles and/or specific mutations that perturb checkpoint silencing but not other essential functions of these genes. For example, the SynCheck strain could be mutagenised using the chemical mutagen, ethyl methanesulfonate (EMS) (Lee et al, 1992). The checkpoint could then be activated by plating to media lacking thiamine. By incubating multiple replica plates at a range of different temperatures, mutations which cause a temperature-sensitive silencing defect could be identified. However, mutagenesis screens are costly and labour-intensive compared to the screening strategy performed here.

6.1.1 Novel candidates identified by SynCheck screen

This study carried out further characterisation of eight of the most promising candidate silencing factors from the screen. It was found that *sol1Δ* and *grh1Δ* mutants have reduced checkpoint silencing efficiency in both SynCheck and the independent checkpoint system, SynCheckABA. This is a novel result, as neither Sol1 nor Grh1 have previously been reported to be associated with spindle checkpoint silencing. Importantly, these genes are conserved in vertebrate cells, and therefore their study could have implications for human health.

Previously unreported phenotypes were detected for some of the shortlisted candidates. When deleted in a wild-type background, both *tls1* and *SPAC227.17c* were temperature sensitive at 32°C. The biological processes in which SPAC227.17c is involved are currently unclear, however this protein is conserved between yeast and vertebrates and so may be of interest for further study. For these reasons, SPAC227.17c has been listed as a priority unstudied gene on PomBase (https://www.pombase.org/status/priority-unstudied-genes). Other phenotypes obtained in our assays agreed with phenotypes reported in the literature. *sol1Δ* was confirmed to be benomyl sensitive, as reported previously, however the cold-sensitive phenotype reported in the same paper was not reproduced in our experiments (Monahan *et al*, 2008).

As discussed in Chapter 4, additional experiments could be performed to test general functions of the candidate silencing factors from the high-throughput screen. For example, chromosome segregation could be monitored by microscopy to check for defects. Growth curve analysis could be performed in different liquid growth media. The most promising factors could be investigated further, e.g. by fluorescently tagging proteins to monitor localisation by microscopy and to allow identification of interactors by co-immunoprecipitation and mass spectrometry analysis.

There are other factors from the screen which were not characterised which might also be worthy of further study. Mss116 is one such factor, which displayed a strong synthetically sick phenotype in the screen. Mss116 is a predicted mitochondrial ATP-dependent RNA helicase. *S. cerevisiae* Mss116 has been shown to be involved in mitochondrial gene expression, e.g. splicing of mitochondrial transcripts (Szczesny et al, 2013). It is possible that *S. pombe* Mss116 could affect transcription of mitochondrial genes, including those involved in the intrinsic apoptotic pathway. The intrinsic apoptotic pathway involves mitochondrial outer membrane permeabilisation (MOMP). Dysregulation of apoptosis by

disruption of mitochondrial function could sensitise *mss116Δ* to the effect of the metaphase arrest induced by SynCheck. In some systems prolonged checkpoint arrest in metaphase is followed by apoptosis, indeed this is thought to be why taxol is such a good chemotherapeutic agent (Jordan *et al*, 1996; Tao *et al*, 2005; Rieder & Maiato, 2004; Gascoigne & Taylor, 2009).

The analysis of the screen data presented has focused on synthetically sick interactions. However, synthetically healthy phenotypes were also identified, in which deletion mutations rescued strains from the mildly reduced growth and low levels of cell death induced by SynCheck (Section 3.4.5 and Appendix 1, 1.6.2). These factors would also be interesting to study in more detail, as they could be negative regulators of silencing pathways.

6.1.2 Evaluation of Sol1 as a possible SAC silencing factor

Sol1 deletion caused severe defects in both SynCheck and SynCheckABA silencing assays. From these results, it seems that *sol1Δ* reduces the efficiency with which cells can exit a SAC arrest, at least in a synthetic, ectopic system.

In SynCheckABA cells, *sol1Δ* is associated with increased Mph1-ABI levels, which is likely to cause higher levels of checkpoint activation. Increased levels of MCC complex may explain the delay in silencing observed in this assay, rather than defects in checkpoint silencing pathways. It has yet to be confirmed whether Sol1 affects the expression level of rTetR-Mph1 in SynCheck strains, or whether it impacts endogenous Mph1 levels. Whether Sol1 exerts its effects at the level of SAC activation or silencing, it is an interesting candidate for further study.

To test whether *sol1Δ* affects silencing of the endogenous spindle checkpoint, this deletion was tested in a microtubule-independent silencing assay, i.e. *nda3-KM311*. No delay in mitotic exit was detected in this assay. However, one drawback of the *nda3-KM311* experiment is that silencing typically takes place very rapidly, so it may be difficult to detect minor defects; in the previous Mph1 overexpression screen (Karen May, Hardwick lab), none of the 9 candidates tested were found to have delayed checkpoint silencing in the *nda3-KM311* arrest, and even the silencing phenotype of confirmed silencing mutant *bub3Δ* was challenging to detect. It will be important to test *sol1Δ* in more sensitive assays. For

example, it would be useful to test the effect of *sol1Δ* on silencing an arrest generated by the endogenous SAC, e.g. by using the spindle poison CBZ.

Sol1 contains a DNA binding domain (ARID, AT-rich interaction domain) (Dallas *et al*, 2000). It also contains an Armidillo-type fold which is thought to mediate protein-protein interactions (Sandhya et al, 2018). Sol1 is a component of SWI/SNF, a highly conserved chromatin remodeling complex.

Sol1 homologs include *S. cerevisiae* Swi1 and human ARID1A (also known as BAF250a) and ARID1B. ARID1A has strong associations with human cancers. ARID1 mutations have been identified across a wide range of tumour lineages, including ovarian clear cell carcinoma, uterine cancers, gastric cancers, breast cancer, hepatocellular carcinoma, and more (Shen *et al*, 2015). The exact role of ARID1A deficiency in cancer development is unclear and may be due to effects of the SWI/SNF complex on transcription of other cancer-associated genes, or due to impaired DNA repair. However, it is possible that dysregulated SAC signalling could also play a role in ARID1A/1B-mediated oncogenesis.

To confirm that SWI/SNF activity is responsible for the observed *sol1Δ* phenotypes, other subunits could be deleted to see if they recapitulate the checkpoint silencing phenotype, e.g. catalytic component Snf22. If other components of SWI/SNF also have an effect on checkpoint silencing, this will suggest that SWI/SNF is involved, rather than an additional unknown function of Sol1.

Since *sol1Δ* practically abolishes silencing in the SynCheckABA assay, synthetic interactions which exacerbate the phenotype are unlikely to be detectable. If deletions of other components of the SWI/SNF complex cause a milder checkpoint silencing defect, it would be possible to use these to test for genetic interactors.

SWI/SNF could play a role in SAC silencing either via effects on transcription or by playing a more direct, non-transcriptional role. The chromatin remodelling activity of SWI/SNF complexes allow them to facilitate the binding of transcription factors or repressors. *S. pombe* SWI/SNF affects the expression of genes involved in multiple processes and is involved in both activation and repression of transcription (Monahan *et al*, 2008). SWI/SNF may play a role in silencing by upregulating expression of checkpoint silencing factors or by downregulating expression of checkpoint activators, e.g. Mph1. This regulation may be direct (for example, increased Mph1-ABI expression could be mediated through a direct effect on the *adh41* promoter) or indirect via effects on expression of intermediate factors.

Other chromatin remodelers play important roles in cell cycle regulation. In some cases, these functions rely on non-transcriptional functions of these complexes. There is evidence to suggest that chromatin state changes during mitosis and may be altered in response to checkpoint activation. For example, mammalian bromodomain protein Brd4 is removed from chromatin upon activation of the checkpoint by adding microtubule poisons (Nishiyama *et al*, 2006). Chromatin remodellers at human centrosomes have been demonstrated to be involved in various processes including microtubule organisation, recruitment of centrosomal proteins, and cytokinesis.

It is also possible that SWI/SNF could have non-chromatin associated roles. In *S. cerevisiae*, SWI/SNF interacts with the checkpoint kinase Mec1. Deletion of the core ATPase subunit of SWI/SNF, Snf2 (homolog of *S. pombe* Snf22), reduces Mec1 activity *in vivo*, and cross-linking experiments showed that SWI/SNF physically interacts with Mec1 (Kapoor *et al*, 2015). It was shown *in vitro* that SWI/SNF complexes are capable of activating Mec1 in the absence of chromatin. The subunit requirements for this activity differ from subunits required for chromatin remodeling. Regulation of kinases involved in SAC signalling by a similar mechanism could be a possible explanation for the SynCheckABA silencing phenotype in *S. pombe*.

6.1.3 Evaluation of Grh1 as a possible SAC silencing factor

Deletion of *grh1* had an effect in both SynCheckABA and the rTetR-based SynCheck screen. In both assays this mutation had a mild phenotype. The effect of *grh1Δ* has not been tested in an endogenous checkpoint silencing assay so far, so this will be an important next step.

It was noted that the *grh1* CDS is in proximity to the CDS of another candidate identified in the screen, *tls1* (Figure 4.3). It is possible that the phenotype of one of these deletion strains in the screen was due to deletion of one gene disrupting flanking sequences of the other gene which are important for regulating its expression. Since *tls1Δ* did not have a phenotype in the SynCheckABA screen, it may be that Tls1 is not a true silencing factor. However, *tls1Δ* had a stronger phenotype than *grh1Δ* in the SynCheck screen, so it is not clear whether *tls1Δ* affects *grh1Δ* or vice versa, or whether these genes have phenotypes which are independent of each other.

To test this, *grh1Δ* and *tls1Δ* SynCheck strains could each be transformed with an exogenous copy of either *grh1* or *tls1*, to see if these rescue the silencing phenotypes. If

tls1Δ causes synthetic sickness in SynCheck by reducing Grh1 expression, exogenous expression of Grh1 should rescue this phenotype. However, if the *tls1Δ* phenotype is rescued by Tls1 expression, it would indicate a more direct involvement of Tls1 in silencing. This hypothesis could be further investigated by tagging these proteins and performing western blots to monitor protein expression levels in wild-type strains compared to strains with the other gene deleted.

6.2 Studying $PP1^{Dis2}$ -mediated silencing with SynCheckABA

$PP1^{Dis2}$ has been demonstrated to be an important, highly conserved checkpoint silencing factor which is found in yeasts, *C. elegans*, Drosophila and humans (Vanoosthuyse & Hardwick, 2009; Pinsky *et al*, 2009; Meadows *et al*, 2011; Espeut *et al*, 2012; Moura *et al*, 2017; Liu *et al*, 2010; Rosenberg *et al*, 2011). However, the mechanisms of $PP1^{Dis2}$ regulation and its important downstream targets remain unclear.

It has been demonstrated *in vitro* that human $PP1^{Dis2}$ is recruited to KNL1 via PP1-binding domains, i.e. the SILK and RVSF domains (Liu *et al*, 2010; Nijenhuis *et al*, 2014; Bajaj *et al*, 2018). These domains are highly conserved, and their importance for PP1-mediated SAC silencing has been demonstrated *in vivo* in yeast and *C. elegans* (Meadows *et al*, 2011; Rosenberg *et al*, 2011; Espeut *et al*, 2012). The *S. pombe* consensus sequences for these motifs are KGILK and RRVSF respectively.

It has been shown that $PP1^{Dis2}$ is also recruited to the mitotic spindle by kinesin-8 motors (Meadows *et al*, 2011). This additional pool of $PP1^{Dis2}$ also makes an important contribution to checkpoint silencing. In *S. pombe*, it has been demonstrated that deleting kinesin-8 homologs (Klp5 and Klp6) reduces silencing efficiency, and that a double mutant with both PP1-binding domains of Spc7 deleted (ΔAB) and Klp5/Klp6 deleted dramatically reduces silencing efficiency, to levels similar to *dis2Δ* strains (Meadows *et al*, 2011).

This study aimed to address whether $PP1^{Dis2}$ plays a role in silencing SynCheckABA and whether this system could be used for studying the mechanisms of this silencing pathway in more detail (Chapter 5).

6.2.1 $PP1^{Dis2}$ appears to be involved in silencing the SynCheckABA arrest

The results obtained in this study indicate that Dis2 is involved in silencing the SynCheckABA signal.

The effect of Dis2 on checkpoint silencing was tested directly in *dis2Δ* cells. *dis2Δ* cells experienced delays in silencing compared to wild-type cells, however these cells were very sick even in the absence of SynCheckABA induction, which complicated the analysis.

Additional results which support Dis2 playing a role in SynCheckABA silencing were obtained from experiments which disrupted pathways involved in endogenous $PP1^{Dis2}$-mediated silencing. We hypothesised that the same pathways might also affect SynCheckABA silencing if Dis2 were involved.

PP1-binding motifs in Spc7 are required for Dis2 recruitment to the endogenous kinetochore. Deletion of these motifs in the Spc7-PYL construct had a detrimental effect on SynCheckABA silencing, presumably due to disruption of $PP1^{Dis2}$ recruitment to the ectopic signalling platform. The fact that that deleting *klp6* also had a detrimental effect on silencing SynCheckABA provides further support for the involvement of Dis2 in SynCheckABA silencing, as Klp6 is involved in the other known mechanism of Dis2 recruitment in the endogenous SAC.

It will be necessary to confirm that the ΔA and ΔAB mutations in Spc7-PYL disrupt $PP1^{Dis2}$ recruitment to the ectopic signalling platform. An important next step will be to perform coimmunoprecipitation experiments with different Spc7-PYL constructs to compare their PP1-binding affinity with the wild-type construct.

6.2.2 Regulation of $PP1^{Dis2}$ silencing in SynCheckABA has similarities to endogenous SAC silencing

The results obtained in Dis2 experiments with the SynCheckABA system are similar in many respects to those from studies of Dis2 in the endogenous SAC. This shows that SynCheckABA is likely to be a good system for studying Dis2 in more detail.

In *S. pombe*, deletion of either the KGILK (A) or RRVSF (B) binding motifs in $KNL1^{Spc7}$ is lethal (Meadows *et al*, 2011). A key study overcame this limitation by complementing deletion of these binding motifs in endogenous Spc7 by co-expressing a non-kinetochore localised wild-type version of Spc7 (residues 1-666 only) (Meadows *et al*, 2011). As other studies

have shown, the N-terminus of KNL1^{Spc7} is sufficient for microtubule binding and the localisation of KNL1^{Spc7} to the mitotic spindle (Kerres *et al*, 2007; Bajaj *et al*, 2018). Spc7$_{1-666}$ may recruit PP1^{Dis2} to the mitotic spindle, allowing it to compensate for endogenous Spc7 mutation (Meadows *et al*, 2011). This rescues cell viability but does not restore silencing efficiency to normal levels, allowing the effects of Dis2 recruitment on checkpoint silencing to be studied. The SynCheckABA system employed here differs from this study in that strain viability is maintained by leaving endogenous Spc7 intact, and only introducing PP1-binding site deletions into the Spc7-PYL construct of the SynCheckABA system.

The fact that deletion of PP1-binding motifs in the Spc7-PYL construct delayed SynCheckABA silencing indicates that recruitment of Dis2 to the ectopic signalling platform itself is important for silencing. Spc7-PYL may act as a scaffold not only for the assembly of spindle checkpoint activators, but also for concentrating downstream targets and/or regulators of Dis2 that are important for its checkpoint silencing functions. This ectopic system avoids the complexity of kinetochores and provides an ideal system for identifying key PP1 interactors involved in checkpoint silencing. Co-immunoprecipitation experiments with Spc7-PYL may produce a subset of Spc7- and Dis2- interactors which are relevant for their checkpoint silencing functions.

The results obtained in this study also provide information on the relative importance of the PP1-binding motifs in SynCheckABA. Although the B motif was not tested in isolation, we can infer from the more severe phenotype of the ΔAB mutant compared to ΔA that the B motif makes a major contribution to this phenotype (Figure 5.4).

These results are similar to what is reported in the literature for endogenous Spc7. The conserved RVSF motif has been widely recognised to be involved in PP1 recruitment and silencing (Meadows *et al*, 2011; Liu *et al*, 2010; Espeut *et al*, 2012; Rosenberg *et al*, 2011; Nijenhuis *et al*, 2014). However, the role of the SILK motif has been the subject of much debate. Several studies have reported evidence for the involvement of SILK in PP1^{Dis2} binding (Meadows *et al*, 2011; Nijenhuis *et al*, 2014; Bajaj *et al*, 2018), however other reports contradict these (Liu *et al*, 2010). Immunoprecipitation of *S. pombe* Spc7 N-terminus showed that deleting either the KGILK or RRVSF motif results in reduced binding to PP1^{Dis2}, although deleting RRVSF has a larger effect (Meadows *et al*, 2011). The importance of SILK for PP1 recruitment is further supported by a recent study, which revealed that the SILK domain directly contacts PP1 in the crystal structure of the human

KNL1:PP1^{Dis2} holoenzyme (Bajaj *et al*, 2018). This study also showed that deletion of the SILK domain causes a 6-fold reduction in PP1 recruitment (Bajaj *et al*, 2018). It has also been shown that deletion of KGILK causes defects in checkpoint silencing *in vivo* in fission yeast (Meadows *et al*, 2011). Deletion of both the KGILK and RRVSF motifs in combination caused a more severe silencing delay (Meadows *et al*, 2011).

In contrast to the previous *S. pombe* study which mutated endogenous Spc7 PP1-binding motifs, it appears as though deleting the A motif alone has an effect on silencing in the SynCheckABA experiments presented in this thesis (Meadows *et al*, 2011). It is possible that the KGILK motif is particularly important at the ectopic SynCheckABA scaffold, in the absence of other kinetochore-based interactions which could promote PP1 binding.

Deletion of the KGILK domain in *S. pombe* has been demonstrated to have defects independent of SAC silencing (i.e. abolishing checkpoint function by deleting Mad2 does not rescue its lethal phenotype, unlike RVSF mutants) (Meadows *et al*, 2011). By conducting our study with the ectopic SynCheckABA, we are likely to have avoided disrupting these other functions of Spc7. Unpublished work by Alicjia Sochaj (Hardwick lab) also suggests that the KGILK motif may function as a nuclear import signal, as its deletion appears to reduce nuclear enrichment of Spc7.

Taken together, the data presented in Chapter 5 of this thesis suggests that not only is the function of PP1^{Dis2} required for silencing the ectopic SynCheckABA arrest, but that this system recapitulates aspects of the regulation of PP1^{Dis2} recruitment to endogenous kinetochores. This will make this system a valuable tool for dissecting these regulatory pathways in more detail.

6.2.3 SynCheckABA as a system for studying PP1^{Dis2} silencing mechanisms

The work done so far in this system has established that SynCheckABA may be used to study PP1^{Dis2} mediated checkpoint silencing in more detail. Aspects of PP1^{Dis2} that could be investigated with this system in the future include phosphoregulation of Spc7-Dis2 interactions as well as the identification of key interactors of Dis2.

PP1^{Dis2} in SynCheckABA silencing – remaining questions

Detailed characterisation of this system will be required to establish which aspects of SynCheckABA silencing are similar to the endogenous checkpoint, and which aspects may differ. These results will be important for interpretation of any other results obtained with this system.

Klp5/Klp6 are capable of recruiting PP1 to spindle microtubules, and it is possible that interactions with endogenous kinetochores are involved in the SynCheckABA system. Although it has been demonstrated that endogenous Mph1 is not required for SynCheckABA arrest, nor for silencing, it remains a possibility that localisation of PP1^{Dis2} to the mitotic spindle improves silencing efficiency by dephosphorylating kinetochore-enriched SAC components (Amin et al, 2019). This possibility could be ruled out by repeating these experiments in an *mph1Δ* background.

It will be particularly important to confirm whether the effect of deleting the KGILK domain on silencing is mediated via PP1-binding, because this domain is also associated with microtubule binding. Microtubule binding function of kinetochore-localised KNL1 is not required for SAC activation or formation of stable KT-MT interactions, but is important for silencing (Espeut *et al*, 2012). The N-terminus of KNL1^{Spc7} binds microtubules (Cheeseman *et al*, 2006; Pagliuca *et al*, 2009; Kerres *et al*, 2007). A basic patch immediately upstream of the SILK domain is essential for this interaction (Welburn *et al*, 2010; Espeut *et al*, 2012; Bajaj *et al*, 2018).

To test whether microtubule binding to Spc7-PYL is required for silencing, a microtubule-independent silencing assay could be performed in a SynCheckABA strain which lacks the endogenous checkpoint (*mph1Δ*). After inducing a SynCheckABA arrest, microtubules could be depolymerised using the temperature-sensitive *nda3-KM311* mutation. ABA would then be washed out to release cells from the arrest, and silencing could be monitored by analysis of cyclin B (Cdc13-GFP) degradation. Comparing the silencing efficiencies of the WT, ΔA and ΔAB Spc7-PYL constructs would indicate whether KGILK plays a role in SynCheckABA silencing independently of microtubule binding.

Phosphoregulation of PP1-binding sites in KNL1

As previously mentioned, the N-terminal of KNL1^{Spc7} contains both PP1- and microtubule-binding sites. Phosphorylation of these motifs by Aurora B appears to be important for negatively regulating this binding in both humans and *C. elegans* (Welburn *et al*, 2010; Espeut *et al*, 2012). Conserved Aurora B phosphorylation sites have been identified in the N-terminus of KNL1. These phosphosites are located adjacent to or within the PP1-binding motifs (Figure 6.1). Phosphomimetic mutants of these sites have been shown to abolish binding of both microtubules and PP1 to KNL1, suggesting that Aurora B can negatively regulate PP1 recruitment to KNL1 (Welburn *et al*, 2010; Liu *et al*, 2010; Nijenhuis *et al*, 2014; Bajaj *et al*, 2018).

Previous work in our lab attempted to address whether this mechanism is conserved in fission yeast (unpublished work by Alicjia Sochaj). Ark1 (Aurora B homolog) phosphorylation sites were identified in the N-terminus of Spc7 (residues S9, S28, S108 and S114) (Figure 6.1). Similar to other organisms, phosphorylation sites (S108 and S114) are closely associated with PP1 binding site 'B' (RRV**S**F motif). However, phosphorylatable sites at PP1-binding site 'A' (human: **S**SILK) are not conserved in *S. pombe* (KGILK).

Residues S9 and S28 of Spc7 are also phosphorylated. These sites are in the region of basic patches which have been demonstrated to be important for microtubule binding. Microtubule binding was assayed by coprecipitation experiments, and it was found that introducing phosphomimics of these residues impaired microtubule binding (work by Alicjia Sochaj).

This previous study from our lab went on to assay PP1^{Dis2} binding to Spc7 phosphomutants by performing co-immunoprecipitation experiments with Spc7-GST bound to beads, and it was found that double phosphomimic mutations of Spc7, either S9D S28D or S108D S114D, did not have much of an effect on affinity of Dis2 for GST-Spc7 (Figure 6.1) (unpublished data by Alicjia Sochaj). It is possible that mutating all four residues would have an effect on binding, and this is something that would be interesting to test in the future. We are also interested in testing whether phosphorylation of these residues plays a role in SynCheckABA regulation.

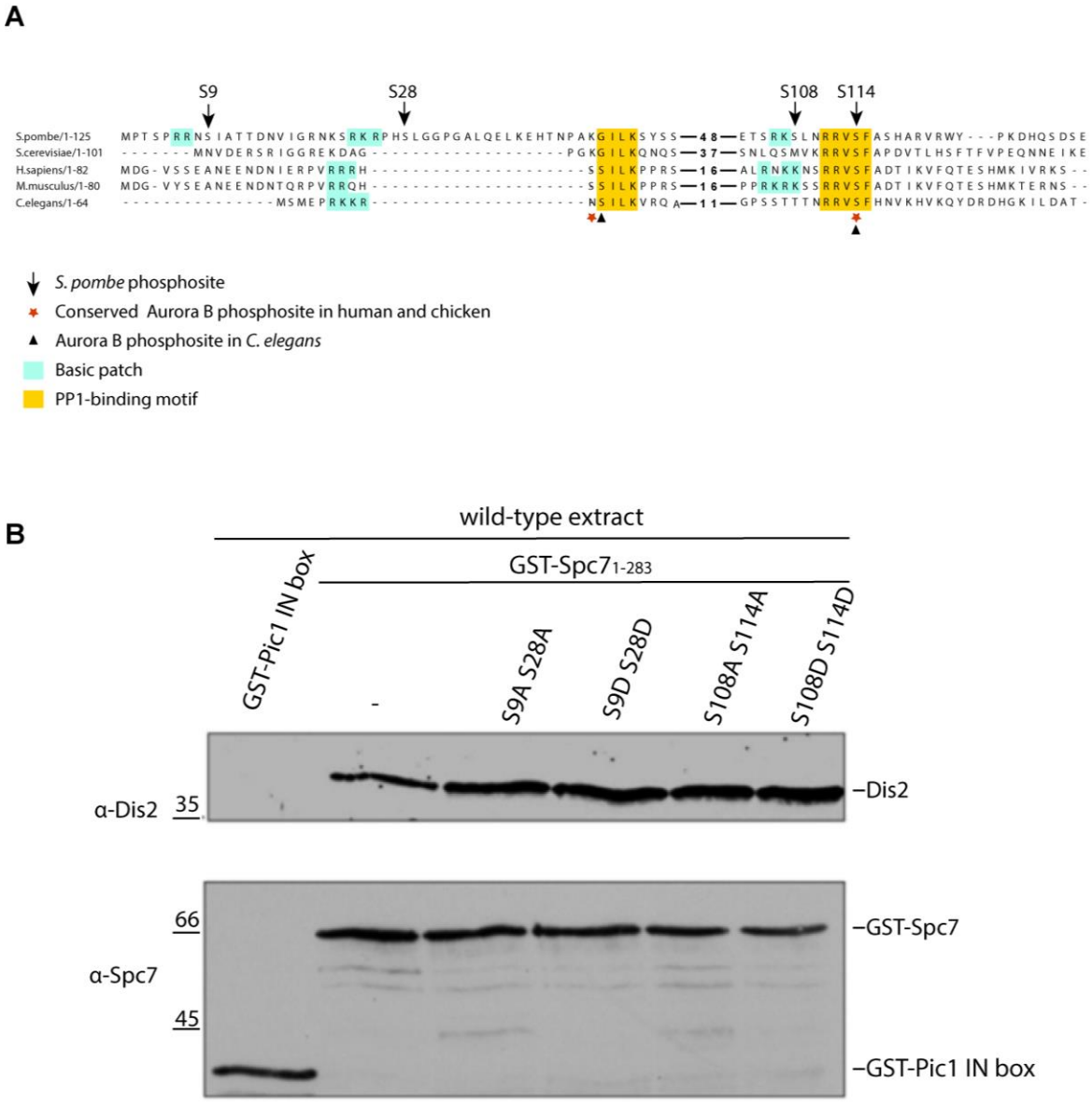

Figure 6.1. Phosphoregulation of PP1-binding sites of KNL1^{Spc7}. (A) Sequence alignment of *S. pombe, S. cerevisiae, H. sapiens, M. musculus,* and *C. elegans* KNL1 homologues. Basic patches are highlighted in blue, and PP1-binding domains in amber (S/GILK and RRVSF). *In vitro* pombe Ark1 sites are indicated (from work by Alicjia Sochaj), as are Aurora B phosphorylation sites in other species (Welburn *et al*, 2010). (B) Immunoblot demonstrating that Dis2 binding to Spc7 does not depend on phosphorylation status of binding sites in *S. pombe*. Pull-downs of GST-Spc7$_{1-283}$ proteins with various phosphosite mutations were run on 10% SDS-PAGE gel. α-Dis2 antibody was used to probe gel. Gel was re-probed with α-Spc7 as a loading control. Data from unpublished work by Alicjia Sochaj.

Targets of PP1^{Dis2}

Another outstanding question about PP1^{Dis2} is what its key downstream targets are. Although we have not directly addressed this question in this work, the system that we have established will be useful for identifying key targets. PP1 may regulate multiple parallel silencing mechanisms, which may vary in their conservation between yeast and higher eukaryotes. It is also possible that PP1 may have multiple targets in the same pathway. Here, I shall discuss various proposed targets of PP1 activity, along with suggestions for how the SynCheckABA system may be used to address these questions in the future.

Inhibition of Mps1 activity at kinetochores is a crucial upstream event in checkpoint silencing (Shepperd *et al*, 2012; Primorac *et al*, 2013; London *et al*, 2012; Yamagishi *et al*, 2012). PP1^{Dis2} may inhibit Mps1 activity in a variety of ways, including prevention of Mps1 recruitment, directly inhibiting Mps1 or by dephosphorylating its key downstream targets.

Experiments in fission yeast have shown that PP1^{Dis2} counteracts the activity of Aurora B homolog, Ark1 (Vanoosthuyse & Hardwick, 2009). It has been shown in other systems that PP1^{Dis2} antagonises Aurora B, thus counteracting Mps1 recruitment. Aurora B phosphorylation of outer kinetochore components, e.g. Ndc80, is important for Mps1 binding (Santaguida *et al*, 2011; Saurin *et al*, 2011; Kemmler *et al*, 2009). In bioriented chromosomes, tension increases spatial separation between Aurora B and its outer kinetochore substrates, allowing the removal of this phosphorylation by PP1^{Dis2}. This activity has not been demonstrated in fission yeast to date. Unfortunately, our system cannot test this hypothesis, because Mps1 recruitment is not regulated by phosphorylation, but rather by dimerisation with Spc7 induced by ABA addition. However, it is worth noting that as PP1^{Dis2} is still required for silencing the SynCheckABA arrest, this indicates that it is important for dephosphorylating targets which function downstream of Mps1 recruitment.

Direct inhibition of Mps1 by PP1 has been demonstrated in Drosophila (Moura *et al*, 2017). In Drosophila, PP1 directly dephosphorylates a T-loop of Mps1 which is required for its activity. It has not been demonstrated that this mechanism is conserved, although mammalian Mps1 does contain PP1-binding motifs.

A key target of Mps1 is KNL1 MELT motifs. These are required for recruiting Bub3-Bub1, and subsequently for Bub1-mediated recruitment of Mad1-Mad2. Dephosphorylation of these motifs abolishes recruitment of SAC proteins to kinetochores, thus inhibiting the

generation of new MCC complexes. Dephosphorylation of KNL1 MELTs has been demonstrated to be dependent on $PP1^{Dis2}$ (London *et al*, 2012)

Although dephosphorylation of KNL1 MELT motifs has been established to be a primary mechanism for PP1 action, it is also possible that PP1 acts on targets downstream of MELTs. This could be tested in SynCheckABA by using Spc7-PYL constructs which have phosphomimic mutations in their MELT motifs. If checkpoint silencing still occurs in phosphomutants, this would suggest that downstream events are able to overcome persistent MELT phosphorylation. If this is the case, it will be possible to test the effects of deleting *dis2Δ*, to see whether it plays an important role in dephosphorylation of downstream targets, or whether its effects are mediated through MELT dephosphorylation. The relative importance of Dis2 for MELT dephosphorylation and for dephosphorylating downstream targets could be tested by comparing the effects of T9E and T12E phosphomutants in wild-type or *dis2Δ* backgrounds.

Additional substrates have been proposed for PP1-dependent dephosphorylation, including Mad3, Cdc20, and Ndc80 (Zich *et al*, 2016; King *et al*, 2007; Kim *et al*, 2017; Kemmler *et al*, 2009).

In summary, the combination of the SynCheckABA system with mutants with impaired $PP1^{Dis2}$-recruitment has provided insights into $PP1^{Dis2}$ silencing mechanisms and will be a useful system for further study.

6.2.4 Broader perspective on $PP1^{Dis2}$

Both the role of $PP1^{Dis2}$ in checkpoint silencing and its specific mechanisms of regulation show high levels of conservation between species. As such, studies of $PP1^{Dis2}$ may have important implications for human health.

PP1 is a commonly mutated factor in cancer. Selective inhibition of PP1 has potential as a cancer therapy. Winkler *et al* (2015) showed that overexpression of NIPP1 (nuclear inhibitor of PP1) causes reduced colony formation and impaired tumour growth in mouse xenografts. NIPP1 overexpression in HeLa cells was shown to cause prometaphase arrests, and led to SAC activation, along with defective spindle formation, chromosome congression and checkpoint silencing defects (Winkler *et al*, 2015). If some cancers are specifically affected by disruption of $PP1^{Dis2}$ activity in checkpoint silencing, more specific inhibition

strategies could be devised. This could result in therapies with reduced toxicity, by avoiding potential side-effects of broad inhibition of PP1.

6.3 SynCheckABA as a system for studying checkpoint silencing

A novel synthetic checkpoint system based on abscisic acid (SynCheckABA) was recently developed (Amin *et al*, 2019). The experiments presented in this thesis demonstrate that this system is suitable for studying spindle checkpoint silencing, establishing this system as a promising new tool for studying the mechanisms of SAC silencing.

In this study SynCheckABA was used both to verify silencing phenotypes of candidates from the screen, and to dissect the mechanisms of silencing pathways in more detail for $PP1^{Dis2}$. The SynCheckABA strains generated as part of this project will be used in future studies into checkpoint silencing, e.g. further characterisation of $PP1^{Dis2}$, Sol1 and Grh1.

SynCheckABA has several advantages as a system for studying SAC signalling, and particularly silencing. Unlike *in vitro* approaches for studying the checkpoint (Minshull *et al*, 1994; Faesen *et al*, 2017), SynCheckABA does not require extensive knowledge of the properties of candidate silencing factors, e.g. stoichiometry, post-translational modifications, or important interactors, to be used to test their function. This makes it particularly well-suited for studying candidates identified from the high-throughput screen, about which we may not have much information. SynCheckABA is also more physiological than other systems; being carried out *in vivo*, downstream checkpoint factors are present at physiological levels and checkpoint silencing can be measured directly by looking at cyclin B degradation. Unlike other *in vivo* systems like *nda3-KM311*, it does not stress cells by imposing cold treatment. The ease with which ABA can be washed out make it ideal for performing release experiments to monitor silencing efficiency.

It has been demonstrated that endogenous Mph1 is not required for either checkpoint activation or silencing in SynCheckABA, however it would be worth checking whether *mph1Δ* affects the kinetics of checkpoint silencing.

SynCheckABA is an example of a synthetic ectopic SAC system. Ectopic systems are emerging as valuable tools for studying the SAC. Another ectopic synthetic checkpoint arrest system has been developed, the eSAC (Chen *et al*, 2019). Similar to the SynCheck and SynCheckABA systems, induction of this arrest relies on dimerisation of Mps1 and KNL1

domains. In the eSAC, a minimal phosphodomain of KNL1 is used, typically with 6 MELT motifs; the kinase domain of Mps1 is used. Again, neither of these constructs localises to endogenous kinetochores, resulting in a soluble cytosolic signalling platform. Dimerisation of the eSAC components is controlled by CID, like SynCheckABA, however the small molecule inducer used in this system is rapamycin, rather than ABA.

The eSAC has provided further evidence of the utility of such ectopic systems for characterising features of SAC signalling. In particular, this system has shed light on the dose-response characteristics of the SAC, i.e. how the number of unattached kinetochores affects the strength of the anaphase inhibitory response (Chen *et al*, 2019). Quantification of the effects of unattached kinetochores would require generating and maintaining specific numbers of unattached chromosomes, whereas quantification of eSAC is far easier. The number of MELT motifs in the eSAC was also varied to test their contributions to signalling. This analysis has revealed that multiple MELT motifs in a phosphodomain can act synergistically to generate more MCC. However, it was shown that the SAC signal saturates at high concentrations of eSAC. This suggests that limited levels of SAC proteins exert an upper limit on the anaphase inhibitory signal. These observations have led to the development of a model in which a single unattached kinetochore can have a relatively strong effect on MCC generation, whereas when many kinetochores are unattached there is competition for binding of MCC components, which means each kinetochore has a relatively weak contribution to MCC generation, but high levels of MCC are produced overall. This model reconciles previous observations that the checkpoint exhibits switch-like behaviour in response to single unattached kinetochores, but also behaves like a rheostat, with greater numbers of unattached kinetochores correlating with increased anaphase inhibition (Dick & Gerlich, 2013; Collin *et al*, 2013).

Thus, ectopic SAC systems are a promising new approach to studying the SAC. SynCheckABA will be particularly useful for studying checkpoint silencing as the arrest is rapidly reversible by washing out ABA. In this respect it has an advantage over the eSAC, since the eSAC uses rapamycin-induced dimerisation which induces very stable, non-reversible binding.

6.4 Final conclusion

In conclusion, the results presented in this thesis have contributed to the important and understudied field of spindle assembly checkpoint silencing and have yielded novel contributions by identifying specific candidates likely to be involved in this process. This project also developed resources and experimental systems which will facilitate future studies of checkpoint silencing mechanisms.

Bibliography

Adams RR, Carmena M & Earnshaw WC (2001) Chromosomal passengers and the (aurora) ABCs of mitosis. *Trends Cell Biol.* **11:** 49–54

Alfieri C, Chang L & Barford D (2018) Mechanism for remodelling of the cell cycle checkpoint protein MAD2 by the ATPase TRIP13. *Nature* **559:** 274–278

Alfieri C, Chang L, Zhang Z, Yang J, Maslen S, Skehel M & Barford D (2016) Molecular basis of APC/C regulation by the spindle assembly checkpoint. *Nature* **536**(7617)**:**431-436.

Alvarez-Tabarés I, Grallert A, Ortiz J-M & Hagan IM (2007) Schizosaccharomyces pombe protein phosphatase 1 in mitosis, endocytosis and a partnership with Wsh3/Tea4 to control polarised growth. *J. Cell Sci.* **120:** 3589–601

Amin P, Soper Ní Chafraidh S, Leontiou I & Hardwick KG (2019) Regulated reconstitution of spindle checkpoint arrest and silencing through chemically induced dimerisation *in vivo*. *J. Cell Sci.* **132:** jcs219766

Aravamudhan P, Goldfarb A a. & Joglekar AP (2015) The kinetochore encodes a mechanical switch to disrupt spindle assembly checkpoint signalling. *Nat. Cell Biol.* **17** (7): 868-880

Aravind L & Koonin E V (1998) The HORMA domain: a common structural denominator in mitotic checkpoints, chromosome synapsis and DNA repair. *Trends Biochem. Sci.* **23:** 284–286

Armstrong J, Bone N, Dodgson J & Beck T (2007) The role and aims of the FYSSION project. *Briefings Funct. Genomics Proteomics* **6:** 3–7

Axton JM, Dombrádi V, Cohen PT & Glover DM (1990) One of the protein phosphatase 1 isoenzymes in Drosophila is essential for mitosis. *Cell* **63:** 33–46

Azzam R, Chen SL, Shou W, Mah AS, Alexandru G, Nasmyth K, Annan RS, Carr SA & Deshaies RJ (2004) Phosphorylation by cyclin B-Cdk underlies release of mitotic exit activator Cdc14 from the nucleolus. *Science* **305:** 516–9

Bajaj R, Bollen M, Peti W & Page R (2018) KNL1 Binding to PP1 and Microtubules Is Mutually Exclusive. *Structure* **26:** 1327–1336.e4

Banerjee R, Russo N, Liu M, Basrur V, Bellile E, Palanisamy N, Scanlon CS, van Tubergen E, Inglehart RC, Metwally T, Mani R-S, Yocum A, Nyati MK, Castilho RM, Varambally S,

Chinnaiyan AM & D'Silva NJ (2014) TRIP13 promotes error-prone nonhomologous end joining and induces chemoresistance in head and neck cancer. *Nat. Commun.* **5:** 4527

Barford D (2011) Structure, function and mechanism of the anaphase promoting complex (APC/C). *Quarterly Rev. Biophysics* **44** (2): 153-190

Baryshnikova A, Costanzo M, Dixon S, Vizeacoumar FJ, Myers CL, Andrews B & Boone C (2010) Synthetic genetic array (SGA) analysis in Saccharomyces cerevisiae and Schizosaccharomyces pombe. *Methods in Enzymology* **470** (7) 145-179

Basi G, Schmid E & Maundrell K (1993) TATA box mutations in the Schizosaccharomyces pombe nmt1 promoter affect transcription efficiency but not the transcription start point or thiamine repressibility. *Gene* **123**: 131-136

Bavetsias V & Linardopoulos S (2015) Aurora Kinase Inhibitors: Current Status and Outlook. *Front. Oncol.* **5:** 278

Behnia R, Barr FA, Flanagan JJ, Barlowe C & Munro S (2007) The yeast orthologue of GRASP65 forms a complex with a coiled-coil protein that contributes to ER to Golgi traffic. *J. Cell Biol.* **176:** 255–61

Beilharz TH, Harrison PF, Miles DM, See MM, Minh U, Le M, Kalanon M, Curtis MJ, Hasan Q, Saksouk J, Margaritis T, Holstege F, Geli V & Dichtl B (2017) Coordination of Cell Cycle Progression and Mitotic Spindle Assembly Involves Histone H3 Lysine 4 Methylation by Set1/COMPASS. *Genetics* **205:** 185–199

Bhaduri S & Pryciak PM (2011) Cyclin-Specific Docking Motifs Promote Phosphorylation of Yeast Signaling Proteins by G1/S Cdk Complexes. *Curr. Biol.* **21:** 1615–1623

Biggins S, Gerring SL, Connelly C, Hieter P & Dann P (2013) The composition, functions, and regulation of the budding yeast kinetochore. *Genetics* **194:** 817–46

Birrell GW, Giaever G, Chu AM, Davis RW & Brown JM (2001) A genome-wide screen in Saccharomyces cerevisiae for genes affecting UV radiation sensitivity. *Proc. Natl. Acad. Sci. U. S. A.* **98:** 12608–13

Bischof L, Převorovský M, Rallis C & Jeffares DC (2017) Spotsizer : High-throughput quantitative analysis of microbial growth. *Biotechniques.* **61:** 191–201

Boyarchuk Y, Salic A, Dasso M & Arnaoutov A (2007) Bub1 is essential for assembly of the functional inner centromere. *J. Cell Biol.* **176:** 919–28

Brady DM & Hardwick KG (2000) Complex formation between Mad1p, Bub1p and Bub3p is crucial for spindle checkpoint function. *Curr. Biol.* **10:** 675–678

Brito DA & Rieder CL (2006) Mitotic Checkpoint Slippage in Humans Occurs via Cyclin B Destruction in the Presence of an Active Checkpoint. *Curr. Biol.* **16:** 1194–1200

Buttrick GJ, Meadows JC, Lancaster TC, Vanoosthuyse V, Shepperd LA, Hoe K-L, Kim D-U, Park H-O, Hardwick KG & Millar JBA (2011) Nsk1 ensures accurate chromosome segregation by promoting association of kinetochores to spindle poles during anaphase B. *Mol. Biol. Cell* **22:** 4486–4502

Buttrick GJ & Millar JBA (2011) Ringing the changes: emerging roles for DASH at the kinetochore–microtubule Interface. *Chromosom. Res.* **19:** 393–407

Campbell MS, Chan GK & Yen TJ (2001) Mitotic checkpoint proteins HsMAD1 and HsMAD2 are associated with nuclear pore complexes in interphase. *J. Cell Sci.* **114** (5): 953-963

Canman JC, Sharma N, Straight A, Shannon KB, Fang G & Salmon ED (2002) Anaphase onset does not require the microtubule-dependent depletion of kinetochore and centromere-binding proteins. *J. Cell Sci.* **115:** 3787–3795

Chan K-S, Koh C-G & Li H-Y (2012) Mitosis-targeted anti-cancer therapies: where they stand. *Cell Death Dis.* **3:** e411–e411

Chao WCH, Kulkarni K, Zhang Z, Kong EH & Barford D (2012) Structure of the mitotic checkpoint complex. *Nature* **484:** 208–213

Cheeseman IM, Anderson S, Jwa M, Green EM, Kang J, Yates JR, Chan CSM, Drubin DG & Barnes G (2002) Phospho-Regulation of Kinetochore-Microtubule Attachments by the Aurora Kinase Ipl1p. *Cell* **111:** 163–172

Cheeseman IM, Chappie JS, Wilson-Kubalek EM & Desai A (2006) The Conserved KMN Network Constitutes the Core Microtubule-Binding Site of the Kinetochore. *Cell* **127:** 983–997

Cheeseman IM & Desai A (2008) Molecular architecture of the kinetochore-microtubule interface. *Nat. Rev. Mol. Cell Biol.* **9:** 33–46

Chen C-TT, Peli-Gulli M-PP, Simanis V & McCollum D (2006) S. pombe FEAR protein orthologs are not required for release of Clp1/Flp1 phosphatase from the nucleolus during mitosis. *J. Cell Sci.* **119:** 4462–4466

Chen C, Whitney IP, Banerjee A, Sacristan C, Sekhri P, Kern DM, Fontan A, Kops GJPL, Tyson JJ, Cheeseman IM & Joglekar AP (2019) Ectopic Activation of the Spindle Assembly Checkpoint Signaling Cascade Reveals Its Biochemical Design. *Curr. Biol.* **29:** 104–119.e10

Chen F, Archambault V, Kar A, Lio' P, D'Avino PP, Sinka R, Lilley K, Laue ED, Deak P, Capalbo L & Glover DM (2007) Multiple protein phosphatases are required for mitosis in Drosophila. *Curr. Biol.* **17:** 293–303

Cheng A, Dean NM & Honkanen RE (2000) Serine/threonine protein phosphatase type 1ɣ1 is required for the completion of cytokinesis in human A549 lung carcinoma cells. *J. Biol. Chem.* **275:** 1846–54

Ciferri C, Pasqualato S, Screpanti E, Varetti G, Santaguida S, Dos Reis G, Maiolica A, Polka J, De Luca JG, De Wulf P, Salek M, Rappsilber J, Moores CA, Salmon ED & Musacchio A (2008) Implications for Kinetochore-Microtubule Attachment from the Structure of an Engineered Ndc80 Complex. *Cell* **133:** 427–439

Ciliberto A & Hauf S (2017) Micromanaging checkpoint proteins. *Elife* **6:** 1–3

Ciliberto A & Shah J V (2009) A quantitative systems view of the spindle assembly checkpoint. *EMBO J.* **28:** 2162–2173

Clute P & Pines J (1999) Temporal and spatial control of cyclin B1 destruction in metaphase. *Nat. Cell Biol.* **1:** 82–87

Cohen-Fix O & Koshland D (1999) Pds1p of budding yeast has dual roles: Inhibition of anaphase initiation and regulation of mitotic exit. *Genes Dev.* **13:** 1950–1959

Colanzi A, Corda D (2007) Mitosis controls the Golgi and the Golgi controls mitosis. *Current Opinion in Cell Biology* **19**(4): 386-393

Colland F, Jacq X, Trouplin V, Mougin C, Groizeleau C, Hamburger A, Meil A, Wojcik J, Legrain P & Gauthier JM (2004) Functional proteomics mapping of a human signaling pathway. *Genome Res.* **14:** 1324–1332

Collin P, Nashchekina O, Walker R & Pines J (2013) The spindle assembly checkpoint works like a rheostat rather than a toggle switch. *Nat. Cell Biol.* **15:** 1378–1385

Corda D, Barretta ML, Cervigni RI, Colanzi A (2012) Golgi complex fragmentation in G2/M transition: An organelle-based cell-cycle checkpoint. *IUBMB Life* **64**(8): 661-670

Courtheoux T, Gay G, Reyes C, Goldstone S, Gachet Y & Tournier S (2007) Dynein participates in chromosome segregation in fission yeast. *Biol. Cell* **99:** 627–637

D'Amours D & Amon A (2004) At the interface between signaling and executing anaphase--Cdc14 and the FEAR network. *Genes Dev.* **18:** 2581–95

Dasso M & Newport JW (1990) Completion of DNA Replication Is Monitored by a Feedback System That Controls the Initiation of Mitosis In Vitro: Studies in Xenopus. *Cell*. **61** (5):811-23.

DeAntoni A, Sala V & Musacchio A (2005) Explaining the oligomerization properties of the spindle assembly checkpoint protein Mad2. *Philos. Trans. R. Soc. B Biol. Sci.* **360:** 637–648

Deshpande GP, Hayles J, Hoe KL, Kim DU, Park HO & Hartsuiker E (2009) Screening a genome-wide S. pombe deletion library identifies novel genes and pathways involved in genome stability maintenance. *DNA Repair (Amst).* **8:** 672–679

DeZwaan TM, Ellingson E, Pellman D & Roof DM (1997) Kinesin-related KIP3 of Saccharomyces cerevisiae is required for a distinct step in nuclear migration. *J. Cell Biol.* **138:** 1023–1040

Dick AE & Gerlich DW (2013) Kinetic framework of spindle assembly checkpoint signalling. *Nat. Cell Biol.* **15:** 1370–1377

Draetta G, Luca F, Westendorf J, Brizuela L, Ruderman J & Beach D (1989) cdc2 Protein Kinase Is Complexed with Both Cyclin A and B: Evidence for Proteolytic Inactivation of MPF. *Cell* **56:** 829–838

Egloff MP, Johnson DF, Moorhead G, Cohen PT, Cohen P & Barford D (1997) Structural basis for the recognition of regulatory subunits by the catalytic subunit of protein phosphatase 1. *EMBO J.* **16:** 1876–87

Emanuele MJ, Lan W, Jwa M, Miller SA, Chan CSM & Stukenberg PT (2008) Aurora B kinase and protein phosphatase 1 have opposing roles in modulating kinetochore assembly. *J. Cell Biol.* **181:** 241–254

Enoch T & Nurse P (1990) Mutation of fission yeast cell cycle control genes abolishes

dependence of mitosis on DNA replication. *Cell* **60:** 665–673

Espeut J, Cheerambathur DK, Krenning L, Oegema K & Desai A (2012) Microtubule binding by KNL-1 contributes to spindle checkpoint silencing at the kinetochore. *J. Cell Biol.* **196:** 469–82

Espeut J, Lara-Gonzalez P, Sassine M, Shiau AK, Desai A & Abrieu A (2015) Natural Loss of Mps1 Kinase in Nematodes Uncovers a Role for Polo-like Kinase 1 in Spindle Checkpoint Initiation. *Cell Rep.* **12:** 58–65

Esposito M, Piatti S, Hofmann L, Frontali L, Delahodde A & Rinaldi T (2011) Analysis of the rpn11-m1 proteasomal mutant reveals connection between cell cycle and mitochondrial biogenesis. *FEMS Yeast Res.* **11:** 60–71

Essex A, Dammermann A, Lewellyn L, Oegema K & Desai A (2009) Systematic analysis in Caenorhabditis elegans reveals that the spindle checkpoint is composed of two largely independent branches. *Mol. Biol. Cell* **20:** 1252–67

Evans T, Rosenthal ET, Youngblom J, Distel D & Hunt T (1983) Cyclin: A protein specified by maternal mRNA in sea urchin eggs that is destroyed at each cleavage division. *Cell* **33:** 389–396

Eytan E, Sitry-Shevah D, Teichner A & Hershko A (2013) Roles of different pools of the mitotic checkpoint complex and the mechanisms of their disassembly. *Proc. Natl. Acad. Sci.* **110:** 10568–10573

Eytan E, Wang K, Miniowitz-Shemtov S, Sitry-Shevah D, Kaisari S, Yen TJ, Liu S-T & Hershko A (2014) Disassembly of mitotic checkpoint complexes by the joint action of the AAA-ATPase TRIP13 and p31(comet). *Proc. Natl. Acad. Sci. U. S. A.* **111:** 12019–24

Faesen AC, Thanasoula M, Maffini S, Breit C, Müller F, Van Gerwen S, Bange T & Musacchio A (2017) Basis of catalytic assembly of the mitotic checkpoint complex. *Nature* **542:** 498–502

Famulski JK, Vos LJ, Rattner JB & Chan GK (2011) Dynein/dynactin-mediated transport of kinetochore components off kinetochores and onto spindle poles induced by Nordihydroguaiaretic acid. *PLoS One* **6** (1): e16494

Fang G (2002) Checkpoint Protein BubR1 Acts Synergistically with Mad2 to Inhibit Anaphase-promoting Complex. *Mol. Biol. Cell* **13:** 755–766

Fernius J & Hardwick KG (2007) Bub1 Kinase Targets Sgo1 to Ensure Efficient Chromosome Biorientation in Budding Yeast Mitosis. *PLoS Genet.* **3:** e213

Foijer F, Xie SZ, Simon JE, Bakker PL, Conte Nathalie, Davis SH, Kregel E, Jonkers J, Bradley A & Sorger PK (2014) Chromosome instability induced by Mps1 and p53 mutation generates aggressive lymphomas exhibiting aneuploidy-induced stress. *Proc. Natl. Acad. Sci. U. S. A.* **111:** 13427–13432

Forsburg SL (2001) The art and design of genetic screens: yeast. *Nat. Rev. Genet.* **2:** 956–966

Francisco L, Wang W & Chan CS (1994) Type 1 protein phosphatase acts in opposition to IpL1 protein kinase in regulating yeast chromosome segregation. *Mol. Cell. Biol.* **14:** 4731–40

Fraschini R, Beretta A, Sironi L, Musacchio A, Lucchini G & Piatti S (2001) Bub3 interaction with Mad2 , Mad3 and Cdc20 is mediated by WD40 repeats and does not require intact kinetochores. **20** (23): 6648-6659

Funabiki H & Wynne DJ (2013) Making an effective switch at the kinetochore by phosphorylation and dephosphorylation. *Chromosoma* **122:** 135–158

Gaitanos TN, Santamaria A, Jeyaprakash AA, Wang B, Conti E & Nigg EA (2009) Stable kinetochore–microtubule interactions depend on the Ska complex and its new component Ska3/C13Orf3. *EMBO J.* **28:** 1442–1452

Gama JB, Pereira C, Simões PA, Celestino R, Barbosa D, Reis RM, Pires HR, Carvalho C, Amorim J, Carvalho AX, Cheerambathur DK & Gassmann R (2017) Molecular mechanism of kinetochore dynein recruitment by the Rod/Zw10/Zwilch complex and Spindly. *J. Cell Biol.* **216:** 654–672

Garcia MA, Koonrugsa N & Toda T (2002a) Two kinesin-like Kin I family proteins in fission yeast regulate the establishment of metaphase and the onset of anaphase A. *Curr. Biol.* **12:** 610–621

Garcia MA, Koonrugsa N & Toda T (2002b) Spindle-kinetochore attachment requires the combined action of Kin I-like Klp5/6 and Alp14/Dis1-MAPs in fission yeast. *EMBO J.* **21:** 6015–24

Gascoigne KE, Taylor SS (2008) Cancer cells display profound intra- and interline variation following prolonged exposure to antimitotic drugs. *Cancer Cell.* **14** (2): 111-122

Gascoigne KE, Taylor SS (2009) How do anti-mitotic drugs kill cancer cells? *J. Cell Sci.* **122** (15): 2579-2585

Gassmann R, Holland AJ, Varma D, Wan X, Civril F, Cleveland DW, Oegema K, Salmon ED & Desai A (2010) Removal of Spindly from microtubule-attached kinetochores controls spindle checkpoint silencing in human cells. *Genes Dev.* **24:** 957–71

Gergely ZR, Crapo A, Hough LE, McIntosh JR & Betterton MD (2016) Kinesin-8 effects on mitotic microtubule dynamics contribute to spindle function in fission yeast. *Mol. Biol. Cell* **27:** 3490–3514

Geymonat M, Jensen S & Johnston LH (2002) Mitotic exit: The Cdc14 double cross. *Curr. Biol.* **12** (14): R482-84

Gossen M & Bujardt H (1992) Tight control of gene expression in mammalian cells by tetracycline-responsive promoters. *Proc. Natl. Acad. Sci. USA* **89**: 5547-5551

Griffis ER, Stuurman N & Vale RD (2007) Spindly, a novel protein essential for silencing the spindle assembly checkpoint, recruits dynein to the kinetochore. *J. Cell Biol.* **177:** 1005–1015

Grissom PM, Fiedler T, Grishchuk EL, Nicastro D, West RR & McIntosh JR (2009) Kinesin-8 from fission yeast: a heterodimeric, plus-end-directed motor that can couple microtubule depolymerization to cargo movement. *Mol. Biol. Cell* **20:** 963–72

Gruneberg U, Glotzer M, Gartner A & Nigg EA (2002) The CeCDC-14 phosphatase is required for cytokinesis in the Caenorhabditis elegans embryo. *J. Cell Biol.* **158:** 901–914

Gupta ML, Carvalho P, Roof DM & Pellman D (2006) Plus end-specific depolymerase activity of Kip3, a kinesin-8 protein, explains its role in positioning the yeast mitotic spindle. *Nat. Cell Biol.* **8:** 913–23

Gutteridge REA, Ndiaye MA, Liu X & Ahmad N (2016) Plk1 Inhibitors in Cancer Therapy: From Laboratory to Clinics. *Mol. Cancer Ther.* **15:** 1427–1435

Habu T, Kim SH, Weinstein J & Matsumoto T (2002) Identification of a MAD2-binding protein, CMT2, and its role in mitosis. *EMBO J.* **21:** 6419–28

Hanisch A, Silljé HHW & Nigg EA (2006) Timely anaphase onset requires a novel spindle and kinetochore complex comprising Ska1 and Ska2. *EMBO J.* **25:** 5504–5515

Hansen KR, Hazan I, Shanker S, Watt S & Verhein-Hansen J (2011) H3K9me-Independent Gene Silencing in Fission Yeast Heterochromatin by Clr5 and Histone Deacetylases. *PLoS Genet* **7:** 1001268

Hartwell LH & Weinert TA (1989) Checkpoints: Controls that Ensure the Order of Cell Cycle Events. *Science* **246** (4930):629-634

Hayles J, Wood V, Jeffery L, Hoe K-L, Kim D-U, Park H-O, Salas-Pino S, Heichinger C & Nurse P (2013) A genome-wide resource of cell cycle and cell shape genes of fission yeast. *Open Biol.* **3:** 130053

He X, Jones MH, Winey M & Sazer S (1998) Mph1, a member of the Mps1-like family of dual specificity protein kinases, is required for the spindle checkpoint in S. pombe. *J. Cell Sci.* **111:** 1635–1647

Heinrich S, Windecker H, Hustedt N & Hauf S (2012) Mph1 kinetochore localization is crucial and upstream in the hierarchy of spindle assembly checkpoint protein recruitment to kinetochores. *J. Cell Sci.* **125:** 4720–4727

Hendrickx A, Beullens M, Ceulemans H, Den Abt T, Van Eynde A, Nicolaescu E, Lesage B & Bollen M (2009) Docking Motif-Guided Mapping of the Interactome of Protein Phosphatase-1. *Chem. Biol.* **16:** 365–371

Hershko A & Ciechanover A (1998) The Ubiquitin System. *Annu. Rev. Biochem.* **67:** 425–479

Hiraga S-I, Alvino GM, Chang F, Lian H-Y, Sridhar A, Kubota T, Brewer BJ, Weinreich M, Raghuraman MK & Donaldson AD (2014) Rif1 controls DNA replication by directing Protein Phosphatase 1 to reverse Cdc7-mediated phosphorylation of the MCM complex. *Genes Dev.* **28:** 372–83

Hiraoka Y, Toda T & Yanagida M (1984) The NDA3 gene of fission yeast encodes beta-tubulin: a cold-sensitive nda3 mutation reversibly blocks spindle formation and chromosome movement in mitosis. *Cell* **39:** 349–358

Hiruma Y, Sacristan C, Pachis ST, Adamopoulos A, Kuijt T, Ubbink M, von Castelmur E, Perrakis A & Kops GJ (2015) Competition between MPS1 and microtubules at kinetochores regulates spindle checkpoint signaling. *Science* **348:** 1264–1267

Hisamoto N, Sugimoto K & Matsumoto K (1994) The Glc7 type 1 protein phosphatase of Saccharomyces cerevisiae is required for cell cycle progression in G2/M. *Mol. Cell. Biol.* **14:** 3158–65

Howell BJ, McEwen BF, Canman JC, Hoffman DB, Farrar EM, Rieder CL & Salmon ED (2001) Cytoplasmic dynein/dynactin drives kinetochore protein transport to the spindle poles and has a role in mitotic spindle checkpoint inactivation. *J. Cell Biol.* **155:** 1159–1172

Hoyt M, Totis L & Roberts BT (1991) S. cerevisiae genes required for cell cycle arrest in response to loss of microtubule function. *Cell* **66:** 507–517

Huang H-C, Shi J, Orth JD & Mitchison TJ (2009) Evidence that Mitotic Exit Is a Better Cancer Therapeutic Target Than Spindle Assembly. *Cancer Cell* **16:** 347–358

Hwang WW & Madhani HD (2009) Nonredundant requirement for multiple histone modifications for the early anaphase release of the mitotic exit regulator Cdc14 from nucleolar chromatin. *PLoS Genet.* **5:** e1000588

Ito H, Fukuda Y, Murata K & Kimura A (1983) Transformation of Intact Yeast Cells Treated with Alkali Cations. *J. Bacteriol.* **153** (1): 163-168

Izawa D & Pines J (2015) The mitotic checkpoint complex binds a second CDC20 to inhibit active APC/C. *Nature* **517:** 631–634

Jackson JR, Patrick DR, Dar MM & Huang PS (2007) Targeted anti-mitotic therapies: can we improve on tubulin agents? *Nat. Rev. Cancer* **7:** 107–17

Jeyaprakash AA, Santamaria A, Jayachandran U, Chan YW, Benda C, Nigg EA & Conti E (2012) Structural and functional organization of the Ska complex, a key component of the kinetochore–microtubule interface. *Mol. Cell* **46**: 274–286

Jordan MA, Wendell K, Gardiner S, Derry WB, Copp H & Wilson L (1996) Mitotic block induced in HeLa cells by low concentrations of paclitaxel (taxol) results in abnormal mitotic exit and apoptotic cell death. *Cancer Res.* **56:** 816–825

Kaisari S, Sitry-Shevah D, Miniowitz-Shemtov S, Teichner A & Hershko A (2017) Role of CCT chaperonin in the disassembly of mitotic checkpoint complexes. *Proc. Natl. Acad. Sci. U. S. A.* **114:** 956–961

Kapoor P, Bao Y, Xiao J, Luo J, Shen J, Persinger J, Peng G, Ranish J, Bartholomew B, Shen X (2015) Regulation of Mec1 kinase activity by the SWI/SNF chromatin remodeling

complex. *Genes Dev.* **29** (6): 591-602.

Kawashima SA, Yamagishi Y, Honda T, Ishiguro K & Watanabe Y (2010) Phosphorylation of H2A by Bub1 prevents chromosomal instability through localizing shugoshin. *Science* **327:** 172–7

Keating P, Rachidi N, Tanaka TU & Stark MJR (2009) Ipl1-dependent phosphorylation of Dam1 is reduced by tension applied on kinetochores. *J. Cell Sci.* **122:** 4375–4382

Kemmler S, Stach M, Knapp M, Ortiz J, Pfannstiel J, Ruppert T & Lechner J (2009) Mimicking Ndc80 phosphorylation triggers spindle assembly checkpoint signalling. *EMBO* **28:** 1099–1110

Kerres A, Jakopec V & Fleig U (2007) The Conserved Spc7 Protein Is Required for Spindle Integrity and Links Kinetochore Complexes in Fission Yeast. *Mol. Biol. Cell* **18:** 2441–2454

Kettenbach AN, Schweppe DK, Faherty BK, Pechenick D, Pletnev AA & Gerber SA (2011) Quantitative phosphoproteomics identifies substrates and functional modules of Aurora and Polo-like kinase activities in mitotic cells. *Sci. Signal.* **4:** rs5

Kim D-U, Hayles J, Kim D, Wood V, Park H-O, Won M, Yoo H-S, Duhig T, Nam M, Palmer G, Han S, Jeffery L, Baek S-T, Lee H, Shim YS, Lee M, Kim L, Heo K-S, Noh EJ, Lee A-R, et al (2010a) Analysis of a genome-wide set of gene deletions in the fission yeast Schizosaccharomyces pombe. *Nat. Biotechnol.* **28:** 617–623

Kim T, Lara-Gonzalez P, Prevo B, Meitinger F, Cheerambathur DK, Oegema K & Desai A (2017) Kinetochores accelerate or delay APC/C activation by directing Cdc20 to opposing fates. *Genes Dev.* **31:** 1089–1094

Kim Y, Holland AJ, Lan W & Cleveland DW (2010b) Aurora kinases and protein phosphatase 1 mediate chromosome congression through regulation of CENP-E. *Cell* **142:** 444–455

Kimelman D, Kirschner M & Scherson T (1987) The Events of the Midblastula Transition in Xenopus Are Regulated by Changes in the Cell Cycle. *Cell* **48:** 399-407

King EMJ, van der Sar SJA & Hardwick KG (2007) Mad3 KEN Boxes Mediate both Cdc20 and Mad3 Turnover, and Are Critical for the Spindle Checkpoint. *PLoS One* **2:** e342

Kirchner J, Gross S, Bennett D & Alphey L (2007) Essential, Overlapping and Redundant Roles of the Drosophila Protein Phosphatase 1α and 1β Genes. *Genetics* **176:** 273–281

Kitajima TS, Hauf S, Ohsugi M, Yamamoto T & Watanabe Y (2005) Human Bub1 Defines the Persistent Cohesion Site along the Mitotic Chromosome by Affecting Shugoshin Localization. *Curr. Biol.* **15:** 353–359

Kitajima TS, Kawashima SA & Watanabe Y (2004) The conserved kinetochore protein shugoshin protects centromeric cohesion during meiosis. *Nature* **427:** 510–517

Klebig C, Korinth D & Meraldi P (2009) Bub1 regulates chromosome segregation in a kinetochore-independent manner. *J. Cell Biol.* **185:** 841–58

Klemm AH, Bosilj A, Glunčić M, Pavin N & Tolić IM (2018) Metaphase kinetochore movements are regulated by kinesin-8 motors and microtubule dynamic instability. *Mol. Biol. Cell* **29:** 1332–1345

Kõivomägi M, Valk E, Venta R, Iofik A, Lepiku M, Morgan DO & Loog M (2011) Dynamics of Cdk1 Substrate Specificity during the Cell Cycle. *Mol. Cell* **42:** 610–623

Kokkoris K, Gallo Castro D & Martin SG (2014) The Tea4–PP1 landmark promotes local growth by dual Cdc42 GEF recruitment and GAP exclusion. *J. Cell Sci.* **127:** 2005–2016

Kops GJPL, Kim Y, Weaver BAA, Mao Y, McLeod I, Yates JR, Tagaya M & Cleveland DW (2005a) ZW10 links mitotic checkpoint signaling to the structural kinetochore. *J. Cell Biol.* **169:** 49–60

Kops GJPL, Weaver BAA & Cleveland DW (2005b) On the road to cancer: aneuploidy and the mitotic checkpoint. *Nat. Rev. Cancer* **5:** 773–785

Kramer ER, Scheuringer N, Podtelejnikov a V, Mann M & Peters JM (2000) Mitotic regulation of the APC activator proteins CDC20 and CDH1. *Mol. Biol. Cell* **11:** 1555–1569

Krenn V & Musacchio A (2015) The Aurora B Kinase in Chromosome Bi-Orientation and Spindle Checkpoint Signaling. *Front. Oncol.* **5:** 225

Krenn V, Wehenkel A, Li X, Santaguida S & Musacchio A (2012) Structural analysis reveals features of the spindle checkpoint kinase Bub1-kinetochore subunit Knl1 interaction. *J. Cell Biol.* **196:** 451–67

Kucsera J, Yarita K & Takeo K (2000) Simple detection method for distinguishing dead and living yeast colonies. *J. Microbiol. Methods.* **41**: 19-21

Kulukian A, Han J & Cleveland D (2009) Unattached Kinetochores Catalyze Production of an

Anaphase Inhibitor that Requires a Mad2 Template to Prime Cdc20 for BubR1 Binding. *Dev. Cell* **16:** 105–117

Larkin SET, Holmes S, Cree IA, Walker T, Basketter V, Bickers B, Harris S, Garbis SD, Townsend PA & Aukim-Hastie C (2012) Identification of markers of prostate cancer progression using candidate gene expression. *Br. J. Cancer* **106:** 157–165

Latif C (2004) DNA damage checkpoint maintenance through sustained Chk1 activity. *J. Cell Sci.* **117:** 3489–3498

Lawless C, Wilkinson DJ, Young A, Addinall SG & Lydall DA (2010) Colonyzer: automated quantification of micro-organism growth characteristics on solid agar. *BMC Bioinformatics* **11**:287

Lee GS-F, Blonskyl KS, Lee Van On D, Savage I EA, Richard Morgan A & von Borstel RC (1992) Base Alterations in Yeast Induced by Alkylating Agents with Differing Swain-Scott Substrate Constants. *J. Mol. Biol.* **223**: 617-626

Lee M & Nurse P (1988) Cell cycle control genes in fission yeast and mammalian cells. *Trends Genet.* **4:** 287–290

Lee MG & Nurse P (1987) Complementation used to clone a human homologue of the fission yeast cell cycle control gene cdc2. *Nature* **327:** 31–35

Li R & Murray a W (1991) Feedback control of mitosis in budding yeast. *Cell* **66:** 519–531 [published erratum appears in *Cell* 79(2):following 388].

Li X & Schimenti JC (2007) Mouse Pachytene Checkpoint 2 (Trip13) is Required for Completing Meiotic Recombination but not Synapsis. *PLoS Genet.* **3:** e130

Li Y, Gorbea C, Mahaffey D, Rechsteiner M & Benezra R (1997) MAD2 associates with the cyclosome/anaphase-promoting complex and inhibits its activity. *Proc. Natl. Acad. Sci. USA* **94**: 12431–12436

Liang F-S, Ho WQ & Crabtree GR (2011) Engineering the ABA plant stress pathway for regulation of induced proximity. *Sci. Signal.* **4:** rs2

Liang F, Richmond D & Wang Y (2013) Coordination of Chromatid Separation and Spindle Elongation by Antagonistic Activities of Mitotic and S-Phase CDKs. *PLoS Genet.* **9**: e1003319

Lie S, Banks P, Lawless C, Lydall D & Petersen J (2018) The contribution of non-essential

Schizosaccharomyces pombe genes to fitness in response to altered nutrient supply and target of rapamycin activity. *Open Biol.* **8**: 180015

Liu D, Vader G, Vromans MJM, Lampson MA & Lens SMA (2009) Sensing chromosome bi-orientation by spatial separation of Aurora B kinase from kinetochore substrates. *Science (80-.).* **323:** 1350–1353

Liu D, Vleugel M, Backer CB, Hori T, Fukagawa T, Cheeseman IM & Lampson MA (2010) Regulated targeting of protein phosphatase 1 to the outer kinetochore by KNL1 opposes Aurora B kinase. *J. Cell Biol.* **188:** 809–820

Lock A, Rutherford K, Harris MA & Wood V (2018) PomBase: The Scientific Resource for Fission Yeast. In pp 49–68. Humana Press, New York, NY

London N & Biggins S (2014) Signalling dynamics in the spindle checkpoint response. *Nat. Rev. Mol. Cell Biol.* **15:** 736–748

London N, Ceto S, Ranish JA & Biggins S (2012) Phosphoregulation of Spc105 by Mps1 and PP1 regulates Bub1 localization to kinetochores. *Curr. Biol.* **22:** 900–906

Löoke M, Kristjuahan K & Kristjuhan A (2011) Extraction of Genomic Dna From Yeasts for PCR- Based Applications. *Biotechniques* **50:** 325–328

Lopez-Girona A, Furnari B, Mondesert O & Russell P (1999) Nuclear localization of Cdc25 is regulated by DNA damage and a 14-3-3 protein. *Nature* **397:** 172–175

Lorincz AL & Reed SI (1984) Primary structure homology between the product of yeast cell division control gene CDC28 and vertebrate oncogenes. *Nature* **307:** 183–185

Lowndes NF & Marguia JR (2000) Sensing and responding to DNA damage. *Curr. Opin. Genet. Dev.* **10:** 17–25

Luo X, Tang Z, Rizo J & Yu H (2002) The Mad2 Spindle Checkpoint Protein Undergoes Similar Major Conformational Changes Upon Binding to Either Mad1 or Cdc20. *Mol. Cel*l **9**: 59–71

Ma HT, Chan YY, Chen X, On KF & Poon RYC (2012) Depletion of p31comet protein promotes sensitivity to antimitotic drugs. *J. Biol. Chem.* **287:** 21561–9

Ma HT & Poon RYC (2016) TRIP13 Regulates Both the Activation and Inactivation of the Spindle-Assembly Checkpoint. *Cell Rep.* **14:** 1086–1099

Maciejowski J, Drechsler H, Grundner-Culemann K, Ballister ER, Rodriguez-Rodriguez J-A,

Rodriguez-Bravo V, Jones MJK, Foley E, Lampson MA, Daub H, McAinsh AD & Jallepalli P V. (2017) Mps1 Regulates Kinetochore-Microtubule Attachment Stability via the Ska Complex to Ensure Error-Free Chromosome Segregation. *Dev. Cell* **41:** 143–156.e6

Maldonado M & Kapoor TM (2011) Constitutive Mad1 targeting to kinetochores uncouples checkpoint signalling from chromosome biorientation. *Nat. Cell Biol.* **13:** 475–482

Malureanu LA, Jeganathan KB, Hamada M, Wasilewski L, Davenport J & van Deursen JM (2009) BubR1 N Terminus Acts as a Soluble Inhibitor of Cyclin B Degradation by APC/C^{Cdc20} in Interphase. *Dev. Cell* **16:** 118–131

Mapelli M, Massimiliano L, Santaguida S & Musacchio A (2007) The Mad2 Conformational Dimer: Structure and Implications for the Spindle Assembly Checkpoint. *Cell* **131:** 730–743

Mason JM, Wei X, Fletcher GC, Kiarash R, Brokx R, Hodgson R, Beletskaya I, Bray MR & Mak TW (2017) Functional characterization of CFI-402257, a potent and selective Mps1/TTK kinase inhibitor, for the treatment of cancer. *Proc. Natl. Acad. Sci.* **114:** 3127–3132

Masui Y (2001) From oocyte maturation to the in vitro cell cycle: the history of discoveries of Maturation-Promoting Factor (MPF) and Cytostatic Factor (CSF). *Differentiation* **69:** 1–17

Matsuyama A, Arai R, Yashiroda Y, Shirai A, Kamata A, Sekido S, Kobayashi Y, Hashimoto A, Hamamoto M, Hiraoka Y, Horinouchi S & Yoshida M (2006) ORFeome cloning and global analysis of protein localization in the fission yeast Schizosaccharomyces pombe. *Nat. Biotechnol.* **24:** 841–847

Maundrell K (1993) Thiamine-repressible expression vectors PREP and pRIP for fission yeast *Gene* **123:** 127–130

Maure J-F, Kitamura E & Tanaka TU (2007) Mps1 Kinase Promotes Sister-Kinetochore Bi-orientation by a Tension-Dependent Mechanism. *Curr. Biol.* **17:** 2175–2182

Mayr MI, Hümmer S, Bormann J, Grüner T, Adio S, Woehlke G & Mayer TU (2007) The Human Kinesin Kif18A Is a Motile Microtubule Depolymerase Essential for Chromosome Congression. *Curr. Biol.* **17:** 488–498

McIntosh JR (2012) Motors or dynamics: What really moves chromosomes? *Nat. Cell Biol.* **14:** 1234–1234

McIntosh JR (2016) Mitosis. *Cold Spring Harb. Perspect. Biol.* **8:** a023218

Meadows JC, Shepperd LA, Vanoosthuyse V, Lancaster TC, Sochaj AM, Buttrick GJ, Hardwick KG & Millar JBAA (2011) Spindle checkpoint silencing requires association of PP1 to both Spc7 and kinesin-8 motors. *Dev. Cell* **20:** 739–750

Meraldi P, Draviam VM & Sorger PK (2004) Timing and checkpoints in the regulation of mitotic progression. *Dev. Cell* **7:** 45–60

Messin LJ & Millar JBA (2014) Role and regulation of kinesin-8 motors through the cell cycle. *Syst. Synth. Biol.* **8:** 205–213

Milross CG, Mason KA, Hunter NR, Chung WK, Peters LJ & Milas L (1996) Relationship of mitotic arrest and apoptosis to antitumor effect of paclitaxel. *J. Natl. Cancer Inst.* **88:** 1308–1314

Miniowitz-Shemtov S, Teichner A, Sitry-Shevah D & Hershko A (2010) ATP is required for the release of the anaphase-promoting complex/cyclosome from inhibition by the mitotic checkpoint. *Proc. Natl. Acad. Sci. U. S. A.* **107:** 5351–6

Minshull J, Straight A, Rudner AD, Dernburg AF, Belmont A & Murray AW (1996) Protein phosphatase 2A regulates MPF activity and sister chromatid cohesion in budding yeast. *Curr. Biol.* **6:** 1609–1620

Minshull J, Sun H, Tonks NK & Murray AW (1994) A MAP kinase-dependent spindle assembly checkpoint in Xenopus egg extracts. *Cell* **79:** 475–86

Miranda JL, Wulf P De, Sorger PK & Harrison SC (2005) The yeast DASH complex forms closed rings on microtubules. *Nat. Struct. Mol. Biol.* **12:** 138–143

Mitchison TJ & Salmon ED (2001) Mitosis: a history of division. *Nat. Cell Biol.* **3:** E17–E21

Miyazono K, Miyakawa T, Sawano Y, Kubota K, Kang H-J, Asano A, Miyauchi Y, Takahashi M, Zhi Y, Fujita Y, Yoshida T, Kodaira K-S, Yamaguchi-Shinozaki K & Tanokura M (2009) Structural basis of abscisic acid signalling. *Nature* **462:** 609–614

Monahan BJ, Villén J, Marguerat S, Bähler J, Gygi SP & Winston F (2008) Fission yeast SWI/SNF and RSC complexes show compositional and functional differences from budding yeast. *Nat. Struct. Mol. Biol.* **15:** 873–80

Moreno S & Nurse P (1990) Substrates for p34cdc2: In vivo veritas? *Cell* **61:** 549–551

Morgan DO (2007) The Cell Cycle - Principles of Control. London: New Science Press Ltd.

Moura M, Osswald M, Leça N, Barbosa J, Pereira AJ, Maiato H, Sunkel CE & Conde C (2017) Protein Phosphatase 1 inactivates Mps1 to ensure efficient Spindle Assembly Checkpoint silencing. *Elife* **6:** e25366

Musacchio A (2015) Closing the Mad2 cycle. *Elife* **4:** e08283

Musacchio A, Desai A, Musacchio A & Desai A (2017) A Molecular View of Kinetochore Assembly and Function. *Biology (Basel).* **6:** 5

Musacchio A & Hardwick KG (2002) The spindle checkpoint: structural insights into dynamic signalling. *Nat. Rev. Mol. Cell Biol.* **3:** 731–741

Nasmyth K (2002) Segregating Sister Genomes: The Molecular Biology of Chromosome Separation. *Sci. New Ser.* **297:** 559–565

Nasmyth K (2005) Review How Do so Few Control so Many? *Cell* **120:** 739–746

Navarro FJ & Nurse P (2012) A systematic screen reveals new elements acting at the G2/M cell cycle control. *Genome Biol.* **13:** R36

Nelson CR, Hwang T, Chen P-H & Bhalla N (2015) TRIP13PCH-2 promotes Mad2 localization to unattached kinetochores in the spindle checkpoint response. *J. Cell Biol.* **211:** 503–516

Nicklas RB & Koch CA (1969) Chromosome micromanipulation. 3. Spindle fiber tension and the reorientation of mal-oriented chromosomes. *J. Cell Biol.* **43:** 40–50

Nijenhuis W, Vallardi G, Teixeira A, Kops GJPL & Saurin AT (2014) Negative feedback at kinetochores underlies a responsive spindle checkpoint signal. *Nat. Cell Biol.* **16:** 1257–1264

Nishiyama A, Dey A, Miyazaki J & Ozato K (2006) Brd4 Is Required for Recovery from Antimicrotubule Drug-induced Mitotic Arrest: Preservation of Acetylated Chromatin. *Mol. Biol. Cell* **17:** 814–823

Norman TC, Smith DL, Sorger PK, Drees BL, O'Rourke SM, Hughes TR, Roberts CJ, Friend SH, Fields S & Murray AW (1999) Genetic selection of peptide inhibitors of biological pathways. *Science* **285** (4527): 591–595

Nurse P (2000) A long twentieth century of the cell cycle and beyond. *Cell* **100:** 71–8

Nurse P & Bissett Y (1981) Gene required in G1 for commitment to cell cycle and in G2 for control of mitosis in fission yeast. *Nature* **292:** 558–560

Nurse P & Thuriaux P (1980) Regulatory genes controlling mitosis in the fission yeast Schizosaccharomyces pombe. *Genetics* **96:** 627–637

O'Connell MJ, Raleigh JM, Verkade HM & Nurse P (1997) Chk1 is a wee1 kinase in the G2DNA damage checkpoint inhibiting cdc2 by Y15 phosphorylation. *EMBO J.* **16:** 545–554

Ohkura H, Adachi Y, Kinoshita N, Niwa O, Toda T & Yanagida M (1988) Cold-sensitive and caffeine-supersensitive mutants of the Schizosaccharomyces pombe dis genes implicated in sister chromatid separation during mitosis. *EMBO J.* **7:** 1465–1473

Ohkura H, Kinoshita N, Miyatani S, Toda T & Yanagida M (1989) The Fission Yeast dis2+ Gene Required for Chromosome Disjoining Encodes One of Two Putative Type 1 Protein Phosphatases. *Cell* **57:** 997–1007

Ooi SL, Shoemaker DD & Boeke JD (2001) A DNA Microarray-Based Genetic Screen for Nonhomologous End-Joining Mutants in Saccharomyces cerevisiae. *Science* **294** (5551):2552-2556

Overlack K, Primorac I, Vleugel M, Krenn V, Maffini S, Hoffmann I, Kops GJPL & Musacchio A (2015) A molecular basis for the differential roles of Bub1 and BubR1 in the spindle assembly checkpoint. *Elife* **4:** 1–24

Pachis ST & Kops GJPL (2018) Leader of the SAC: molecular mechanisms of Mps1/TTK regulation in mitosis. *Open Biol.* **8**: 180109

Pagano M, Pepperkok R, Verde F, Ansorge W & Draetta G (1992) Cyclin A is required at two points in the human cell cycle. *EMBO J.* **11:** 961–971

Pagliuca C, Draviam VM, Marco E, Sorger PK & De Wulf P (2009) Roles for the Conserved Spc105p/Kre28p Complex in Kinetochore-Microtubule Binding and the Spindle Assembly Checkpoint. *PLoS One* **4:** e7640

Pan X, Lei B, Zhou N, Feng B, Yao W, Zhao X, Yu Y & Lu H (2012) Identification of novel genes involved in DNA damage response by screening a genome-wide Schizosaccharomyces pombe deletion library. *BMC Genomics* **13:** 662

Parker LL, Atherton-Fessler S & Piwnica-Worms H (1992) P107Wee1 Is a Dual-Specificity Kinase That Phosphorylates P34Cdc2 on Tyrosine 15. *Proc. Natl. Acad. Sci.* **89:** 2917–2921

Parker LL & Piwnica-worms H (1992) Inactivation of the p34cdc2-Cyclin B Complex by the Human WEEl Tyrosine Kinase. **257:** 1955–1958

Parua PK, Booth GT, Sansó M, Benjamin B, Tanny JC, Lis JT & Fisher RP (2018) A Cdk9–PP1 switch regulates the elongation–termination transition of RNA polymerase II. *Nature* **558:** 460–464

Pereira AJ, Dalby B, Stewart RJ, Doxsey SJ & Goldstein LSB (1997) Mitochondrial association of a plus end-directed microtubule motor expressed during mitosis in Drosophila. *J. Cell Biol.* **136:** 1081–1090

Perpelescu M & Fukagawa T (2011) The ABCs of CENPs. *Chromosoma* **120:** 425–446

Peters J-M (2006) The anaphase promoting complex/cyclosome: a machine designed to destroy. *Nat. Rev. Mol. Cell Biol.* **7:** 644–656

Petrovic A, Keller J, Liu Y, Overlack K, John J, Dimitrova YN, Jenni S, van Gerwen S, Stege P, Wohlgemuth S, Rombaut P, Herzog F, Harrison SC, Vetter IR & Musacchio A (2016) Structure of the MIS12 Complex and Molecular Basis of Its Interaction with CENP-C at Human Kinetochores. *Cell* **167:** 1028–1040.e15

Petrovic A, Mosalaganti S, Keller J, Mattiuzzo M, Overlack K, Krenn V, De Antoni A, Wohlgemuth S, Cecatiello V, Pasqualato S, Raunser S & Musacchio A (2014) Modular Assembly of RWD Domains on the Mis12 Complex Underlies Outer Kinetochore Organization. *Mol. Cell* **53:** 591–605

Pinsky BA, Kotwaliwale C V, Tatsutani SY, Breed CA & Biggins S (2006) Glc7/protein phosphatase 1 regulatory subunits can oppose the Ipl1/aurora protein kinase by redistributing Glc7. *Mol. Cell. Biol.* **26:** 2648–60

Pinsky BA, Nelson CR & Biggins S (2009) Protein Phosphatase 1 Regulates Exit from the Spindle Checkpoint in Budding Yeast. *Curr. Biol.* **19:** 1182–1187

Primorac I, Weir JR, Chiroli E, Gross F, Hoffmann I, van Gerwen S, Ciliberto A & Musacchio A (2013) Bub3 reads phosphorylated MELT repeats to promote spindle assembly checkpoint signaling. *Elife* **2:** e01030

Raff JW & Glover DM (1988) Nuclear and Cytoplasmic Mitotic Cycles Continue in Drosophila Embryos in which DNA Synthesis Is Inhibited with Aphidicolin. *J. Cell Biol.* **107:** 2009–2019

Raleigh JM & O'Connell MJ (2000) The G(2) DNA damage checkpoint targets both Wee1 and Cdc25. *J. Cell Sci.* **113** (1): 1727–1736

Rao PN & Johnson RT (1970) Mammalian Cell Fusion: Studies on the Regulation of DNA Synthesis and Mitosis. *Nature* **225**: 159–164

Reddy SK, Rape M, Margansky WA & Kirschner MW (2007) Ubiquitination by the anaphase-promoting complex drives spindle checkpoint inactivation. *Nature* **446:** 921–925

Rieder CL, Cole RW, Khodjakov A & Sluder G (1995) The checkpoint delaying anaphase in response to chromosome monoorientation is mediated by an inhibitory signal produced by unattached kinetochores. *J. Cell Biol.* **130:** 941–948

Rieder CL, Maiato H (2004) Stuck in division or passing through: What happens when cells cannot satisfy the spindle assembly checkpoint *Dev. Cell* **7**(5): 637-651

Roccuzzo M, Visintin C, Tili F & Visintin R (2015) FEAR-mediated activation of Cdc14 is the limiting step for spindle elongation and anaphase progression. *Nat. Cell Biol.* **17:** 251–61

Rodriguez-Bravo V, Maciejowski J, Corona J, Buch HK, Collin P, Kanemaki MT, Shah J V. & Jallepalli P V. (2014) Nuclear pores protect genome integrity by assembling a premitotic and mad1-dependent anaphase inhibitor. *Cell* **156:** 1017–1031

Roguev A, Schaft D, Shevchenko A, Aasland R, Shevchenko A & Stewart AF (2003) High Conservation of the Set1/Rad6 Axis of Histone 3 Lysine 4 Methylation in Budding and Fission Yeasts. *J. Biol. Chem.* **278:** 8487–8493

Roguev A, Wiren M, Weissman JS & Krogan NJ (2007) High-throughput genetic interaction mapping in the fission yeast Schizosaccharomyces pombe. *Nat. Methods* **4:** 861–866

Roguev A, Xu J & Krogan N (2018) Genetic interaction mapping in schizosaccharomyces pombe using the pombe epistasis mapper (PEM) system and a ROTOR HDA colony replicating robot in a 1536 array format. *Cold Spring Harb. Protoc.* **2018:** 112–118

Rosenberg JS, Cross FR & Funabiki H (2011) KNL1/Spc105 recruits PP1 to silence the spindle assembly checkpoint. *Curr. Biol.* **21:** 942–7

Rossio V, Galati E, Ferrari M, Pellicioli A, Sutani T, Shirahige K, Lucchini G & Piatti S (2010) The RSC chromatin-remodeling complex influences mitotic exit and adaptation to the

spindle assembly checkpoint by controlling the Cdc14 phosphatase. *J. Cell Biol.* **191:** 981–997

Rual J-F, Venkatesan K, Hao T, Hirozane-Kishikawa T, Dricot A, Li N, Berriz GF, Gibbons FD, Dreze M, Ayivi-Guedehoussou N, Klitgord N, Simon C, Boxem M, Milstein S, Rosenberg J, Goldberg DS, Zhang L V., Wong SL, Franklin G, Li S, et al (2005) Towards a proteome-scale map of the human protein–protein interaction network. *Nature* **437:** 1173–1178

Rudner AD, Hardwick KG & Murray AW (2000) Cdc28 Activates Exit from Mitosis in Budding Yeast *J. Cell Biol.* **149** (7): 1361-1376

Ryan CJ, Roguev A, Patrick K, Xu J, Jahari H, Tong Z, Beltrao P, Shales M, Qu H, Collins SR, Kliegman JI, Jiang L, Kuo D, Tosti E, Kim H-S, Edelmann W, Keogh M-C, Greene D, Tang C, Cunningham P, et al (2012) Hierarchical modularity and the evolution of genetic interactomes across species. *Mol. Cell* **46:** 691–704

Samejima I, Spanos C, Alves F de L, Hori T, Perpelescu M, Zou J, Rappsilber J, Fukagawa T & Earnshaw WC (2015) Whole-proteome genetic analysis of dependencies in assembly of a vertebrate kinetochore. *J. Cell Biol.* **211:** 1141–1156

San-Segundo PA & Roeder GS (1999) Pch2 links chromatin silencing to meiotic checkpoint control. *Cell* **97:** 313–324

Santaguida S, Vernieri C, Villa F, Ciliberto A & Musacchio A (2011) Evidence that Aurora B is implicated in spindle checkpoint signalling independently of error correction. *EMBO J.* **30:** 1508–1519

Saurin AT, van der Waal MS, Medema RH, Lens SMA & Kops GJPL (2011) Aurora B potentiates Mps1 activation to ensure rapid checkpoint establishment at the onset of mitosis. *Nat. Commun.* **2:** 316

Scott RJ, Lusk CP, Dilworth DJ, Aitchison JD & Wozniak RW (2005) Interactions between Mad1p and the nuclear transport machinery in the yeast Saccharomyces cerevisiae. *Mol. Biol. Cell* **16:** 4362–4374

Shah J V, Botvinick E, Bonday Z, Funrari F, Berns M & Cleveland DW (2004) Dynamics of centromere and kinetochore proteins: Implications for checkpoint signaling and silencing. *Curr. Biol.* **14:** 942–952

Shen J, Peng Y, Wei L, Zhang W, Yang L, Lan L, Kapoor P, Ju Z, Mo Q, Shih I-M, Uray IP, Wu X, Brown PH, Shen X, Mills GB, Peng G & Peng G (2015) ARID1A Deficiency Impairs the

DNA Damage Checkpoint and Sensitizes Cells to PARP Inhibitors HHS Public Access. *Cancer Discov* **5:** 752–767

Shepperd LA, Meadows JC, Sochaj AM, Lancaster TC, Zou J, Buttrick GJ, Rappsilber J, Hardwick KG & Millar JBA (2012) Phosphodependent Recruitment of Bub1 and Bub3 to Spc7/KNL1 by Mph1 Kinase Maintains the Spindle Checkpoint. *Curr. Biol.* **22:** 891–899

Sherr CJ (1993) Mammalian G1 cyclins. *Cell* **73:** 1059–1065

Shevchenko A, Roguev A, Schaft D, Buchanan L, Habermann B, Sakalar C, Thomas H, Krogan NJ, Shevchenko A & Stewart F (2008) Chromatin Central: towards the comparative proteome by accurate mapping of the yeast proteomic environment. *Genome Biol.* **9:** R167

Shi J, Orth JD & Mitchison T (2008) Cell type variation in responses to antimitotic drugs that target microtubules and kinesin-5. *Cancer Res.* **68:** 3269–3276

Shou W, Azzam R, Chen SL, Huddleton MJ, Baskerville C, Charbonneau H, Annan RS, Carr SA & Deshaies RJ (2002) Cdc5 influences phosphorylation of Net1 and disassembly of the RENT complex. *BMC Mol. Biol.* **3:** 3

Sillibourne JE, Delaval B, Redick S, Sinha M & Doxsey SJ (2007) Chromatin remodeling proteins interact with pericentrin to regulate centrosome integrity. *Mol. Biol. Cell* **18:** 3667–80

Simanis V & Nurse P (1986) The cell cycle control gene cdc2+ of fission yeast encodes a protein kinase potentially regulated by phosphorylation. *Cell* **45:** 261–268

Sitry-Shevah D, Kaisari S, Teichner A, Miniowitz-Shemtov S & Hershko A (2018) Role of ubiquitylation of components of mitotic checkpoint complex in their dissociation from anaphase-promoting complex/cyclosome. *PNAS* **115:** 1777–1782

Stegmeier F, Huang J, Rahal R, Zmolik J, Moazed D & Amon A (2004) The replication fork block protein Fob1 functions as a negative regulator of the FEAR network. *Curr. Biol.* **14:** 467–480

Stegmeier F, Visintin R & Amon A (2002) Separase, polo kinase, the kinetochore protein Slk19, and Spo12 function in a network that controls Cdc14 localization during early anaphase. *Cell* **108:** 207–220

Stelzl U, Worm U, Lalowski M, Haenig C, Brembeck FH, Goehler H, Stroedicke M, Zenkner M, Schoenherr A, Koeppen S, Timm J, Mintzlaff S, Abraham C, Bock N, Kietzmann S, Goedde A, Toksöz E, Droege A, Krobitsch S, Korn B, et al (2005) A human protein-protein interaction network: a resource for annotating the proteome. *Cell* **122:** 957–68

Stout JR, Yount AL, Powers JA, LeBlanc C, Ems-McClung SC & Walczak CE (2011) Kif18B interacts with EB1 and controls astral microtubule length during mitosis. *Mol. Biol. Cell* **22:** 3070–3080

Stumpff J, von Dassow G, Wagenbach M, Asbury C & Wordeman L (2008) The kinesin-8 motor Kif18A suppresses kinetochore movements to control mitotic chromosome alignment. *Dev. Cell* **14:** 252–62

Sudakin V, Chan GKT & Yen TJ (2001) Checkpoint inhibition of the APC/C in HeLa cells is mediated by a complex of BUBR1, BUB3, CDC20, and MAD2. *J. Cell Biol.* **154:** 925–936

Sullivan M & Morgan DO (2007) Finishing mitosis, one step at a time. *Nat. Rev. Mol. Cell Biol.* **8:** 894–903

Sullivan M & Uhlmann F (2003) A non-proteolytic function of separase links the onset of anaphase to mitotic exit. *Nat. Cell Biol.* **5:** 249–254

Tabba S, Mangat S, Mccartney R & Schmidt MC (2010) PP1 phosphatase-binding motif in Reg1 protein of Saccharomyces cerevisiae is required for interaction with both the PP1 phosphatase Glc7 and the Snf1 protein kinase. *Cell Signal* **22:** 1013–1021

Takeuchi K & Fukagawa T (2012) Molecular architecture of vertebrate kinetochores. *Exp. Cell Res.* **318:** 1367–1374

Tanaka K, Chang HL, Kagami A & Watanabe Y (2009) CENP-C functions as a scaffold for effectors with essential kinetochore functions in mitosis and meiosis. *Dev. Cell* **17:** 334–43

Tanaka TU (2010) Kinetochore-microtubule interactions: steps towards bi-orientation. *EMBO J.* **29:** 4070–4082

Tanenbaum ME, Macůrek L, Janssen A, Geers EF, Alvarez-Fernández M & Medema RH (2009) Kif15 Cooperates with Eg5 to Promote Bipolar Spindle Assembly. *Curr. Biol.* **19:** 1703–1711

Tang Z, Bharadwaj R, Li B & Yu H (2001) Mad2-Independent Inhibition of APC^{Cdc20} by the Mitotic Checkpoint Protein BubR1. *Dev. Cell* **1:** 227–237

Tange Y & Niwa O (1995) A selection system for diploid and against haploid cells in Schizosaccharomyces pombe. *Mol. Gen. Genet.* **248:** 644-648

Tao W, South VJ, Zhang Y, Davide JP, Farrell L, Kohl NE, Sepp-Lorenzino L & Lobell RB (2005) Induction of apoptosis by an inhibitor of the mitotic kinesin KSP requires both activation of the spindle assembly checkpoint and mitotic slippage. *Cancer Cell* **8:** 49–59

Teichner A, Eytan E, Sitry-Shevah D, Miniowitz-Shemtov S, Dumin E, Gromis J & Hershko A (2011) p31comet Promotes disassembly of the mitotic checkpoint complex in an ATP-dependent process. *Proc. Natl. Acad. Sci. U. S. A.* **108:** 3187–92

Tinker-Kulberg RL & Morgan DO (1999) Pds1 and Esp1 control both anaphase and mitotic exit in normal cells and after DNA damage. *Genes Dev.* **13:** 1936–1949

Tipton AR, Wang K, Oladimeji P, Sufi S, Gu Z & Liu S-T (2012) Identification of novel mitosis regulators through data mining with human centromere/kinetochore proteins as group queries. *BMC Cell Biol.* **13:** 15

Toda K, Naito K, Mase S, Ueno M, Uritani M, Yamamoto A & Ushimaru T (2012) APC/C-Cdh1-dependent anaphase and telophase progression during mitotic slippage. *Cell Div.* **7:** 4

Trautmann S, Wolfe BA, Jorgensen P, Tyers M, Gould KL & McCollum D (2001) Fission yeast Clp1p phosphatase regulates G2/M transition and coordination of cytokinesis with cell cycle progression. *Curr. Biol.* **11:** 931–940

Tu J & Carlson M (1995) REG1 binds to protein phosphatase type 1 and regulates glucose repression in Saccharomyces cerevisiae. *EMBO J.* **14:** 5939–46

Vanoosthuyse V & Hardwick KG (2009) A Novel Protein Phosphatase 1-Dependent Spindle Checkpoint Silencing Mechanism. *Curr. Biol.* **19:** 1176–1181

Vanoosthuyse V, Hardwick KG, Akiyoshi B, Nelson CR & Ranish J a (2009a) Overcoming inhibition in the spindle checkpoint. *Genes Dev.*: 2799–2805

Vanoosthuyse V, Legros P, van der Sar SJA, Yvert G, Toda K, Le Bihan T, Watanabe Y, Hardwick K & Bernard P (2014) CPF-associated phosphatase activity opposes

condensin-mediated chromosome condensation. *PLoS Genet.* **10:** e1004415

Vanoosthuyse V, Meadows JC, van der Sar SJA, Millar JBA & Hardwick KG (2009b) Bub3p Facilitates Spindle Checkpoint Silencing in Fission Yeast. *Mol. Biol. Cell* **20:** 5096–5105

Varga V, Helenius J, Tanaka K, Hyman AA, Tanaka TU & Howard J (2006) Yeast kinesin-8 depolymerizes microtubules in a length-dependent manner. *Nat. Cell Biol.* **8:** 957–62

Vink M, Simonetta M, Transidico P, Ferrari K, Mapelli M, De Antoni A, Massimiliano L, Ciliberto A, Faretta M, Salmon ED & Musacchio A (2006) In vitro FRAP identifies the minimal requirements for Mad2 kinetochore dynamics. *Curr. Biol.* **16:** 755–66

Visintin R, Stegmeier F & Amon A (2003) The Role of the Polo Kinase Cdc5 in Controlling Cdc14 Localization. *Mol. Biol. Cell* **14:** 4486–4498

Vleugel M, Hoogendoorn E, Snel B & Kops GJPL (2012) Evolution and Function of the Mitotic Checkpoint. *Dev. Cell* **23:** 239–250

Wagih O & Parts L (2014) gitter: A Robust and Accurate Method for Quantification of Colony Sizes From Plate Images. *G3 Genes Genomes Genet.* **4:** 547–552

Wagih O, Usaj M, Baryshnikova A, VanderSluis B, Kuzmin E, Costanzo M, Myers CL, Andrews BJ, Boone CM & Parts L (2013) SGAtools: one-stop analysis and visualization of array-based genetic interaction screens. *Nucleic Acids Res.* **41:** W591-6

Walworth N, Davey S & Beach D (1993) Fission yeast chk1 protein kinase links the rad checkpoint pathway to cdc2. *Nature* **363:** 368–371

Wan J, Zhu F, Zasadil LM, Yu J, Wang L, Johnson A, Berthier E, Beebe DJ, Audhya A & Weaver BA (2014) A Golgi localized pool of the mitotic checkpoint component Mad1 controls integrin secretion and cell migration. *Curr Biol* **24:** 2687–2692

Wang H-W, Ramey VH, Westermann S, Leschziner AE, Welburn JPI, Nakajima Y, Drubin DG, Barnes G & Nogales E (2007) Architecture of the Dam1 kinetochore ring complex and implications for microtubule-driven assembly and force-coupling mechanisms. *Nat. Struct. Mol. Biol.* **14:** 721–726

Wang J, Tadeo X, Hou H, Andrews S, Moresco JJ, Yates JR, Nagy PL, Jia S & Jia S (2014a) Tls1 regulates splicing of shelterin components to control telomeric heterochromatin assembly and telomere length. *Nucleic Acids Res.* **42:** 11419–32

Wang J, Wang Z, Yu T, Yang H, Virshup DM, Kops GJPL, Lee SH, Zhou W, Li X, Xu W & Rao Z

(2016) Crystal structure of a PP2A B56-BubR1 complex and its implications for PP2A substrate recruitment and localization. *Protein Cell* **7:** 516–526

Wang K, Sturt-Gillespie B, Hittle JC, Macdonald D, Chan GK, Yen TJ & Liu S-T (2014b) Thyroid hormone receptor interacting protein 13 (TRIP13) AAA-ATPase is a novel mitotic checkpoint-silencing protein. *J. Biol. Chem.* **289:** 23928–37

Wang W, Stukenberg PT & Brautigan DL (2008) Phosphatase Inhibitor-2 Balances Protein Phosphatase 1 and Aurora B Kinase for Chromosome Segregation and Cytokinesis in Human Retinal Epithelial Cells. *Mol. Biol. Cell* **19:** 4852–4862

Warren CD, Brady DM, Johnston RC, Hanna JS, Hardwick KG & Spencer FA (2002) Distinct Chromosome Segregation Roles for Spindle Checkpoint Proteins. *Mol. Biol. Cell* **13:** 3029–3041

Wei RR, Al-Bassam J & Harrison SC (2007) The Ndc80/HEC1 complex is a contact point for kinetochore-microtubule attachment. *Nat. Struct. Mol. Biol.* **14:** 54–59

Weinert TA & Hartwell LH (1988) The RAD9 gene controls the cell cycle response to DNA damage in Saccharomyces cerevisiae. *Science* **241:** 317–22

Welburn JPI, Grishchuk EL, Backer CB, Wilson-Kubalek EM, Yates JR & Cheeseman IM (2009) The Human Kinetochore Ska1 Complex Facilitates Microtubule Depolymerization-Coupled Motility. *Dev. Cell* **16:** 374–385

Welburn JPI, Vleugel M, Liu D, Yates JR, Lampson MA, Fukagawa T & Cheeseman IM (2010) Aurora B phosphorylates spatially distinct targets to differentially regulate the kinetochore-microtubule interface. *Mol. Cell* **38:** 383–92

West RR, Malmstrom T & McIntosh JR (2002) Kinesins klp5+ and klp6+ are required for normal chromosome movement in mitosis. *J. Cell Sci.* **115:** 931–940

West RR, Malmstrom T, Troxell CL & McIntosh JR (2001) Two related kinesins, klp5+ and klp6+ , foster microtubule disassembly and are required for meiosis in fission yeast. *Mol. Biol. Cell* **12:** 3919–3932

Westermann S, Avila-Sakar A, Wang H-W, Niederstrasser H, Wong J, Drubin DG, Nogales E & Barnes G (2005) Formation of a Dynamic Kinetochore- Microtubule Interface through Assembly of the Dam1 Ring Complex. *Mol. Cell* **17:** 277–290

Westhorpe FG, Tighe A, Lara-Gonzalez P & Taylor SS (2011) p31 comet-mediated extraction

of Mad2 from the MCC promotes efficient mitotic exit. *J. Cell Sci.* **124:** 3905–3916

Williams GL, Roberts TM & Gjoerup O V. (2007) Bub1: Escapades in a Cellular World. *Cell Cycle* **6:** 1699–1704

Winey M, Goetsch L, Baum P & Byers B (1991) MPS1 and MPS2: novel yeast genes defining distinct steps of spindle pole body duplication. *J. Cell Biol.* **114:** 745–754

Winkler C, Munter S De, Dessel N Van, Lesage B & Heroes E (2015) The selective inhibition of protein phosphatase-1 results in mitotic catastrophe and impaired tumor growth.

Winzeler EA, Shoemaker DD, Astromoff A, Liang H, Anderson K, Andre B, Bangham R, Benito R, Boeke JD, Bussey H, Chu AM, Connelly C, Davis K, Dietrich F, Dow SW, El Bakkoury M, Foury F, Friend SH, Gentalen E, Giaever G, et al (1999) Functional characterization of the S. cerevisiae genome by gene deletion and parallel analysis. *Science* **285:** 901–906

Wolfe BA & Gould KL (2004) Fission yeast Clp1p phosphatase affects G2/M transition and mitotic exit through Cdc25p inactivation. *EMBO* **23:** 919–929

Wood V, Harris MA, McDowall MD, Rutherford K, Vaughan BW, Staines DM, Aslett M, Lock A, Bähler J, Kersey PJ & Oliver SG (2012) PomBase: A comprehensive online resource for fission yeast. *Nucleic Acids Res.* **40:** 695–699

Wood V, Lock A, Harris MA, Rutherford K, Bähler J & Oliver SG (2019) Hidden in plain sight: what remains to be discovered in the eukaryotic proteome? *Open Biol.* **9:** 180241

Wu H-Y & Burgess SM (2006) Two Distinct Surveillance Mechanisms Monitor Meiotic Chromosome Metabolism in Budding Yeast. *Curr. Biol.* **16:** 2473–2479

Xia G, Luo X, Habu T, Rizo J, Matsumoto T & Yu H (2004) Conformation-specific binding of p31(comet) antagonizes the function of Mad2 in the spindle checkpoint. *EMBO J.* **23:** 3133–3143

Yam AY, Xia Y, Lin HTJ, Burlingame A, Gerstein M & Frydman J (2008) Defining the TRiC/CCT interactome links chaperonin function to stabilization of newly made proteins with complex topologies. *Nat. Struct. Mol. Biol.* **15:** 1255–1262

Yamagishi Y, Yang C-H, Tanno Y & Watanabe Y (2012) MPS1/Mph1 phosphorylates the kinetochore protein KNL1/Spc7 to recruit SAC components. *Nat. Cell Biol.* **14:** 746–752

Yang M, Li B, Tomchick DR, Machius M, Rizo J, Yu H & Luo X (2007) p31comet Blocks Mad2

Activation through Structural Mimicry. *Cell* **131:** 744–755

Ye Q, Rosenberg SC, Moeller A, Speir JA, Su TY & Corbett KD (2015) TRIP13 is a protein-remodeling AAA+ ATPase that catalyzes MAD2 conformation switching. *Elife* **4:**

Ying WC, Fava LL, Uldschmid A, Schmitz MHA, Gerlich DW, Nigg EA & Santamaria A (2009) Mitotic control of kinetochore-associated dynein and spindle orientation by human Spindly. *J. Cell Biol.* **185:** 859–874

Yuan I, Leontiou I, Amin P, May KM, Soper Ní Chafraidh S, Zlámalová E & Hardwick KG (2016) Generation of a Spindle Checkpoint Arrest from Synthetic Signaling Assemblies. *Curr. Biol.***:** 137–143

Zhang K, Lin W, Latham JA, Riefler GM, Schumacher JM, Chan C, Tatchell K, Hawke DH, Kobayashi R & Dent SYR (2005) The Set1 Methyltransferase Opposes Ipl1 Aurora Kinase Functions in Chromosome Segregation. *Cell* **122:** 723–734

Zhu C & Jiang W (2005) Cell cycle-dependent translocation of PRC1 on the spindle by Kif4 is essential for midzone formation and cytokinesis. *Proc. Natl. Acad. Sci. U. S. A.* **102:** 343–348

Zich J, May K, Paraskevopoulos K, Sen O, Syred HM, van der Sar S, Patel H, Moresco JJ, Sarkeshik A, Yates JR, Rappsilber J & Hardwick KG (2016) Mps1Mph1 Kinase Phosphorylates Mad3 to Inhibit Cdc20Slp1-APC/C and Maintain Spindle Checkpoint Arrests. *PLOS Genet.* **12:** e1005834

Appendices

Appendix 1

1.1 rTetR-Mph1$_{(\Delta 1\text{-}302)}$ expression levels in SynCheck gene deletion strains

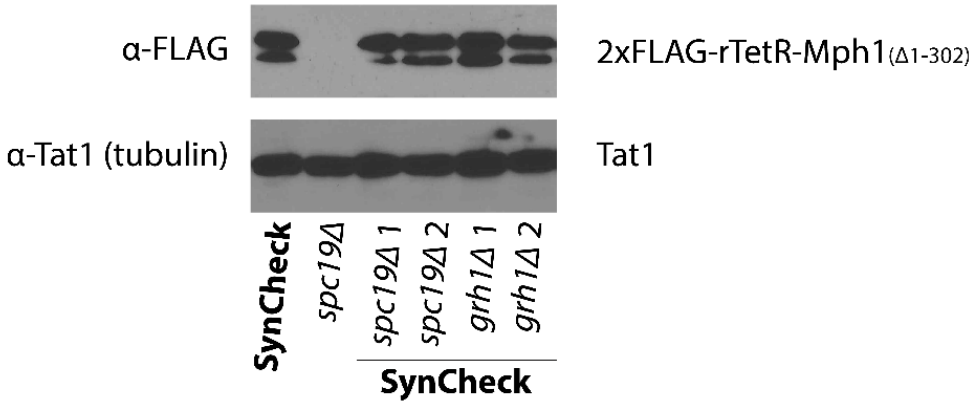

SynCheck: *rTetR-Spc7$_{1\text{-}666}$, rTetR-Mph1$_{(\Delta 1\text{-}302)}$, Mad2-GFP*

Figure S1.1 Expression levels of rTetR-Mph1$_{(\Delta 1\text{-}302)}$ construct are similar between the original SynCheck strain and SynCheck strains with single gene deletions. SynCheck strains with deletions of candidate checkpoint silencing genes were tested (same strains as used in Figure 3.2). Immunoblots were probed with α-FLAG antibody to detect the FLAG-tagged rTetR-Mph1$_{(\Delta 1\text{-}302)}$ construct. Tat1 (tubulin) was used as a loading control.

1.2 rTetR-Mph1$_{(\Delta 1\text{-}302)}$ expression in query strain for high-throughput screen

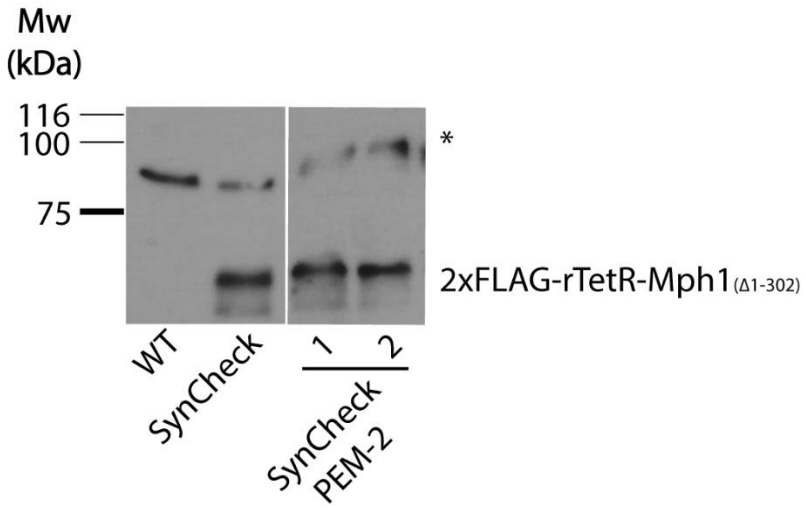

Figure S1.2 Expression levels of rTetR-Mph1$_{(\Delta 1\text{-}302)}$ construct are similar between the original SynCheck strain (Yuan *et al*, 2016) and the reconstructed SynCheck strain in a PEM-2 background. SynCheck PEM-2 was constructed by transforming the PEM-2 strain by electroporation with the rTetR-Spc7$_{(1\text{-}666)}$ and rTetR-Mph1$_{(\Delta 1\text{-}302)}$. Immunoblots were probed with α-FLAG antibody to detect the FLAG-tagged rTetR-Mph1$_{(\Delta 1\text{-}302)}$ construct. * indicates a non-specific band (also seen in the wild-type), which gives an indication of protein loading levels.

1.3 CHX and G418 serial dilution growth assays

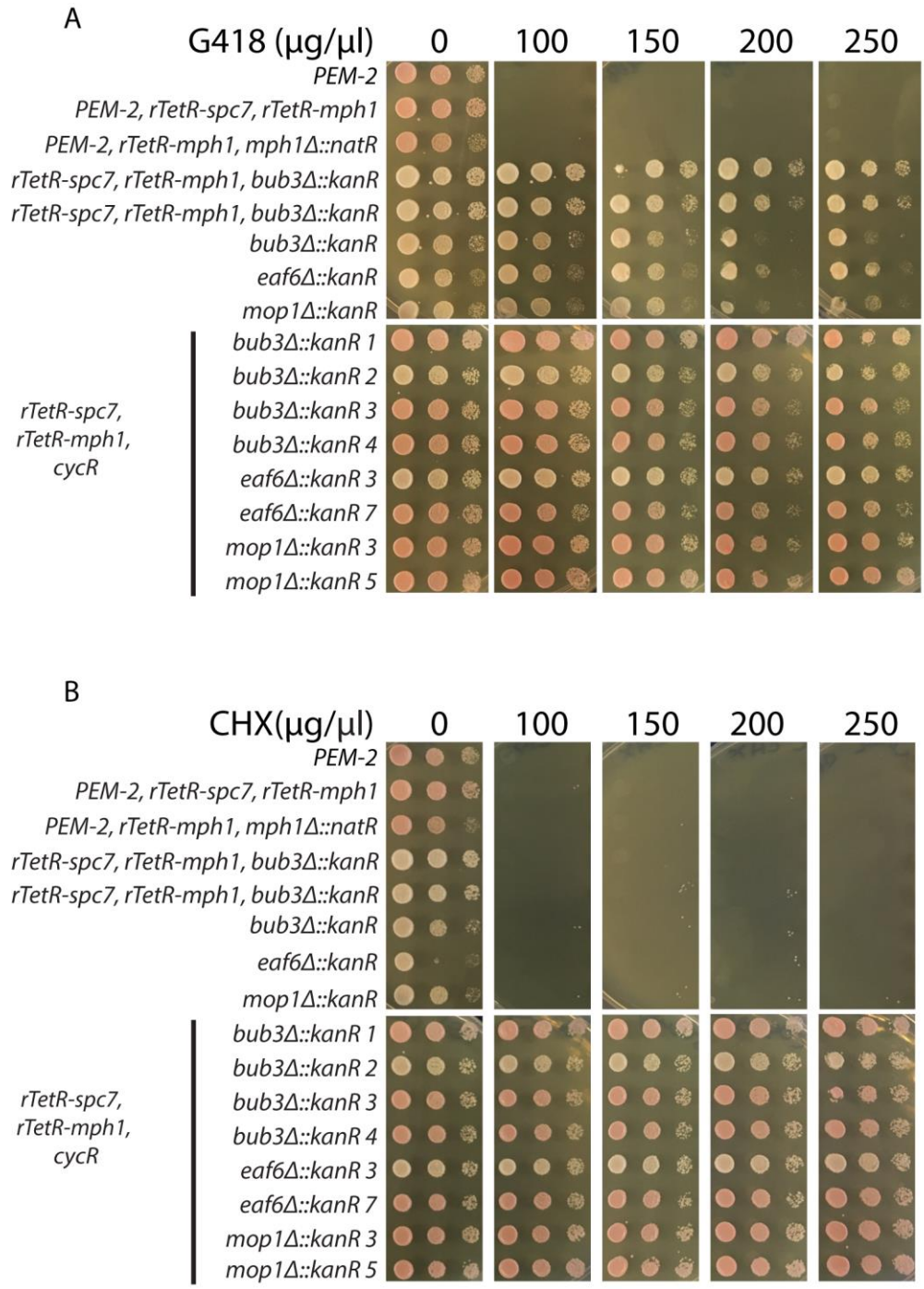

Figure S1.3 Optimisation of drug concentrations for use in high-throughput genetic screen. To determine suitable concentrations of (A) G418 and (B) cyclohexamide (CHX), serial dilution assays were performed on YES plates containing a range of drug concentrations (0-250µg/µl). Strains from the Bioneer library were crossed with the query strain used for the high-throughput screen and progeny were selected based on cycloheximide resistance (Section 2.6), and leucine and uracil auxotrophy. Strains with G418 resistance were used as positive controls (*bub3Δ*, *eaf6Δ* and *mop1Δ* strains from the

Bioneer library). Cycloheximide sensitive controls were also tested (e.g. PEM-2 strains). Multiple isolates were tested from each cross (individual isolates identified by numbers).

1.4 Additional information on high-throughput pilot plate

1.4.1 Deletion strains included on high-throughput pilot plate (gene IDs)

SPAC589.11	SPAC6C3.06c	SPBC1198.01	SPBC17D1.06	SPBC29A10.09c	SPBC8D2.02c
SPAC1002.01	SPAC6C3.07	SPBC11C11.07	SPBC17D1.07c	SPBC29A10.12	SPBC8D2.04
SPAC11D3.02c	SPAC6F6.02c	SPBC11C11.09c	SPBC17F3.01c	SPBC29A10.14	SPBC947.05c
SPAC12G12.13c	SPAC6F6.09	SPBC1215.01	SPBC17G9.05	SPBC29A3.05	SPBC947.15c
SPAC12G12.15	SPAC6F6.11c	SPBC1271.05c	SPBC17G9.12c	SPBC29A3.08	SPBCPT2R1.01c
SPAC14C4.04	SPAC6G9.01c	SPBC1271.12	SPBC1861.02	SPBC29A3.09c	SPBCPT2R1.02
SPAC1786.01c	SPAC6G9.09c	SPBC12C2.02c	SPBC1861.03	SPBC29A3.18	SPBCPT2R1.03
SPAC17A2.07c	SPAC750.08c	SPBC12C2.05c	SPBC1861.05	SPBC29A3.21	SPBCPT2R1.08c
SPAC17H9.13c	SPAC823.02	SPBC12D12.06	SPBC1861.06c	SPBC29B5.03c	SPBP22H7.08
SPAC1834.04	SPAC869.06c	SPBC1347.03	SPBC18E5.14c	SPBC2A9.03	SPBP23A10.14c
SPAC186.06	SPAC869.09	SPBC1347.12	SPBC18H10.07	SPBC2A9.04c	SPBP4H10.08
SPAC22E12.03c	SPAC890.06	SPBC1348.01	SPBC18H10.13	SPBC2D10.09	SPBP4H10.12
SPAC22E12.06c	SPAC8C9.19	SPBC1348.14c	SPBC1921.01c	SPBC2D10.15c	SPBP4H10.17c
SPAC23A1.16c	SPAC8E11.04c	SPBC13E7.08c	SPBC19C2.04c	SPBC2D10.16	SPBP4H10.18c
SPAC23C11.02c	SPAC9.02c	SPBC13E7.09	SPBC19C2.10	SPBC2D10.20	SPBP8B7.22
SPAC23C4.09c	SPAC9.12c	SPBC13E7.11	SPBC19C7.02	SPBC2F12.05c	SPBP8B7.28c
SPAC23D3.11	SPAC9.13c	SPBC146.09c	SPBC19C7.09c	SPBC2F12.11c	SPCC1020.05
SPAC23H3.08c	SPAC922.07c	SPBC146.10	SPBC19F8.01c	SPBC2F12.12c	SPCC1020.09

SPAC25B8.01	SPAC926.05c	SPBC14C8.04	SPBC19F8.02	SPBC2G2.05	SPCC11E10.06c
SPAC25B8.15c	SPAC959.05c	SPBC14F5.13c	SPBC19F8.04c	SPBC2G5.02c	SPCC1223.10c
SPAC25G10.02	SPACUNK4.19	SPBC1539.06	SPBC19F8.08	SPBC30B4.01c	SPCC1259.08
SPAC25H1.06	SPAP11E10.01	SPBC1539.07c	SPBC19G7.04	SPBC30B4.02c	SPCC1259.14c
SPAC26A3.17c	SPAP27G11.15	SPBC1539.08	SPBC19G7.10c	SPBC30B4.03c	SPCC126.13c
SPAC27D7.08c	SPAP27G11.16	SPBC1539.10	SPBC20F10.06	SPBC30D10.09c	SPCC126.15c
SPAC27D7.10c	SPAP32A8.02	SPBC15C4.05	SPBC20F10.10	SPBC30D10.18c	SPCC1442.07c
SPAC29B12.12	SPAP32A8.03c	SPBC15D4.02	SPBC215.01	SPBC31F10.03	SPCC1442.11c
SPAC29B12.13	SPAP7G5.05	SPBC15D4.06	SPBC215.06c	SPBC31F10.05	SPCC1450.08c
SPAC29E6.09	SPAPB17E12.02	SPBC15D4.15	SPBC215.07c	SPBC31F10.07	SPCC1494.08c
SPAC2E1P5.03	SPAPB17E12.03	SPBC1604.08c	SPBC215.11c	SPBC31F10.09c	SPCC14G10.03c
SPAC2F3.07c	SPAPB17E12.04c	SPBC1604.16c	SPBC216.02	SPBC31F10.15c	SPCC162.03
SPAC30D11.04c	SPAPB17E12.05	SPBC1604.18c	SPBC216.04c	SPBC32F12.08c	SPCC162.12
SPAC31G5.03	SPAPB17E12.08	SPBC1683.06c	SPBC21B10.03c	SPBC32H8.01c	SPCC1795.10c
SPAC3G6.01	SPAPB17E12.12c	SPBC1683.07	SPBC21B10.04c	SPBC32H8.05	SPCC1840.09
SPAC3G9.07c	SPAPB17E12.14c	SPBC1683.13c	SPBC21B10.05c	SPBC336.10c	SPCC23B6.05c
SPAC3H1.08c	SPAPB18E9.04c	SPBC1685.01	SPBC21B10.07	SPBC337.09	SPCC24B10.10c
SPAC3H5.10	SPAPB1A10.03	SPBC1685.10	SPBC21B10.08c	SPBC337.16	SPCC285.14
SPAC4A8.07c	SPAPB1A11.04c	SPBC16A3.07c	SPBC21C3.06	SPBC36.06c	SPCC297.04c
SPAC4A8.09c	SPAPB1E7.07	SPBC16A3.17c	SPBC21C3.08c	SPBC365.16	SPCC306.07c
SPAC4D7.06c	SPAPB21F2.03	SPBC16C6.03c	SPBC21C3.09c	SPBC36B7.06c	SPCC330.03c
SPAC4F10.19c	SPAPB24D3.02c	SPBC16C6.05	SPBC21C3.11	SPBC3B8.10c	SPCC338.02

SPAC4G8.10	SPAPB24D3.08c	SPBC16C6.09	SPBC21C3.13	SPBC3B9.05	SPCC338.08
SPAC4G8.11c	SPAPB2B4.06	SPBC16E9.14c	SPBC21D10.08c	SPBC3B9.13c	SPCC364.01
SPAC4H3.14c	SPAPB8E5.02c	SPBC16E9.15	SPBC23E6.05	SPBC3D6.04c	SPCC4B3.11c
SPAC513.04	SPAPB8E5.05	SPBC16G5.05c	SPBC23E6.08	SPBC3D6.06c	SPCC4G3.02
SPAC56E4.07	SPAPB8E5.10	SPBC16G5.15c	SPBC23E6.10c	SPBC3D6.09	SPCC576.17c
SPAC57A10.08c	SPAPJ691.02	SPBC16G5.16	SPBC23G7.07c	SPBC409.17c	SPCC613.03
SPAC57A7.09	SPAPJ691.03	SPBC16H5.08c	SPBC23G7.11	SPBC409.20c	SPCC613.11c
SPAC5D6.01	SPAPJ698.02c	SPBC16H5.11c	SPBC23G7.15c	SPBC4B4.06	SPCC622.01c
SPAC5D6.07c	SPAPYUG7.06	SPBC1703.03c	SPBC23G7.16	SPBC4C3.12	SPCC63.06
SPAC5D6.08c	SPAPYUK71.03c	SPBC1703.06	SPBC24C6.05	SPBC4F6.10	SPCC63.13
SPAC5H10.05c	SPBC106.01	SPBC1703.08c	SPBC25B2.03	SPBC609.04	SPCC645.07
SPAC630.10	SPBC106.02c	SPBC1703.11	SPBC25B2.04c	SPBC651.04	SPCC736.09c
SPAC630.11	SPBC106.03	SPBC1709.11c	SPBC25H2.05	SPBC660.05	SPCC737.05
SPAC630.15	SPBC106.10	SPBC1709.18	SPBC25H2.08c	SPBC660.17c	SPCC757.02c
SPAC664.10	SPBC1105.09	SPBC1711.14	SPBC27.04	SPBC685.04c	SPCC777.08c
SPAC683.03	SPBC1105.11c	SPBC1711.15c	SPBC27B12.05	SPBC83.04	SPCC965.08c
SPAC694.03	SPBC115.02c	SPBC1718.02	SPBC28E12.04	SPBC83.19c	SPCC965.09
SPAC6B12.06c	SPBC115.03	SPBC1773.03c	SPBC28E12.06c	SPBC839.13c	SPCC965.13
SPAC6B12.14c	SPBC119.04	SPBC1773.17c	SPBC28F2.02	SPBC839.14c	SPCC965.14c
SPAC6B12.15	SPBC119.06	SPBC1778.03c	SPBC28F2.05c	SPBC887.08	SPCC970.05
SPAC6C3.02c	SPBC119.12	SPBC17A3.10	SPBC28F2.08c	SPBC887.15c	SPCP31B10.05
SPAC6C3.05					

1.4.2 Synthetically rescued strains from high-throughput pilot plate

Gene ID (Δ)	Gene name	Gene description
SPBC16C6.09	*ogm4*	protein O-mannosyltransferase Ogm4
SPCC338.02	*mug112*	sequence orphan
SPBC83.04	*apc15*	anaphase-promoting complex, platform subcomplex scaffold subunit Apc15
SPBC20F10.06	*mad2*	mitotic spindle checkpoint protein Mad2

1.5 Complete list of manually identified synthetically sick strains from screen

Gene ID (Δ)	Gene name	Gene function	Darker	Smaller
SPAC14C4.11	*vtc2*	polyphosphate synthetase	2	2
SPCC1223.02	*nmt1/thi3*	no message in thiamine Nmt1	2	2
SPCC18B5.05c		phosphomethylpyrimidine kinase	2	2
SPAC227.15	*reg1*	protein phosphatase regulatory subunit Reg1	2	2
SPBC30B4.04c	*sol1*	SWI/SNF complex subunit Sol1	2	2
SPAC4F10.18		WD repeat protein, human NUP37 family	2	2
SPAC926.03	*rlc1*	myosin II regulatory light chain	2	1
SPAC589.02c	*med13*	mediator complex subunit Srb9	2	0
SPBC3B8.02	*php5*	CCAAT-binding factor complex subunit Php5	2	0
SPAPJ696.01c	*vps17*	retromer complex subunit Vps17	2	0
SPCC1672.04c	*cox 19*	mitochondrial copper ion transport protein	2	0
SPBC691.04	*mss116*	mitochondrial ATP-dependent RNA helicase	2	0
SPBP8B7.18c		phosphomethylpyrimidine kinase	1	1
SPBC216.01c	*psy2*	DNA damage response protein	1	1
SPCC1259.11c	*gyp2*	GTPase activating protein Gyp2	1	1
SPAC1D4.01	*tls1*	sequence orphan	1	1
SPAC1B3.16c	*vht1*	vitamin H transporter Vth1	1	1
SPBC29A10.06c		conserved fungal protein	1	1
SPAC23H3.08c	*bub3*	mitotic spindle checkpoint protein Bub3	1	1
SPAC823.03	*ppk15*	serine/threonine protein kinase Ppk15	1	0
SPAC1D4.02c	*grh1*	human GRASP protein homolog	1	0
SPAC227.17c		conserved protein (fungal and plant)	1	0
SPBP4H10.13	*rps2302*	40S ribosomal protein S23	1	0
SPBC28E12.04		sequence orphan	1	1
SPCC24B10.10c	*yta4*	mitochondrial outer membrane ATPase	1	0
SPBC3E7.16c	*leu3*	2-isopropylmalate synthase	0	1
SPCC576.17c		membrane transporter	0	1
SPCC777.08c	*bit61*	HbrB family protein	0	1
SPBC11B10.05c	*rsp1*	random septum position protein Rsp1	0	1

SPAC19G12.16c	*adg2*	conserved fungal protein	0	1

1.6 Quantification of high-throughput SynCheck (rTetR) screen with SGATools

1.6.1 Synthetically sick strains in SynCheck (rTetR) screen

Gene ID (Δ)	Gene name	Gene description	Score -Th	Score +Th	Adjusted score (-Th)-(+Th)
SPBCPT2R1.03		hypothetical protein	-0.094	0.83	**-0.924**
SPAC1751.04	*loc1*	ribosome biogenesis protein Loc1 (predicted)	-0.318	0.564	**-0.882**
SPBC1711.15c		sequence orphan	-0.631	0.19	**-0.821**
SPAC869.02c	*yhb1*	nitric oxide dioxygenase	-0.735	0.046	**-0.781**
SPBP8B7.26		sequence orphan	-0.174	0.575	**-0.749**
SPBC3D6.09	*dpb4*	DNA polymerase epsilon subunit Dpb4	-0.327	0.37	**-0.697**
SPBC713.09		sequence orphan	-0.233	0.442	**-0.675**
SPAP27G11.16		sequence orphan	0	0.674	**-0.674**
SPAC227.15	*reg1*	protein phosphatase regulatory subunit Reg1	-0.764	-0.133	**-0.631**
SPBC530.01	*gyp1*	GTPase activating protein	1.106	1.719	**-0.613**
SPBC30D10.14		dienelactone hydrolase family	-0.638	-0.045	**-0.592**
SPCC4G3.05c	*mus81*	Holliday junction resolvase subunit Mus81	0.271	0.828	**-0.557**
SPAC13F5.05	*mpd1*	thioredoxin family protein	-0.274	0.265	**-0.539**
SPAC10F6.06	*vip1*	RNA-binding protein Vip1	-0.527	-0.013	**-0.514**
SPAC18B11.09c		N-acetyltransferase	-0.426	0.087	**-0.513**
SPBC146.10	*mug57*	meiotically upregulated gene Mug57	-0.461	0.05	**-0.511**
SPAC25A8.01c	*fft3*	fun thirty related protein Fft3	-0.253	0.25	**-0.503**
SPAC24H6.11c		sulfate transmembrane transporter (predicted)	0.050	0.548	**-0.498**
SPAC23C11.10	*mpn1*	poly(U)-specific exoribonuclease, producing 3' uridine cyclic phosphate ends Mpn1	-0.17	0.324	**-0.494**
SPAC16E8.18	*tam5*	sequence orphan	-0.585	-0.091	**-0.493**
SPBC1685.11	*Rlp1*	RecA family ATPase Rlp1	-0.192	0.283	**-0.476**
SPAC17H9.19c	*cdt2*	WD repeat protein Cdt2	-0.276	0.193	**-0.469**
SPCC1183.10	*wtf10*	wtf element Wtf10	0.114	0.572	**-0.459**
SPAC1B1.02c		NAD/NADH kinase (predicted)	-0.008	0.447	**-0.454**
SPAC607.06c		metallopeptidase (predicted)	-0.06	0.382	**-0.442**
SPAC1142.08	*fhl1*	forkhead transcription factor Fhl1	-0.174	0.264	**-0.437**
SPAC27F1.10		sequence orphan	0.073	0.508	**-0.436**

SPBC19G7.02	*abz2*	4-amino-4-deoxychorismate lyase Abz2 (predicted)	-0.099	0.335	**-0.433**
SPAC694.03		conserved fungal protein	-0.795	-0.365	**-0.43**
SPAC1B3.16c	*vht1*	vitamin H transporter Vht1	-0.329	0.093	**-0.421**
SPAC2E1P3.04	*cao1*	copper amine oxidase	-0.304	0.116	**-0.42**
SPAC3F10.09		isomerase	-0.323	0.094	**-0.417**
SPBC19F8.01c	*spn7*	meiotic septin Spn7	-0.1	0.313	**-0.413**
SPAC227.14	*yfh7*	uridine kinase Yfh7 (predicted)	0.072	0.481	**-0.409**
SPAC1B3.08		TREX2 complex subunit (predicted)	0.446	0.852	**-0.406**
SPAC343.16	*lys2*	homoaconitate hydratase Lys2	-0.653	-0.247	**-0.406**
SPAC23A1.14c		cystathionine gamma-synthase	-0.448	-0.044	**-0.404**
SPCC4G3.19	*alp16*	gamma tubulin complex subunit Alp16	0.085	0.487	**-0.403**
SPAC25G10.01		RNA-binding protein	-0.307	0.089	**-0.396**
SPAC1486.02c	*ucp14, dsc2*	Golgi Dsc E3 ligase complex subunit Dsc2	-0.695	-0.301	**-0.394**
SPAC1952.08c		pyridoxamine 5'-phosphate oxidase (predicted)	-0.059	0.334	**-0.393**
SPAC4G9.19		DNAJ domain protein DNAJB family (predicted)	0.044	0.434	**-0.39**
SPAC57A7.13		RNA-binding protein, involved in splicing (predicted)	0.162	0.549	**-0.387**
SPAC22F3.07c	*atp20*	F0-ATPase subunit G	-0.468	-0.082	**-0.386**
SPBC2A9.13		sequence orphan	-0.29	0.093	**-0.383**
SPAPB1A10.15	*arv1*	Arv1-like family protein (predicted)	-0.28	0.085	**-0.366**
SPAC227.03c	*yea6*	mitochondrial NAD+ transporter	-0.423	-0.057	**-0.365**
SPCC1183.09c	*pmp31*	plasma membrane proteolipid Pmp31	0.418	0.782	**-0.364**
SPCC320.04c	*gem1*	ERMES complex GTPase subunit Gem1 (predicted)	-0.181	0.175	**-0.356**
SPAC630.07c		sequence orphan	1.044	1.4	**-0.355**
SPAC823.16c	*atg1802*	autophagy associated WD repeat protein Atg18b	0.368	0.722	**-0.354**
SPCC126.08c		lectin family glycoprotein receptor (predicted)	-0.494	-0.144	**-0.351**
SPBC725.10	*tps0*	mitochondrial lipid translocator protein, tspO	0.089	0.439	**-0.35**
SPAPB17E12.03	*pex12*	ubiquitin-protein ligase E3 Pex12 involved in peroxisome organization and biogenesis (predicted)	0.266	0.614	**-0.348**
SPBC32F12.06	*pch1*	cyclin Pch1	-0.237	0.107	**-0.343**
SPAC8E11.06		sequence orphan	-0.406	-0.076	**-0.33**
SPCC4B3.02c	*got1*	Golgi transport protein Got1 (predicted)	-0.131	0.195	**-0.326**

SPBC1105.14	*rsv2*	transcription factor Rsv2	-0.465	-0.141	**-0.324**
SPAC890.05	*pxr1*	ribosome biogenesis protein	-0.436	-0.121	**-0.315**
SPAPJ691.03	*mic10*	MICOS complex subunit Mic10 (predicted)	-0.159	0.154	**-0.313**
SPAC1952.15c	*rec24*	meiotic recombination protein Rec24	-0.04	0.273	**-0.313**
SPAPB8E5.02c	*rpn502*	19S proteasome regulatory subunit Rpn502	-0.042	0.259	**-0.301**
SPBC16G5.05c	*scs2*	VAP family protein Scs2	0.132	0.426	**-0.294**
SPAC26A3.10		Arf GAP protein	-0.247	0.04	**-0.287**
SPAC3C7.10	*pex13*	peroxin 13 (predicted)	0.122	0.401	**-0.279**
SPAC6F6.09	*eaf6*	NuA4 histone acetyltransferase complex subunit	-0.309	-0.031	**-0.278**
SPAC29B12.03	*spd1*	ribonucleotide reductase (RNR) inhibitor	-0.32	-0.046	-0.274
SPCC1281.07c		glutathione S-transferase Gst3	-0.369	-0.1	-0.269
SPAC17C9.07	*alg8*	dolichyl pyrophosphate Glc1Man9GlcNAc2 alpha-1,3-glucosyltransferase Alg8 (predicted)	-0.06	0.209	**-0.268**
SPCC622.17	*apn1*	AP endonuclease Apn1	-0.215	0.053	**-0.268**
SPBC1921.01c	*rpl35b*	60S ribosomal protein L35a (predicted)	0.492	0.76	**-0.268**
SPCC1919.03c	*amk2*	AMP-activated protein kinase beta subunit	-0.256	0.009	**-0.266**
SPBC1685.08	*cti6*	histone deacetylase complex subunit Cti6	-0.364	-0.099	**-0.265**
SPAC9.10	*thi9*	plasma membrane thiamine/proton high affinity transmembrane transporter Thi9	-0.671	-0.41	**-0.262**
SPBC106.04	*ada1*	adenosine deaminase Ada1	0.098	0.36	**-0.261**
SPAPB17E12.02	*yip12*	SMN family protein Yip12	-0.277	-0.017	**-0.261**
SPAC5D6.01	*rps2202*	40S ribosomal protein S15a (predicted)	0.224	0.483	**-0.259**
SPBC29A10.01	*ccr1*	NADPH-cytochrome p450 reductase	-0.017	0.24	**-0.257**
SPBC19C2.09	*sre1*	sterol regulatory element binding protein Sre1	-0.547	-0.292	**-0.256**
SPAC3C7.03c	*rad55*	RecA family ATPase Rad55/Rhp55	-0.183	0.069	**-0.252**
SPACUNK4.16c	*tps3*	alpha,alpha-trehalose-phosphate synthase (predicted)	-0.152	0.099	**-0.251**
SPBC16D10.02	*trm11*	tRNA (guanine-N2-)-methyltransferase catalytic subunit Trm11 (predicted)	-0.121	0.127	**-0.248**
SPBC543.10	*get1*	GET complex subunit	-0.222	0.025	**-0.248**
SPBC32F12.07c		membrane associated ubiquitin-protein ligase E3, MARCH family (predicted)	-0.101	0.147	**-0.248**

SPBC26H8.12		cytochrome c heme lyase Cyc3 (predicted)	-0.023	0.223	**-0.246**
SPAC16A10.05c	*dad1*	DASH complex subunit Dad1	0.021	0.261	**-0.241**
SPAC1D4.02c	*grh1*	human GRASP protein homolog	-0.414	-0.174	**-0.24**
SPBC4F6.12	*pxl1*	paxillin-like protein Pxl1	0.3641	0.604	**-0.24**
SPAPB2B4.04c	*pmc1*	P-type ATPase, calcium transporting Pmc1	-0.384	-0.146	**-0.238**
SPCP1E11.07c	*cwf18*	complexed with Cdc5 protein Cwf18	-0.354	-0.118	**-0.237**
SPCC777.08c	*bit61*	HbrB family protein	-0.48	-0.245	**-0.235**
SPAC589.10c	*ubi5*	ribomal-ubiquitin fusion protein Ubi5	-0.957	-0.723	**-0.234**
SPAC4H3.01		DNAJ domain protein Caj1/Djp1 type (predicted)	-0.109	0.125	**-0.234**
SPAC806.04c		DUF89 family protein (phosphatase)	-0.309	-0.079	**-0.231**
SPBC24C6.04	*put2*	delta-1-pyrroline-5-carboxylate dehydrogenase Put2 (predicted)	0.376	0.607	**-0.23**
SPAC11D3.18c		nicotinic acid plasma membrane transporter	-0.261	-0.031	**-0.23**
SPBC3H7.07c		phosphoserine phosphatase	-0.291	-0.065	**-0.226**
SPCC736.02		sequence orphan	0.066	0.292	**-0.225**
SPBC12C2.09c	*izh2*	Haemolysin-III family plasma membrane receptor implicated in zinc ion homeostasis Izh2 (predicted)	-0.196	0.029	**-0.225**
SPBC32H8.03	*bem46*	esterase/lipase, human ABHD13 ortholog (predicted)	0.213	0.438	**-0.225**
SPAC5D6.02c	*mug165*	sequence orphan	-0.224	-6E-04	**-0.224**
SPAC22A12.16	*acl2*	ATP-citrate synthase subunit 2 (predicted)	-0.019	0.205	**-0.223**
SPBC21B10.06c	*inp2*	myosin binding vezatin family protein involved in peroxisome inheritance Inp2 (predicted)	0.047	0.27	**-0.223**
SPBC14F5.09c	*ade8*	adenylosuccinate lyase Ade8	-0.076	0.143	**-0.219**
SPBC215.13	*mtl3*	plasma membrane-associated serine-rich cell wall sensor Mtl1/Mtl3	-0.168	0.05	**-0.218**
SPBC30B4.01c	*wsc1*	transmembrane receptor Wsc1	-0.318	-0.099	**-0.218**
SPAC22F8.09	*rrp16*	rRNA processing protein Rrp16	-0.336	-0.118	**-0.218**
SPCC1795.06	*map2*	P-factor pheromone Map2	0.061	0.279	**-0.218**
SPBC24C6.05	*sec28*	coatomer epsilon subunit (predicted)	-0.131	0.087	**-0.218**
SPBC1198.11c	*reb1*	RNA polymerase I transcription termination factor/ RNA polymerase II transcription factor Reb1	-0.169	0.049	**-0.218**
SPAC12G12.01c	*sea4*	ubiquitin-protein ligase E3	-0.413	-0.195	**-0.217**

SPAC31G5.18c	*sde2*	intron-specific pre-mRNA splicing-ubiquitin fusion protein Sde2	-0.009	0.208	**-0.217**
SPAC23C11.13c	*hpt1*	guanine/xanthine/hypoxanthine phosphoribosyltransferase Hpt1	0.519	0.735	**-0.217**
SPCC962.04	*rps1201*	40S ribosomal protein S12	-0.387	-0.172	**-0.216**
SPCC13B11.02c		sequence orphan	0.105	0.32	**-0.215**
SPAC23C4.17	*trm402*	tRNA (cytosine-5-)-methyltransferase (predicted)	0.049	0.264	**-0.215**
SPAC2C4.14c	*ppk11*	PAK-related kinase Ppk11	-0.376	-0.164	**-0.212**
SPAC637.07	*moe1*	translation initiation factor eIF3d Moe1	-0.252	-0.042	**-0.209**
SPAC1952.06c	*trm402*	spliceosomal complex subunit (predicted)	0.085	0.294	**-0.209**
SPCC895.07	*alp14*	microtubule plus end tracking polymerase Alp14	-0.575	-0.366	**-0.209**
SPAC3H5.07	*rpl702*	60S ribosomal protein L7b involved in cytoplasmic translation	-0.085	0.123	**-0.209**
SPCC576.01c	*xan1*	alpha-ketoglutarate-dependent xanthine dioxygenase Xan1	-0.183	0.024	**-0.207**
SPCC1393.09c	*gir2*	RWD domain protein, involved in cytoplasmic translation Gir2	0.076	0.282	**-0.207**
SPBC2D10.17	*clr1*	SHREC complex intermodule linker subunit Clr1	0.033	0.24	**-0.207**
SPAC1556.01c	*rad50*	DNA repair protein Rad50	-0.024	0.182	**-0.206**
SPAC5H10.01	*dgc1*	mitochondrial D-glutamate cyclase Dgc1 (predicted)	-0.075	0.131	**-0.206**
SPCC18B5.05c		phosphomethylpyrimidine kinase (predicted)	-0.147	0.058	**-0.206**
SPAC11H11.04	*mam2*	pheromone p-factor receptor	0.154	0.36	**-0.206**
SPCC4B3.12	*set9*	histone lysine H4-K20 methyltransferase Set9	0.210	0.413	**-0.203**
SPAP8A3.12c	*tpp2*	tripeptidyl-peptidase II Tpp2	-0.057	0.145	**-0.202**
SPCC777.10c	*ubc12*	NEDD8-conjugating enzyme Ubc12	-0.156	0.047	**-0.202**
SPBC23G7.16	*ctr6*	copper transporter Ctr6	-0.253	-0.051	**-0.201**
SPAPB21F2.02	*dop1*	Dopey family protein Dop1	-0.115	0.086	**-0.201**

1.6.2 Synthetically rescued strains in SynCheck (rTetR) screen

Gene ID (Δ)	Gene name	Gene description	Score -Th	Score +Th	Adjusted score (-Th)-(+Th)
SPBC947.14c		sequence orphan	0.613	-0.57	**1.179**
SPCC1223.11	*ptc2*	protein phosphatase 2C Ptc2	1.208	0.173	**1.036**
SPAC1952.02		ribosome biogenesis protein	-0.027	-1.01	**0.982**
SPCC663.03	*pmd1*	leptomycin efflux transporter Pmd1	0.449	-0.46	**0.913**
SPCC1223.15c	*spc19*	DASH complex subunit Spc19	0.948	0.095	**0.853**

SPBC354.03	*swd3*	WD repeat protein Swd3	0.386	-0.41	**0.8**
SPBC2F12.11c	*rep2*	transcriptional activator Rep2	0.275	-0.5	**0.772**
SPAC4A8.06c		esterase/lipase	0.659	-0.09	**0.753**
SPAC15A10.16	*bud6*	actin interacting protein 3 homolog Bud6	0.368	-0.38	**0.745**
SPBC21B10.13c		transcription factor	-0.093	-0.8	**0.71**
SPAC29A4.09		rRNA processing protein Rrp17	0.313	-0.39	**0.701**
SPBC1539.08	*arf6*	ADP-ribosylation factor, Arf family	1.12	0.432	**0.688**
SPAC105.03c		transcription factor	0.181	-0.5	**0.682**
SPAC139.06	*hat1*	histone acetyltransferase Hat1	0.99	0.316	**0.674**
SPCC970.05	*rpl3601*	60S ribosomal protein L36	-0.333	-0.98	**0.65**
SPBC29B5.03c	*rpl26*	60S ribosomal protein L26	-0.185	-0.83	**0.642**
SPBC3H7.03c		2-oxoglutarate dehydrogenase (lipoamide) (e1 component of oxoglutarate dehydrogenase complex)	-0.22	-0.85	**0.626**
SPBC646.06c	*agn2*	glucan endo-1,3-alpha-glucosidase Agn2	-0.001	-0.62	**0.621**
SPBC887.08		sequence orphan	1.25	0.629	**0.621**
SPBC1105.04c	*cbp1*	CENP-B homolog	-0.491	-1.11	**0.621**
SPAC1851.03	*ckb1*	CK2 family regulatory subunit	0.312	-0.3	**0.617**
SPAC13A11.03	*mcp7*	meiosis specific coiled-coil protein Mcp7	0.928	0.314	**0.613**
SPAC14C4.12c		SWIRM domain protein	0.471	-0.13	**0.606**
SPCC297.05		diacylglycerol binding protein	-0.212	-0.8	**0.584**
SPBP4H10.03	*oxa102*	mitochondrial inner membrane translocase Oxa102	-0.004	-0.57	**0.57**
SPAC1F5.08c	*yam8*	calcium transport protein	0.548	-0.01	**0.562**
SPAC227.18	*lys3*	saccharopine dehydrogenase [NAD+, L-lysine forming]	0.764	0.206	**0.558**
SPCC24B10.09	*rps1702*	40S ribosomal protein S17	0.198	-0.36	**0.556**
SPBC31F10.02		thioesterase superfamily protein	-0.092	-0.63	**0.543**
SPBC16C6.05		translation initiation factor	0.559	0.021	**0.538**
SPBC29A3.03c		ubiquitin-protein ligase E3	0.317	-0.22	**0.535**
SPBC29A10.12		HMG-box variant	1.019	0.503	**0.517**
SPAC29A4.14c		peroxin-3	-0.13	-0.64	**0.511**
SPCC550.15c		ribosome biogenesis protein	-0.113	-0.62	**0.511**
SPAC12G12.03	*cip2*	RNA-binding protein Cip2	1.093	0.583	**0.51**
SPAC1F3.09	*mug161*	CwfJ family protein	-0.083	-0.59	**0.509**
SPBC1105.09	*ubc15*	ubiquitin conjugating enzyme Ubc15	0.824	0.327	**0.497**
SPBC13E7.06	*msd1*	spindle pole body protein Msd1	0.62	0.154	**0.466**
SPAC2C4.08		conserved fungal protein	0.442	-0.02	**0.466**
SPBC56F2.08c		RNA-binding protein	0.717	0.257	**0.46**
SPBC13E7.04	*atp16*	F1-ATPase delta subunit	0.22	-0.23	**0.453**
SPAC13G6.09		zf-MYND type	0.523	0.076	**0.447**

SPBC29A3.12	*rps902*	40S ribosomal protein S9	-0.33	-0.76	**0.426**
SPBC365.03c	*rpl2101*	60S ribosomal protein L21	1.306	0.888	**0.419**
SPAC13G6.15c		calcipressin	0.481	0.064	**0.417**
SPCC297.04c	*set7*	histone lysine methyltransferase Set7	-0.059	-0.47	**0.414**
SPAC823.10c		mitochondrial carrier with solute carrier repeats	-0.129	-0.54	**0.413**
SPBC947.10		ubiquitin-protein ligase E3	0.103	-0.3	**0.403**
SPCC553.08c		GTPase Ria1	0.093	-0.3	**0.397**
SPAC4F10.20	*grx1*	glutaredoxin Grx1	0.331	-0.07	**0.397**
SPAC1486.01		manganese superoxide dismutase (AF069292)	-0.093	-0.49	**0.392**
SPBC36.10		mitochondrial intermembrane space protein sorting protein	0.423	0.033	**0.391**
SPBC21C3.11	*ubx4*	UBX domain protein Ubx4	0.576	0.188	**0.388**
SPAC15A10.10	*mde6*	Muskelin homolog	-0.273	-0.66	**0.387**
SPACUNK4.19	*mug153*	sequence orphan	0.16	-0.23	**0.386**
SPAC11E3.05		ubiquitin-protein ligase E3	0.603	0.22	**0.382**
SPAC140.02	*gar2*	GAR family	-0.184	-0.56	**0.379**
SPCC1223.02	*nmt1*	no message in thiamine Nmt1	0.167	-0.21	**0.378**
SPAC11G7.06c	*mug132*	S. pombe specific UPF0300 family protein 3	0.193	-0.19	**0.378**
SPBC30B4.04c	*sol1*	SWI/SNF complex subunit Sol1	0.013	-0.36	**0.374**
SPAC25B8.10		trans-aconitate 3-methyltransferase	0.165	-0.21	**0.371**
SPAC664.01c	*swi6*	chromodomain protein Swi6	0.379	0.018	**0.362**
SPAC27D7.11c		S. pombe specific But2 family protein	0.227	-0.13	**0.36**
SPBC29A3.10c	*atp14*	F1-ATPase subunit H	-0.346	-0.7	**0.357**
SPBP18G5.03	*toc1*	sequence orphan	-0.645	-1	**0.356**
SPBC1105.10	*rav1*	RAVE complex subunit Rav1	0.667	0.313	**0.354**
SPBC3E7.16c	*leu3*	2-isopropylmalate synthase	-0.315	-0.67	**0.354**
SPBC1347.02	*fkbp39*	FKBP-type peptidyl-prolyl cis-trans isomerase	0.339	-0.01	**0.349**
SPBP35G2.04c		sequence orphan	-0.279	-0.63	**0.347**
SPAC6G10.06		amino acid oxidase	-0.05	-0.4	**0.347**
SPAC9G1.03c	*rpl3001*	60S ribosomal protein L30	-0.387	-0.73	**0.347**
SPBC651.05c	*dot2*	EAP30 family protein Dot2	0.099	-0.24	**0.341**
SPBC13G1.10c	*mug81*	ATP-dependent RNA helicase Slh1	0.97	0.633	**0.337**
SPAC1834.09	*mug51*	conserved fungal protein	-0.081	-0.42	**0.336**
SPCC24B10.18		human Leydig cell tumor 10 kDa protein homolog	-0.405	-0.74	**0.336**
SPBC577.11		sequence orphan	0.149	-0.18	**0.334**
SPBC1D7.04	*mlo3*	RNA annealing factor Mlo3	1.751	1.418	**0.333**
SPBC25H2.10c		tRNA acetyltransferase	0.468	0.142	**0.326**
SPAC4F10.19c		zf-HIT protein Hit1	0.292	-0.03	**0.325**

SPAC328.04		AAA family ATPase, unknown biological role	0.081	-0.24	**0.322**
SPAC19D5.03	*cid1*	poly(A) polymerase Cid1	-0.091	-0.41	**0.322**
SPBC1348.02		S. pombe specific 5Tm protein family	0.069	-0.25	**0.315**
SPAC3C7.08c	*elf1*	AAA family ATPase ELf1	-0.395	-0.71	**0.314**
SPAC644.07		Rieske ISP assembly protein	-0.118	-0.43	**0.31**
SPBC18H10.04c	*sce3*	translation initiation factor eIF4B	0.373	0.066	**0.306**
SPAC18G6.02c	*chp1*	chromodomain protein Chp1	-0.221	-0.53	**0.306**
SPBC106.05c	*tim11*	F0-ATPase subunit E	0.037	-0.27	**0.303**
SPAC630.14c	*tup12*	transcriptional corepressor Tup12	0.825	0.525	**0.3**
SPAC22H10.09		sequence orphan	-0.012	-0.31	**0.298**
SPBC16G5.09		serine carboxypeptidase	0.143	-0.15	**0.297**
SPBC887.04c	*lub1*	WD repeat protein Lub1	-0.168	-0.46	**0.293**
SPBC1604.09c		exoribonuclease Rex4	0.054	-0.24	**0.293**
SPBC16C6.02c	*vps1302*	chorein homolog	0.067	-0.23	**0.292**
SPAC977.15		dienelactone hydrolase family	0.488	0.196	**0.291**
SPAC19A8.05c	*sst4*	sorting receptor for ubiquitinated membrane proteins	-0.116	-0.41	**0.29**
SPAC1250.04c	*atl1*	alkyltransferase-like protein Atl1	-0.253	-0.54	**0.289**
SPCC777.17c		mitochondrial ribosomal protein subunit L9	0.6	0.311	**0.289**
SPAC4C5.03		CTNS domain protein	-0.896	-1.18	**0.288**
SPBC354.10		RNAPII degradation factor	-0.026	-0.31	**0.288**
SPAC4H3.02c		sequence orphan	0.175	-0.11	**0.287**
SPAC3H5.12c	*rpl501*	60S ribosomal protein L5	0	-0.28	**0.284**
SPAC13G6.08		Cdc20/Fizzy family WD repeat protein	0.245	-0.04	**0.284**
SPBC17G9.02c		RNA polymerase II accessory factor, Cdc73 family	0.226	-0.06	**0.283**
SPBC30D10.04	*swi3*	replication fork protection complex subunit Swi3	0.676	0.394	**0.282**
SPCC794.15		sequence orphan	0.18	-0.1	**0.28**
SPAC56F8.04c	*coq2*	para-hydroxybenzoate--polyprenyltransferase Coq2	-0.751	-1.03	**0.28**
SPAC1142.03c	*swi2*	Swi5 complex subunit Swi2	0.398	0.121	**0.276**
SPCC1739.04c		sequence orphan	0.175	-0.1	**0.276**
SPAC869.08	*pcm2*	protein-L-isoaspartate O-methyltransferase	0.164	-0.11	**0.274**
SPAC1B2.04	*cox6*	cytochrome c oxidase subunit VI	0.031	-0.24	**0.274**
SPBC1778.10c	*ppk21*	serine/threonine protein kinase Ppk21	0.188	-0.09	**0.274**
SPAC6B12.14c		conserved fungal protein	0.153	-0.12	**0.274**
SPAC31A2.02	*trm112*	tRNA (guanine-N2-)-methyltransferase regulatory subunit Trm112	-0.186	-0.46	**0.273**

SPAC23H4.17c	*srb10*	cyclin-dependent protein kinase Srb10	0.135	-0.14	**0.273**
SPAC222.04c	*ies6*	chromatin remodeling complex subunit Ies6	1.648	1.377	**0.271**
SPBC3B9.13c	*rpp102*	60S acidic ribosomal protein Rpp1-2	0.059	-0.21	**0.27**
SPAC13G7.07	*arb2*	argonaute binding protein 2	-0.195	-0.46	**0.27**
SPAC23G3.08c	*ubp7*	ubiquitin C-terminal hydrolase Ubp7	0.479	0.211	**0.268**
SPBC19C2.13c	*ctu2*	conserved eukaryotic protein	0.502	0.239	**0.263**
SPCP1E11.11		Puf family RNA-binding protein	-0.021	-0.28	**0.261**
SPAC17A2.06c	*vps8*	WD repeat protein Vps8	0.245	-0.02	**0.26**
SPBPB7E8.02		conserved protein (fungal bacterial protazoan)	0.227	-0.03	**0.26**
SPAC13D6.04c	*btb3*	BTB/POZ domain protein Btb3	0.014	-0.24	**0.258**
SPBC839.05c	*rps1701*	40S ribosomal protein S17	-0.079	-0.34	**0.257**
SPAC4F10.11	*spn1*	septin Spn1	0.396	0.139	**0.257**
SPAC19D5.06c	*din1*	Dhp1p-interacting protein Din1	-0.325	-0.58	**0.255**
SPAC31G5.19		ATPase with bromodomain protein	-0.022	-0.28	**0.254**
SPAC22F3.06c	*lon1*	Lon protease homolog Lon1	0.431	0.178	**0.253**
SPAC630.04c		sequence orphan	-0.13	-0.38	**0.253**
SPAC4H3.03c		glucan 1,4-alpha-glucosidase	0.051	-0.2	**0.251**
SPBC337.09	*erg28*	Erg28 protein	0.351	0.102	**0.248**
SPAC323.05c		S-adenosylmethionine-dependent methyltransferase	0.32	0.072	**0.248**
SPAC24B11.06c	*sty1*	MAP kinase Sty1	0.078	-0.17	**0.247**
SPAC458.06		phosphoinositide binding protein	-0.027	-0.27	**0.246**
SPAC24C9.16c	*cox8*	cytochrome c oxidase subunit VIII	-0.007	-0.25	**0.244**
SPBC31E1.02c	*pmr1*	P-type ATPase, calcium transporting Pmr1	0.008	-0.24	**0.244**
SPAC1687.16c	*erg3*	C-5 sterol desaturase Erg3	-0.477	-0.72	**0.244**
SPAC1071.08	*rpp203*	60S acidic ribosomal protein P2C subunit	0.171	-0.07	**0.242**
SPAC4F10.04		protein phosphatase type 2A, intrinsic regulator	0.637	0.399	**0.237**
SPAC27D7.03c	*mei2*	RNA-binding protein involved in meiosis Mei2	0.179	-0.06	**0.236**
SPAC343.06c		scramblase	-0.259	-0.49	**0.233**
SPBC32F12.11	*tdh1*	glyceraldehyde-3-phosphate dehydrogenase Tdh1	0.594	0.362	**0.232**
SPBPB10D8.07c		membrane transporter	-0.044	-0.28	**0.232**
SPAC17H9.10c	*ddb1*	damaged DNA binding protein Ddb1	0.189	-0.04	**0.232**
SPBC947.05c		ferric-chelate reductase	0.409	0.18	**0.23**
SPAC22E12.11c	*set3*	histone lysine methyltransferase Set3	0.013	-0.21	**0.227**
SPBC530.08		transcription factor	0.13	-0.1	**0.227**

SPCC613.06	*rpl902*	60S ribosomal protein L9	0.078	-0.15	**0.226**
SPBC31F10.14c	*hip3*	HIRA interacting protein Hip3	-0.375	-0.6	**0.225**
SPCC1259.11c	*gyp2*	GTPase activating protein Gyp2	0.103	-0.12	**0.224**
SPAC57A10.12c	*ura3*	dihydroorotate dehydrogenase Ura3	0.12	-0.1	**0.223**
SPBPB10D8.06c		membrane transporter	-0.163	-0.39	**0.222**
SPAC4G9.10	*arg3*	ornithine carbamoyltransferase Arg3	-0.025	-0.25	**0.222**
SPAC24H6.13		DUF221 family protein	0.253	0.032	**0.221**
SPAC15F9.02	*seh1*	nucleoporin Seh1	-0.08	-0.3	**0.221**
SPAC26F1.10c	*pyp1*	tyrosine phosphatase Pyp1	0.26	0.039	**0.22**
SPAC767.01c	*vps1*	dynamin family protein Vps1	-0.125	-0.35	**0.22**
SPAC18G6.04c	*shm2*	serine hydroxymethyltransferase Shm2	-0.227	-0.44	**0.218**
SPAC26H5.04		vacuolar import and degradation protein Vid28	0.047	-0.17	**0.216**
SPAC212.01c		S. pombe specific DUF999 family protein 2	0.252	0.036	**0.216**
SPAC1782.09c	*clp1*	Cdc14-related protein phosphatase Clp1/Flp1	0.047	-0.17	**0.215**
SPBC26H8.05c		serine/threonine protein phosphatase	-0.111	-0.32	**0.213**
SPAPB2B4.06		conserved fungal protein	0.093	-0.12	**0.212**
SPCC1450.12		conserved fungal protein	-0.673	-0.88	**0.212**
SPBC3B8.02	*php5*	CCAAT-binding factor complex subunit Php5	-0.215	-0.43	**0.212**
SPAC1F7.09c		allantoicase	0.127	-0.08	**0.211**
SPAC1002.20		sequence orphan	-0.02	-0.23	**0.211**
SPCC4B3.08		C-terminal domain kinase I (CTDK-I) gamma subunit	0.261	0.051	**0.21**
SPAC212.04c		S. pombe specific DUF999 family protein 1	0.156	-0.05	**0.209**
SPCC4G3.15c		CCR4-Not complex subunit Not2	0.127	-0.08	**0.209**
SPBC336.13c		mitochondrial inner membrane peptidase complex catalytic subunit 2	-0.197	-0.4	**0.208**
SPAC513.06c		dihydrodiol dehydrogenase	-0.025	-0.23	**0.206**
SPCC1223.05c	*rpl3702*	60S ribosomal protein L37	0.423	0.218	**0.205**
SPBC1703.08c		5-formyltetrahydrofolate cyclo-ligase	-0.029	-0.23	**0.204**
SPAC959.05c		protein disulfide isomerase	0.243	0.039	**0.204**
SPCC4G3.04c	*coq5*	C-methytransferase	-0.234	-0.44	**0.204**
SPCC1020.06c	*tal1*	transaldolase	0.274	0.07	**0.204**
SPBC15D4.15	*pho2*	4-nitrophenylphosphatase	0.093	-0.11	**0.202**
SPCC584.01c		sulfite reductase NADPH flavoprotein subunit	0.98	0.778	**0.202**
SPAC4F8.01	*did4*	vacuolar sorting protein Did4	-0.128	-0.33	**0.202**

SPAC890.03	*ppk16*	serine/threonine protein kinase Ppk16	0.433	0.233	**0.2**

Appendix 2

Co-authored papers

Yuan I, Leontiou I, Amin P, May KM, Soper Ní Chafraidh S, Zlámalová E & Hardwick KG (2017) Generation of a Spindle Checkpoint Arrest from Synthetic Signaling Assemblies. *Curr. Biol.* **27:** 137–143

Amin P, Soper Ní Chafraidh S, Leontiou I & Hardwick KG (2019) Regulated reconstitution of spindle checkpoint arrest and silencing through chemically induced dimerisation *in vivo*. *J. Cell Sci.* **132:** jcs219766

Report

Current Biology

Generation of a Spindle Checkpoint Arrest from Synthetic Signaling Assemblies

Graphical Abstract

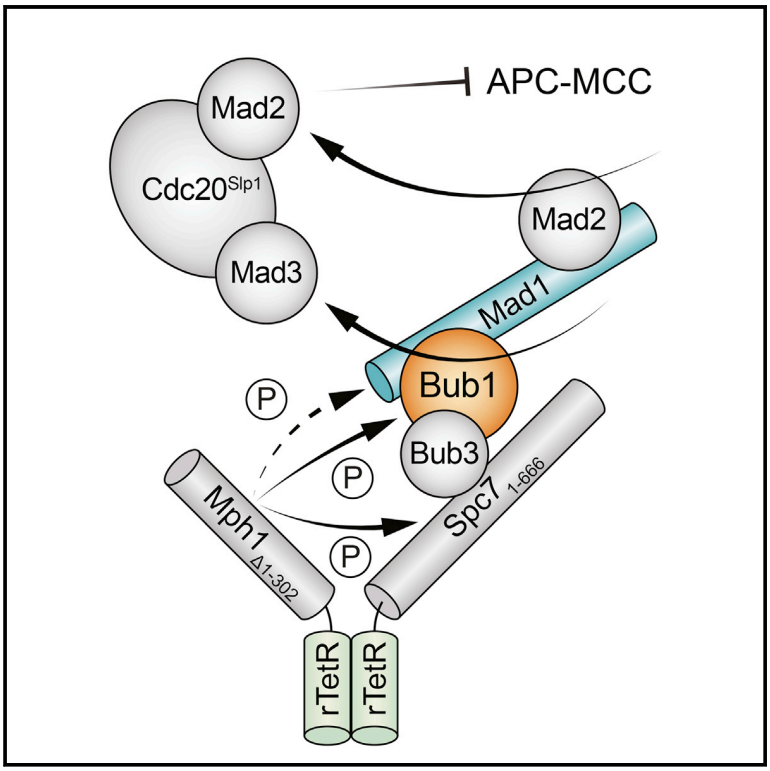

Authors

Ivan Yuan, Ioanna Leontiou, Priya Amin, Karen M. May, Sadhbh Soper Ní Chafraidh, Eliška Zlámalová, Kevin G. Hardwick

Correspondence

kevin.hardwick@ed.ac.uk

In Brief

Yuan et al. employ synthetic protein assemblies to generate a robust spindle checkpoint arrest in fission yeast. Formation of artificial heterodimers between a checkpoint kinase and one of its key substrates is shown to be sufficient for mitotic arrest, entirely independently of the location of this complex in the yeast nucleus.

Highlights

- Synthetic signaling scaffolds generate a spindle checkpoint arrest
- The combination of KNL1^{Spc7} and Mps1^{Mph1} kinase generates a robust arrest
- Kinetochore, spindle, and nuclear envelope enrichment of the scaffold is not required
- Bub3 acts to inhibit premature checkpoint activation

Yuan et al., 2017, Current Biology *27*, 137–143
January 9, 2017 © 2017 The Author(s). Published by Elsevier Ltd.
http://dx.doi.org/10.1016/j.cub.2016.11.014

CellPress

Current Biology
Report

Generation of a Spindle Checkpoint Arrest from Synthetic Signaling Assemblies

Ivan Yuan,[1,2] Ioanna Leontiou,[1,2] Priya Amin,[1] Karen M. May,[1] Sadhbh Soper Ní Chafraidh,[1] Eliška Zlámalová,[1] and Kevin G. Hardwick[1,3,*]
[1]Wellcome Trust Centre for Cell Biology, University of Edinburgh King's Buildings, Max Born Crescent, Edinburgh EH9 3BF, UK
[2]Co-first author
[3]Lead Contact
*Correspondence: kevin.hardwick@ed.ac.uk
http://dx.doi.org/10.1016/j.cub.2016.11.014

SUMMARY

The spindle checkpoint acts as a mitotic surveillance system, monitoring interactions between kinetochores and spindle microtubules and ensuring high-fidelity chromosome segregation [1–3]. The checkpoint is activated by unattached kinetochores, and Mps1 kinase phosphorylates KNL1 on conserved MELT motifs to generate a binding site for the Bub3-Bub1 complex [4–7]. This leads to dynamic kinetochore recruitment of Mad proteins [8, 9], a conformational change in Mad2 [10–12], and formation of the mitotic checkpoint complex (MCC: Cdc20-Mad3-Mad2 [13–15]). MCC formation inhibits the anaphase-promoting complex/cyclosome (Cdc20-APC/C), thereby preventing the proteolytic destruction of securin and cyclin and delaying anaphase onset. What happens at kinetochores after Mps1-dependent Bub3-Bub1 recruitment remains mechanistically unclear, and it is not known whether kinetochore proteins other than KNL1 have significant roles to play in checkpoint signaling and MCC generation. Here, we take a reductionist approach, avoiding the complexities of kinetochores, and demonstrate that co-recruitment of KNL1^{Spc7} and Mps1^{Mph1} is sufficient to generate a robust checkpoint signal and prolonged mitotic arrest. We demonstrate that a Mad1-Bub1 complex is formed during synthetic checkpoint signaling. Analysis of *bub3Δ* mutants demonstrates that Bub3 acts to suppress premature checkpoint signaling. This synthetic system will enable detailed, mechanistic dissection of MCC generation and checkpoint silencing. After analyzing several mutants that affect localization of checkpoint complexes, we conclude that spindle checkpoint arrest can be independent of their kinetochore, spindle pole, and nuclear envelope localization.

RESULTS AND DISCUSSION

Genetic and proteomic approaches have revealed that kinetochores are highly complex molecular machines (with ~100 kinetochore components in vertebrates [16] and ~50 in yeast [17]) and that there are approximately ten components of the spindle checkpoint machinery [2]. Amidst such complexity, separating kinetochore bi-orientation, error-correction, and microtubule attachment functions from true checkpoint activation and signaling functions is problematic. Kinetochore tethering of, e.g., Mph1-Ndc80 and Mis12-Mad1 can initiate checkpoint arrests [18, 19]. However, it is very likely that in such experiments endogenous kinetochore function is being perturbed and that these perturbations then activate the spindle checkpoint, making interpretation of the experiments complicated and rather unsatisfactory. To improve on this tethering strategy, we set out to generate a spindle checkpoint arrest from a site quite distinct from an unattached kinetochore. We employed a fission yeast strain with 112 tandem repeats of the tet operator (tetO) integrated on the arm of chromosome 1 (at the *arg3* locus, see Figure 1A). This is ~1.5 Mb away from cen1 and can thus be imaged as a distinct spot in live fission yeast cells (see Figure S1A). When we expressed the phosphomimic mutant Spc7(1-666)-9TE fused to the Tet repressor in these cells it resulted in constitutive recruitment of Bub1, Bub3, and Mad3 to the tetO array, throughout the cell cycle and independently of Mph1 kinase (Figure 1B). Note, this fusion protein only contains the first half of Spc7 (1-666) and so completely lacks its C-terminal kinetochore targeting domain. Expression of TetR-Spc7-9TA failed to recruit checkpoint proteins to the tetO array (see Figure S1B), whereas wild-type TetR-Spc7 was able to recruit Bub1, Bub3, and Mad3 but at much lower levels than TetR-Spc7-9TE and in a way that was dependent on endogenous Mph1 kinase action (see Figure S1B). This demonstrates that the "activated" Spc7-9TE binding platform is sufficient to recruit these three checkpoint proteins constitutively, and that this works ectopically and thus does not require additional kinetochore factors. Bub1p, Bub3p, and Mad3p are recruited to the array with the expected dependencies (see Figures S1C–S1E): thus, we believe that this Spc7-Bub-Mad3 complex likely acts as an independent signaling module (Figure 1C).

Co-tethering KNL1^{Spc7} and Mps1^{Mph1} Kinase Generates a Robust Mitotic Arrest

At unattached kinetochores, Bub1 is thought to recruit Mad1 [20]. However, when we expressed TetR-Spc7-9TE no detectable Mad1-Mad2 proteins were recruited to the array, and no cell-cycle delay was observed (data not shown). When we co-expressed TetR-Mad1 with TetR-Spc7-9TE, again no cell-cycle

This is an open access article under the CC BY license (http://creativecommons.org/licenses/by/4.0/).

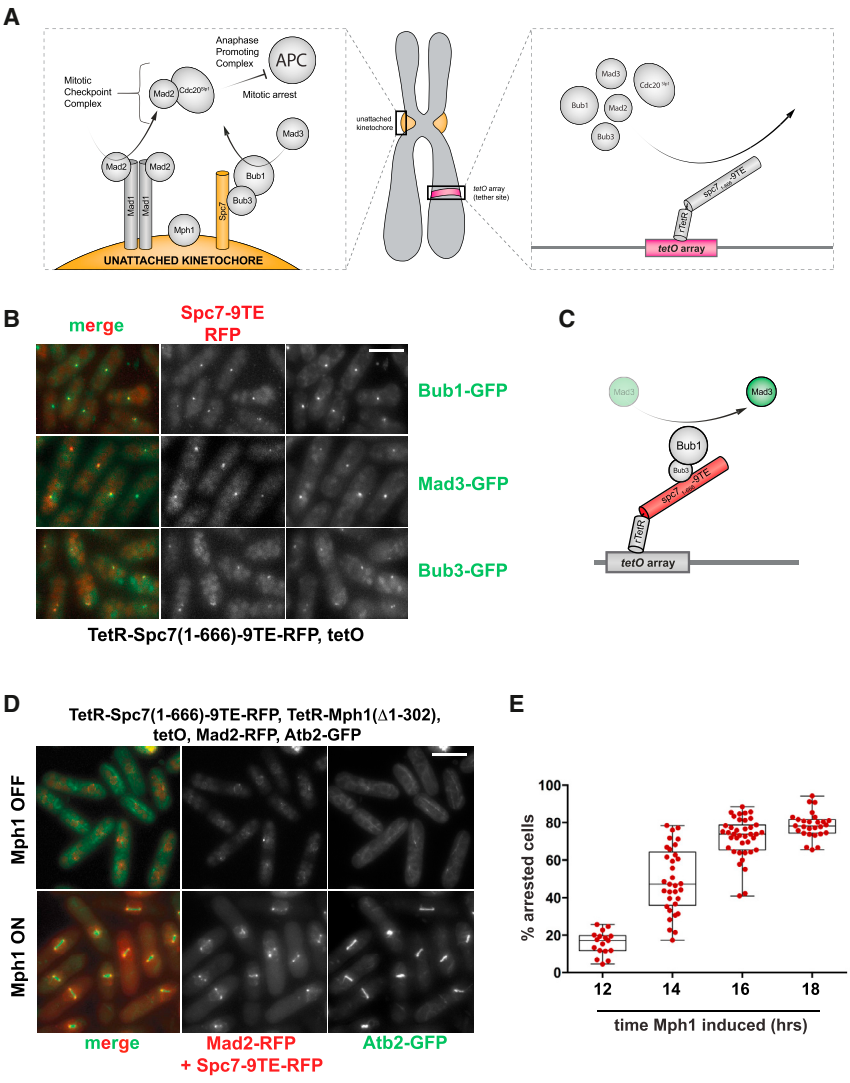

Figure 1. Co-tethering of Spc7-9TE and TetR-Mph1ΔN Generates a Robust Checkpoint Arrest

(A) Schematic model of kinetochore-based checkpoint signaling versus the synthetic tetO platform.

(B) TetR-Spc7-9TE is sufficient to recruit Bub1-GFP, Bub3-GFP, and Mad3-GFP to an array of Tet operators on a chromosome arm. Scale bar, 10 μm. See Figure S1 for TetR-Spc7wt and TetR-Spc7-9TA images.

(C) Schematic summary of Spc7-9TE tethering.

(D) Co-expression of TetR-Spc7-9TE and TetR-Mph1ΔN produces a robust mitotic arrest with short metaphase spindles. Scale bar, 10 μm.

(E) Quantitation of arrested cells after 12, 14, 16, and 18 hr of Mph1 induction (cells grown without thiamine). The plus thiamine control culture does not arrest, containing just a few mitotic cells. 36 experiments were performed and data points are plotted along with the mean and SD.

See also Figure S1.

effects were observed (data not shown). This suggests that co-recruitment of Mad1 and Bub1 is not sufficient for checkpoint signaling at least on this tetO platform. We thought that this might be because the synthetic signaling scaffold assembled there (Spc7-Bub-Mad) lacked Mph1 kinase. Therefore, instead of Mad1, we co-expressed TetR-Spc7-9TE with TetR-Δ(1-302) Mph1, being very careful not to overexpress Mph1 kinase. We particularly wanted to avoid activating the checkpoint from kinetochores, and so the N terminus of Mph1 was removed to prevent this kinase from targeting to endogenous kinetochores [21] where it might be activated and could then recruit other checkpoint complexes. Figures 1D and 1E show a very striking result: co-expression of TetR-Spc7-9TE with TetR-Δ(1-302)Mph1 was sufficient to arrest cells in mitosis. This is seen very clearly in Figure 1D where we used GFP-labeled tubulin to image the short metaphase spindles in arrested cells. Figure 1E shows that, after 16 hr of Mph1 induction, we typically see ~80% metaphase cells (cf. ~5% in strains not inducing Mph1, +thiamine). When we imaged Mad2-GFP/RFP in the arrested cells, we saw that, rather than accumulate at the tetO array with the Bub proteins, Mad2-GFP accumulated at the poles of the metaphase spindles (Figure 2A, and see Figure 3A for co-localization). Importantly, this arrest requires co-expression of both TetR-Spc7-9TE and TetR-Δ(1-302)Mph1: neither alone is sufficient for an arrest (Figures 2B and S2A–S2D), and their arrest does not require endogenous Mph1 kinase (Figures S2D–S2G).

Next, we analyzed Spc7-wt and Spc7-9TA: while Spc7-9TA had little effect on the cell cycle, we were surprised to find that Spc7-wt arrested significantly faster than Spc7-9TE (Figure 2C), with ~60% mitotic arrest after 12 hr compared to 16 hr for Spc7-9TE. To analyze this in more detail, we compared Spc7-wt and Spct-9TE arrests in strains expressing TetR-Δ(1-302)Mph1 both with and without endogenous Mph1 kinase. Figure S2D confirms that the wild-type form of this signaling scaffold is more efficient than the Spc7-9TE phosphomimic at generating a checkpoint signal. There are several possible reasons for this: perhaps the nine glutamic acid residues do not fully mimic phosphorylation, or perhaps having all nine sites modified on a single molecule is not optimal for scaffolding function (see Mad2 recruitment below).

Next, we wanted to test what level of co-enrichment of TetR-Spc7-9TE and TetR-Δ(1-302)Mph1 was necessary for initiation of an arrest (each yeast kinetochore is thought to have approximately five molecules of Spc7 [22]), and so we modified our strains by reducing the number of tet operators present, and thus the number of Spc7 and Mph1 binding sites. Strains containing four tandem copies of tetO arrested well (data not shown) and to our surprise so did strains without any tetO sequences at all (Figures 2D and S2J). Consistent with this observation, we found that addition of anhydro-tetracycline (aTc), which enhances TetR binding to the tetO array in this system, had no

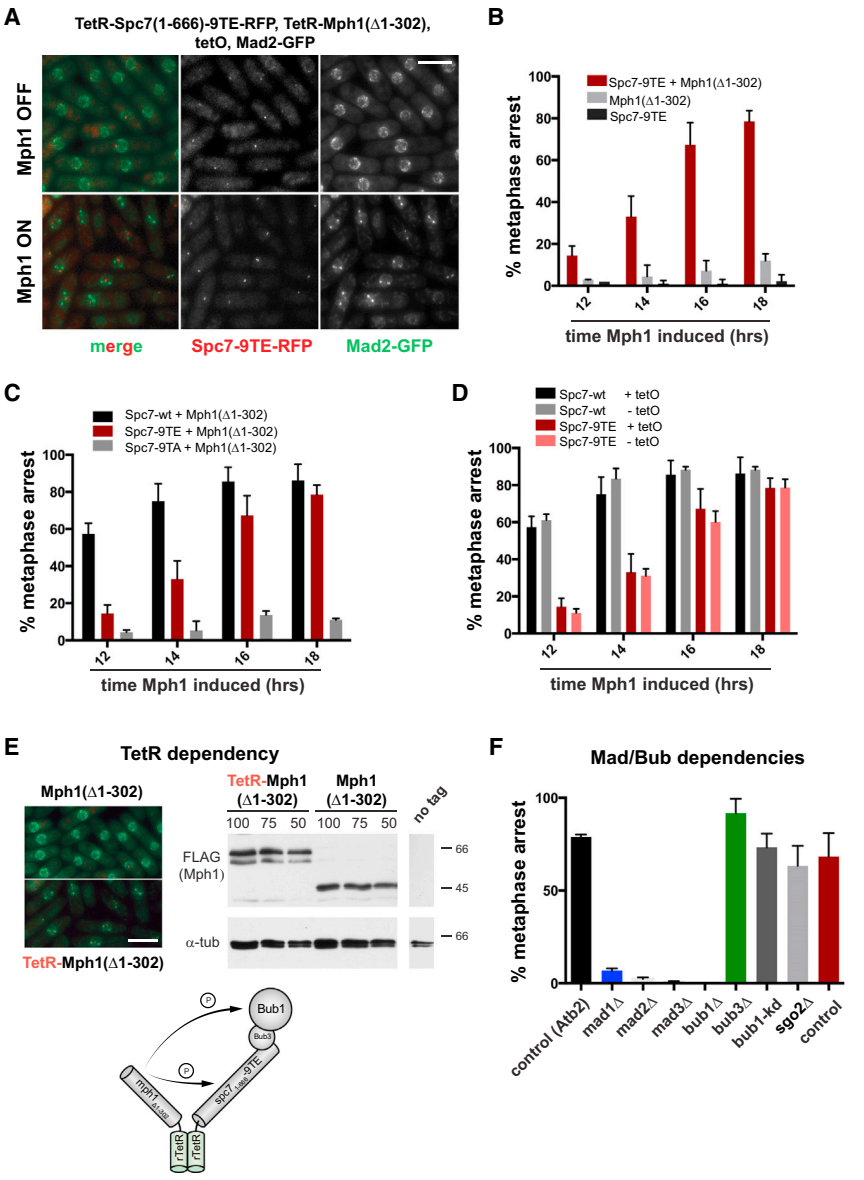

Figure 2. Dependencies for Synthetic Checkpoint Arrest

(A) Co-expression of TetR-Spc7-9TE and TetR-Mph1ΔN leads to a metaphase arrest with Mad2-GFP accumulating at the spindle poles (analyzed in detail in Figure 3). Scale bar, 10 μm.

(B) Expression of either TetR-Spc7-9TE or TetR-Mph1ΔN alone is not sufficient for robust arrest. This experiment was repeated three times and is plotted as the mean ± SD.

(C) Comparison of TetR-Spc7-9TE, TetR-wild-type Spc7 (Spc7-wt), and TetR-Spc7-9TA. The latter is unable to arrest cells, whereas the wild-type protein arrests better than Spc7-9TE. This experiment was repeated three times and is plotted as the mean ± SD.

(D) The tetO array is not necessary for Mad2-GFP accumulation at spindle poles or metaphase arrest. The mitotic arrest, for both TetR-Spc7-wt and TetR-Spc7-9TE, was compared in strains containing either 112xtetO or no tet operators. This experiment was repeated three times and is plotted as the mean ± SD.

(E) No arrest was observed when TetR was removed from the Mph1 fusion protein (Mad2-GFP did not accumulate at spindle poles). Scale bar, 10 μm. Anti-Flag (Mph1) immunoblot of whole cell extracts demonstrates that similar levels of Mph1 were expressed with and without TetR.

(F) The mitotic arrest is Mad1, Mad2, Mad3, and Bub1 dependent, but independent of Bub3, Bub1 kinase activity, and Sgo2. These strains were analyzed at least three times and data plotted as the mean ± SD. The control strain (TetR-Spc7-9TE) on the left has Atb2-GFP as reporter and on the right Mad2-RFP. All strains contained the tetO array, apart from *sgo2*Δ and its corresponding control strain. Representative images are presented in Figure S2J.

See also Figure S2.

significant effect on this arrest (Figure S2H). Our interpretation is that soluble, heterodimeric complexes formed between TetR-Spc7 and TetR-Mph1 in the nucleoplasm are sufficient for checkpoint activation. To test this directly, we removed TetR from the Mph1 construct: the resulting strains no longer arrest, and Mad2-GFP does not accumulate at spindle poles (Figure 2E). We conclude that forced interaction of these two critical upstream checkpoint components is sufficient for activation of the spindle checkpoint, and that their enrichment at the tetO array is unnecessary for these signals to induce a metaphase arrest.

If these arrests reflect a normal mode of checkpoint signaling, they should be dependent on downstream checkpoint components. We tested the dependence of this metaphase arrest on the Mad/Bub proteins and found that it required Mad1, Mad2, Mad3, and Bub1. Importantly it did not require "upstream" kinetochore-based signaling: the arrest was independent of endogenous Mph1 and Bub1 kinase activities, of Sgo2, and of Bub3 (Figures 2F and S2I–S2J). The latter is not surprising, as Bub3 is known to be unnecessary for fission yeast spindle checkpoint arrests [23, 24].

Arrested Cells Accumulate Several Checkpoint Proteins at Their Spindle Poles

Co-expression of Mps1 kinase and an Spc105 fragment has previously been demonstrated to induce a cell-cycle delay in budding yeast [25]. In that study, the rapamycin-induced heterodimers (of Mps1-Spc105) usually became enriched at endogenous kinetochores, which could then serve as a platform to generate or amplify the checkpoint signal. Some evidence was presented suggesting that the cell-cycle delay could be generated independently of kinetochores, using the *ndc10-1* mutation where kinetochores are thought to be destroyed at the restrictive temperature. The possible role of endogenous kinetochores is an important issue, and one we were keen to avoid in our system: our Mph1 construct lacks the N-terminal 302 residue kinetochore

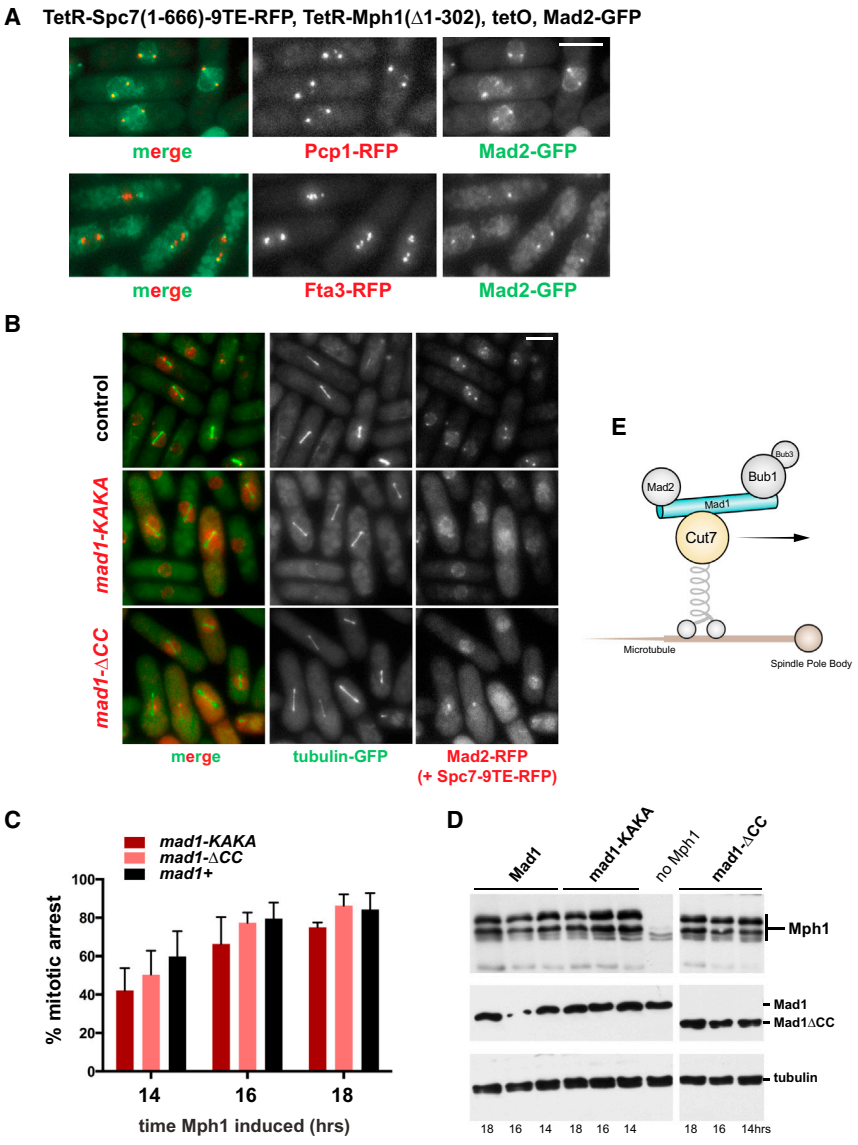

Figure 3. Mad2p Accumulates at Spindle Poles in the Synthetic Arrest, but This Is Not Necessary for the Arrest

(A) Cells were arrested with co-expression of TetR-Mph1ΔN and TetR-Spc7-9TE. Co-localization of the spindle pole marker Pcp1-RFP and Mad2-GFP is observed. The Mad2-GFP does not co-localize well with the kinetochore marker Fta3-RFP in arrested cells, although in a few cases kinetochores are close to the poles. Scale bar, 5 μm. Figure S3A demonstrates co-immunoprecipitation of Mad2 with gamma tubulin complex proteins.

(B) Strains co-expressing Spc7 and Mph1 do not accumulate Mad2-GFP at spindle poles in strains containing the *mad1-KAKA* mutation that disrupts the Mad1-Cut7 kinesin motor interaction. Other motor mutants were analyzed (*dynein*, *klp2*Δ, *klp5/6*Δ) but found to have no effect on the arrest or Mad2-GFP localization to spindle poles (see Figure S3G). Scale bar, 10 μm.

The *mad1-ΔCC* allele still arrests even though localization of Mad1 and Mad2 to the nuclear periphery/envelope and spindle poles is lost. This N-terminal coiled-coil domain also includes the Cut7 interaction site.

(C) Quantitation of the *mad1-KAKA* and *mad1-ΔCC* mutant arrests. This experiment was repeated five times and data plotted as the mean ± SD.

(D) The levels of Mph1 expression and Mad1 protein stability are not affected in these *mad1* mutants. Time of Mph1 induction (after thiamine wash-out) is indicated.

(E) Model with the Cut7 kinesin moving the Mad-Bub complex to spindle poles. This predicts that the movement of Bub1 to spindle poles is Bub3 independent, which was found to be the case (see Figure S3D).

See also Figure S3.

targeting domain, our Spc7 construct lacks the C-terminal half of the protein that targets it to kinetochores, and most of our strains lack endogenous Mph1 kinase, thereby preventing all the Mad/Bub proteins from being recruited to endogenous kinetochores [21]. We carried out co-localization experiments with kinetochore (Fta3 [26]) and spindle pole (Pcp1 [27]) markers in our arrested fission yeast cells. Figure 3A demonstrates that Mad2-GFP was not recruited to endogenous fission yeast kinetochores but instead overlapped well with gamma-tubulin and spindle pole body markers. Mad1 and Mad2 proteins have been observed at spindle poles previously, and direct interaction with the gamma-tubulin protein Alp4 and Mad2 has been described in fission yeast cells late in mitosis (post-metaphase), but its roles there remain unclear [28]. Co-immunoprecipitation confirms that Mad2-GFP interacts with Alp4 in these synthetically arrested cells (see Figure S3A). We analyzed which other checkpoint proteins were enriched at spindle poles in the arrested cells, by crossing in GFP-tagged forms of Mad1, Mad3, Bub3, and Bub1 (Figures S3B–S3D). Mad3-GFP and Bub1-GFP were recruited both to the tetO array and to spindle poles in cells co-expressing TetR-Spc7-9TE with TetR-Δ(1-310)Mph1 (see Figures S3B–S3D), as is Bub3-GFP (data not shown). Interestingly, Bub1-GFP recruitment to spindle poles did not require Bub3. Similar observations were made with TetR-Spc7-wt experiments with one important exception: in cells co-expressing TetR-Spc7-wt with TetR-Δ(1-310)Mph1, we could also detect Mad2-GFP on the tetO array (Figure S2E). This interesting observation might explain why these cells arrest faster than Spc7-9TE, as it suggests that the Mad1-Mad2 complex associates more stably with the TetR-Spc7-wt platform than with TetR-Spc7-9TE and that this stable complex may then be better able to generate the mitotic checkpoint complex (MCC) and inhibit the anaphase-promoting complex/cyclosome (APC/C).

Spindle Pole Localization Is Not Necessary for Checkpoint Arrest

We wanted to test whether the spindle pole localization was relevant to generation of the checkpoint arrest in these cells. In

human cells, checkpoint proteins are stripped from the outer kinetochore upon microtubule attachment and transported to spindle poles in a dynein-dependent fashion [29]. This is thought to be one way vertebrate cells silence the spindle checkpoint, although it is not essential for silencing [30]. However, there is no evidence that dynein is involved in checkpoint protein targeting in yeast mitosis [31]. We tested dynein, *klp2*, *klp5*, and *klp6* mutants and found no effect on Mad2 localization in our synthetic checkpoint strain (see Figure S3G). An interaction between Mad1 and Cut7 (fission yeast Kinesin 5) was recently reported by Watanabe et al. [32]. They found that recruitment of Cut7 to kinetochores was Mad1 dependent, and that this interaction could be disrupted through mutation of the Mad1 N terminus (with the *mad1-KAKA* mutation) without affecting spindle checkpoint function. We note that the Cut7 kinesin motor has been demonstrated to be bi-directional in vitro [33] and that this motor localizes to spindle poles in addition to the spindle and midzone [34]. When we introduced the *mad1-KAKA* allele into our synthetic checkpoint system, we observed a dramatic decrease in spindle pole localization of Mad2-GFP (Figure 3B). Our interpretation is that fission yeast kinesin 5 is required for spindle pole enrichment of spindle checkpoint proteins in the synthetic arrest. However, imaging revealed that the *mad1-KAKA* cells still efficiently arrested at metaphase, with a diffuse nuclear pool of Mad2-RFP (Figures 3B and 3C). Thus, spindle pole enrichment of checkpoint proteins is not critical for the synthetic arrest, and we conclude that spindle poles are unlikely to be an important site of MCC generation in these cells. Mad1 and Mad2 interact with the nuclear periphery, via Mlp/TPR protein interactions [35, 36], and this has been demonstrated to be an important site of MCC assembly early in vertebrate mitosis [37]. Therefore, we analyzed another *mad1* mutant where the first 136 amino acids of Mad1 containing a coiled-coil region (CC) were removed, preventing Mad1-Mad2 interaction with Mlps and the nuclear envelope and also removing the Cut7 interaction site. These *mad1*-ΔCC cells were also able to arrest efficiently when TetR-Spc7-9TE and TetR-Δ(1-302)Mph1 were co-expressed (Figure 3E). We conclude that the Mad and Bub proteins do not need to be enriched at kinetochores, spindle poles, or the nuclear periphery for a robust checkpoint arrest to be generated in fission yeast. Most likely a diffuse, soluble pool of Spc7-Bub-Mad signaling assemblies is sufficient.

Checkpoint Signaling Generates a Mad1-Bub1 Complex and Is Inhibited by Bub3

A biochemical hallmark of active spindle checkpoint signaling in budding yeast is formation of a Bub1-Mad1 complex [20, 38], but this complex has proved challenging to detect in other systems. We immunoprecipitated Bub1-GFP from synthetically arrested cells (both with and without a tetO array), after cross-linking with dithiobis[succinimidylpropionate] (DSP) and were able to pull down complexes containing Mad1 and Mad2 (Figure 4A; data not shown). While our previous experiments suggested that this complex is rather labile in fission yeast extracts, we have also been able to co-immunoprecipitate these proteins in extracts made from *nda3* arrested cells after DSP cross-linking (data not shown). We propose that the synthetic checkpoint arrest is generated from a TetR-Spc7-Bub1 platform and that co-tethered TetR-Mph1 kinase then activates this further by phosphorylating Bub1 [20] to recruit the Mad1-Mad2 complex (Figure 4F). To directly test the importance of the Bub1-Mad1 interaction, we used the *bub1-CD1* mutant, where conserved phospho-sites thought to be needed for Mad1 interaction have been mutated to alanine [20, 39], and we found that these cells were unable to checkpoint arrest (Figure 4B). Co-immunoprecipitation experiments confirm that the Mad1-Bub1 interaction is efficiently generated from the TetR-Spc7-wt platform (data not shown), consistent with our ability to detect Mad2-GFP on the tetO array in the cells with tethered TetR-Spc7-wt (see Figure S2E). Detailed structural studies will be needed to explain this intriguing, partial "separation of function" with the Spc7-9TE allele: it recruits Bub1 better than Spc7-wt to the tetO array (Figure 1), yet it is less effective at recruiting Mad1&2 than Spc7-wt.

Watanabe et al. proposed that Bub3 might act as a chaperone to "suppress the ectopic activation of non-kinetochore Bub1" [6]. If so, one would expect to see a significant effect on the efficiency of ectopic TetR-Spc7-TetR-Mph1-induced checkpoint arrest in *bub3*Δ cells. Consistent with this prediction, Figure 4C demonstrates a striking advance (by ~4 hr) in the timing of arrest in *bub3*Δ cells arresting due to Spc7-9TE cells (although there is no effect with Spc7-wt, see Figure S4C). Deletion of *bub3* even allowed TetR-Spc7-9TA, TetR-Δ(1-302)Mph1 to arrest cells, again demonstrating the inhibitory effect of Bub3 (Figure 4D). Figure 4E shows a corresponding increase in the level of the Mad1-Bub1 complex in *bub3*Δ cells. We also note that in *bub3*Δ cells Bub1-GFP becomes hyperphosphorylated during mitotic arrest. This suggests one possible mode of Bub3 action: Bub3 binding might inhibit Bub1 auto-phosphorylation and thereby negatively impact Mad1p binding (see model in Figure 4F). We conclude that Bub3 likely acts to prevent ectopic spindle checkpoint signaling. Future experiments will address whether it does this by inhibiting the checkpoint activation pathway, or enhancing spindle checkpoint silencing [24]. In normal cells, Bub3 would prevent early nucleoplasmic signaling, and this effect would later be overcome when Mad-Bub complexes assemble at kinetochores and Spc7-Bub3-Bub1 interactions induce conformational changes in the Bub proteins, thereby activating Bub1 for downstream signaling. These Bub3 findings from our synthetic arrest are entirely consistent with a recent study published while our manuscript was in revision [40].

Conclusions

We have assembled a simple, synthetic, signaling system (SynCheck), avoiding the complexities of kinetochores, and generated a robust checkpoint arrest in fission yeast cells. $KNL1^{Spc7}$ acts as a platform to recruit Bub complexes and co-targeted $Mps1^{Mph1}$ kinase is sufficient to activate them for downstream signaling. This leads to assembly of a Mad1-Bub1 complex, MCC generation, and metaphase arrest. We note that the resulting cells arrest for several hours and eventually *cut* and die. This is possibly due to inefficient checkpoint silencing and that is currently under investigation.

It is clear from this and previous studies that checkpoint signals can be initiated from several sites: kinetochores, nuclear pores, possibly spindle poles, a tetO array, and soluble heterodimers of $KNL1^{Spc7}$-$Mps1^{Mph1}$ in the nucleoplasm. For a field

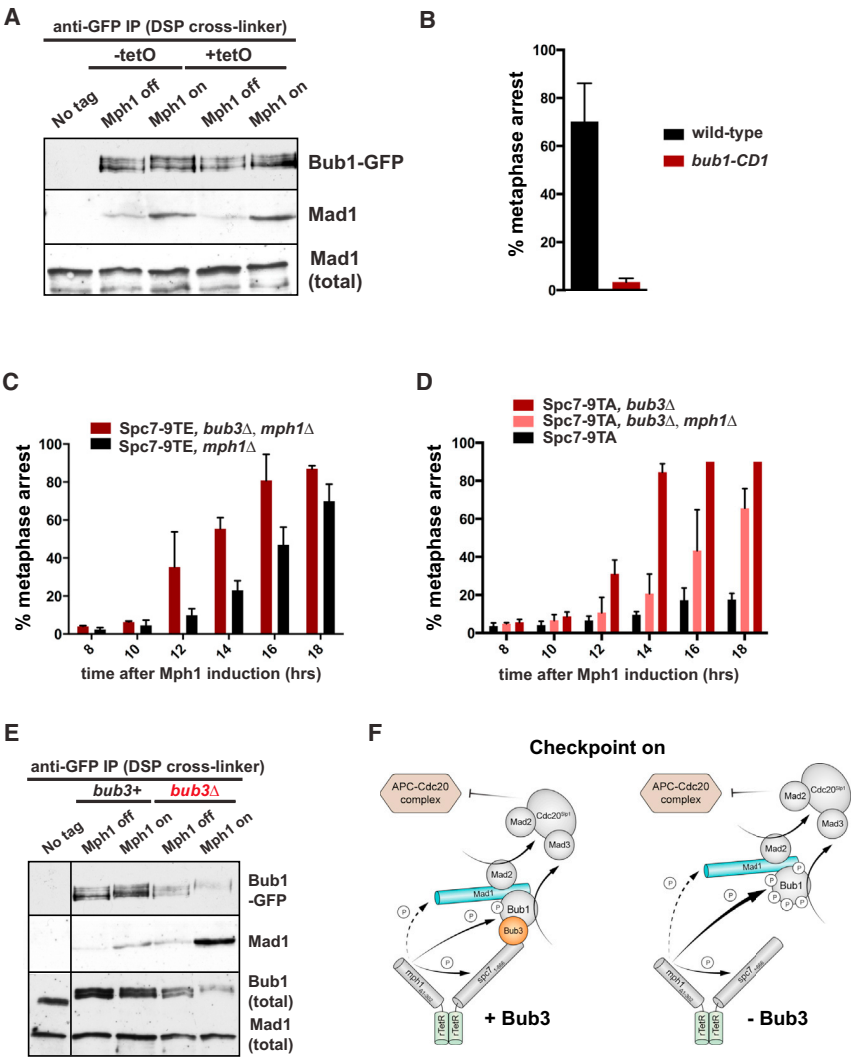

Figure 4. Synthetic Checkpoint Arrest Requires Mad1-Bub1 Complex Formation and Is Inhibited by Bub3

(A) Cells containing Bub1-GFP, TetR-Spc7-9TE, and TetR-Mph1ΔN were arrested as above for 16 hr then cross-linked with DSP before harvesting. Mad1 co-immunoprecipitates with Bub1-GFP in the arrested cells, both in the presence and absence of the tetO array. On the immunoblots, Bub1-GFP was detected with anti-Bub1 antibody and Mad1 with anti-Mad1 (see Supplemental Experimental Procedures).

(B) There is no arrest in the *bub1-CD1* mutant, which disrupts the Bub1-Mad1 interaction (see Figure S4A for images). This experiment was repeated three times, and data were plotted as the mean ± SD. The mutant Bub1-CD1 protein is stable (see Figure S4B).

(C) *bub3*Δ mutants containing TetR-Spc7-9TE arrest significantly faster than *bub3*$^{+}$, TetR-Spc7-9TE. This experiment was repeated three times, and data were plotted as the mean ± SD.

(D) TetR-Spc7-T9A combined with TetR-Mph1ΔN is able to arrest cells in the absence of Bub3. This experiment was repeated three times, and data were plotted as the mean ± SD.

(E) Higher levels of the Mad1-Bub1 complex are generated in *bub3*Δ cells. These cells contained TetR-Mph1ΔN and TetR-Spc7-9TE and were harvested after 12 hr of TetR-Mph1 induction. On the immunoblots, Bub1-GFP was detected with polyclonal anti-Bub1 antibodies, and Mad1 with anti-Mad1 antibodies (see Supplemental Experimental Procedures).

(F) Working model: diffusible heterodimers of TetR-Mph1ΔN and TetR-Spc7(1-666) actively produce a phospho-dependent Bub1-Mad1 complex, that than acts as an assembly platform for MCC production. In the absence of Bub3, shown to the right, Bub1 becomes hyperphosphorylated, which can enhance Bub1-Mad1 complex assembly and MCC production.

See also Figure S4.

that often equates kinetochore localization with checkpoint action, it is rather humbling to observe that none of this localized enrichment is necessary for checkpoint arrest, at least in the relatively small yeast cells studied here. It will be very interesting to see whether similar ectopic platforms can arrest larger vertebrate cells and, if so, whether apoptosis is induced as this could have therapeutic implications.

SUPPLEMENTAL INFORMATION

Supplemental Information includes four figures and Supplemental Experimental Procedures and can be found with this article online at http://dx.doi.org/10.1016/j.cub.2016.11.014.

AUTHOR CONTRIBUTIONS

This project was conceived by K.G.H. Most of the experiments were carried out by I.L. and I.Y., with the exception of *mad1ΔCC* and some *bub3*Δ experiments (K.M.M.), Bub1-Mad1 co-immunoprecipitations (P.A.), some *bub3*Δ, *sgo2*Δ and Cen2-GFP experiments (S.S.N.C. and I.L.), and the kinesin and dynein motor mutant analyses (E.Z. and I.L.). The manuscript was written by K.G.H. with help from I.Y., I.L., K.M.M., P.A., and S.S.N.C.

ACKNOWLEDGMENTS

We thank Robin Allshire, Yoshi Watanabe, and Silke Hauf for yeast strains; Robin Allshire, Ken Sawin, and Jonathan Millar for plasmids; Dave Kelly for imaging advice; Rachael Barton for cross-linking advice; and all members of K.G.H.'s group for their encouragement and comments on the manuscript. This work was supported by a Seed Award from the Wellcome Trust to K.G.H. (108105) and the Wellcome Trust Centre for Cell Biology core grant (092076). I.L. is supported by the Darwin Trust of Edinburgh, P.A. by the Medical Research Council (MR/K501293/1), and S.S.N.C. by the Wellcome Trust (105258).

Received: April 26, 2016
Revised: October 14, 2016
Accepted: November 3, 2016
Published: December 22, 2016

REFERENCES

1. Jia, L., Kim, S., and Yu, H. (2013). Tracking spindle checkpoint signals from kinetochores to APC/C. Trends Biochem. Sci. *38*, 302–311.
2. London, N., and Biggins, S. (2014). Signalling dynamics in the spindle checkpoint response. Nat. Rev. Mol. Cell Biol. *15*, 736–747.

3. Musacchio, A. (2015). The molecular biology of spindle assembly checkpoint signaling dynamics. Curr. Biol. *25*, R1002–R1018.
4. Shepperd, L.A., Meadows, J.C., Sochaj, A.M., Lancaster, T.C., Zou, J., Buttrick, G.J., Rappsilber, J., Hardwick, K.G., and Millar, J.B. (2012). Phosphodependent recruitment of Bub1 and Bub3 to Spc7/KNL1 by Mph1 kinase maintains the spindle checkpoint. Curr. Biol. *22*, 891–899.
5. London, N., Ceto, S., Ranish, J.A., and Biggins, S. (2012). Phosphoregulation of Spc105 by Mps1 and PP1 regulates Bub1 localization to kinetochores. Curr. Biol. *22*, 900–906.
6. Yamagishi, Y., Yang, C.H., Tanno, Y., and Watanabe, Y. (2012). MPS1/Mph1 phosphorylates the kinetochore protein KNL1/Spc7 to recruit SAC components. Nat. Cell Biol. *14*, 746–752.
7. Vleugel, M., Omerzu, M., Groenewold, V., Hadders, M.A., Lens, S.M., and Kops, G.J. (2015). Sequential multisite phospho-regulation of KNL1-BUB3 interfaces at mitotic kinetochores. Mol. Cell *57*, 824–835.
8. Shah, J.V., Botvinick, E., Bonday, Z., Furnari, F., Berns, M., and Cleveland, D.W. (2004). Dynamics of centromere and kinetochore proteins; implications for checkpoint signaling and silencing. Curr. Biol. *14*, 942–952.
9. Howell, B.J., Moree, B., Farrar, E.M., Stewart, S., Fang, G., and Salmon, E.D. (2004). Spindle checkpoint protein dynamics at kinetochores in living cells. Curr. Biol. *14*, 953–964.
10. De Antoni, A., Pearson, C.G., Cimini, D., Canman, J.C., Sala, V., Nezi, L., Mapelli, M., Sironi, L., Faretta, M., Salmon, E.D., and Musacchio, A. (2005). The Mad1/Mad2 complex as a template for Mad2 activation in the spindle assembly checkpoint. Curr. Biol. *15*, 214–225.
11. Mapelli, M., Massimiliano, L., Santaguida, S., and Musacchio, A. (2007). The Mad2 conformational dimer: Structure and implications for the spindle assembly checkpoint. Cell *131*, 730–743.
12. Yang, M., Li, B., Liu, C.J., Tomchick, D.R., Machius, M., Rizo, J., Yu, H., and Luo, X. (2008). Insights into mad2 regulation in the spindle checkpoint revealed by the crystal structure of the symmetric mad2 dimer. PLoS Biol. *6*, e50.
13. Sudakin, V., Chan, G.K., and Yen, T.J. (2001). Checkpoint inhibition of the APC/C in HeLa cells is mediated by a complex of BUBR1, BUB3, CDC20, and MAD2. J. Cell Biol. *154*, 925–936.
14. Hardwick, K.G., Johnston, R.C., Smith, D.L., and Murray, A.W. (2000). MAD3 encodes a novel component of the spindle checkpoint which interacts with Bub3p, Cdc20p, and Mad2p. J. Cell Biol. *148*, 871–882.
15. Chao, W.C., Kulkarni, K., Zhang, Z., Kong, E.H., and Barford, D. (2012). Structure of the mitotic checkpoint complex. Nature *484*, 208–213.
16. Samejima, I., Spanos, C., Alves, Fde.L., Hori, T., Perpelescu, M., Zou, J., Rappsilber, J., Fukagawa, T., and Earnshaw, W.C. (2015). Whole-proteome genetic analysis of dependencies in assembly of a vertebrate kinetochore. J. Cell Biol. *211*, 1141–1156.
17. Biggins, S. (2013). The composition, functions, and regulation of the budding yeast kinetochore. Genetics *194*, 817–846.
18. Ito, D., Saito, Y., and Matsumoto, T. (2012). Centromere-tethered Mps1 pombe homolog (Mph1) kinase is a sufficient marker for recruitment of the spindle checkpoint protein Bub1, but not Mad1. Proc. Natl. Acad. Sci. USA *109*, 209–214.
19. Maldonado, M., and Kapoor, T.M. (2011). Constitutive Mad1 targeting to kinetochores uncouples checkpoint signalling from chromosome biorientation. Nat. Cell Biol. *13*, 475–482.
20. London, N., and Biggins, S. (2014). Mad1 kinetochore recruitment by Mps1-mediated phosphorylation of Bub1 signals the spindle checkpoint. Genes Dev. *28*, 140–152.
21. Heinrich, S., Windecker, H., Hustedt, N., and Hauf, S. (2012). Mph1 kinetochore localization is crucial and upstream in the hierarchy of spindle assembly checkpoint protein recruitment to kinetochores. J. Cell Sci. *125*, 4720–4727.
22. Joglekar, A.P., Bouck, D., Finley, K., Liu, X., Wan, Y., Berman, J., He, X., Salmon, E.D., and Bloom, K.S. (2008). Molecular architecture of the kinetochore-microtubule attachment site is conserved between point and regional centromeres. J. Cell Biol. *181*, 587–594.
23. Tange, Y., and Niwa, O. (2008). *Schizosaccharomyces pombe* Bub3 is dispensable for mitotic arrest following perturbed spindle formation. Genetics *179*, 785–792.
24. Vanoosthuyse, V., Meadows, J.C., van der Sar, S.J., Millar, J.B., and Hardwick, K.G. (2009). Bub3p facilitates spindle checkpoint silencing in fission yeast. Mol. Biol. Cell *20*, 5096–5105.
25. Aravamudhan, P., Goldfarb, A.A., and Joglekar, A.P. (2015). The kinetochore encodes a mechanical switch to disrupt spindle assembly checkpoint signalling. Nat. Cell Biol. *17*, 868–879.
26. Liu, X., McLeod, I., Anderson, S., Yates, J.R., 3rd, and He, X. (2005). Molecular analysis of kinetochore architecture in fission yeast. EMBO J. *24*, 2919–2930.
27. Flory, M.R., Morphew, M., Joseph, J.D., Means, A.R., and Davis, T.N. (2002). Pcp1p, an Spc110p-related calmodulin target at the centrosome of the fission yeast Schizosaccharomyces pombe. Cell Growth Differ. *13*, 47–58.
28. Mayer, C., Filopei, J., Batac, J., Alford, L., and Paluh, J.L. (2006). An extended anaphase signaling pathway for Mad2p includes microtubule organizing center proteins and multiple motor-dependent transitions. Cell Cycle *5*, 1456–1463.
29. Howell, B.J., McEwen, B.F., Canman, J.C., Hoffman, D.B., Farrar, E.M., Rieder, C.L., and Salmon, E.D. (2001). Cytoplasmic dynein/dynactin drives kinetochore protein transport to the spindle poles and has a role in mitotic spindle checkpoint inactivation. J. Cell Biol. *155*, 1159–1172.
30. Vanoosthuyse, V., and Hardwick, K.G. (2009). Overcoming inhibition in the spindle checkpoint. Genes Dev. *23*, 2799–2805.
31. Courtheoux, T., Gay, G., Reyes, C., Goldstone, S., Gachet, Y., and Tournier, S. (2007). Dynein participates in chromosome segregation in fission yeast. Biol. Cell *99*, 627–637.
32. Akera, T., Goto, Y., Sato, M., Yamamoto, M., and Watanabe, Y. (2015). Mad1 promotes chromosome congression by anchoring a kinesin motor to the kinetochore. Nat. Cell Biol. *17*, 1124–1133.
33. Edamatsu, M. (2014). Bidirectional motility of the fission yeast kinesin-5, Cut7. Biochem. Biophys. Res. Commun. *446*, 231–234.
34. Hagan, I., and Yanagida, M. (1990). Novel potential mitotic motor protein encoded by the fission yeast cut7+ gene. Nature *347*, 563–566.
35. Iouk, T., Kerscher, O., Scott, R.J., Basrai, M.A., and Wozniak, R.W. (2002). The yeast nuclear pore complex functionally interacts with components of the spindle assembly checkpoint. J. Cell Biol. *159*, 807–819.
36. Lee, S.H., Sterling, H., Burlingame, A., and McCormick, F. (2008). Tpr directly binds to Mad1 and Mad2 and is important for the Mad1-Mad2-mediated mitotic spindle checkpoint. Genes Dev. *22*, 2926–2931.
37. Rodriguez-Bravo, V., Maciejowski, J., Corona, J., Buch, H.K., Collin, P., Kanemaki, M.T., Shah, J.V., and Jallepalli, P.V. (2014). Nuclear pores protect genome integrity by assembling a premitotic and Mad1-dependent anaphase inhibitor. Cell *156*, 1017–1031.
38. Brady, D.M., and Hardwick, K.G. (2000). Complex formation between Mad1p, Bub1p and Bub3p is crucial for spindle checkpoint function. Curr. Biol. *10*, 675–678.
39. Heinrich, S., Sewart, K., Windecker, H., Langegger, M., Schmidt, N., Hustedt, N., and Hauf, S. (2014). Mad1 contribution to spindle assembly checkpoint signalling goes beyond presenting Mad2 at kinetochores. EMBO Rep. *15*, 291–298.
40. Mora-Santos, M.D., Hervas-Aguilar, A., Sewart, K., Lancaster, T.C., Meadows, J.C., and Millar, J.B. (2016). Bub3-Bub1 binding to Spc7/KNL1 toggles the spindle checkpoint switch by licensing the interaction of Bub1 with Mad1-Mad2. Curr. Biol. *26*, 2642–2650.

© 2018. Published by The Company of Biologists Ltd | Journal of Cell Science (2019) 132, jcs219766. doi:10.1242/jcs.219766

TOOLS AND RESOURCES

SPECIAL ISSUE: RECONSTITUTING CELL BIOLOGY

Regulated reconstitution of spindle checkpoint arrest and silencing through chemically induced dimerisation *in vivo*

Priya Amin, Sadhbh Soper Ní Chafraidh, Ioanna Leontiou and Kevin G. Hardwick*

ABSTRACT

Chemically induced dimerisation (CID) uses small molecules to control specific protein–protein interactions. We employed CID dependent on the plant hormone abscisic acid (ABA) to reconstitute spindle checkpoint signalling in fission yeast. The spindle checkpoint signal usually originates at unattached or inappropriately attached kinetochores. These are complex, multiprotein structures with several important functions. To bypass kinetochore complexity, we took a reductionist approach to studying checkpoint signalling. We generated a synthetic checkpoint arrest ectopically by inducing heterodimerisation of the checkpoint proteins Mph1 (the fission yeast homologue of Mps1) and Spc7 (the fission yeast homologue of KNL1). These proteins were engineered such that they cannot localise to kinetochores, and only form a complex in the presence of ABA. Using this novel assay we were able to checkpoint arrest a synchronous population of cells within 30 min of ABA addition. This assay allows detailed genetic dissection of checkpoint activation and, importantly, also provides a valuable tool for studying checkpoint silencing. To analyse silencing of the checkpoint and the ensuing mitotic exit, we simply washed out the ABA from arrested fission yeast cells. We show here that silencing is critically dependent on protein phosphatase 1 (PP1) recruitment to Mph1-Spc7 signalling platforms.

KEY WORDS: Mps1, Checkpoint, Dimerisation, Mitosis, Reconstitution, Spindle

INTRODUCTION

Spindle checkpoint signalling was initially reconstituted in *Xenopus* egg extracts (Kulukian et al., 2009; Minshull et al., 1994) and most recently using recombinant complexes of human checkpoint proteins (Faesen et al., 2017). Major advantages of such *in vitro* assays are that complex systems can be simplified through biochemical fractionation and manipulated through immunodepletion. They also enable the regulated addition of specific components, whereby the timing, concentration and activity of these can all be varied.

In parallel, yeast genetics has driven the identification of most of the molecular components of this pathway, such as the mitotic arrest deficient (Mad) and budding uninhibited by benzimidazoles (Bub) proteins (Hoyt et al., 1991; Li and Murray, 1991) and their Cdc20 effector (Hwang et al., 1998; Kim et al., 1998). This combination of yeast genetics and *in vitro* reconstitution has proven invaluable in dissecting the molecular mechanism of action of spindle checkpoint signals and inhibition of the downstream effector Cdc20-APC/C (London and Biggins, 2014; Musacchio, 2015).

Here, we have employed a hybrid approach, using yeast genetics and partial reconstitution of the pathway *in vivo*. We used synthetic biology to re-wire and simplify the upstream part of the checkpoint signalling pathway and chemically induced dimerisation (CID) to add an extra level of regulation that can be easily controlled experimentally in intact cells. Employing this strategy, we were able to achieve the following outcomes. (1) We simplified the system through regulated, ectopic activation of the spindle checkpoint, enabling kinetochore-independent studies. (2) We used yeast genetics to enable rapid iterative analyses. (3) We employed synthetic biology and CID to generate specific complexes in an experimentally controlled fashion. (4) We used abscisic acid (ABA) addition and wash-out to provide tight temporal control of the initiation and termination of checkpoint signalling.

More specifically, we generated a synthetic checkpoint arrest ectopically by inducing heterodimerisation of the checkpoint proteins Mph1 (the fission yeast homologue of Mps1) and Spc7 (the fission yeast homologue of KNL1) in fission yeast. This led to checkpoint arrest in a synchronous population of cells within 30 min of addition of the plant phytohormone ABA. As expected, this checkpoint response required the downstream Mad and Bub factors. To analyse silencing of the checkpoint, we simply washed out the ABA from arrested cells and analysed mitotic exit. We found that the kinetics of release was critically dependent on recruitment of protein phosphatase 1 (PP1) to the Mph1-Spc7 signalling platform.

RESULTS

We previously published a synthetic checkpoint arrest assay (SynCheck) in which we activated the spindle checkpoint in fission yeast using heterodimers of TetR-Spc7 and TetR-Mph1 kinase (Yuan et al., 2017). However, in those experiments, dimerisation was constitutive, being driven by formation of Tet repressor dimers (TetR). Thus, checkpoint signalling was challenging to regulate, both in terms of initiation and termination. We controlled checkpoint arrest at the transcriptional level using an *nmt* promoter to drive expression of the TetR-Mph1 fusion protein. Unfortunately, the fission yeast *nmt1* promoter requires induction in medium lacking thiamine for several hours. As a consequence, the peak of arrest was observed ∼14 h after induction and was not as synchronous as hoped. To improve both timing and control, we modified our approach by employing CID to give tight temporal control over the initiation and termination of checkpoint signalling.

Generation of SynCheckABA

Following the strategy of Crabtree and colleagues (Liang et al., 2011), we fused the PYL domain (residues 33-209) of the ABA receptor after the N-terminal 666 amino acids of fission yeast Spc7.

Institute of Cell Biology, School of Biological Sciences, University of Edinburgh, King's Buildings, Max Born Crescent, Edinburgh, EH9 3BF, UK.

*Author for correspondence (Kevin.Hardwick@ed.ac.uk)

K.G.H., 0000-0002-6462-1047

This is an Open Access article distributed under the terms of the Creative Commons Attribution License (http://creativecommons.org/licenses/by/3.0), which permits unrestricted use, distribution and reproduction in any medium provided that the original work is properly attributed.

Received 30 April 2018; Accepted 4 September 2018

Journal of Cell Science (2019) 132, jcs219766. doi:10.1242/jcs.219766

By deleting the C-terminal half of Spc7, this protein is unable to be targeted to kinetochores because it lacks the Mis12-interacting region (Petrovic et al., 2016; Petrovic et al., 2014). This fusion protein was expressed from the constitutive *adh21* promoter (Tanaka et al., 2009). The ABI domain (residues 126-423) of ABI1 was fused to the C-terminus of the Mph1 spindle checkpoint kinase. We also deleted the first 301 amino acids of Mph1 to prevent it going to kinetochores (Heinrich et al., 2012). This Mph1-ABI fusion protein was expressed from the adh41 promoter (Tanaka et al., 2009). In the presence of ABA, the PYL and ABI domains are sufficient to form a tight complex (Miyazono et al., 2009), thus forming complexes of Mph1-ABI and Spc7-PYL (Fig. 1A). We combined these constructs in a strain that also had the *cdc25-22* mutation, enabling synchronisation in G2, the Bub1 checkpoint protein tagged with GFP and microtubules labelled with mCherry-Atb2 (α-tubulin).

Inducing Spc7-Mph1 heterodimers to trigger metaphase arrest

Cells were synchronised in G2 using a temperature-sensitive *cdc25-22* mutant that blocks cells in G2 after 3.5 h at 36°C. When cells were shifted to 25°C, they were 'released' from the block, enabling progression through the cell cycle. After 5 min, ABA was added to activate the spindle checkpoint through the formation of Spc7-PYL and Mph1-ABI heterodimers (Fig. 1B). We observed that 60 min after ABA addition to the synchronous population of cells, over

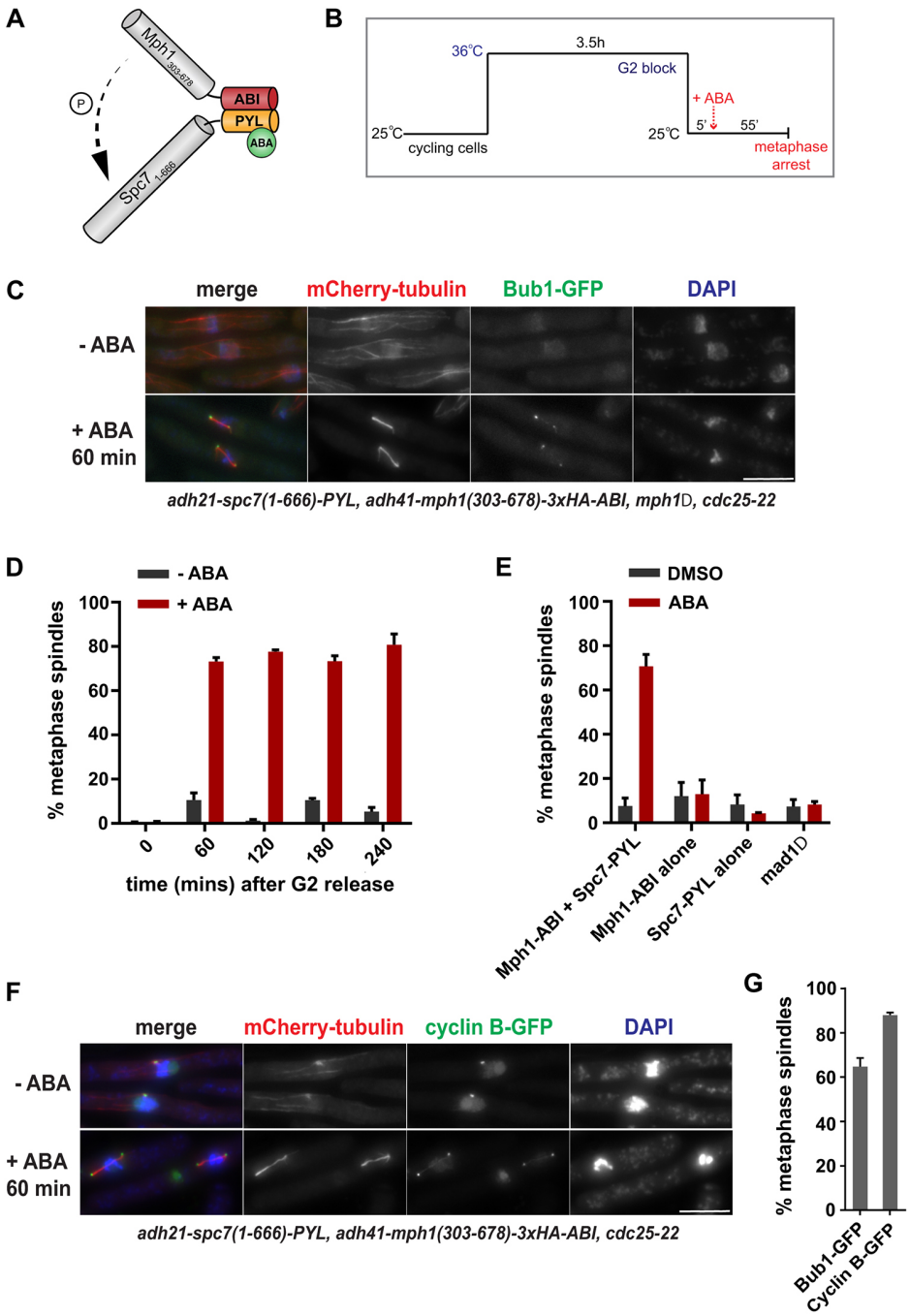

Fig. 1. Rapid induction of spindle checkpoint arrest using ABA for CID of Mph1-Spc7. (A) Representation of the Mph1-Spc7 heterodimer induced by ABA addition. (B) Work flow of the pre-synchronisation in G2 (*cdc25-22*), followed by release into mitosis at 25°C and then induction of checkpoint arrest through the addition of ABA. (C) Fixed cell images taken of the arrested ABA-induced strain 60 min after ABA addition. Microtubules are seen in red (mCherry-Atb2), the checkpoint protein in green (Bub1-GFP) and chromatin in blue (DAPI). (D) Quantification of cultures (±ABA addition) through a 4 h time course after release from G2. Samples were fixed every 60 min and scored as metaphase arrested if they had short metaphase spindles and a single mass of condensed chromatin. More than 100 cells were analysed per strain at each time point. The experiment was repeated three times. (E) Quantification of the strains indicated at the 60 min time point after release from the G2 block (ABA added 5 min after release). *mad1Δ* is the Mph1-ABI Spc7-PYL strain with *mad1* deleted. Cells were scored as metaphase arrested as for D. At least 100 cells were analysed per strain at each time point. The experiment was repeated three times for each strain. (F) Fixed cell images taken of the SynCheckABA strain with Cdc13–GFP at spindle poles bodies 60 min after ABA addition. Microtubules are seen in red (mCherry-Atb2 is labelled fission yeast tubulin), cyclin B in green (Cdc13-GFP) and chromatin in blue (DAPI). (G) Comparison of ABA-induced metaphase arrest at 60 min for an Mph1-ABI Spc7-PYL strain containing Bub1-GFP or another Cdc13-GFP. This experiment was repeated twice. All data are plotted as mean±s.d. Scale bars: 10 µm

Journal of Cell Science (2019) 132, jcs219766. doi:10.1242/jcs.219766

70% of cells had short metaphase spindles (Fig. 1C,D). The metaphase arrest could be sustained for at least 4 h (Fig. 1D). We tested a range of ABA concentrations (0-500 µM) and found that 250 µM was optimal for reproducible, robust arrests (Fig. S1A). The ABA can be added later (e.g. 20 min after *cdc25* release) and cells arrest with similar efficiency to that observed after anti-microtubule drug treatment with carbendazim (see Fig. S1B). Without pre-synchronisation in G2, the mitotic index increases over time and reaches a peak 4 h after ABA addition (Fig. S1C). In our previous SynCheck studies, cells arrested for several hours but then died (Yuan et al., 2017). We wanted to determine whether the ABA arrest also had a significant effect on cell viability or whether our ability to release this arrest (through ABA wash-out) meant that viability was maintained. After ABA treatment, we found a gradual drop in cell viability (see Fig. 2E), which was similar to that observed upon anti-microtubule drug treatment (data not shown).

In the arrested cells, we observed Bub1 enrichment at the spindle poles (Fig. 1C). This is consistent with our previous SynCheck assay, where movement of all spindle checkpoint proteins to spindle poles was reported to be Mad1-Cut7 kinesin driven (Yuan et al., 2017). As expected, deleting the first N-terminal coiled coil (136 amino acids) of Mad1, required for its interaction with Cut7 (Akera et al., 2015), prevented Bub1 accumulation at spindle poles. This de-localisation of checkpoint proteins from spindle poles did not affect the efficiency of the arrest (Fig. S1D), as found in SynCheck (Yuan et al., 2017).

ABA-induced metaphase arrest is dependent on heterodimerisation of Spc7-PYL and Mph1-ABI. Strains lacking either the Mph1-ABI component or the Spc7-PYL component failed to arrest in the presence of ABA (Fig. 1E). Deleting the downstream checkpoint protein Mad1 abolished the arrest (Fig. 1E), showing that ABA-induced arrest is checkpoint dependent. In these constructs, Spc7 and Mph1 lack their kinetochore-binding domains, making initiation of this arrest ectopic and independent of the complexities of the kinetochore. The Mph1-ABI, Spc7-PYL strain used above lacks endogenous *mph1*, which prevents all Mad and Bub checkpoint proteins from targeting to kinetochores (Heinrich et al., 2012). As an additional measure, to confirm kinetochore

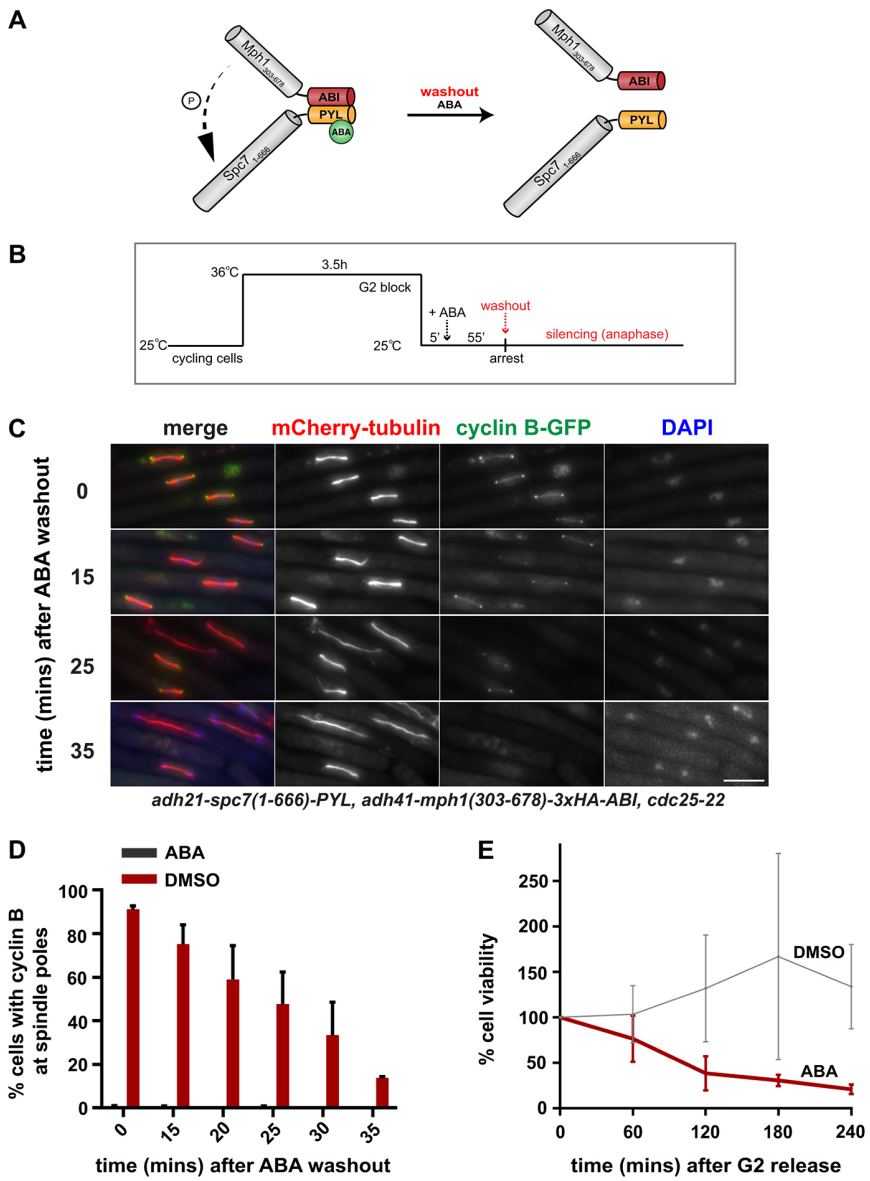

Fig. 2. Silencing of spindle checkpoint signalling after ABA wash-out. (A) Representation of the dissociation of Mph1-Spc7 heterodimers after ABA wash-out. (B) Silencing work flow: pre-synchronisation in G2 (*cdc25-22*), induction of checkpoint arrest through the addition of ABA, subsequent wash-out of ABA 60 min later. (C) Fixed cell images taken of the arrested SynCheckABA strain at 0, 15, 25 and 35 min after ABA wash-out. Microtubules are seen in red (mCherry-Atb2), cyclin B in green (Cdc13-GFP) and chromatin in blue (DAPI). Scale bar: 10 µm. See Fig. S2B for an alternatively coloured version of similar images. (D) Quantification of Cdc13-GFP at spindle pole bodies in the SynCheckABA cultures (plus ABA or DMSO). Samples were fixed and scored for the presence of Cdc13 at spindle pole bodies. The +DMSO control did not arrest in metaphase. More than 150 cells were analysed per strain at each time point. This experiment was repeated three times. (E) The viability of SynCheckABA-arrested strains was determined by plating cells 0, 60, 120, 180 and 240 min after release from a G2 block, where DMSO or ABA was added 5 min after release from the G2 block. Cell viability over time was plotted as a percentage relative to that at time zero. Cells were plated in triplicate. The experiment was repeated three times. All data are plotted as mean±s.d.

independence, we employed a strain containing the *spc7-12A* MELT mutant allele (Mora-Santos et al., 2016; Yamagishi et al., 2012). This mutant Spc7 kinetochore component cannot be phosphorylated by Mph1, preventing recruitment of Bub3-Bub1, and thereby Mad1-Mad2 complexes, to kinetochores. The *spc7-12A* mutant arrested with very similar efficiency to *spc7+* cells under ABA control (Fig. S1F), indicating that the Spc7wt-PYL Mph1-ABI heterodimer does not need to be aided by endogenous kinetochore-based checkpoint signalling to generate a checkpoint arrest. Importantly, *spc7-12A-PYL* fusion protein was unable to generate an arrest in combination with Mph1-ABI, demonstrating that the ectopic signalling scaffold needs to be phosphorylated on conserved Spc7 MELT motifs to recruit Bub3-Bub1 complexes for active signalling (Fig. S1G).

Crucial consequences of checkpoint action are the stabilisation of cyclin B and securin. Using a modified strain, we analysed cyclin B (Cdc13) levels in the ABA-induced arrest. Fig. 1F shows that Cdc13-GFP accumulated on short metaphase spindles and was enriched at mitotic spindle poles, as expected. As a technical aside, we found that different tags can affect the efficiency of the ABA-induced arrest. For example, this Cdc13-GFP strain reproducibly arrests more efficiently than the strain containing Bub1-GFP (Fig. 1G). This is probably a result of a partial loss of function when C-terminally tagging the Bub1 checkpoint protein. The Cdc13-GFP strain also contains the endogenous wild-type *Mph1* gene, but we found that this did not significantly impact the efficiency of arrest (see Fig. S1E).

Thus, we have reconstituted a robust, kinetochore-independent checkpoint arrest that can be initiated very simply *in vivo* through ABA addition to culture media. This works efficiently in both minimal (PMG) and rich (YES) fission yeast growth media. Hereafter, we refer to this assay as SynCheckABA.

A novel spindle checkpoint silencing assay

A significant advantage of SynCheckABA is the ability to reverse the effects of ABA by simply washing cells with fresh medium lacking ABA and thereby releasing them from metaphase arrest (Fig. 2A,B). We can use this to study spindle checkpoint silencing, which has proven to be technically challenging in the past. Fig. 2C,D demonstrates that washing out the ABA results in rapid cyclin degradation and spindle elongation (see also Fig. S2A).

Regulation of spindle checkpoint silencing

Previous work has shown that PP1 (Dis2) is a key spindle checkpoint silencing factor in yeasts (Meadows et al., 2011; Pinsky et al., 2009; Vanoosthuyse and Hardwick, 2009). The N-terminus of Spc7 has two conserved motifs (SILK and RRVSF, also referred to as the A and B motifs) that mediate stable PP1 association (Fig. 3A). Mutation of both binding sites leads to a lethal metaphase block in *Saccharomyces cerevisiae* and *Schizosaccharomyces pombe* (Meadows et al., 2011; Rosenberg et al., 2011). There are additional kinetochore-binding sites for PP1 such as Klp5 and Klp6 (Meadows et al., 2011) and these are relevant to checkpoint silencing, although binding to Spc7 appears to be the major player. In human cells, similar motifs are found at the N-terminus of KNL1; PP1 binding is regulated by Aurora B activity as this kinase can directly phosphorylate the B motif, disrupting PP1 association (Liu et al., 2010).

Employing SynCheckABA, we tested mutations of the A and B motifs at the N-terminus of Spc7 and removal of the Klp6 kinesin. For these experiments (Figs 3 and 4), all strains contained endogenous wild-type *Mph1* kinase and thus were able to recruit checkpoint proteins to their kinetochores. These include the Mph1 and Bub1 kinases, which are also thought to also have 'error correction' functions. Thus, silencing probably needs to take place not only at the ectopic Mph1-Spc7 signalling scaffold, but also at kinetochores. Strains were pre-synchronised in G2 using *cdc25*, released and arrested at metaphase using ABA, and then washed to terminate checkpoint signalling. Progression through anaphase was scored through analysis of spindle elongation and/or cyclin B degradation (using Cdc13-GFP) over a 90 min time course. Mutation of the A motif delayed spindle elongation by 30 min and the A/B double mutant was delayed even more profoundly (Fig. 3B,C). This indicates that PP1 activity on or near the Spc7 protein (previously phosphorylated by Mph1 kinase) is a limiting factor in checkpoint silencing. This system will prove useful for dissecting the regulation of PP1 binding to Spc7 in more detail, and for analysis of putative regulators of PP1 activity.

Mutation of fission yeast kinesin 8 (either Klp5 or Klp6) leads to stabilisation of microtubules, aberrant chromosome movements and long metaphase spindles (Gergely et al., 2016; Klemm et al., 2018; Meadows et al., 2011; West et al., 2002). In these mutants, checkpoint silencing defects cannot simply be analysed through spindle elongation. Instead, we imaged Cdc13-GFP and used the decrease in the number of cells with cyclin B enriched at their spindle poles as a measure of checkpoint silencing. Fig. 4A,B demonstrates that deletion of Klp6 significantly reduces the efficiency of silencing and cyclin B degradation. Finally, we analysed the silencing defect upon deletion of PP1 phosphatase (*dis2Δ*). In the *dis2Δ* strain, which is rather sick, checkpoint silencing was extremely defective with no significant drop in Cdc13-GFP levels over the 90 min time course (Fig. 4C). It should be noted that these *dis2Δ* strains display significant mitotic delays, even in the absence of ABA addition, presumably because the lack of this mitotic phosphatase leads to pleiotropic mitotic defects (see Fig. S4 for images of these cells).

Thus, SynCheckABA neatly recapitulates the balance of opposing kinase and phosphatase activities between Mph1-dependent checkpoint activation and PP1-driven checkpoint silencing on Spc7 and kinesin 8-dependent pathways (see general model in Fig. 4D).

DISCUSSION

Here, we employed CID to generate a rapid, controlled spindle checkpoint arrest. Addition of ABA to SynCheckABA strains induces the heterodimerisation of Mph1-ABI and Spc7-PYL fusion proteins and this is sufficient to generate an activated signalling scaffold and metaphase arrest within minutes. Like our original SynCheck assay, which was driven by constitutive TetR homodimers (Yuan et al., 2017), this arrest acts independently of spindle checkpoint signalling at endogenous kinetochores, but is dependent on downstream checkpoint components such as Mad1.

A significant advantage of SynCheckABA is that we can wash out the ABA and study the kinetics and mechanism of spindle checkpoint silencing. This was not possible with the original SynCheck strain as we were unable to control TetR dimerisation and thus unable to dissociate the Mph1-TetR–Spc7-TetR signalling scaffold.

Using this new assay, we confirmed that PP1 is crucial for silencing the Mph1-Spc7 scaffold (Figs 3 and 4). PP1 binds to the N-terminus of Spc7, not far from the conserved MELT motifs that, once phosphorylated by Mph1, bind Bub3-Bub1 complexes to initiate generation of the mitotic checkpoint complex (MCC) (Shepperd et al., 2012). Thus, Spc7 acts as the platform for both checkpoint activation and silencing and appears to be a major site of

Journal of Cell Science (2019) 132, jcs219766. doi:10.1242/jcs.219766

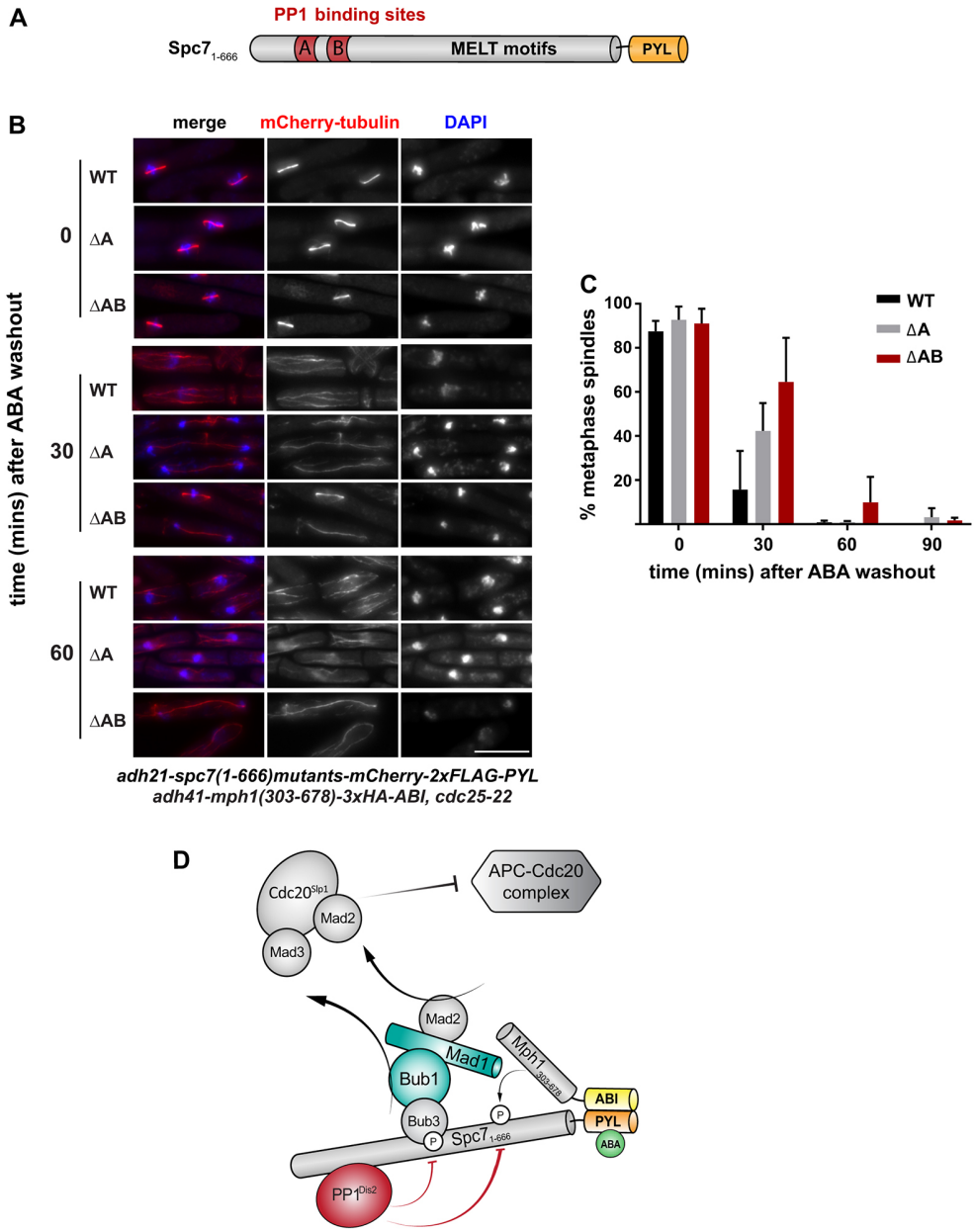

Fig. 3. Checkpoint silencing in SynCheckABA is dramatically slowed when the Spc7^{KNL1} binding sites for PP1^{Dis2} are deleted. (A) Schematic of Spc7^{KNL1} indicating the N-terminal PP1-binding motifs (A motif, SILK; B motif, RRVSF). The MELT motifs form binding sites for Bub3-Bub1 complexes once they have been phosphorylated by Mph1 kinase. (B) Images of cells expressing wild-type Spc7$_{1\text{-}666}$ (WT) or mutants with deletion of the A motif (ΔA) or both the A and B motifs (ΔAB). Time points were analysed at the time of ABA wash-out (time zero) and 30 and 60 min post-wash. Scale bar: 10 µm. See Fig. S3 for non-red-green colour scheme. (C) Quantification of release from checkpoint arrest in WT, ΔA or ΔAB strains. The experiment was repeated three times. More than 100 cells were analysed per strain at each time point. Data are plotted as mean±s.d. (D) Schematic of SynCheckABA: activating (Mph1) and silencing (PP1) factors bind nearby on the Spc7 scaffold. The balance of their activities determines how much MCC is generated and thus whether anaphase onset is inhibited.

action for both checkpoint activation kinases and silencing phosphatases (Meadows et al., 2011). It is important to note that not all aspects of silencing are recapitulated in our ectopic assay, as some of these relate to specific kinetochore processes that are not captured.

Kinesin 8 is also confirmed as a PP1 recruitment site relevant for checkpoint silencing in SynCheckABA. The phenotypes of the *klp6Δ* mutant suggest that targeting of PP1 to spindle microtubules and kinetochores is also relevant to mitotic exit from an ABA-induced arrest, even though the arrest is initiated away from the kinetochore (see Fig. 4D).

Advantages of SynCheckABA, over other forms of reconstitution

We believe that all forms of spindle checkpoint reconstitution are useful for mechanistic dissection of this dynamic signalling pathway, whether this be *in vitro* within cytoplasmic extracts (Minshull et al., 1994), *in vitro* with purified recombinant proteins (Faesen et al., 2017) or *in vivo* with synthetically re-wired and simplified signalling pathways (SynCheckABA). The advantages of the latter system are as follows.

(1) The signalling pathway downstream of Spc7 and the downstream effectors are present at normal physiological levels and there are simple, quantitative physiological read-outs (cyclin B degradation, sister chromatid separation and/or anaphase spindle elongation).

(2) Checkpoint arrest is induced in the absence of additional stresses; simple addition of ABA (low toxicity) to the growth media is sufficient for checkpoint activation. There is no need for cold shock (to depolymerise tubulin, *nda3* arrest), heat shock (to perturb temperature-sensitive kinetochore mutants) or overexpression of checkpoint activators.

(3) The PYL and ABI domains have limited cross-reaction in yeast as they are derived from plant proteins. Although we have not

Journal of Cell Science (2019) 132, jcs219766. doi:10.1242/jcs.219766

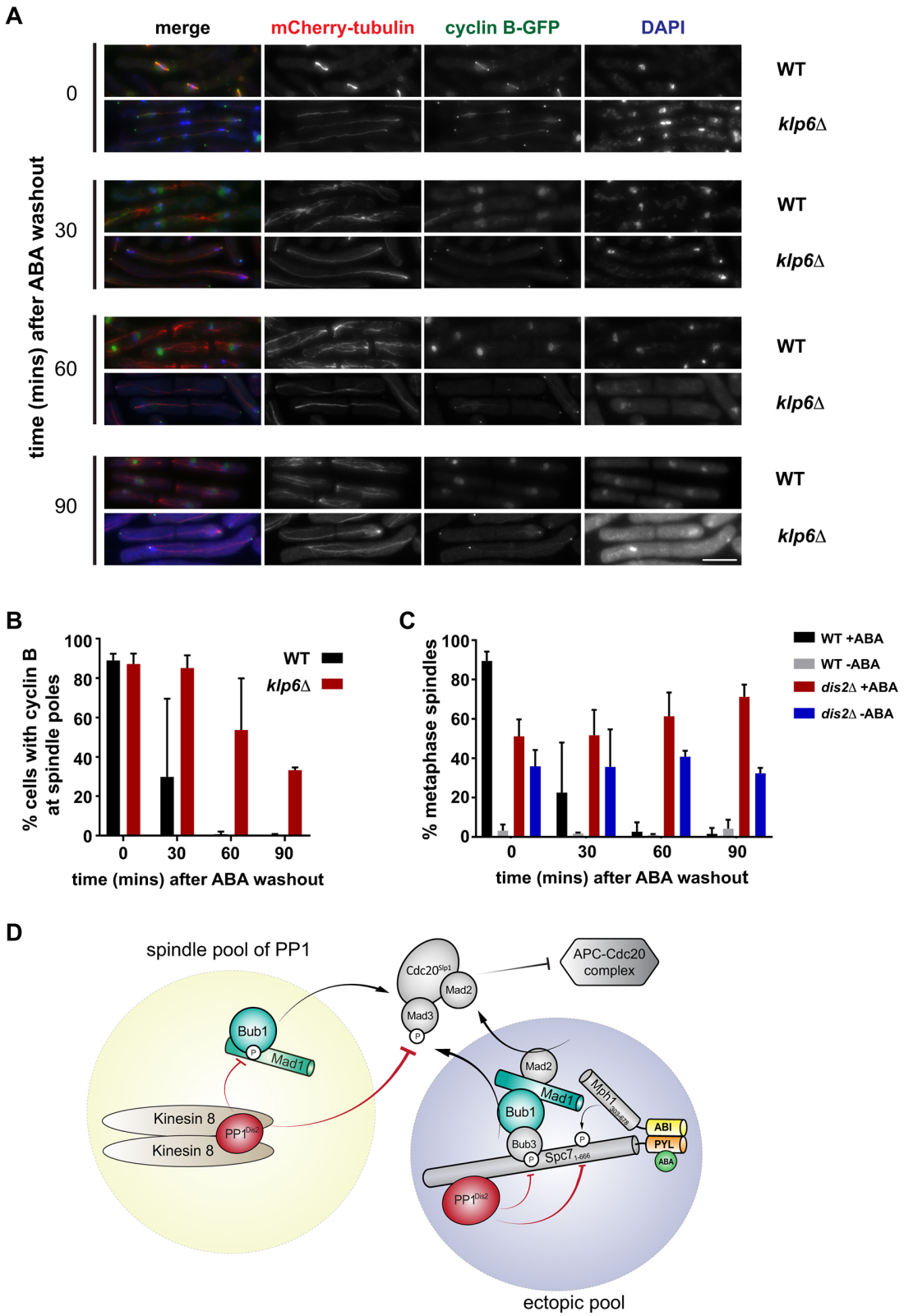

Fig. 4. See next page for legend.

compared them directly, we believe that ABA has certain advantages over the use of rapamycin, a very popular CID. To use rapamycin in fission yeast one needs to engineer strains to remove endogenous rapamycin-binding proteins, such as by deleting the *fkh1*+ gene that encodes a native FKBP12 domain (Ding et al., 2014). Importantly, because ABA does not bind tightly

Journal of Cell Science

Journal of Cell Science (2019) 132, jcs219766. doi:10.1242/jcs.219766

Fig. 4. Checkpoint silencing in SynCheckABA is also slowed when other recruitment sites for PP1 are removed from spindles. (A) Deletion of kinesin 8 (Klp6) leads to reduced silencing efficiency. Images of cells with and without Klp6 deleted are shown after ABA wash-out (time zero) and 30, 60 and 90 min post-wash. Microtubules are seen in red (mCherry-Atb2), cyclin B in green (Cdc13-GFP) and chromatin in blue (DAPI). Scale bar: 10 µm. (B) Quantification of this release from checkpoint arrest in strains with (WT) and without Klp6 (*klp6Δ*). Cells were scored as arrested if Cdc13-GFP was enriched at spindle poles. This experiment was repeated three times. More than 100 cells were analysed per strain at each time point. (C) *dis2Δ* mutants have profound silencing defects. Quantification of the release from the checkpoint arrest is shown for wild-type and *dis2Δ* cells (plus ABA or DMSO). Cells were scored as metaphase arrested if they had short metaphase spindles and a single mass of condensed chromatin. Results for DMSO controls show that *dis2Δ* cells are generally sick, but that ABA addition induces the SynCheckABA, resulting in elevated levels of metaphase-arrested cells. This arrest persists for >60 m after ABA wash-out as *dis2Δ* cells struggle to silence the checkpoint. This experiment was repeated three times. More than 200 cells were analysed per strain at each time point. See Fig. S4 for fixed cell images from this timecourse. (D) General model of relevant PP1-dependent silencing pathways. The schematic describes two pools of PP1, one that is recruited to the ectopic Spc7-Mph1 signalling scaffold, via the A and B motifs on Spc7, and a second pool that is more generally recruited to the spindle through interaction with kinesin 8 (Klp6). These two pools act together to inhibit MCC-APC/C assembly and thereby enable checkpoint silencing and mitotic exit. All data are plotted as mean±s.d.

to the PYL domain, we can wash ABA out easily to initiate checkpoint silencing. By comparison, rapamycin is very difficult to wash out, making efficient release experiments unrealistic.

(4) Compared to *in vitro* studies with large, recombinant complexes, these fission yeast experiments are simple, cheap and fast. The system also enables rapid iterative studies, because of the ease of further genetic manipulation in yeast.

(5) Importantly, we can easily test candidate regulators (e.g. silencing factors) without needing to know what complexes they are part of, purifying them and worrying about their relevant concentration and post-translational modifications.

(6) Compared with our transcriptionally controlled SynCheck (which employs *nmt-tetR-Mph1*), the ABI-PYL system is less leaky, enabling sick strains (such as the *dis2* mutant analysed in Fig. 4) to be constructed. Previously, we were unable to isolate *nmt-tetR-Mph1, dis2Δ* strains because of leaky expression from the weak *nmt81* promoter.

Our ongoing studies with SynCheckABA will enable a detailed mechanistic dissection of PP1-mediated spindle checkpoint silencing in fission yeast. We believe that ABA holds promise as an alternative CID to rapamycin and that it has significant advantages.

MATERIALS AND METHODS

P_{adh41}-$Mph1_{303-678}$-3xHA-ABI

Mph1 (residues 303-678) was amplified from a pDONR 201 plasmid containing Mph1 (303-678) (Yuan et al., 2017). 3×HA was amplified from a plasmid from the Allshire laboratory (University of Edinburgh) containing codon-optimised PYL-3×HA. ABI was amplified from a pMT_CID_ABI_VS_H vector from the Patrick Heun laboratory (University of Edinburgh). These PCR fragments were treated with Dpn1 and assembled into a Sma1-digested and antarctic phosphatase-treated gel-purified pRad41 yeast expression vector by Gibson assembly.

P_{adh21}-$Spc7_{1-666}$-PYL

The yeast expression vector pIY03 (Yuan et al., 2017) was digested with *Nhe*1 and *Xho*1 and gel purified. The insert (mCherry-2×FLAG-$Spc7_{1-666}$) was used as a template to amplify $Spc7_{1-666}$. PYL was amplified from a bVNI-221 vector from the Heun laboratory. The fragments were then assembled into the digested pIY03 vector backbone using Gibson assembly.

P_{adh21}-$spc7_{1-666}$-mCherry-2×FLAG-PYL (PP1-binding site mutants)

Plasmids containing full-length Spc7 PP1-binding mutants (ΔA, deletion of residues 136–150; ΔAB, deletion of residues 136-150 and residues 331–345) (provided by the Millar laboratory, University of Warwick) were used as templates to amplify mutant versions of $Spc7_{1-666}$. NheI-NLS and PacI sites were introduced during amplification, allowing Spc7 constructs to be digested and ligated into digested pIY03-derived vector backbone, which also contained a C-terminal mCherry-2×FLAG-PYL tag.

Fission yeast strains

The fission yeast strains used are listed in Table S1.

cdc25-22 synchronisation

Cells were grown at 25°C for 1-2 days on YES (rich yeast media, with additional leucine, arginine, lysine, histidine and uracil) plates. They were then pre-cultured in 10 ml of liquid YES containing amino acid supplements at 25°C over the day and inoculated into a larger culture of YES overnight. The following day, log phase cultures were shifted to 36°C for 3.5 h to block in G2. After this, cultures were cooled quickly in iced water to rapidly shift them back to 25°C and release them from the G2 block.

Synthetic arrest assay

Following a *cdc25-22* block, 250 mM ABA stock (Sigma Aldrich A1049) was added to cultures 5 min after release (20 min if comparing to a carbendazim arrest) to achieve a final concentration of 250 µM (unless otherwise stated).

Synthetic arrest assay wash-out

Following an ABA-induced synthetic arrest, the cells were washed three times with 50 ml YES.

Fixing cells and microscopy

Culture (1-1.5 ml) was centrifuged for 1 min at 6000 rpm. The cell pellet was fixed in 200–500 µl of 100% ice-cold methanol. To image cells, 8 µl of the cell suspension in methanol was added to a glass slide; when the methanol evaporated, 1-2 µl DAPI (0.4 µg/ml) was added to the sample and a glass cover slip was placed on top.

Cells were imaged immediately using a 100× oil immersion lens and a Zeiss Axiovert 200M microscope (Carl Zeiss), equipped with a CoolSnap CCD camera (Photometrics) and Slidebook 5.0 software (3i, Intelligent Imaging Innovations). Typical acquisition settings were 300 ms exposure (FITC and TRITC) and 100 ms exposure (DAPI), 2× binning, Z-series over 3 µm range in 0.5 µm steps (seven planes).

Carbendazim arrest

Following a cdc25-22 block, 3.75 mg/ml stock of carbendazim (Sigma Aldrich) was added to cultures 20 min after release to achieve a final concentration of 100 µg/ml.

Cell viability assay

Following a synthetic arrest assay, cells from 1 ml of culture were harvested by centrifugation at 6000 rpm for 1 min and re-suspended in 1 ml of distilled water. Tenfold serial dilutions were made in distilled water. Cells were diluted by factors of 100 and 1000, and 0.1 ml plated in triplicate. Colony forming units (cfu) per millilitre of culture was calculated and cell viability over time was plotted as a percentage relative to that at time zero.

Acknowledgements

We would like to thank Patrick Heun and Eftychia Kyriacou for providing constructs containing the ABA-binding heterodimerisation domains of PYL and ABI; Jonathan Millar for the PP1-binding *spc7* mutants and the *klp6* mutants; and Ken Sawin for the mCherry-Atb2 strain.

Competing interests

The authors declare no competing or financial interests.

Author contributions

P.A. carried out the experiments and produced the data presented in Figs 1 and 2, Figs S1 and S2. S.S.N.C. carried out the experiments and produced the data

presented in Figs 3 and 4, Figs S3 and S4. I.L. assisted with experiments, figure production and Fig. 4D model generation. Conceptualization: P.A., K.G.H.; Methodology: P.A., S.S.N.C., I.L.; Formal analysis: P.A., S.S.N.C., I.L.; Investigation: P.A., S.S.N.C., I.L.; Writing - original draft: K.G.H.; Writing - review and editing: P.A., S.S.N.C., I.L.; Visualization: P.A., S.S.N.C., I.L.; Supervision: K.G.H.; Project administration: K.G.H.; Funding acquisition: K.G.H.

Funding

This work was supported by a Seed Award from the Wellcome Trust to K.G.H. (108105) and the Wellcome Centre for Cell Biology core grant (203149). P.A. was supported by the Medical Research Council (MR/K501293/1), S.S.N.C. by the Wellcome Trust (105258) and I.L. by the Darwin Trust of Edinburgh. Deposited in PMC for immediate release.

Supplementary information

Supplementary information available online at http://jcs.biologists.org/lookup/doi/10.1242/jcs.219766.supplemental

References

Akera, T., Goto, Y., Sato, M., Yamamoto, M. and Watanabe, Y. (2015). Mad1 promotes chromosome congression by anchoring a kinesin motor to the kinetochore. *Nat. Cell Biol.* **17**, 1124-1133.

Ding, L., Laor, D., Weisman, R. and Forsburg, S. L. (2014). Rapid regulation of nuclear proteins by rapamycin-induced translocation in fission yeast. *Yeast* **31**, 253-264.

Faesen, A. C., Thanasoula, M., Maffini, S., Breit, C., Müller, F., van Gerwen, S., Bange, T. and Musacchio, A. (2017). Basis of catalytic assembly of the mitotic checkpoint complex. *Nature* **542**, 498-502.

Gergely, Z. R., Crapo, A., Hough, L. E., McIntosh, J. R. and Betterton, M. D. (2016). Kinesin-8 effects on mitotic microtubule dynamics contribute to spindle function in fission yeast. *Mol. Biol. Cell* **27**, 3490-3514.

Heinrich, S., Windecker, H., Hustedt, N. and Hauf, S. (2012). Mph1 kinetochore localization is crucial and upstream in the hierarchy of spindle assembly checkpoint protein recruitment to kinetochores. *J. Cell Sci.* **125**, 4720-4727.

Hoyt, M. A., Totis, L. and Roberts, B. T. (1991). S. cerevisiae genes required for cell cycle arrest in response to loss of microtubule function. *Cell* **66**, 507-517.

Hwang, L. H., Lau, L. F., Smith, D. L., Mistrot, C. A., Hardwick, K. G., Hwang, E. S., Amon, A. and Murray, A. W. (1998). Budding yeast Cdc20: a target of the spindle checkpoint. *Science* **279**, 1041-1044.

Kim, S. H., Lin, D. P., Matsumoto, S., Kitazono, A. and Matsumoto, T. (1998). Fission yeast Slp1: an effector of the Mad2-dependent spindle checkpoint. *Science* **279**, 1045-1047.

Klemm, A. H., Bosilj, A., Glunčić, M., Pavin, N. and Tolic, I. M. (2018). Metaphase kinetochore movements are regulated by kinesin-8 motors and microtubule dynamic instability. *Mol. Biol. Cell* **29**, 1332-1345.

Kulukian, A., Han, J. S. and Cleveland, D. W. (2009). Unattached kinetochores catalyze production of an anaphase inhibitor that requires a Mad2 template to prime Cdc20 for BubR1 binding. *Dev. Cell* **16**, 105-117.

Li, R. and Murray, A. W. (1991). Feedback control of mitosis in budding yeast. *Cell* **66**, 519-531.

Liang, F.-S., Ho, W. Q. and Crabtree, G. R. (2011). Engineering the ABA plant stress pathway for regulation of induced proximity. *Sci. Signal.* **4**, rs2.

Liu, D., Vleugel, M., Backer, C. B., Hori, T., Fukagawa, T., Cheeseman, I. M. and Lampson, M. A. (2010). Regulated targeting of protein phosphatase 1 to the outer kinetochore by KNL1 opposes Aurora B kinase. *J. Cell Biol.* **188**, 809-820.

London, N. and Biggins, S. (2014). Signalling dynamics in the spindle checkpoint response. *Nat. Rev. Mol. Cell Biol.* **15**, 736-748.

Meadows, J. C., Shepperd, L. A., Vanoosthuyse, V., Lancaster, T. C., Sochaj, A. M., Buttrick, G. J., Hardwick, K. G. and Millar, J. B. (2011). Spindle checkpoint silencing requires association of PP1 to both Spc7 and kinesin-8 motors. *Dev. Cell* **20**, 739-750.

Minshull, J., Sun, H., Tonks, N. K. and Murray, A. W. (1994). A MAP kinase-dependent spindle assembly checkpoint in Xenopus egg extracts. *Cell* **79**, 475-486.

Miyazono, K., Miyakawa, T., Sawano, Y., Kubota, K., Kang, H. J., Asano, A., Miyauchi, Y., Takahashi, M., Zhi, Y., Fujita, Y. et al. (2009). Structural basis of abscisic acid signalling. *Nature* **462**, 609-614.

Mora-Santos, M. D., Hervas-Aguilar, A., Sewart, K., Lancaster, T. C., Meadows, J. C. and Millar, J. B. (2016). Bub3-Bub1 binding to Spc7/KNL1 toggles the spindle checkpoint switch by licensing the interaction of Bub1 with Mad1-Mad2. *Curr. Biol.* **26**, 2642-2650.

Musacchio, A. (2015). The molecular biology of spindle assembly checkpoint signaling dynamics. *Curr. Biol.* **25**, R1002-R1018.

Petrovic, A., Mosalaganti, S., Keller, J., Mattiuzzo, M., Overlack, K., Krenn, V., De Antoni, A., Wohlgemuth, S., Cecatiello, V., Pasqualato, S. et al. (2014). Modular assembly of RWD domains on the Mis12 complex underlies outer kinetochore organization. *Mol. Cell* **53**, 591-605.

Petrovic, A., Keller, J., Liu, Y., Overlack, K., John, J., Dimitrova, Y. N., Jenni, S., van Gerwen, S., Stege, P., Wohlgemuth, S. et al. (2016). Structure of the MIS12 complex and molecular basis of its interaction with CENP-C at human kinetochores. *Cell* **167**, 1028-1040.e1015.

Pinsky, B. A., Nelson, C. R. and Biggins, S. (2009). Protein phosphatase 1 regulates exit from the spindle checkpoint in budding yeast. *Curr. Biol.* **19**, 1182-1187.

Rosenberg, J. S., Cross, F. R. and Funabiki, H. (2011). KNL1/Spc105 recruits PP1 to silence the spindle assembly checkpoint. *Curr. Biol.* **21**, 942-947.

Shepperd, L. A., Meadows, J. C., Sochaj, A. M., Lancaster, T. C., Zou, J., Buttrick, G. J., Rappsilber, J., Hardwick, K. G. and Millar, J. B. (2012). Phosphodependent recruitment of Bub1 and Bub3 to Spc7/KNL1 by Mph1 kinase maintains the spindle checkpoint. *Curr. Biol.* **22**, 891-899.

Tanaka, K., Chang, H. L., Kagami, A. and Watanabe, Y. (2009). CENP-C functions as a scaffold for effectors with essential kinetochore functions in mitosis and meiosis. *Dev. Cell* **17**, 334-343.

Vanoosthuyse, V. and Hardwick, K. G. (2009). A novel protein phosphatase 1-dependent spindle checkpoint silencing mechanism. *Curr. Biol.* **19**, 1176-1181.

West, R. R., Malmstrom, T. and McIntosh, J. R. (2002). Kinesins klp5(+) and klp6(+) are required for normal chromosome movement in mitosis. *J. Cell Sci.* **115**, 931-940.

Yamagishi, Y., Yang, C.-H., Tanno, Y. and Watanabe, Y. (2012). MPS1/Mph1 phosphorylates the kinetochore protein KNL1/Spc7 to recruit SAC components. *Nat. Cell Biol.* **14**, 746-752.

Yuan, I., Leontiou, I., Amin, P., May, K. M., Soper Ni Chafraidh, S., Zlámalová, E. and Hardwick, K. G. (2017). Generation of a spindle checkpoint arrest from synthetic signaling assemblies. *Curr. Biol.* **27**, 137-143.

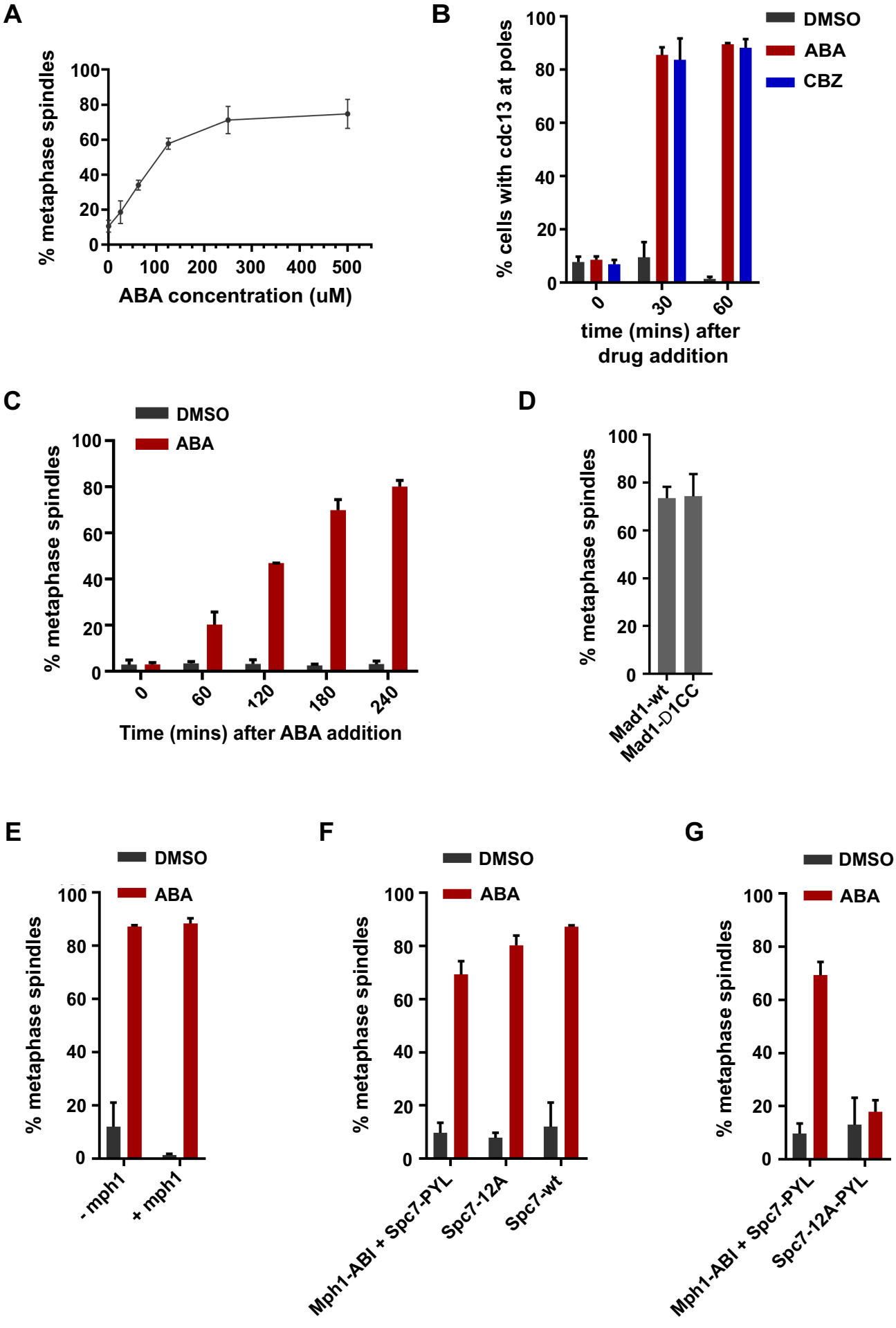

Figure S1 Amin et al

Journal of Cell Science • Supplementary information

Figure S1

(A) The effect of ABA concentration on Mph1-ABI Spc7-PYL driven arrest. Different concentrations (0, 25, 62.5, 125, 250, 500 μM) of ABA were used to induce arrest in cultures 5 mins after release from the G2 block. Samples were fixed at 60 mins and scored as metaphase arrested if they had short metaphase spindles and a single mass of condensed chromatin. >100 cells were analysed per strain at each time point. This experiment was repeated 3 times. Data plotted as mean +/- SD.

(B) Quantification of SynCheckABA strain containing Cdc13-GFP at 60 minutes after treatment with either DMSO, ABA or CBZ (added 20 minutes after release from G2 block). Cells were scored as arrested if Cdc13 was enriched at spindle poles and/or if short metaphase spindle was present. >240 cells were analysed per strain at each time point. This experiment was repeated 2 times. Data plotted as mean +/- SD.

(C) Quantification of Mph1-ABI Spc7-PYL cultures (plus ABA or DMSO) through a 4 hour time course at 25°C without synchronisation in G2. Samples were fixed every 60 minutes and scored as metaphase arrested if they had short metaphase spindles and a single mass of condensed chromatin. >250 cells were analysed per strain at each time point. This experiment was repeated 2 times. Data plotted as mean +/- SD.

(D) Quantification of Mph1-ABI Spc7-PYL arrest in strains with and without the N-terminal coiled-coil of Mad1, 60 minutes after release from G2 block (ABA added at 5 minutes). In its absence, Mad1p fails to localise to the nuclear periphery or bind to the Cut7 kinesin which would otherwise take it to spindle poles. >150 cells were analysed per strain at each time point. This experiment was repeated 3 times. Data plotted as mean +/- SD.

(E) Quantification of ABA-induced arrest in strains with and without endogenous mph1 60 minutes after release from G2 block (ABA added at 5 minutes). >100 cells were analysed per strain at each time point. This experiment was repeated 2 times. Data plotted as mean +/- SD.

(F) Quantification of the strains indicated at the 60 minute time point after release from the G2 block (ABA added 5 mins after release). The spc7-12A strain has the endogenous spc7 gene deleted and expresses this non-phosphorylatable 12A (MELA) allele from its own promoter integrated at the C locus. Spc7-wt is the wild-type control for this strain. > 100 cells were analysed per strain at each time point. This experiment was repeated 3 times. Data plotted as mean +/- SD.

(G) Quantification of the strains indicated at the 60 minute time point after release from the G2 block (ABA added 5 mins after release). Spc7-12A-PYL is a non-phosphorylatable 12A (MELA) mutant tagged with PYL, which does not generate an arrest when co-recruited with Mph1-ABI in the presence of ABA. >220 cells were analysed per strain at each time point. This experiment was repeated ≥ 2 times. Data plotted as mean +/- SD.

Journal of Cell Science • Supplementary information

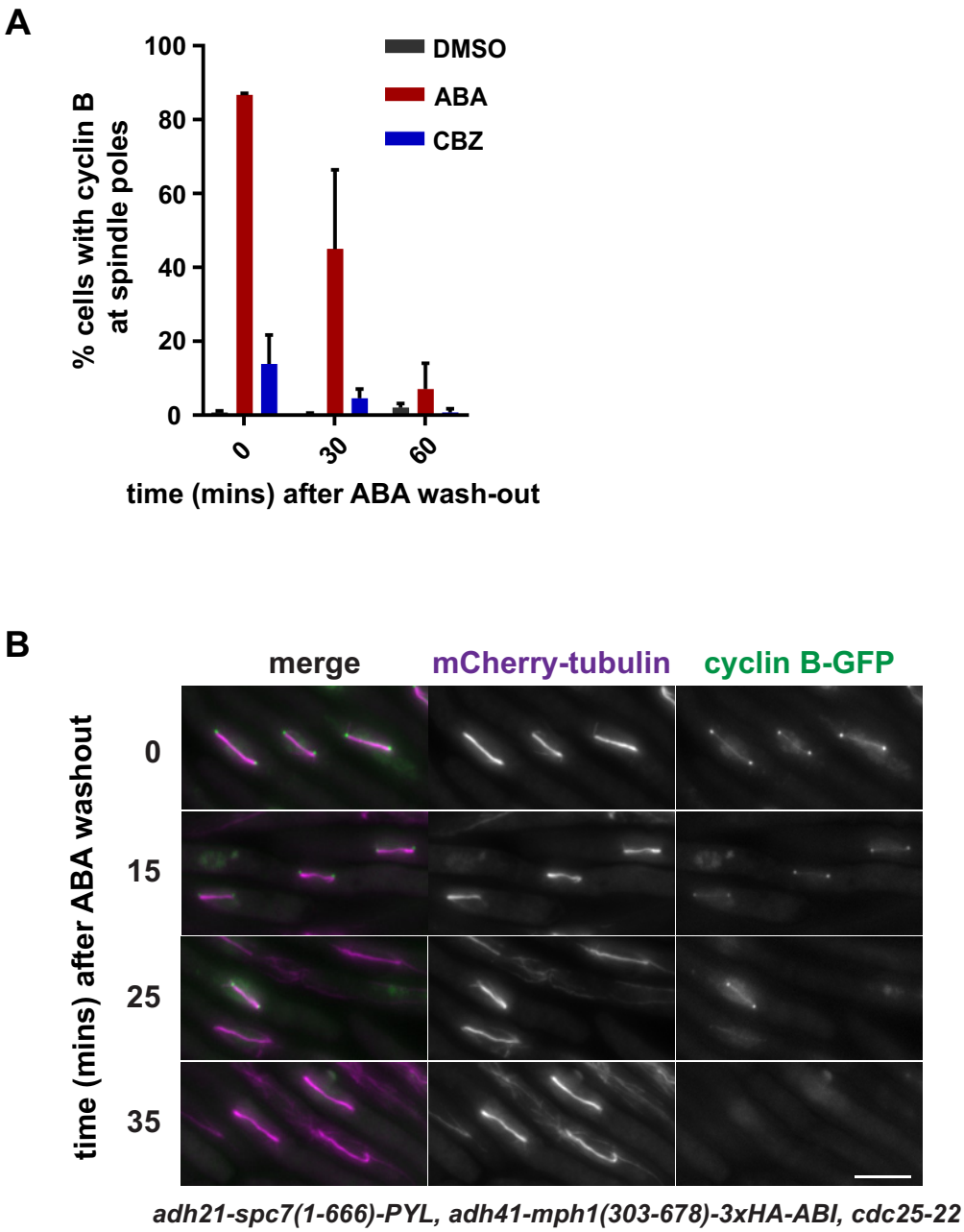

(A) Quantification of DMSO/ABA/CBZ wash-out in SynCheckABA strain following 60 minutes of treatment with solvent (added 20 minutes after release from G2 block).
Cells were scored as arrested if Cdc13 was enriched at spindle poles.
>160 cells were analysed per strain at each time point.
This experiment was repeated 2 times and data are plotted as mean +/- SD.

(B) Fixed cell images taken of the arrested SynCheckABA strain at 0, 15, 25 and 35 minutes after ABA wash-out. Microtubules are seen in purple (mCherry-tubulin) and cyclin B in green (cyclin B-GFP). Scale bar is 10 μm.

Figure S2 Amin et al

Journal of Cell Science • Supplementary information

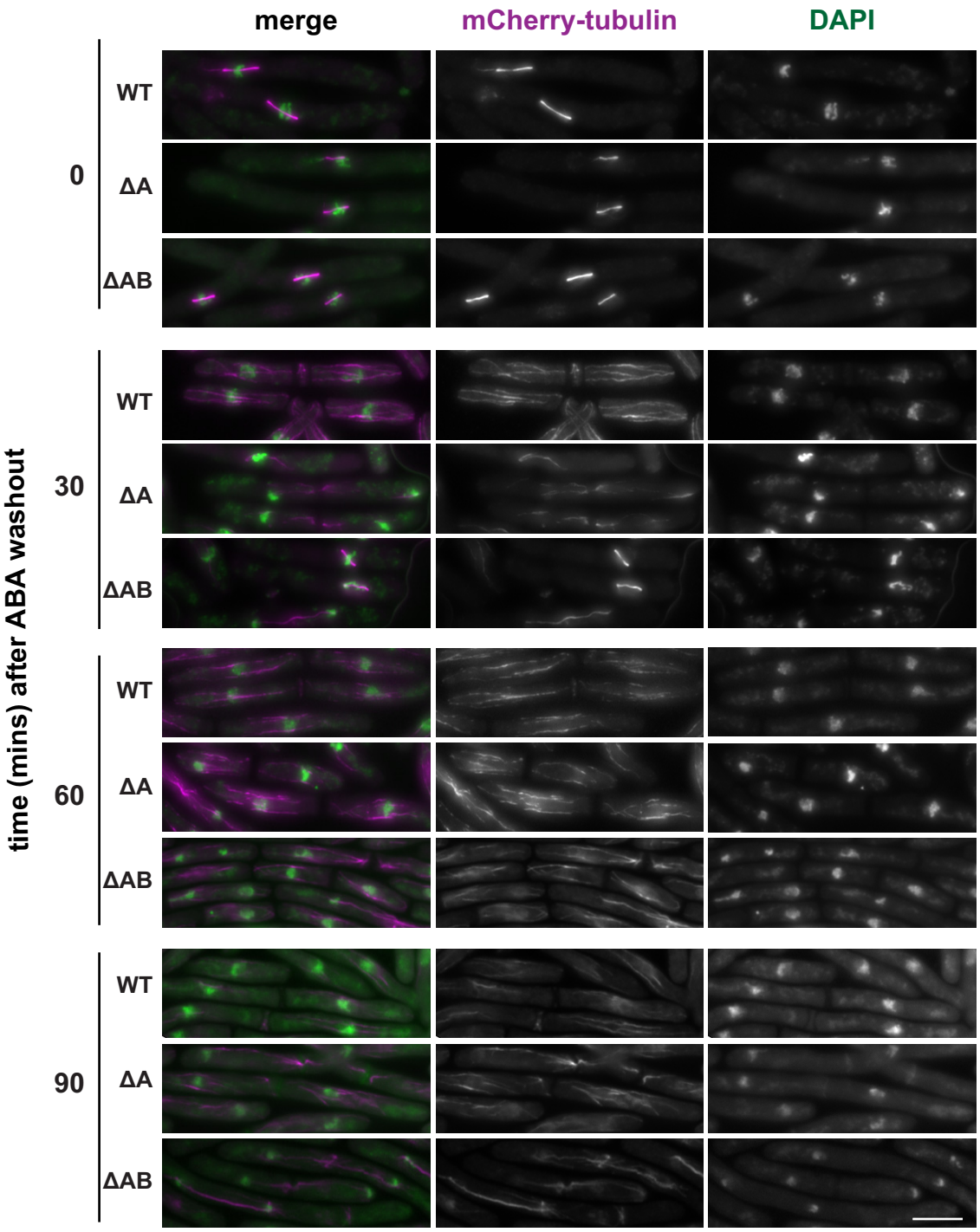

Fixed cell images taken of the arrested Spc7 mutant strains at 0, 15, 25 and 35 minutes after ABA wash-out. Microtubules are seen in purple (mCherry-tubulin) and DAPI in green. Scale bar is 10 μm.

Figure S3 Amin et al

Journal of Cell Science • Supplementary information

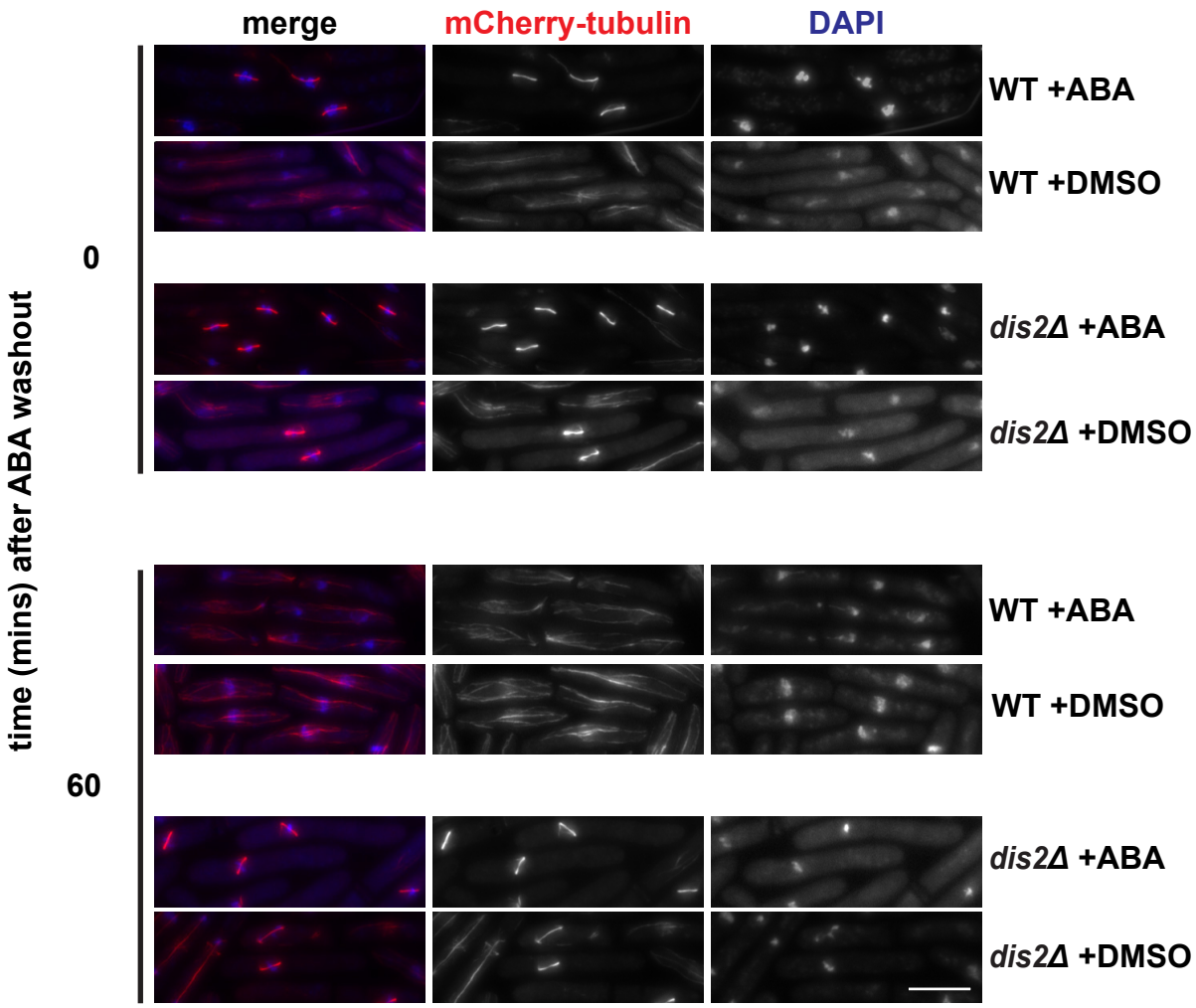

*dis2*Δ mutants have profound silencing defects. Fixed cell images of wild-type and *dis2*Δ cells after ABA washout (time zero) and 60 minutes post-wash. Microtubules are seen in red (mCherry-tubulin) and chromatin in stained with DAPI. Scale bar is 10 µm.

Figure S4 Amin et al

Journal of Cell Science • Supplementary information

Supplementary Table 1

Figure	Strain	Genotype
Figure 1	PA252	Padh41-mph1(303-678)-3xHA-ABI:LEU2 mph1Δ::nat lys1::Padh21-spc7(1-666)-PYL:ura4 cdc25-22 Z:Padh15-mCherry-atb2:natMX6 bub1-GFP:his
	PA269	Padh41-mph1(303-678)-3xHA-ABI:LEU2 mph1Δ::nat cdc25-22 Z:Padh15-mCherry-atb2:natMX6 bub1GFP:his
	PA286	lys1::Padh21-spc7(1-666)-PYL:ura4 cdc25-22 Z:Padh15-mCherry-atb2:natMX6 bub1-GFP:his
	PA260	mad1Δ::hyg Padh41-mph1(303-678)-3xHA-ABI:LEU2 mph1Δ::nat lys1::adh21-spc7(1-666)-PYL:ura4 cdc25-22 Z:Padh15-mCherry-atb2:natMX6; bub1-GFP:his
	PA338	Padh41-mph1(303-678)-3xHA-ABI:LEU2 lys1::Padh21-spc7(1-666)-PYL:ura4 cdc25-22 Z:Padh15-mCherry-atb2:natMX6 cdc13-GFP:leu
Figure 2	PA338	Padh41-mph1(303-678)-3xHA-ABI:LEU2 lys1::Padh21-spc7(1-666)-PYL:ura4 cdc25-22 Z:Padh15-mCherry-atb2:natMX6 cdc13-GFP:leu
	PA252	Padh41-mph1(303-678)-3xHA-ABI:LEU2 mph1Δ::nat lys1::Padh21-spc7(1-666)-PYL:ura4 cdc25-22 Z:Padh15-mCherry-atb2:natMX6 bub1-GFP:his
Figure 3	SS123	Padh41-mph1(303-678)-3xHA-ABI:LEU2 lys1::Padh21-spc7(1-666)-mCherry-2xFLAG-PYL:ura4 cdc25-22 Z:Padh15-mCherry atb2:natMX6
	SS121	Padh41-mph1(303-678)-3xHA-ABI:LEU2 lys1::Padh21-spc7(1-666, Δ136-150)-mCherry-2xFLAG-PYL:ura4 cdc25-22 Z:Padh15-mCherry-atb2:natMX6
	SS122	Padh41-mph1(303-678)-3xHA-ABI:LEU2 lys1::Padh21-spc7(1-666, Δ136-150, Δ331-345)-mCherry-2xFLAGPYL:ura4 cdc25-22 Z:Padh15-mCherry-atb2:natMX6
Figure 4	PA338	Padh41-mph1(303-678)-3xHA-ABI:LEU2 lys1::Padh21-spc7(1-666)-PYL:ura4 cdc25-22 Z:Padh15-mCherry-atb2:natMX6 cdc13-GFP:leu
	SS130	klp6Δ::ura4 Padh41-mph1(303-678)-3xHA-ABI:LEU2 lys1::Padh21-spc7(1-666)-mCherry-2xFLAG-PYL:ura4 cdc25-22 Z:Padh15-mCherry-atb2:natMX6 cdc13-GFP:leu
	SS123	Padh41-mph1(303-678)-3xHA-ABI:LEU2 lys1::Padh21-spc7(1-666)-mCherry-2xFLAG-PYL:ura4 cdc25-22 Z:Padh15-mCherry-

Journal of Cell Science • Supplementary information

		atb2:natMX6
	SS128	dis2Δ::hyg Padh41-mph1(303-678)-3xHA-ABI:LEU2 lys1::Padh21-spc7(1-666)-mCherry-2xFLAG-PYL:ura4 cdc25-22 Z:Padh15-mCherry-atb2:natMX6 cdc13-GFP:leu
Figure S1	PA252	Padh41-mph1(303-678)-3xHA-ABI:LEU2 mph1D::nat lys1::Padh21-spc7(1-666)-PYL:ura4 cdc25-22 Z:Padh15-mCherry-atb2:natMX6 bub1-GFP:his
	PA338	Padh41-mph1(303-678)-3xHA-ABI:LEU2 lys1::Padh21-spc7(1-666)-PYL:ura4 cdc25-22 Z:Padh15-mCherry-atb2:natMX6 cdc13-GFP:leu
	PA253	Padh41-mph1(303-678)-3xHA-ABI:LEU2 mph1D::nat lys1::Padh21-spc7(1-666)-PYL:ura4 2xflag-mad1-Δ1CC:hyg cdc25-22 Z:Padh15-mCherry-atb2:natMX6 bub1-GFP:his
	PA 254	Padh41-mph1(303-678)-3xHA-ABI:LEU2 mph1D::nat lys1::Padh21-spc7(1-666)-PYL:ura 2xflag-mad1-Δ1CC:hyg cdc25-22 Z:Padh15-mCherry-atb2:natMX6 bub1-GFP:his
	PA264	spc7Δ::G418 spc7:hyg lys1::Padh21-spc7(1-666)-PYL:ura4 Padh41-mph1(303-678)-3xHA-ABI:LEU2 mph1Δ::nat cdc25-22 Z:Padh15-mCherry-atb2:natMX6
	PA262	spc7Δ::G418 spc7-T12A:hyg lys1::Padh21-spc7(1-666)-PYL:ura4 Padh41-mph1(303-678)-3xHA-ABI:LEU2 mph1Δ::nat cdc25-22 Z:Padh15-mCherry-atb2:natMX6
	PA317	Padh41-mph1(303-678)-3xHA-ABI:LEU2 lys1::Padh21-spc7(1-666)12A-PYL:ura4 cdc25-22 Z:Padh15-mCherry-atb2:natMX6
Figure S2	PA338	Padh41-mph1(303-678)-3xHA-ABI:LEU2 lys1::Padh21-spc7(1-666)-PYL:ura4 cdc25-22 Z:Padh15-mCherry-atb2:natMX6 cdc13-GFP:leu
Figure S3	SS123	Padh41-mph1(303-678)-3xHA-ABI:LEU2 lys1::Padh21-spc7(1-666)-mCherry-2xFLAG-PYL:ura4 cdc25-22 Z:Padh15-mCherry atb2:natMX6
	SS121	Padh41-mph1(303-678)-3xHA-ABI:LEU2 lys1::Padh21-spc7(1-666, Δ136-150)-mCherry-2xFLAG-PYL:ura4 cdc25-22 Z:Padh15-mCherry-atb2:natMX6
	SS122	Padh41-mph1(303-678)-3xHA-ABI:LEU2 lys1::Padh21-spc7(1-666, Δ136-150, Δ331-345)-mCherry-2xFLAGPYL:ura4 cdc25-22 Z:Padh15-mCherry-atb2:natMX6
Figure S4	SS128	dis2Δ::hyg Padh41-mph1(303-678)-3xHA-ABI:LEU2 lys1::Padh21-spc7(1-666)-mCherry-2xFLAG-PYL:ura4 cdc25-22 Z:Padh15-mCherry-atb2:natMX6 cdc13-GFP:leu
	SS123	Padh41-mph1(303-678)-3xHA-ABI:LEU2 lys1::Padh21-spc7(1-666)-mCherry-2xFLAG-PYL:ura4 cdc25-22 Z:Padh15-mCherry-atb2:natMX6